Interactions matière organique contaminants inorganiques dans des dépôts de solutions de traitement des eaux fondées sur la nature : Approche combinée ultrafiltration-modélisation

Camille Banc

N°d'ordre NNT : 2021LYSEI066

THESE de DOCTORAT DE L'UNIVERSITE DE LYON
opérée au sein de
L'Institut National des Sciences Appliquées de Lyon

Ecole Doctorale N° 206
Ecole doctorale de Chimie de Lyon

Spécialité de doctorat/ Discipline : Environnement

Soutenue publiquement le 15/10/2021, par :
Camille Banc

Interactions matière organique-contaminants inorganiques dans des dépôts de solutions de traitement des eaux fondées sur la nature. Approche combinée ultrafiltration-modélisation

Devant le jury composé de :

Béchet, Béatrice	Directrice de Recherche Université Gustave Eiffel	Rapporteure
Pokrovsky, Oleg	Directeur de Recherche CNRS Géoscience Environnement Toulouse	Rapporteur
Bataillard, Phillipe	Chercheur BRGM	Examinateur
Marsac, Rémi	Chargé de Recherche CNRS Géosciences Rennes	Examinateur
Molle, Pascal	Directeur de Recherche INRAE	Examinateur
Gourdon, Rémy	Professeur des Universités INSA LYON	Directeur de thèse
Gautier, Mathieu	Maître de Conférences INSA LYON	Co-directeur de thèse
Blanc, Denise	Maître de Conférences INSA LYON	Encadrante de thèse

Membres invités :

Lupsea-Toader, Maria	Maître de Conférences INSA LYON	Encadrante de thèse
Lassabatère, Laurent	IDTPE, ENTPE	Examinateur

Département FEDORA – INSA Lyon - Ecoles Doctorales

SIGLE	ECOLE DOCTORALE	NOM ET COORDONNEES DU RESPONSABLE
CHIMIE	**CHIMIE DE LYON** **https://www.edchimie-lyon.fr** Sec. : Renée EL MELHEM Bât. Blaise PASCAL, 3e étage secretariat@edchimie-lyon.fr	**M. Stéphane DANIELE** C2P2-CPE LYON-UMR 5265 Bâtiment F308, BP 2077 43 Boulevard du 11 novembre 1918 69616 Villeurbanne **directeur@edchimie-lyon.fr**
E.E.A.	**ÉLECTRONIQUE, ÉLECTROTECHNIQUE, AUTOMATIQUE** **https://edeea.universite-lyon.fr** Sec. : Stéphanie CAUVIN Bâtiment Direction INSA Lyon Tél : 04.72.43.71.70 secretariat.edeea@insa-lyon.fr	**M. Philippe DELACHARTRE** INSA LYON Laboratoire CREATIS Bâtiment Blaise Pascal, 7 avenue Jean Capelle 69621 Villeurbanne CEDEX Tél : 04.72.43.88.63 **philippe.delachartre@insa-lyon.fr**
E2M2	**ÉVOLUTION, ÉCOSYSTÈME, MICROBIOLOGIE, MODÉLISATION** **http://e2m2.universite-lyon.fr** Sec. : Sylvie ROBERJOT Bât. Atrium, UCB Lyon 1 Tél : 04.72.44.83.62 secretariat.e2m2@univ-lyon1.fr	**M. Philippe NORMAND** Université Claude Bernard Lyon 1 UMR 5557 Lab. d'Ecologie Microbienne Bâtiment Mendel 43, boulevard du 11 Novembre 1918 69 622 Villeurbanne CEDEX **philippe.normand@univ-lyon1.fr**
EDISS	**INTERDISCIPLINAIRE SCIENCES-SANTÉ** **http://ediss.universite-lyon.fr** Sec. : Sylvie ROBERJOT Bât. Atrium, UCB Lyon 1 Tél : 04.72.44.83.62 secretariat.ediss@univ-lyon1.fr	**Mme Sylvie RICARD-BLUM** Institut de Chimie et Biochimie Moléculaires et Supramoléculaires (ICBMS) - UMR 5246 CNRS - Université Lyon 1 Bâtiment Raulin - 2ème étage Nord 43 Boulevard du 11 novembre 1918 69622 Villeurbanne Cedex Tél : +33(0)4 72 44 82 32 **sylvie.ricard-blum@univ-lyon1.fr**
INFOMATHS	**INFORMATIQUE ET MATHÉMATIQUES** **http://edinfomaths.universite-lyon.fr** Sec. : Renée EL MELHEM Bât. Blaise PASCAL, 3e étage Tél : 04.72.43.80.46 infomaths@univ-lyon1.fr	**M. Hamamache KHEDDOUCI** Université Claude Bernard Lyon 1 Bât. Nautibus 43, Boulevard du 11 novembre 1918 69 622 Villeurbanne Cedex France Tél : 04.72.44.83.69 **hamamache.kheddouci@univ-lyon1.fr**
Matériaux	**MATÉRIAUX DE LYON** **http://ed34.universite-lyon.fr** Sec. : Yann DE ORDENANA Tél : 04.72.18.62.44 yann.de-ordenana@ec-lyon.fr	**M. Stéphane BENAYOUN** Ecole Centrale de Lyon Laboratoire LTDS 36 avenue Guy de Collongue 69134 Ecully CEDEX Tél : 04.72.18.64.37 **stephane.benayoun@ec-lyon.fr**
MEGA	**MÉCANIQUE, ÉNERGÉTIQUE, GÉNIE CIVIL, ACOUSTIQUE** **http://edmega.universite-lyon.fr** Sec. : Stéphanie CAUVIN Tél : 04.72.43.71.70 Bâtiment Direction INSA Lyon mega@insa-lyon.fr	**M. Jocelyn BONJOUR** INSA Lyon Laboratoire CETHIL Bâtiment Sadi-Carnot 9, rue de la Physique 69621 Villeurbanne CEDEX **jocelyn.bonjour@insa-lyon.fr**
ScSo	**ScSo*** **https://edsciencessociales.universite-lyon.fr** Sec. : Mélina FAVETON INSA : J.Y. TOUSSAINT Tél : 04.78.69.77.79 melina.faveton@univ-lyon2.fr	**M. Christian MONTES** Université Lumière Lyon 2 86 Rue Pasteur 69365 Lyon CEDEX 07 **christian.montes@univ-lyon2.fr**

*ScSo : Histoire, Géographie, Aménagement, Urbanisme, Archéologie, Science politique, Sociologie, Anthropologie

Table des matières

PRODUCTION SCIENTIFIQUE

Article en revue à comité de lecture

Camille Banc, Mathieu Gautier, Denise Blanc-Biscarat, Maria Lupsea-Toader, Rémi Marsac, Rémy Gourdon. Influence of pH on the release of colloidal and dissolved organic matter from Vertical Flow Constructed Wetland surface sludge deposits. *Chemical Engineering Journal*, Elsevier, 2021, 418, pp.129353. ⟨10.1016/j.cej.2021.129353⟩.

Camila Maria Trein, Camille Banc, Kévin Maciejewski, Amanda de Moraes Motta, Rémy Gourdon, Pascal Molle, Mathieu Gautier, Marcos von Sperling. French vertical flow treatment wetlands in a subtropical climate: Characterization of the organic deposit layer and comparison with systems in France. *Science of the Total Environment*, Elsevier, 2020, 742, pp.140608. ⟨10.1016/j.scitotenv.2020.140608⟩.

Communications orales

Camila Maria Trein, Camille Banc, Kévin Maciejewski, Mathieu Gautier, Marcos von Sperling. Caracterização da fração orgânica da camada de depósito de lodo na primeira etapa de um Sistema Francês em operação no Brasil. *V Conferência Panamericana de Sistemas Wetlands para Tratamento e Melhoramento da Qualidade da Água / 5º Simpósio Brasileiro sobre Aplicação de Wetlands Construídos no Tratamento de Águas Residuárias*, Apr 2021, Florianopolis, Brazil.

Camille Banc, Denise Blanc, Mathieu Gautier, Maria Lupsea-Toader, Rémy Gourdon. La modélisation géochimique comme outil d'aide à la décision pour les gestionnaires. *Association scientifique et technique pour l'eau et l'environnement*, Sep 2020, Lyon, France. 2020.

Camille Banc, Mathieu Gautier, Denise Blanc, Maria Lupsea-Toader, Remi Marsac. Release of Metals from Wastewater Residue at Different pHs: An Ultrafiltration Investigation. *Goldschmidt 2020, Geochemical Society*, Jun 2020, online, United States. pp.118-118, ⟨10.46427/gold2020.118⟩.

Camille Banc, Mathieu Gautier, Denise Blanc, Maria Lupsea-Toader, Remi Marsac, Rémy Gourdon. Influence of pH on the formation of organic colloïds and the associated release of various elements from surface sludge deposits of vertical flow constructed wetlands. *EGU2020: Sharing Geoscience Online*, May 2020, Vienna, Austria.

Kévin Maciejewski, Mathieu Gautier, Camille Banc, Boram Kim, Manon Kania, Rémy Gourdon. Récupérer les ressources de l'eau par traitement par filtres plantés de roseaux. *CODEGEPRA - SFGP Sud-Est*, Nov 2019, Lyon, France.

Kévin Maciejewski, Mathieu Gautier, Manon Kania, Camille Banc, Philippe Michel, Pascal Molle, Rémy Gourdon. Challenges in nitrogen removal in french vertical flow constructed wetlands. *WETPOL 2019*, Jun 2019, Aarhus, Denmark.

Camille Banc, Denise Blanc, Mathieu Gautier, Maria Lupsea-Toader, Rémy Gourdon. Modelling of pollutants partition between soluble and particulate organic matter in French Vertical Flow Constructed Wetlands sludge deposits. *AMARE 2019 : International conference on Applications of Multi-scale Approaches in Environmental chemistry*, Apr 2019, Rennes, France.

Camille Banc, Maria Lupsea-Toader, Mathieu Gautier, Denise Blanc, Rémy Gourdon. Geochemical modelling of a sludge deposit: first results. *16th IWA International Conference on Wetland Systems for Water Pollution Control (ICWS)*, Sep 2018, Valencia, Spain.

Camille Banc, Mathieu Gautier, Maria Lupsea-Toader, Denise Blanc, Rémy Gourdon. Modélisation géochimique d'un dépôt organique : premiers résultats. *FROG4 (4ème Réunion des Géochimistes Organiciens Français)*, Jul 2018, Lyon, France.

Communications par affiches

Kévin Maciejewski, Mathieu Gautier, Camille Banc, Boram Kim, Manon Kania, Rémy Gourdon. Récupérer les ressources de l'eau par traitement par filtres plantés de roseaux. *CODEGEPRA - SFGP Sud-Est*, Nov 2019, Lyon, France.

Kévin Maciejewski, Mathieu Gautier, Camille Banc, Boram Kim, Manon Kania, Rémy Gourdon. Récupérer les ressources de l'eau par traitement par filtres plantés de roseaux : Du déchet à la ressource. *SFGP 2019*, Oct 2019, Nantes, France.

Camille Banc, Mathieu Gautier, Denise Blanc, Maria Lupsea-Toader, Rémy Gourdon. Modelling of trace metals behaviour capacity into a high organic sludge deposit. *19th European Meeting on Environmental Chemistry (EMEC 19)*, Dec 2018, Royat, France.

SIGLES ET ABREVIATIONS

CW	Constructed wetlands
DOC	Dissolved Organic carbon
FA (AF)	Fulvic acids (Acides fulviques)
HA	Humic acids (Acides humiques)
HAO	Hydrous aluminium oxides
HFO	Hydrous ferric oxides
HS(SH)	Humic substance (Substances humiques)
IB (BI)	Infiltration bassin (bassin d'infiltration)
IBS	Infiltration basin sediment
LOC	Large organic colloids
OC	Organic carbon
OM	Organic matter
SD	Sludge deposit
SOC	Small organic colloids
SOM	Solid organic matter
tDOC	Truly dissolved organic carbon
TOC	Total organic carbon
VFCW	Verticlal flow constructed wetlands
MW	Molecular weight
BOD	Biological oxygen demand
FPR	Filtre planté de roseaux
SUVA	Specific ultraviolet absorbance
SC	Small colloids
LC	Large colloids

RESUME

Dans les systèmes de traitement des eaux qualifiés de « solutions fondées sur la nature » (*i.e.* filtres plantés de roseaux et bassin d'infiltration), la rétention des particules en suspensions peut conduire à la formation d'une couche de dépôts de surface. Tant du point de vue de sa capacité à interagir avec les polluants lors de sa présence sur l'unité de traitement, que lors de sa réutilisation notamment en épandage après curage, la spéciation des éléments au sein de ces dépôts et les mécanismes de remobilisation des polluants interrogent. Après évacuation, ces dépôts peuvent constituer une ressource intéressante notamment en agriculture en raison de la quantité de nutriments et de matière organique qu'ils contiennent. Ce travail avait pour objectifs de mieux décrire l'assemblage organo-minéral de ces matrices et de fournir une meilleure compréhension de l'influence des phases colloïdales sur la remobilisation d'éléments majeurs et traces afin de pouvoir fournir des modèles de prédictions, à la fois quantitatif et qualitatif, sur la remobilisation de polluants des dépôts soumis à des variations de pH.

Un dépôt de surface de filtre planté de roseaux à écoulement vertical a été soumis à différentes conditions de pH et les phases colloïdales ont été étudiées. La remobilisation de phases colloïdales organiques s'est montrée particulièrement sensible aux variations de pH. Dans la gamme de pH acide, de petites molécules organiques (< 3 kDa) sont majoritairement remobilisées des dépôts. Pour des pH proches de la neutralité et alcalins, les gros colloïdes organiques (> 30 kDa) prévalent en solutions. Ce relargage de matière organique semble favoriser la remobilisation d'oxydes de fer et d'aluminium au sein de colloïdes organo-minéraux. La nature et la quantité des phases colloïdales remobilisées exercent une large influence sur le relargage d'éléments majeurs et traces depuis les dépôts de filtre planté de roseaux. Cependant, l'affinité des éléments pour ces phases colloïdales est aussi contrôlée par la classe chimique de l'élément considéré, son état d'oxydation ainsi que le pH de la solution.

L'utilisation de ces données expérimentales a permis le développement et la calibration d'un modèle géochimique multi-surfacique capable de reproduire la spéciation d'une large gamme d'éléments (Fe, Al, P, Ca, Mg, Cu, Cd, Cr, Zn, Pb, As) contenue au sein d'une boue de filtre planté de roseaux et ainsi de reproduire le relargage de ces éléments. De par la concentration importante en matière organique mesurée dans la boue et leur importance dans le relargage et la spéciation des éléments, la modélisation de la complexation des métaux sur la matière organique par WHAM-ModelVII a fait l'objet d'un développement particulier. Les essais de modélisation combinés aux résultats d'ultrafiltrations ont permis l'obtention d'un ratio de matière organique active permettant d'améliorer la prédiction des concentrations en éléments. Afin d'évaluer la robustesse de la méthodologie

employée sur cette première boue, la stratégie de modélisation a été appliquée à d'autres échantillons (*i.e* une deuxième boue de filtre planté de roseaux et deux sédiments de bassin d'infiltration). Les modèles multisurfaciques développés dans cette thèse ont tous montré leur efficacité à calculer le relargage de nombreux éléments quel que soit les conditions de pH et malgré des concentrations initiales en élément majeurs et traces très variables. Les informations fournies par ces travaux se sont avérées fondamentales dans la compréhension des risques associés notamment au relargage d'éléments traces métalliques. A terme ces modèles pourraient donc faire partie du panel d'outil d'aide à la décision à disposition des gestionnaires de ces dépôts.

Mots-clefs : solution fondée sur la nature, métaux traces, nutriments, spéciation, distribution phase solide et liquide, évaluation du risque

ABSTRACT

In water treatment systems described as "nature-based solutions" (i.e. constructed wetlands and infiltration basins), the retention of suspended solids can lead to the formation of a surface deposit layer. Both from the point of view of its capacity to interact with the pollutants during its presence on the treatment unit, and during its reuse, notably in land application after curing, pollutants speciation within the deposits and their prossess of remobilization are questioned. After removal, these deposits constitute an interesting resource, particularly in agriculture, due to the quantity of nutrients and organic matter they contain. The objectives of this work was to better describe the organo-mineral assemblage of these deposits and to provide a better understanding of the influence of colloidal phases on the remobilization of major and trace elements in order to be able to provide predictive models, both quantitative and qualitative, on the remobilization of pollutants from deposits subjected to pH variations.

A vertical flow constructed wetland sludge deposit was subjected to different pH conditions and the colloidal phases were studied. Remobilization of organic colloidal phases was found to be particularly sensitive to pH changes. In the acidic pH range, small organic molecules (<3 kDa) are predominantly remobilized from the deposits. For near-neutral and alkaline pH, large organic colloids (>30 kDa) prevail in solution. This release of organic matter seems to favor the remobilization of iron and aluminum oxides within organo-mineral colloids. The nature and quantity of the remobilized colloidal phases have a large influence on the release of major and trace elements from the constructed wetland's sludge deposits. However, the affinity of the elements for these colloidal phases is also controlled by the chemical class of the element considered, its oxidation state and the pH of the solution.

The use of these experimental data allowed the development and calibration of a multi-surface geochemical model able to reproduce the release and speciation of a wide range of elements (Fe, Al, P, Ca, Mg, Cu, Cd, Cr, Zn, Pb, As) retained within a reed filter sludge. Due to the high concentration of organic matter measured in the sludge and their importance in the release and speciation of elements, the modeling of metal complexation on organic matter by WHAM-ModelVII has been the subject of numerous experiments. The modeling tests combined with the ultrafiltration results allowed to obtain a ratio of active organic matter allowing to improve the prediction of the elemental concentrations. In order to evaluate the robustness of the methodology used on this first sludge, the modeling strategy was applied to other samples (i.e. a second constructed wetland sludge and two infiltration basin sediments). The multisurface models developed in this thesis have all shown their efficiency in calculating the release of many elements whatever the pH conditions and despite very variable initial concentrations of major and trace elements. The information provided by this thesis have been

fundamental in understanding the risks associated with the emission of trace metals in particular. In time these models could therefore be part of the decision supporting tools available to managers of these solid deposits.

Keywords: nature-based solution, trace metals, nutrients, organo-mineral colloids, speciation, solid-solution partitioning, risks assessment

INTRODUCTION GENERALE

Naturellement présents dans notre environnement, les éléments traces métalliques, métalloïdes et nutriments (azote et phosphore) sont la trace du passé géologique. Cependant, certaines activités humaines comme la combustion du pétrole ou encore l'activité métallurgique et minière viennent bousculer la répartition, mais aussi la spéciation de ces éléments au sein des écosystèmes (Nriagu and Pacyna, 1988). Pouvant être émis dans l'atmosphère, dans les eaux superficielles ou de surfaces ces éléments détériorent la qualité des sols, des eaux et des écosystèmes dans leurs ensembles. Le rejet de 20 millions de tonnes de « boues rouges » industrielles entre 1966 et 2016 dans le parc naturel régional des calanques de la mer méditerranée est un exemple récent de scandale environnemental et sanitaire lié à la pollution par les éléments traces métalliques (Juanals, 2021; Pagano et al., 2002). Ces « boues rouges » constituent le principal déchet produit lors de l'extraction chimique de l'alumine à partir de Bauxite. Leur teneur élevée en oxides de fer leur confère un fort pouvoir complexant pour les métaux traces comme le zinc ou encore le plomb (Santona et al., 2006) à l'origine de la pollution des milieux récepteurs en métaux trace. La récupération, le traitement des eaux usées (domestiques et industrielles) et de ruissellement permettent de limiter les rejets dans l'environnement mais peuvent engendrer la création de boue résiduaire, encore appelée dépôt, potentiellement chargée en nutriments, en éléments traces métalliques et en métalloïdes.

La majeure proportion de ces contaminants se trouve dans la fraction solide des dépôts, inaccessible pour la plupart des organismes vivants (Semple et al., 2000). Mais leur remobilisation dans la solution du dépôt pourrait augmenter leur biodisponibilité et leur potentiel transfert vers les eaux de surface et souterraine (de Vries et al., 2007; Semple et al., 2000). La meilleure compréhension des mécanismes de remobilisation et la spéciation des éléments chimiques contenues dans ces dépôts est donc un enjeu important pour permettre une bonne appréciation de leurs risques environnementaux et sanitaires (de Vries et al., 2007; Smolders et al., 2009). Ces connaissances sont d'autant plus importantes que les dépôts se formant à la surface de solutions de traitement fondées sur la nature sont régulièrement soumis à l'arrivé de nouvelles eaux aux caractéristiques chimiques pouvant varier (*i.e.* pH, force ionique). Les risques de remobilisation des polluants stockés dans la phase solide, et donc la pollution des zones de rejets, existent donc. De même, plus de 60 % des dépôts issus de l'ensemble de la filière du traitement des eaux usées sont réutilisés en agriculture (Agence de la transition écologique, 2016). La réutilisation de ces boues s'inscrit dans un contexte agricole récent de pression sur la ressource et d'augmentation importante du prix des amendements organiques, des engrais organiques azotés et phosphatés nécessitant plus que jamais la réutilisation des ressources déjà disponibles sur le territoire. La nécessité de renforcer la compréhension de l'impact de l'ajout de ces dépôts sur le sol, ses microorganismes et ses plantes est aussi l'objet de la mise en place d'une nouvelle réglementation d'épandage rentrant en vigueur à partir du 1er Juillet 2021 (article 86 de la

loi AGEC). Celle-ci a pour objectif d'harmoniser la réglementation sur les épandages de matières fertilisantes en venant apporter de nouveaux seuils de pollutions aux éléments traces métalliques et en ajoutant des tests d'écotoxicité à l'arrêté de 1998 précisant les modalités d'épandage des boues d'épuration. Finalement, c'est donc à ce double titre que l'amélioration de la description de l'émission de polluants depuis les boues de traitement des eaux usées et eaux de ruissellement est importante.

De nombreux chercheurs ont déjà étudié des milieux poreux naturels avec pour objectif final de mieux contrôler et mieux prévoir la remobilisation de ces polluants depuis la fraction solide. C'est ainsi que le rôle prépondérant de la remobilisation des colloïdes, organiques et inorganiques, dans le transfert de polluants a été mis en évidence (Aiken et al., 2011; de Jonge et al., 2004; Pokrovsky and Schott, 2002a; Raudina et al., 2021a; Stolpe et al., 2013). Les colloïdes sont des particules de taille comprise entre 1 µm et 1-3 nm (Aiken et al., 2011) possédant une grande surface spécifique et donc une grande quantité de sites de complexation pour les éléments contenus en solution. L'influence des conditions pédoclimatiques (Bradford et al., 2002; Xu et al., 2019a), biogéochimiques (Grybos et al., 2007a, 2009a; Pédrot et al., 2009a; Xu et al., 2018) et hydrologiques (Durce et al., 2018; C. Wang et al., 2020; Zhuang et al., 2009) sur la remobilisation, la nature et la capacité de complexation de ces colloïdes a donc fait l'objet de plusieurs études de caractérisation et de modélisation.

Bien que plusieurs études (Clozel et al., 2006a; Drapeau et al., 2017; Kania et al., 2019; Kim et al., 2016) se soient intéressées à la remobilisation de polluants depuis ces dépôts solides, celles-ci apportent des informations essentiellement quantitatives. A l'instar des études effectuées en milieu naturel, il est nécessaire d'améliorer notre compréhension de la spéciation des polluants en phase solide et liquide, de la nature, de la complexité des colloïdes remobilisés et de l'influence des facteurs environnementaux sur leur remobilisation afin de pouvoir offrir une vision plus globale sur les mécanismes de rétention et de remobilisation des polluants aux gestionnaires de ces dépôts.

Ce travail a été effectué au sein du laboratoire Déchets Eaux Environnement et Pollutions (DEEP) de l'INSA de Lyon qui se focalise particulièrement sur la compréhension des mécanismes physiques et biogéochimiques à l'origine de la rétention des polluants au sein de systèmes fondés sur la nature conçus pour le traitement des eaux usées et de ruissellement. L'étude de la remobilisation des contaminants inorganiques contenus au sein de dépôts va d'abord passer par l'obtention de données relatives à l'influence du pH sur le relargage de ces contaminants et des phases colloïdales afin de comprendre les mécanismes de remobilisation. Ces données vont ensuite permettre d'ajuster, calibrer des modèles de spéciations géochimiques permettant d'obtenir des informations fondamentales sur la spéciation et donc sur la mobilité et la toxicité d'un relargage.

Références :

Aiken, G.R., Hsu-Kim, H., Ryan, J.N., 2011. Influence of Dissolved Organic Matter on the Environmental Fate of Metals, Nanoparticles, and Colloids. Environ. Sci. Technol. 45, 3196–3201. https://doi.org/10.1021/es103992s

Bradford, S.A., Yates, S.R., Bettahar, M., Simunek, J., 2002. Physical factors affecting the transport and fate of colloids in saturated porous media: FACTORS AFFECTING THE FATE OF COLLOIDS. Water Resour. Res. 38, 63-1-63–12. https://doi.org/10.1029/2002WR001340

Clozel, B., Ruban, V., Durand, C., Conil, P., 2006. Origin and mobility of heavy metals in contaminated sediments from retention and infiltration ponds. Applied Geochemistry 21, 1781–1798. https://doi.org/10.1016/j.apgeochem.2006.06.017

de Jonge, L.W., Kjaergaard, C., Moldrup, P., 2004. Colloids and Colloid-Facilitated Transport of Contaminants in Soils. Vadose Zone Journal 3, 321–325. https://doi.org/10.2136/vzj2004.0321

de Vries, W., Lofts, S., Tipping, E., Meili, M., Groenenberg, J.E., Schütze, G., 2007. Impact of Soil Properties on Critical Concentrations of Cadmium, Lead, Copper, Zinc, and Mercury in Soil and Soil Solution in View of Ecotoxicological Effects, in: Reviews of Environmental Contamination and Toxicology, Reviews of Environmental Contamination and Toxicology. Springer, New York, NY, pp. 47–89. https://doi.org/10.1007/978-0-387-69163-3_3

Drapeau, C., Delolme, C., Chatain, V., Gautier, M., Blanc, D., Benzaazoua, M., Lassabatère, L., 2017. Spatial and Temporal Stability of Major and Trace Element Leaching in Urban Stormwater Sediments. Open Journal of Soil Science 07, 347. https://doi.org/10.4236/ojss.2017.711025

Durce, D., Aertsens, M., Jacques, D., Maes, N., Van Gompel, M., 2018. Transport of dissolved organic matter in Boom Clay: Size effects. Journal of Contaminant Hydrology 208, 27–34. https://doi.org/10.1016/j.jconhyd.2017.12.004

Grybos, M., Davranche, M., Gruau, G., Petitjean, P., 2007. Is trace metal release in wetland soils controlled by organic matter mobility or Fe-oxyhydroxides reduction? Journal of Colloid and Interface Science 314, 490–501. https://doi.org/10.1016/j.jcis.2007.04.062

Grybos, M., Davranche, M., Gruau, G., Petitjean, P., Pédrot, M., 2009. Increasing pH drives organic matter solubilization from wetland soils under reducing conditions. Geoderma 154, 13–19. https://doi.org/10.1016/j.geoderma.2009.09.001

Juanals, B., 2021. La crise environnementale et sanitaire des « boues rouges » dans la presse locale en Provence. Anthropologie & Santé. Revue internationale francophone d'anthropologie de la santé. https://doi.org/10.4000/anthropologiesante.9148

Kania, Gautier, M., Blanc, D., Lupsea-Toader, M., Merlot, L., Quaresima, M.-C., Gourdon, R., 2019. Leaching behavior of major and trace elements from sludge deposits of a French vertical flow constructed wetland. Science of The Total Environment 649, 544–553. https://doi.org/10.1016/j.scitotenv.2018.08.364

Kim, B., Gautier, M., Simidoff, A., Sanglar, C., Chatain, V., Michel, P., Gourdon, R., 2016. pH and Eh effects on phosphorus fate in constructed wetland's sludge surface deposit. Journal of Environmental Management 183, 175–181. https://doi.org/10.1016/j.jenvman.2016.08.064

Nriagu, J.O., Pacyna, J.M., 1988. Quantitative assessment of worldwide contamination of air, water and soils by trace metals. Nature 333, 134–139. https://doi.org/10.1038/333134a0

Pagano, G., Biase, A. de, Iaccarino, M., Meric, S., Petruzzelli, D., Tünay, O., Warnau, M., Trieff, N.M., 2002. Bauxite manufacturing residues from Gardanne (France) and Portovesme (Italy) exert different patterns of pollution and toxicity to sea urchin embryos. Environmental Toxicology and Chemistry 21, 1272–1278. https://doi.org/10.1002/etc.5620210623

Pédrot, M., Dia, A., Davranche, M., 2009. Double pH control on humic substance-borne trace elements distribution in soil waters as inferred from ultrafiltration. Journal of Colloid and Interface Science 339, 390–403. https://doi.org/10.1016/j.jcis.2009.07.046

Pokrovsky, O.S., Schott, J., 2002. Iron colloids/organic matter associated transport of major and trace elements in small boreal rivers and their estuaries (NW Russia). Chemical Geology 190, 141–179. https://doi.org/10.1016/S0009-2541(02)00115-8

Raudina, T.V., Loiko, S.V., Kuzmina, D.M., Shirokova, L.S., Kulizhskiy, S.P., Golovatskaya, E.A., Pokrovsky, O.S., 2021. Colloidal organic carbon and trace elements in peat porewaters across a permafrost gradient in Western Siberia. Geoderma 390, 114971. https://doi.org/10.1016/j.geoderma.2021.114971

Santona, L., Castaldi, P., Melis, P., 2006. Evaluation of the interaction mechanisms between red muds and heavy metals. Journal of Hazardous Materials 136, 324–329. https://doi.org/10.1016/j.jhazmat.2005.12.022

Semple, K., Doick, K.J., Jones, K., Burauel, P., Craven, A., Harms, H., 2000. Defining BIOAVAILABILITY and Bioaccessibility of Contaminated Soil and Sediment is Complicated. Stationery Office, London.

Smolders, E., Oorts, K., Sprang, P.V., Schoeters, I., Janssen, C.R., McGrath, S.P., Mclaughlin, M.J., 2009. Toxicity of Trace Metals in Soil as Affected by Soil Type and Aging After Contamination: Using Calibrated Bioavailability Models to Set Ecological Soil Standards. Environmental Toxicology and Chemistry 28, 1633–1642. https://doi.org/10.1897/08-592.1

Stolpe, B., Guo, L., Shiller, A.M., Aiken, G.R., 2013. Abundance, size distributions and trace-element binding of organic and iron-rich nanocolloids in Alaskan rivers, as revealed by field-flow fractionation and ICP-MS. Geochimica et Cosmochimica Acta 105, 221–239. https://doi.org/10.1016/j.gca.2012.11.018

Wang, C., Wang, R., Huo, Z., Xie, E., Dahlke, H.E., 2020. Colloid transport through soil and other porous media under transient flow conditions—A review. WIREs Water 7, e1439. https://doi.org/10.1002/wat2.1439

Xu, H., Ji, L., Kong, M., Jiang, H., Chen, J., 2019. Molecular weight-dependent adsorption fractionation of natural organic matter on ferrihydrite colloids in aquatic environment. Chemical Engineering Journal 363, 356–364. https://doi.org/10.1016/j.cej.2019.01.154

Xu, H., Lin, H., Jiang, H., Guo, L., 2018. Dynamic molecular size transformation of aquatic colloidal organic matter as a function of pH and cations. Water Research 144, 543–552. https://doi.org/10.1016/j.watres.2018.07.075

Zhuang, J., Tyner, J.S., Perfect, E., 2009. Colloid transport and remobilization in porous media during infiltration and drainage. Journal of Hydrology 377, 112–119. https://doi.org/10.1016/j.jhydrol.2009.08.011

CHAPITRE I. SYNTHESE BIBLIOGRAPHIQUE

La matière organique joue un rôle prépondérant dans la dynamique des métaux et métalloïdes des sols/sédiments (Raudina et al., 2021a; M. Wang et al., 2020; Xu et al., 2019c). Celle-ci impacte notamment largement la spéciation et donc la mobilité et la biodisponibilité de ces éléments pouvant constituer une menace pour nos environnements. La nature des mécanismes physico-chimique intervenant à l'interface liquide/solide entre la matière organique et ces polluants peuvent être particulièrement complexe. Les principales intéractions pouvant survenir à l'interface liquide/solide ont par exemple été largement décrites par Manceau et al. (2002). Un des enjeux lié aux dépôts, résidus du traitement des eaux, concerne d'ailleurs la prise en compte des interactions entre la matière organique et les polluants au sein de ces milieux complexes (Cross et al., 2021). C'est pourquoi la première partie de cette synthèse bibliographique s'intéressera à la matière organique, à sa structure, sa réactivité et sa prise en compte au sein de modèles de prédictions géochimiques. Dans un deuxième temps, les deux structures de traitement des eaux fondées sur la nature dont les dépôts ont été étudiés seront décrites (*i.e* filtre planté de roseaux et bassin d'infiltration). Les mécanismes de rétention à l'origine de la création de ces dépôts et les caractéristiques physico-chimique de ces derniers seront aussi présentés.

I. La matière organique

1.1 Généralités

La matière organique est produite par l'ensemble des organismes vivant de la planète. Dans la suite de ce document, le terme « matière organique naturelle » désignera l'ensemble des molécules organiques issues de la décomposition des plantes, des animaux, ainsi que les molécules provenant du métabolisme microbien. Les stocks de matière organique ou plus spécifiquement de carbone organique dans un sol sont temporellement et spatialement variables (Weissert et al., 2016). La mesure du stock de carbone organique dans les sols à l'échelle de la planète est complexe mais estimé à 2000 milliards de tonne de carbone dans les premiers 200 cm du sol (Batjes, 2016). Les zones humides et les tourbières sont les principaux puits de carbone organique dans les couches superficielles de terre. Les tourbières, caractérisées par une accumulation de matière végétale inerte en décomposition et des conditions de saturation en eau permanente (FAO, 2017; Tanneberger et al., 2017), concentrent plus de 30 % du carbone organique du sol sur seulement 3 % de la surface émergée des terres (FAO, 2017). Le carbone organique joue un rôle important sur la qualité physique, chimique et biologique des sols, ces trois paramètres étant fondamentaux dans le maintien de la fertilité des sols. Mais la fertilité des sols n'est pas le seul enjeu. En effet, les matières organiques sont également à la base de nombreuses fonctions écosystémiques des sols comme l'épuration des eaux et la régulation du climat au travers de la séquestration du carbone (FAO, 2017).

En 1978, Hayes et Swift ont considéré une nouvelle fraction de molécules au sein des matières organiques naturelles : les molécules organiques résultant de la transformation chimique ou microbienne de débris organiques ainsi appelée processus d'humification produisant *in fine* les substances humiques (SH). Plus tard, Stevenson en 1994, différenciera aussi les molécules organiques du sol en fraction active, regroupant les molécules organiques labiles, biodisponibles n'ayant pas subi de processus d'humification et en fraction stable regroupant les substances humiques (SH). Retrouvées dans des milieux poreux sous forme solide ou dissoute et dans des eaux naturelles, les SH englobent plus de 80 % du carbone organique disponible dans nos écosystèmes (Stevenson, 1994).

1.2 Caractéristiques des substances humiques

L'influence des débris organiques à l'origine des SH, ainsi que l'impact des conditions pédoclimatiques sur ces mêmes SH complexifie la caractérisation de ces molécules. Face à tant d'hétérogénéité, Stevenson (1994) voit en ces SH des molécules polymériques synthétisées *de novo*, polyfonctionnelles et de haut poids moléculaire (fig 1 a). Ces structures sont hypothétiquement composées de chaines aliphatiques et de groupements aromatiques substitués par des groupements fonctionnels principalement carboxyliques et phénoliques. D'importantes différences de solubilité dans la famille des SH amènent les scientifiques à considérer l'existence de trois structures différentes : (i) les acides humiques (AH) solubles en conditions alcalines, (ii) les acides fulviques (AF) solubles dans l'eau quelles que soient les conditions de pH et (iii) les humines insolubles dans l'eau. Comparativement aux AH, les AF seraient plus aliphatiques, avec un nombre de groupes aromatiques réduit (Clapp et al., 2005; Stevenson, 1994). Cette vision macromoléculaire des substances humiques a été supportée pendant plusieurs années par plusieurs théories s'appuyant sur des évidences scientifiques (Kononova, 2013; Schulten and Schnitzer, 1993; Swift, 1999). La similarité entre les analyses élémentaires et les dosages des groupements fonctionnels de SH provenant de sols aux qualités différentes ont rendu évidente l'existence de ces structures macromoléculaires prédéfinies (Kononova, 2013). Les principales théories sur la formation et l'origine de SH restent cohérentes avec la vision macromoléculaire établie. Parmi celles-ci, la théorie de la lignine (Waksman, 1931), la théorie des polyphénols (Flaig et al., 1975) et la théorie de la condensation amine-sucre (Maillard, 1913) font intervenir des résidus de la dégradation de végétaux et d'animaux, ainsi que des procédés de transformations biologiques dans la polymérisation des substances humiques et leur synthèse *de novo.*

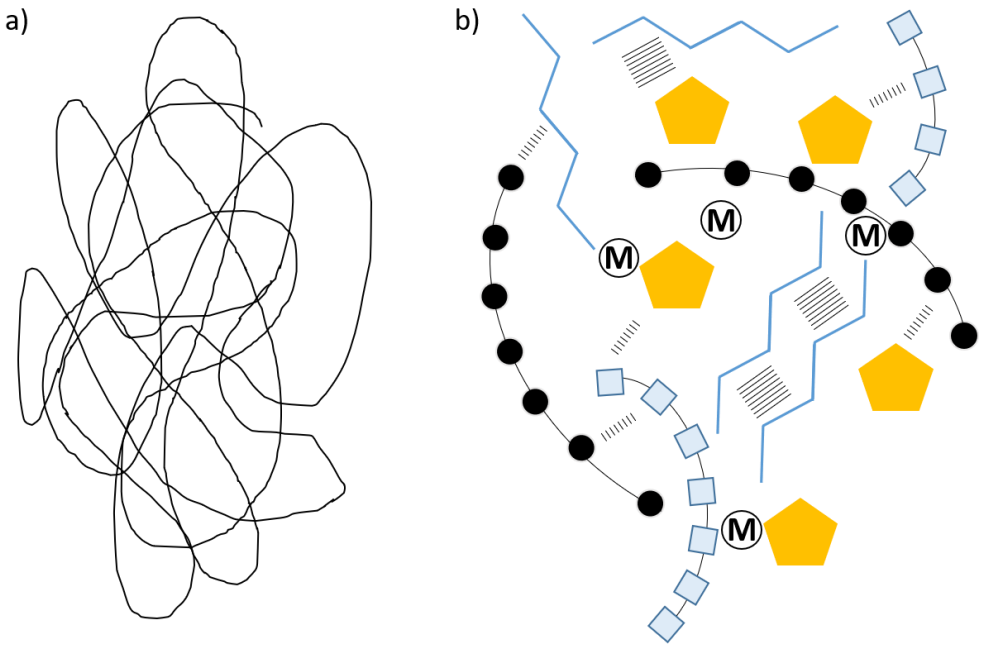

Fig.1. Description schématique de la structure moléculaire des substances humiques selon, a) la théorie macromoléculaire (Stevenson, 1994) ou, b) la théorie supramoléculaire (adaptée de Simpson et al. 2002). Les structures supramoléculaires sont le fruit d'associations entre molécules organiques de faible poids moléculaire (<1-2 kDa). Parmi ces composés, on retrouve des polysaccharides (sphères noires), des polypeptides (carrés bleus), des chaines aliphatiques (traits bleus) et des groupement aromatiques (hexagone orange). Ces composés s'assemblent à l'aide de différentes liaisons faibles comme les ponts cationiques (M), des interactions hydrophobes (grands tirets) et liaisons hydrogène (petits tirets).

Avec le développement des techniques analytiques comme la chromatographie à exclusion stérique ou la résonnance magnétique nucléaire, une description plus précise de la structure chimique des SH est proposée par d'autres scientifiques (Pédrot et al., 2010; Piccolo, 2001; Simpson et al., 2002). Les SH seraient des entités supramoléculaires formées par l'assemblage de différentes molécules organiques de faible poids moléculaire (< 1 kDa) comme présenté à la Fig. 1b. Ces petits composés organiques, issus de la dégradation des biopolymères constitutifs de la matière vivante, s'assemblent en structure métastable par une combinaison de liaisons hydrogène, de van der Waals ou électrostatiques (ponts cationiques)(Piccolo, 2001). L'organisation de ces structures supramoléculaires et leur réactivité sont largement influencées par les conditions chimiques des milieux dans lesquels elles évoluent (Pédrot et al., 2010). Ainsi la baisse du pH favorise les liaisons hydrogène quand une augmentation de la concentration en métaux peut favoriser la formation de ponts cationiques. La stabilité dans le temps des SH ne s'explique plus uniquement par leur structure polymérique composée de lignine récalcitrante, mais par l'augmentation de la concentration en composés hydrophobes et groupements fonctionnels favorisant les interactions avec les particules minérales solides (Gu et al., 1995; Specht et al., 2000). Ces complexes organo-minéraux réduisent la biodisponibilité et augmentent la longévité des substances humiques dans leurs écosystèmes. En reconsidérant les substances

humiques comme des structures supramoléculaires, Piccolo a réactualisé en 2001 la définition des acides humiques et fulviques. Les AF sont donc principalement composés d'associations entre molécules hydrophiles, dont les groupements fonctionnels acides sont suffisamment nombreux et forts afin de permettre la dispersion des AF à n'importe quel pH. Les AH résultent d'associations entre composés principalement hydrophobes (chaine aliphatique, acide gras, composé aromatique) dont les forces hydrophobes permettent de stabiliser la structure supramoléculaire et, ainsi, éviter leur dissolution dans l'eau. Comparativement aux AF, leur solubilité est donc faible aux pH acides, du fait de la forte hydrophobicité et de la faible déprotonation des groupements acides qui les composent. De plus, aux pH acides, l'augmentation de la concentration en ions H^+ permet l'augmentation du nombre de liaisons hydrogène aboutissant à l'augmentation de la taille moléculaire des AH et à leur coagulation.

Les deux visions précédemment décrites ne sont pourtant pas totalement antagonistes. Certaines études basées sur des techniques d'ultrafiltration des SH suggèrent la co-existence de ces deux formes (macromolécules et entités supramoléculaires) de substances humiques (Baigorri et al., 2007; Pédrot et al., 2010), dont la prévalence fluctue selon les conditions chimiques dans lesquelles elles évoluent.

1.3 Influence des conditions chimiques du milieu sur la structure des SH et leur pouvoir complexant

a. Substances humiques en solution

Comme évoqué précédemment, la structure des matières organiques en solution est contrôlée par les conditions chimiques dans lesquelles elles évoluent. En d'autres termes, ces molécules ont des structures dynamiques qui évoluent avec les conditions chimiques du milieu (Chen et al., 2007; Xu et al., 2018). La compréhension de ces phénomènes est déterminante pour apprécier la réactivité de ces structures moléculaires et supramoléculaires et ainsi mieux décrire leurs interactions avec les polluants (Pédrot et al., 2010; Xu et al., 2019a, 2018).

Le pH semble largement impacter la structure des matières organiques en solution. Pédrot et al. (2010) ont pu mettre en évidence la dissolution des structures comprises entre 5 et 30 kDa, soumises à des pH inférieurs à 6, en de petites molécules organiques inférieures à 2 kDa. Les auteurs ont attribué ce phénomène à la perturbation de la structure supramoléculaire, résultant de l'augmentation des liaisons hydrogène dans la structure. Bien que de petit poids moléculaire, ces molécules organiques gardent la capacité de complexer des cations et notamment les métaux de transitions divalents, comme le cuivre (Pokrovsky et al., 2005; Worms et al., 2019). Cependant, d'après Xu et al. (2018),

l'impact des conditions de pH sur la structure moléculaire des colloïdes organiques est largement dépendant de l'origine des molécules étudiées.

Des études ont pu montrer la faible influence de la force ionique sur la structure supramoléculaire des SH (Baigorri et al., 2007; Pédrot et al., 2010). En revanche, l'augmentation de la concentration en électrolytes dans la solution entraine une contraction des structures macromoléculaires (Baigorri et al., 2007; Durce et al., 2016; Kipton et al., 1992) en réduisant les forces intra et intermoléculaires répulsives. Cette contraction peut aussi s'accompagner par une expulsion des cations compris dans la sphère d'hydratation de ces molécules (Kipton et al., 1992). D'autres études ont pu mettre en évidence l'importance du ratio métal/SH sur le poids moléculaire des SH en solution (Kalinichev et al., 2011; Suteerapataranon et al., 2006). Avec l'augmentation de ce ratio, l'augmentation du nombre de ponts cationiques entre molécules organiques aboutit à l'augmentation du poids moléculaire des SH. *In fine*, ce phénomène peut conduire à la précipitation des molécules organiques.

b. Fractionnement des substances humiques dans un milieu poreux

Au sein des milieux poreux, la complexation des SH aux surfaces minérales constitutives du milieu change la nature des SH retrouvées en solution. Les minéraux sont à la fois responsables de la séquestration des matières organiques dans la fraction solide des sols, mais aussi à l'origine de leur relargage (Avena and Koopal, 1998; Gu et al., 1995). Il existe plusieurs mécanismes contrôlant l'adsorption des SH sur des minéraux (Gu et al., 1995, 1994) : (i) l'attraction électrostatique, (ii) l'échange de ligands, (iii) des liaisons H, (iv) ponts cationiques et (v) les interactions hydrophobes. Mais les paramètres chimiques retrouvés à l'interface solide-liquide, impactent la stabilité des agrégats organo-minéraux et donc la quantité et la qualité des SH en solution (Murphy and Zachara, 1995; You et al., 2006). Plusieurs études ont pu montrer l'affinité entre les surfaces minérales des sols (argiles, oxydes métalliques) et les groupements hydrophobes des substances humiques (El-sayed et al., 2019; Kaiser and Guggenberger, 2000; Meier et al., 1999; Specht et al., 2000; Wiseman and Püttmann, 2006; Xu et al., 2019c). Ces groupements hydrophobes s'accumulent préférentiellement au sein de molécules organiques de haut poids moléculaire (Meier et al., 1999; Piccolo, 2001). Avec l'augmentation des conditions alcalines, les SH et les surfaces minérales se repoussent, conduisant ainsi au relargage de molécules organiques, majoritairement de haut poids moléculaire et hydrophobes. Ce phénomène a déjà été observé sur des solutions de sol provenant de zones humides (Grybos et al., 2009a; Pédrot et al., 2009a), ainsi que sur d'autres types de sols (You et al., 2006). De même, la réduction des oxydes métalliques peut aussi provoquer le relargage des matières organiques qu'ils adsorbent ou enrobent (Bongoua-Devisme et al., 2013; Quantin et al., 2001). Ce phénomène de réduction peut survenir dans des conditions de sursaturation en eaux notamment rencontrées dans

des zones humides. Au contraire, en cas d'acidification d'un milieu poreux, l'augmentation du nombre de liaisons hydrogène entre matière organique et surface minérale, ainsi que l'augmentation de l'hydrophobicité des SH tend à augmenter la stabilité de ces agrégats (Specht et al., 2000), limitant le relargage de matière organique. En revanche, la charge de surface plus importante de certaines petites molécules organiques peut favoriser leur solubilisation (Pédrot et al., 2009a).

1.4 Interaction métaux substances humiques

La sorption des cations métalliques par les matières organiques est un enjeu environnemental important. En effet, ces molécules sont une des sources de mobilité et de transfert de cations métalliques depuis les milieux poreux vers les écosystèmes aquatiques environnants (Li et al., 2019; Raudina et al., 2021a; Shi et al., 2013a). La sorption des cations par ces composés organiques s'est révélée dépendante de plusieurs facteurs dont : (i) les conditions chimiques du milieu comme le pH, les conditions redox et la force ionique (Christl, 2012; Pédrot et al., 2009a; Shaheen et al., 2019), (ii) les caractéristiques physico-chimiques des molécules organiques (Amery et al., 2008; Li et al., 2019; Xu et al., 2019c) et (iii) le type de cation métallique considéré (Pédrot et al., 2008; Pokrovsky et al., 2005).

La capacité de sorption des molécules organiques est essentiellement supportée par ces groupements carboxyliques et phénoliques (Evangelou and Marsi, 2001; Tipping et al., 2011). Des études ont donc dosé ces groupements à l'aide de titration potentiométrique (Plaza et al., 2005; Senesi et al., 2007; Zhou et al., 2005) afin d'évaluer la capacité de complexation des molécules organiques en présence. Plaza et al. 2005, 2006, ont ainsi pu mettre en évidence la baisse de l'affinité des matières organiques solides pour le cuivre dans un sol amendé avec des boues de stations d'épuration comparativement aux matières organiques initialement présentes dans les sols non amendés, conséquence d'une diminution du nombre de groupements carboxyliques et phénoliques. L'aromaticité des molécules est l'un des indicateurs les plus utilisés afin d'appréhender la capacité de sorption des molécules organiques (Amery et al., 2008; Tang et al., 2016; Yang et al., 2015). Amery et al. (2008) ont pu corréler positivement l'aromaticité de la matière organique de 250 solutions de sols naturels à leur capacité à complexer le cuivre. En revanche, dans des milieux plus fortement anthropisés (*e.g.* eaux de surfaces recevant des eaux usées, sols amendés), la capacité de sorption des matières organiques n'est plus corrélée à leur aromaticité (Baken et *al.,* 2011 ; Laurent et *al.,* 2020 ; Matar et *al.,* 2015 ; Kikuchi et *al.,* 2017). Les ligands organiques d'origine anthropique comme les aminopolycarboxylates montrent une faible aromaticité, mais une forte affinité pour le cuivre. D'autres molécules retrouvées dans des eaux de rivières fortement soumises à la pression urbaine, plus hydrophiles et de faible poids moléculaire, sont aussi responsables de la complexation du Cu et du Zn (Matar et al., 2018 ; Louis et *al.,* 2014).

Bien qu'influente, l'impact de la qualité des molécules organiques sur leur capacité de sorption reste moins importante que celle des paramètres de la solution (Fernández-Calviño et al., 2010). En conditions très acide, la protonation des groupements fonctionnels réduit, non seulement, le potentiel de surface des molécules, mais aussi, la quantité de sites disponibles (Tipping et al., 2011), soit, *in fine*, la capacité de sorption des composés organiques (Havelcová et al., 2009). La force ionique de la solution, la composition et la concentration des électrolytes présents dans cette solution influencent aussi la complexation des métaux (Imoto and Yasutaka, 2020; Tipping et al., 2011). Par exemple, l'augmentation de la concentration en électrolyte réduit la capacité de sorption des métaux (Christl, 2012; Christl et al., 2005; Imoto and Yasutaka, 2020; Liu and Gonzalez, 2000) en diminuant notamment le volume de la double couche diffuse et en entrant en compétition pour les sites de liaison organique.

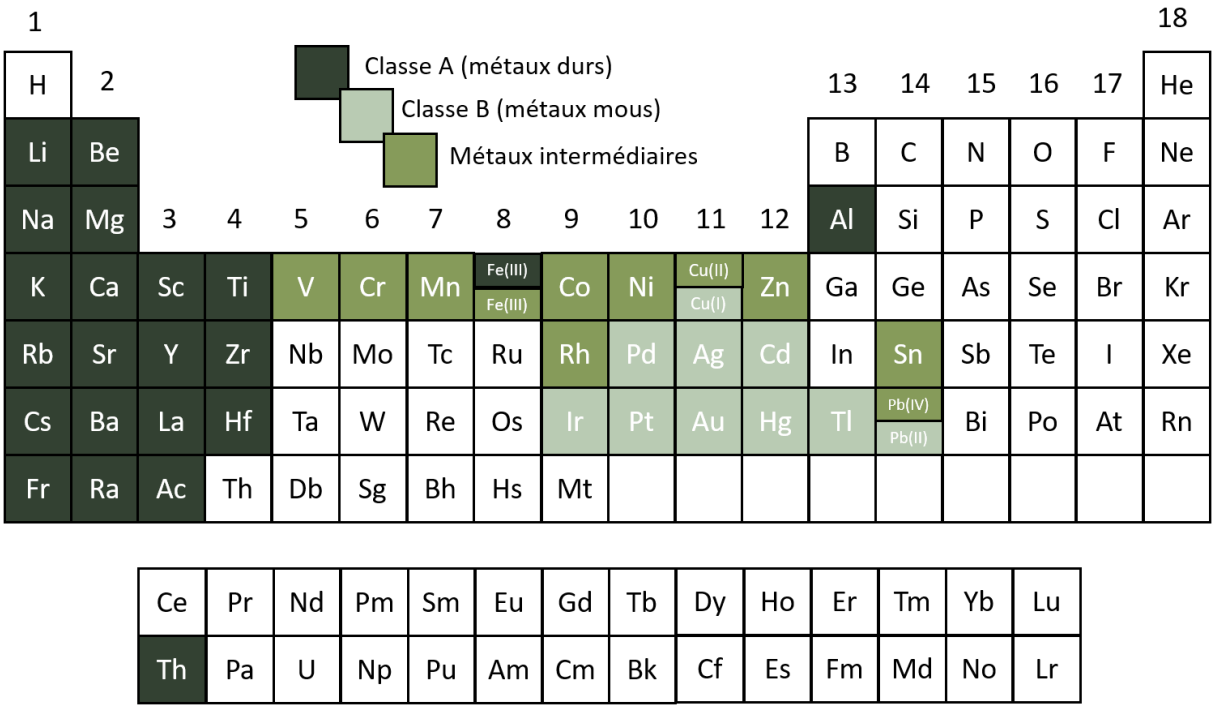

Fig.2. Tableau périodique présentant les différentes classes de métaux décrites par Duffus, (2002) et Nieboer and Richardson, (1980).

Les cations métalliques ne montrent pas tous la même affinité pour les ligands organiques (Pourret et al., 2007a). De nombreuses études (Brezonik et al., 1991; Demey et al., 2018; Pourret et al., 2007a) se réfèrent à la classification des métaux développée par Nieboer et Richardson en 1980 (Fig. 2) afin d'expliquer le comportement de métaux. Cette classification s'appuie sur les propriétés acido-basiques des métaux afin d'établir leur réactivité vis-à-vis de ligands organiques. En effet, la capacité des métaux à accepter des électrons va déterminer leur propension à lier des ligands organiques mais aussi influer sur la nature de ces interactions. La Fig. 2 situe les 3 différentes classes de métaux obtenues par Nieboer et Richardson en 1980 sur le tableau périodique des éléments. La classe A, aussi appelée

« métaux durs », regroupe les éléments non polarisables comme les éléments alcalins et alcalino-terreux. Ces éléments vont principalement interagir électrostatiquement avec des ligands dits « durs » pour former des complexes en sphère externe. Parmi ces ligands durs, ou bases dures, on retrouve des groupements fortement chargés contenant des atomes très électronégatifs, à l'instar des groupements carboxylique et phénolique. La classe B composée des « métaux mous », se lient de manière préférentiellement covalente à des ligands « intermédiaires », comme les groupements contenant de l'azote (amines…) et des ligands « mous », comme les groupements contenant du souffre (thiol, thioéther). Ces groupements sont généralement peu électronégatifs et très polarisables. A la frontière entre ces deux ensembles, on retrouve les « métaux intermédiaires », regroupant des métaux de transition divalents d'intérêt environnemental comme le cobalt ou le cuivre. Ces métaux vont avoir la capacité de former des liaisons fortes avec n'importe quel ligand organique.

De manière générale, les acides forts préfèrent se lier aux bases fortes et les acides faibles aux bases faibles. Il est important de noter que cette classification n'est pas figée. Un même élément peut être considéré dans deux familles différentes en fonction des études. Le cuivre, un métal intermédiaire selon Nieboer et Richardson, 1980, est considéré comme un métal fort dans l'étude réalisé par Pourret et al. 2007. Dans cette même étude, les terres rares de la classification périodique sont discutées comme étant des métaux forts. Les différents types de sorption présentés précédemment vont, en partie, régir le comportement du métal considéré dans l'environnement. Les métaux faibles formant des complexes covalents avec des bases faibles seront donc plus stables dans l'environnement. Ce phénomène contraste avec les métaux dits forts dont les complexes en sphères externes sont plus labiles, plus influencés par les conditions chimiques du milieu. Ces éléments sont donc potentiellement plus mobiles.

II. La modélisation géochimique

2.1 Généralités sur la modélisation géochimique multisurfacique

La répartition des contaminants entre phases liquides et solides, mais aussi leur spéciation à l'intérieur de ces deux phases sont deux paramètres fondamentaux dans l'évaluation de la toxicité d'une matrice, d'un relargage (Almas et al., 2007; Dijkstra et al., 2009; Matar et al., 2015). Ces paramètres sont influencés par les conditions chimiques du milieu, la complexation par des ligands inorganiques, la complexation de surface par les phases solide et colloïdale et la précipitation minérale. Les modèles géochimique sont devenus des outils majeurs dans l'étude de la spéciation, du relargage et de la biodisponibilité de nombreux contaminants (métaux traces, nutriments…) (Dijkstra et al., 2009;

Groenenberg et al., 2012; Paquin et al., 2002). Deux approches différentes peuvent être utilisées pour décrire la répartition solide-liquide à l'intérieur des milieux poreux (Groenenberg et al., 2012). La première consiste en l'utilisation d'équations empiriques reliant la concentration en éléments à différentes propriétés de l'échantillon considéré. Ces équations ont montré une bonne capacité à reproduire la concentration en métaux dans la gamme de pH et de force ionique dans laquelle elles ont été définies, mais perdent en efficacité en dehors de cette zone (Groenenberg et al., 2012). La deuxième approche possible, la modélisation multi-surfacique, peut être définie comme étant la description des phases solide et liquide d'un milieu poreux avec un ensemble de sous-modèles de surface disponibles où les ions peuvent être échangés ou complexés (Molina, 2016). Ces modèles multi-surfaciques permettent une meilleure compréhension des processus géochimiques. Les sous-modèles intégrés à ces modèles multi-surfaciques sont basés sur une combinaison de paramètres génériques, de constantes thermodynamiques (Dzombak and Morel, 1990; Tipping et al., 2011) obtenus sur une large gamme de conditions chimiques. Ces modèles sont notamment indépendants des conditions de pH et de force ionique élargissant ainsi leur domaine d'application. L'utilisation d'un modèle multi-surfacique offre la possibilité de tester l'impact d'une très grande variété de conditions environnementales, parfois extrême et/ou difficilement reproductible en laboratoire (Groenenberg et al., 2012). Parmi les études référencées dans le tableau 3, la capacité de sorption des oxydes métalliques, des argiles et de la matière organique est conjointement utilisée au sein des modèles multi-surfaciques. Le Windermere Humic Aqueous Model (WHAM-ModelVII) développé par Tipping en 2001 et le Non-ideal Competitive Adsorption model (NICA-Donnan) développé par Benedetti en 1996 sont les deux principaux modèles décrivant la capacité de sorption des SH. La capacité de sorption des (hydr)oxides métalliques (principalement l'aluminium et le fer) est couramment prise en compte en utilisant le Generalized Two Layer Model (GTLM) de Dzomback et Model (1990) et/ou le Charge Distribution-Multisite Complexation model (CD-MUSIC) de Hiemstra et Van Riemsdijk (1996). La capacité de sorption des argiles est, quant-à-elle, principalement modélisée en utilisant le Constant Capacitance Model (Lofts and Tipping, 1998).

Les modèles décrits dans cette section ont tous pour objectif de représenter le pouvoir de complexation de la matière organique naturelle et, plus précisément, des substances humiques. Les modèles de complexation aux surfaces minérales ne seront pas présentés en détail dans cette thèse mais Molina en 2016 a fait une large revue des différents modèles existant (Molina, 2016). Durant les sections précédentes, l'hétérogénéité physico-chimique des SH a été expliquée. Cette hétérogénéité se traduit par une pluralité des groupements fonctionnels, de poids moléculaires et de surfaces spécifiques variables modulant la capacité de sorption des SH (Tipping et al., 2011). Cette complexité, les créateurs des modèles l'ont réduite et généralisée en conservant une capacité de sorption

représentative des SH ayant différentes origines et en permettant leur utilisation pour une large gamme de conditions environnementales. Parmi les 3 principaux modèles utilisés dans la littérature scientifique (WHAM, SHM et NICA), tous considèrent des interactions spécifique et électrostatique (Koopal et al., 2005; Milne et al., 2001; Tipping et al., 2011). Dans ces modèles, le large panel de sites de sorption organiques est représenté par un « spectre d'affinité » pouvant être (i) discret (WHAM, SHM), (ii) continu (NICA) ou (iii) basé sur la structure moléculaire (Molina, 2016).

2.2 Modélisation de la sorption des ions aux substances humiques

a. WHAM-MODELVII

Comme précédemment décrit, les modèles WHAM utilisent un spectre d'affinité à distribution discrète pour calculer la sorption de protons et de cations aux substances humiques. Quatre sites carboxyliques (appelés sites A) et quatre sites phénoliques (appelés sites B) sont ainsi définis. La densité des quatre sites de type A est identique, tout comme celle des quatre sites de type B. En revanche, comme spécifié dans le tableau 1, la densité globale des sites de type A est deux fois plus importante que celle des sites de type B. La réaction de déprotonation de chacun des 8 sites est identique et s'écrit de la manière suivante :

$$\mathrm{R-OH} \leftrightarrow R-O^- + H^+ \qquad 1$$

Cette dissociation est régie par des constantes de dissociations protonique spécifiques aux sites de types A et B et est décrit comme suit :

$$\mathrm{p}K_{H,i} = \mathrm{p}K_A + \frac{2i-5}{6}\Delta\mathrm{p}K_A, 1 \leq i \leq 4 \qquad 2$$

$$\mathrm{p}K_{H,i} = \mathrm{p}K_B + \frac{2i-13}{6}\Delta\mathrm{p}K_B, 5 \leq i \leq 8 \qquad 3$$

Avec :

- $\mathrm{p}K_A$ et $\mathrm{p}K_B$ les valeurs intrinsèques de dissociation protonique spécifiées (Tableau 1) pour les sites de types A et B respectivement,
- ΔpKA et ΔpKB termes affinés expérimentalement permettant de moduler les valeurs des constantes précédemment décrites.

Dans Model VII, les cations peuvent complexer des sites monodentés, bidentés et tridentés. La sorption des cations aux sites monodentés carboxylique et phénolique suit l'équation bilan 4 et 5 dont la constante d'équilibre est appelée K_{MA} et K_{MB} pour les sites de types A et B respectivement.

$$(\mathrm{SH})\mathrm{H} + \mathrm{M}^{z+} \leftrightarrow (\mathrm{SH})\mathrm{M}^{(z-1)} + \mathrm{H}^{+} \quad 4$$

$$(\mathrm{SH})^{-} + \mathrm{M}^{z+} \leftrightarrow (\mathrm{SH})\mathrm{M}^{(z-1)} \quad 5$$

Avec :

- M : cation,
- z : nombre de charge ionique du cation M.

La sorption d'un cation sur les sites monodentés déprotonés de type A (eq. 6) et de type B (eq. 7) a une constante d'équilibre $logK_{MA,i}$ et $logK_{MB,i}$ respectivement, calculée selon la méthode suivante :

$$logK_{MA,i} = logK_{MA} + \frac{2i-5}{6}\Delta\mathrm{LK}_1, \qquad 1 \le i \le 4 \quad 6$$

Et

$$logK_{MB,i} = logK_{MB} + \frac{2i-13}{6}\Delta\mathrm{LK}_1, \qquad 1 \le i \le 8 \quad 7$$

Avec :

- i : indice représentant les 4 sites carboxyliques et les 4 sites phénoliques (sites monodentés),
- $\Delta\mathrm{LK}_1$: paramètre modulant la distribution des $logK_{MA,i}$ et $logK_{MB,i}$.

La valeur de $logK_{MA}$ est déterminée expérimentalement et spécifiée pour chaque cation. Dans Model VII, dans un souci de simplification, les valeurs de $logK_{MB}$ spécifique à chaque cation sont calculées à partir des valeurs obtenues sur les sites de type A selon la relation 8 :

$$logK_{MB} = logK_{MA} \times \frac{\mathrm{p}K_B}{\mathrm{p}K_A} \quad 8$$

Avec :

- $\mathrm{p}K_A$ et $\mathrm{p}K_B$ les valeurs intrinsèques de dissociation protonique spécifiées (tableau 1) pour les sites de types A et B respectivement.

Les cations peuvent aussi être complexés par des sites bidentés et tridentés dont l'occurrence a été calculée en fonction de la probabilité que 2 ou 3 sites de types A et B soient suffisamment proches de la surface de la molécule organique pour pouvoir se recombiner. La prise en compte de ces sites a été l'objet de plusieurs modifications au long du processus d'amélioration de ce modèle (Tipping et al., 2011). Dans Model VII, la quantité de sites bidentés a été limitée à 6 et les sites tridentés à 8. L'abondance de ces sites multidentés est modulée par deux facteurs, f_B et f_T (Tableau 1) pour les sites bidentés et tridentés respectivement. Comparativement aux sites monodentés, la constante d'équilibre de la complexation d'un cation sur un site bidenté (eq. 9) et un site tridenté (eq. 10) est la somme des constantes des différents sites impliqués. En 2011, Tipping et al. ont proposé en

complément la découpe des sites bidentés et tridentés en 3 familles : les sites faibles, les sites modérés et les sites forts pour un total de 18 sites bidentés et de 24 sites tridentés. L'abondance des sites faibles, modérés et forts correspondant à respectivement 90,1, 9 et 0,9 % des sites. L'ajout de ces sites permet d'élargir la gamme de valeurs des constantes de complexation cationique disponible. Pour cela, comme cela est décrit dans les équations suivantes, trois nouveaux paramètres sont introduits. Il s'agit de x, y et $\Delta \mathrm{LK}_2$. Ce dernier paramètre (*i.e.* $\Delta \mathrm{LK}_2$), propre à chaque cation, va permettre d'accroitre les constantes de sorptions des sites modérés et forts. x et y vont permettre de moduler l'impact du $\Delta \mathrm{LK}_2$ sur les constantes d'équilibres des sites bi et tridentés, respectivement.

$$\log K_{M,\mathrm{j,k}} = \log K_{M,\mathrm{j}} + \log K_{M,\mathrm{k}} + x \times \Delta \mathrm{LK}_2 \qquad 9$$

$$\log K_{M,\mathrm{j,k},l} = \log K_{M,\mathrm{j}} + \log K_{M,\mathrm{k}} + \log K_{M,\mathrm{l}} + y \times \Delta \mathrm{LK}_2 \qquad 10$$

Avec :

- M : indice représentant le cation concerné,
- j, k, l : indices relatifs aux sites monodentés constituant les sites bidentés et/ou tridentés,
- x : paramètre modulant l'impact du $\Delta \mathrm{LK}_2$ sur les constantes d'équilibres des sites bidentés ; prend la valeur de 0, 1 et 2 pour les sites bidentés faibles, modérés et forts respectivement,
- y : paramètre modulant l'impact du $\Delta \mathrm{LK}_2$ sur les constantes d'équilibres des sites tridentés ; prend la valeur de 0, 1,5 et 3 pour les sites tridentés faibles, modérés et forts respectivement,
- $\Delta \mathrm{LK}_2$: paramètre permettant d'accroitre les sites de sorption des modérés et forts.

Au total, Model VII décrit la complexation des cations sur un total de 50 sites dont l'abondance (*i.e.* le nombre de mol de site par g de SH) et l'étalement des constantes de dissociation protonique est représenté sur la fig. 3.

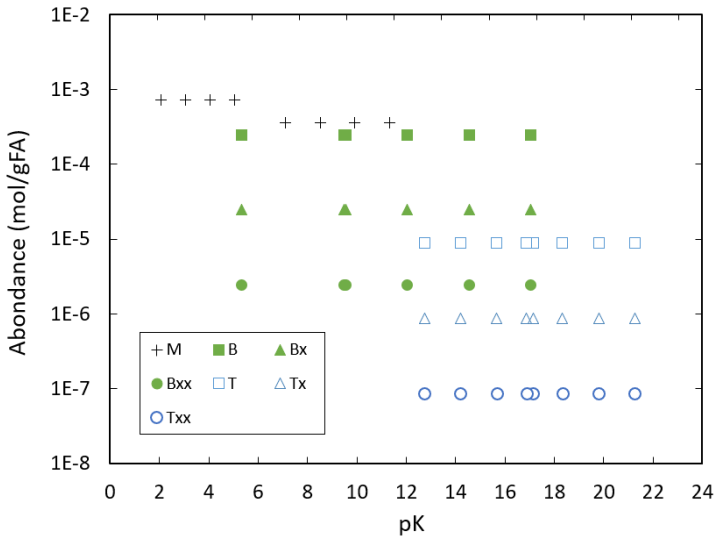

Fig.3. Distribution des pK protonique des acides fulviques et leur abondance décrite dans Model VII. Les valeurs des constantes utilisées sont identiques à celles décrites dans le tableau 1. M, B et T représentent les sites mono, bi et tridentés respectivement. Les sites bidentés et tridentés sans indice représentent les sites dits faibles. Les sites modérés et forts sont appelés x, et xx respectivement.

Les effets électrostatiques de Model VII permettent, à la fois, de moduler les constantes de sorptions précédemment décrites et d'ajouter une sorption non-spécifique. Dans Model VII, les acides humiques et fulviques sont considérés comme des sphères imperméables. La prise en compte des effets électrostatiques est similaire à un modèle de complexation de surface. La constante de sorption obtenue en l'absence de charge moléculaire $\left(K_i^{intr}\right)$ est modulée par le facteur électrostatique $\left(K_i^{elec}\right)$ comme décrit dans l'équation 11.

$$K_i = K_i^{intr} \times K_i^{elec} \qquad 11$$

où $$K_i^{elec} = e^{2\omega z Z_h} \qquad 12$$

et $$\omega = P \times \log(I) \qquad 13$$

Avec :

- i : indice représentant les différents site de sorption ?
- Z_h (eq.g-1) : charge globale de la molécule organique
- z : changement de charge survenu lors de la complexation du cation
- I (mol.L-1) : force ionique du milieu
- P : paramètre électrostatique

Une sorption non spécifique des cations est aussi intégrée. Les acides fulviques et humiques sont considérés comme des sphères imperméables de tailles fixes et chargés négativement, entourés d'un

volume, le volume de Donnan (V_D en L.gSH^{-1}), à l'intérieur duquel s'accumulent des « contre-ions » de charge positive. Ce volume non fixe est calculé à partir de l'équation 14 :

$$V_D = \frac{N_A}{M_r}\frac{4\pi}{3}\left[\left(r + \frac{1}{\kappa}\right)^3 - r^3\right] \quad 14$$

Avec :

- Mr : poids moléculaire de la molécule considérée,
- r : rayon moléculaire,
- κ : longueur de Debye,
- N_A : constante d'Avogadro.

La longueur de Debye est calculée selon la relation suivante :

$$\kappa = \sqrt{\frac{2F^2 I}{\varepsilon RT}} \quad 15$$

Avec

- ε : constante diélectrique de la substance humique,
- F : constante de Faraday,
- R : constante des gaz parfaits,
- I (mol.L-1) : force ionique du milieu
- T : température absolue.

A travers la longueur de Debye, V_D est largement dépendant de la force ionique de la solution. Alors que l'augmentation de celle-ci réduit ce volume, sa diminution engendre l'augmentation du volume de Donnan (Fig. 4). Ce paramètre est particulièrement important puisqu'il dépend des conditions expérimentales. Il a d'ailleurs été précédemment noté que dans des conditions de basse concentration en électrolytes, cette méthode de calcul à tendance à surestimer largement ce volume (Town et al., 2019). Dans des conditions de fortes concentrations en matière organique et/ou de force ionique ≥ 1 M, ce volume de Donnan est assez faible pour pouvoir négliger son impact sur la sorption des cations.

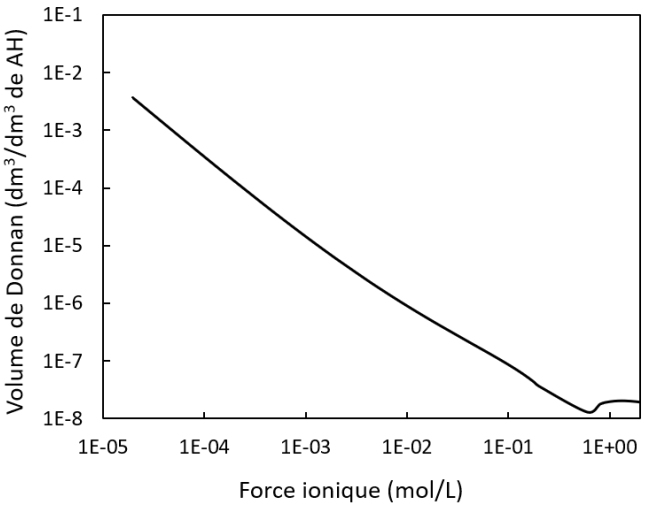

Fig.4. Evolution du volume de Donnan entourant les acides humiques (notés AH) en fonction de la force ionique de la solution.

L'équation d'électroneutralité comprenant la somme des charges de surfaces négatives des substances humiques (eq. 16) et la somme des charges positives des « contres-ions » doit aboutir à une neutralité électrostatique. La charge de la substance humique Z_h (eq.g^{-1}) est dépendante du volume de Donnan selon la relation suivante :

$$Z_h = -V_D \times \sum_{1}^{x} C_{D,x} \times z_x \qquad 16$$

Avec :

- V_D : volume de Donnan
- x : indice représentant les cations à l'intérieur du volume,
- ($C_{D,x}$) : concentration d'un cation x,
- z_x : charge ionique du cation x.

La concentration ($C_{D,x}$) d'un cation x à l'intérieur du volume de Donnan est calculée à partir de l'équation suivante :

$$C_{D,x} = C_{S,x} \times K_{sel,x} \times R^{|z_x|} \qquad 17$$

Avec :

- $C_{S,x}$: concentration du cation dans la solution,
- $K_{sel,x}$: coefficient d'accumulation déterminé expérimentalement,
- z_x : charge ionique du cation x,
- R : constante ajustée afin que la somme de toutes les charges des contres-ions compense la charge de la SH (Z_h) respectant ainsi la neutralité globale de la molécule.

Tableau 1. Définition des principaux paramètres utilisés dans WHAM-Model VII. Adapté de Tipping et al., (2011)

Paramètre	Description	Origine
Q_A	Abondance de site de type A (carboxylique)	Affiné expérimentalement
Q_B	Abondance de site de type B (phénolique)	Calculé
pK_A	Constant de dissociation pour les sites de type A	Affiné expérimentalement
pK_B	Constant de dissociation pour les sites de type B	Affiné expérimentalement
ΔpK_A	Terme de distribution modulant les pK_A	Affiné expérimentalement
ΔpK_B	Terme de distribution modulant les pK_B	Affiné expérimentalement
Log K_{MA}	Constant d'équilibre intrinsèque aux sites de type A	Affiné expérimentalement
Log K_{MB}	Constant d'équilibre intrinsèque aux sites de type B	Calculé à partir des Log K_{MA}
ΔLK_2	Terme de modulation de l'affinité aux sites forts	Affiné expérimentalement
P	Paramètre électrostatique	Affiné expérimentalement
K_{sel}	Coefficient de sélectivité pour l'accumulation de contre-ion	Affiné expérimentalement
f_b	Fraction de site protonique pouvant former des sites bidentés	Calculé
f_t	Fraction de site protonique pouvant former des sites tridentés	Calculé
M	Masse moléculaire	Estimé à partir de la littérature
r	Rayon moléculaire	Estimé à partir de la littérature

b. NICA-DONNAN

A l'image de WHAM-Model VII, NICA-Donnan présente à la fois une sorption spécifique en intégrant l'isotherme « non ideal competitive adsorption » (NICA, Koopal et al., 1994) et une sorption non-spécifique via l'utilisation du volume de Donnan. Bien que continue, la distribution de l'affinité

protonique et des cations se fait aussi autour de deux principaux sites : les sites carboxyliques (indicés 1 et présentant un $\log \overline{K}_{H,1} = 4$) et les sites phénoliques (indicés 2 et présentant un $\log \overline{K}_{H,2} = 9$) dont la distribution est décrite sur la Fig. 5.

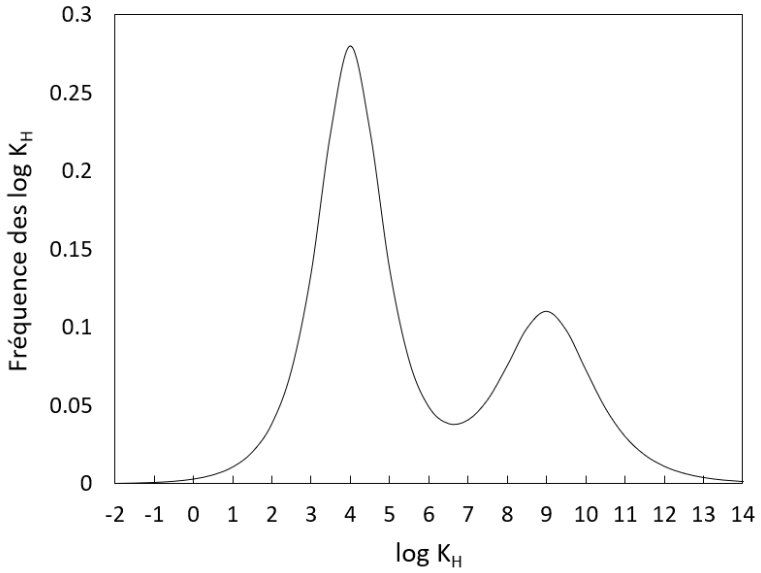

Fig.5. Distribution des constantes d'acidité d'une substance humique typique du spectre de Sips (1948) utilisé dans NICA-Donnan.

Koopal et *al.* (1994) ont proposé l'utilisation d'une isotherme proche de celle de Langmuir-Freunclich pour décrire l'adsorption locale (T) d'une espèce (*i*). L'équation 18, décrit la proportion de sites occupés, notée ($\theta_{i,T}$) par l'espèce i (Sips, 1948).

$$\theta_{i,T} = \frac{(\widetilde{K}_i c_i)^{n_i}}{\sum_i (\widetilde{K}_i c_i)^{n_i}} \times \frac{\left[\sum_i (\widetilde{K}_i c_i)^{n_i}\right]^p}{1 + \left[\sum_i (\widetilde{K}_i c_i)^{n_i}\right]^p} \qquad 18$$

Avec :

- $\widetilde{K}_i$: moyenne des constantes d'affinité de l'espèce i pour les sites T.
- c_i : la concentration de l'espèce *i*
- n_i : constante permettant de prendre en compte les effets de coopérativité spécifique à chaque ion i (*i.e.* effet de l'adsorption sur l'affinité d'autres sites de liaisons)
- p : constante permettant de prendre en compte la largeur de la distribution pour décrire le site complexant.

La constante n_i est l'équivalent des sites multidentés proposés dans WHAM-MODEL VII. Autrement dit, avec cette constante, des quantités d'ions adsorbés différentes peuvent refléter une occupation de

sites identiques. La quantité totale d'ions i adsorbés peut être calculée à l'aide de l'équation suivante qui est la somme de la quantité d'ions adsorbés sur les sites 1 et les sites 2 :

$$Q_i = \theta_{i,1}\left(\frac{n_{i,1}}{n_{H,1}}\right)Q_{max,1} + \theta_{i,2}\left(\frac{n_{i,2}}{n_{H,2}}\right)Q_{max,2} \qquad 19$$

Avec :

- $n_{i,1}$ et $n_{i,2}$: paramètres de non idéalité pour la sorption des cations aux sites de type 1 et 2
- $n_{H,1}$et $n_{H,2}$: paramètre de non idéalité de la sorption des H^+ aux sites de type 1 et 2
- $Q_{max,1}$ et $Q_{max,2}$: capacité maximale d'adsorption d'un site

Afin de prendre en compte la sorption non-spécifique des ions, Koopal (1996) et Benedetti et al. (1996) ont choisi de considérer les SH comme des sphères perméables constituées d'un volume interne variable décrit par le volume de Donnan (V_D, L.kg^{-1}) à l'intérieur duquel viennent s'accumuler des contres-ions en réponse au développement de la charge des SH. Dans ce volume le potentiel électrostatique est constant et vaut 0 en dehors de ce volume. La charge cumulée de ces contres-ions à l'intérieur de V_D doit venir compenser la charge de la molécule humique :

$$\frac{q}{V_D} = \sum_i Z_i\left(c_{i,D}\right) = 0 \qquad 20$$

Avec :

- $c_{i,D}$: concentration de l'ion i à l'intérieur du volume de Donnan,
- Z_i : charge de l'ion i
- q : charge nette de la SH (meq.kg^{-1}).

Le facteur de Boltzman peut être appliqué pour relier la concentration de l'ion à l'intérieur du volume de Donnan, $c_{i,D}$, à celle mesurée dans la solution notée c_i :

$$c_{i,D} = c_i \times e^{\frac{Z_i F \Psi_D}{RT}} \qquad 21$$

Avec :

- c_i : concentration en ion i dans la solution,
- Z_i : charge de l'ion i,
- Ψ_D : potentiel électrique (V) à l'intérieur du volume de Donnan, considéré comme constant,
- F: constante de Faraday,
- R: constante des gaz parfaits,
- T : température.

Lorsque la valeur du volume de Donnan est obtenue (calculée à partir de l'équation 22 d'après Benedetti et al. 1996), la charge nette de la molécule q mesurée par titrage potentiométrique, il est possible de retrouver la valeur du Ψ_D.

$$log\, V_D = -1 + b(1 - logI) \qquad 22$$

Avec :

- I : force ionique (mol.L-1)
- b : paramètre ajusté en fonction du type de SH.

Le paramètre b permet de mieux décrire l'accumulation des cations dans le volume de Donnan pour des conditions de faible force ionique (Koopal et al., 2005; Milne et al., 2001). Cette relation permet donc de décrire l'effet de I sur la charge et l'encombrement stérique des molécules (Marang, 2007).

Tableau 2. Définition des principaux paramètres utilisés dans NICA-Donnan. Depuis Molina, (2016).

Paramètre	Description	Origine
$Q_{max,1}$	Abondance site de type 1 (carboxylique)	Affiné expérimentalement
$Q_{max,2}$	Abondance site de type 2 (phénolique)	Affiné expérimentalement
Log $\widetilde{K}_{H,1}$ Log $\widetilde{K}_{H,2}$	Valeur moyenne de la constante de dissociation protonique des sites de type 1 et 2	Affiné expérimentalement
$n_{H,1}$ $n_{H,2}$	Paramètre de non idéalité de la sorption des H^+ aux sites de type 1 et 2	Affiné expérimentalement
p_1	Paramètre d'hétérogénéité pour les sites de type 1	Affiné expérimentalement ou considéré comme constante universelle
p_2	Paramètre d'hétérogénéité pour les sites de type 2	Affiné expérimentalement ou considéré comme constante universelle
Log $K_{M,1}$	Valeur moyenne de la constante d'affinité de cations pour les sites de type 1	Affiné expérimentalement
Log $K_{M,2}$	Valeur moyenne de la constante d'affinité de cations pour les sites de type 2	Affiné expérimentalement ou estimé depuis la littérature
$ni_{,1}$	Paramètre de non idéalité pour la sorption des cations aux sites de type 1	Affiné expérimentalement
$ni_{,2}$	Paramètre de non idéalité pour la sorption des cations aux sites de type 2	Affiné expérimentalement ou estimé
b	Paramètre du volume de Donnan	Affiné expérimentalement

2.3 Utilisation de modèle multisurfacique au sein de milieu poreux

Un large référencement des études ayant intégré une modélisation de la répartition de différents métaux entre phases solide et liquide a été réalisé en 2014 puis actualisé en 2018 par Di Bonito et al (2018). Le tableau 3 permet de continuer ce référencement avec des études postérieures à 2018. Dans ce tableau, sont extraites les informations reflétant la stratégie de modélisation et pouvant avoir une influence sur la qualité des calculs effectués. On retrouve notamment un référencement des surfaces réactives implémentées, leur quantité, ainsi que le modèle utilisé. Également, sont listés les différents éléments d'intérêts modélisés, ainsi que leur fraction utilisée en données d'entrée. Comparativement au formalisme initial proposé par Di Bonito en 2018, un focus particulier a été fait sur les moyens utilisés afin de définir les quantités de matières organiques solides et dissoutes réactives. Dans la suite de ce document, seront repris en détail les méthodes d'implémentation des oxydes métalliques, de la matière organique et de la quantité d'ion à intégrer au modèle.

a. Méthode d'implémentation de la capacité de sorption des oxydes métalliques

La grande majorité des études modélisant la distribution de métaux entre les phases solide et liquide de milieux poreux intègre l'influence des oxydes métalliques (voir tableau 3). Ce sont majoritairement les oxydes de fer et d'aluminium qui sont modélisés. Les études utilisant d'autres oxydes, comme les oxydes de manganèse sont moins fréquentes (Cancès et al., 2003; Marzouk et al., 2013a, 2013b). Bien que moins abondants que les oxydes de fer ou d'aluminium, les oxydes de manganèse sont pourtant ubiquitaires. Leur large charge de surface négative présente pour de très faibles valeurs de pH (McKenzie, 1981) leur permet de jouer un rôle important dans la mobilité et la biodisponibilité des métaux et métalloïdes (Holguera et al., 2018) d'environnements naturels. Cependant, la faible optimisation des constantes de sorption à l'intérieur de modèle de complexation de surface complique leur implémentation (Huang et al., 2017; Tonkin et al., 2004).

Globalement l'influence des différents oxydes métalliques sur la spéciation des éléments est largement dépendante (i) des conditions chimiques (pH, pE…), (ii) de la quantité relative d'oxydes métalliques et de matière organique solide et (iii) de l'élément considéré. Par exemple, l'acidification des conditions diminue drastiquement l'influence de ces surfaces (largement chargées positivement) sur la spéciation des métaux (Dijkstra et al., 2004; Fang et al., 2016a). Parmi les métaux divalents, le plomb montre la plus grande affinité pour les oxydes métalliques (Dijkstra et al., 2009; Peng et al., 2018). La zone d'influence de ces oxydes métalliques ne s'arrête pas seulement au compartiment solide (> 0,45 µm). Le relargage de nanoparticules de fer et/ou d'aluminium dans des solutions de sol est une notion largement établie dans de nombreux environnements (Aiken et al., 2011; Pokrovsky et al., 2005; Pokrovsky and Schott, 2002a; Pourret et al., 2007a). L'influence de ces oxydes colloïdaux sur le

relargage d'éléments associés peut être fondamentale. Sjöstedt et al., (2018) ont montré que la modélisation de colloïdes d'oxydes de fer permet d'améliorer qualitativement et quantitativement la modélisation du comportement du Pb. Et pourtant, les études de modélisation prenant en compte ce phénomène sont peu nombreuses (Almås et al., 2007a; Sjöstedt et al., 2018; Tipping et al., 2003).

Quelles quantités réactives d'(hydr)oxydes métalliques sont à implémenter aux modèles multi-surfaciques ? Les oxydes métalliques peuvent se retrouver sous deux principales formes : cristallisés ou amorphes. Ces deux formes se caractérisent notamment par des réactivités différentes, conséquence d'une plus grande surface spécifique des formes amorphes (Dzombak and Morel, 1990). Les études de modélisation, en combinant différentes techniques d'extraction chimique d'Al, de Fe ou de Mn, peuvent mesurer et implémenter distinctement ces différentes formes (tableau 3). La quantité totale d'oxyde métallique est extraite avec des solutions de dithionite-citrate-bicarbonate, DCB (Fisher-Power et al., 2019; ISO 12782-2, 2012). La différence entre les concentrations de fer mesurées après extraction au DCB et celles mesurées après extraction à l'acide ascorbique permet de remonter jusqu'à la quantité de Fe-oxyhydroxydes cristallin (Fisher-Power et al., 2019; ISO 12782-2, 2012). L'intégration de ces mesures au sein des modèles peut, aussi, être sujette à quelques variations. Dans l'étude de Van Eynde et *al.* 2020, les mesures d'oxydes de fer et d'aluminium, sous formes cristallisés et amorphes (ou faiblement cristallisés) sont modélisées via une seule et unique phase. L'importance des différents oxydes est en revanche pondérée : le poids des oxydes cristallisés ne représentant qu'un sixième du poids des formes amorphes afin de prendre en compte la plus faible surface réactive des oxydes cristallisés. Zhu et *al.* (2018) considèrent aussi la sorption de métaux sur des oxydes amorphes et d'autres formes plus cristallisées. Cependant, CD-MUSIC est utilisé pour décrire la complexation sur les formes cristallisées et le « generalized double layer model » de Dzomback et Morel (1990) pour calculer la complexation sur les formes amorphes avec des surfaces spécifiques de 50 et 600 $m^2.g^{-1}$, respectivement.

Finalement, d'autres études utilisent les constantes de solubilité présentes dans leur base de données afin de modéliser la précipitation des oxydes de fer et d'aluminium à partir des quantités réactives de Fe et de Al (Almas et al., 2007; Bonten et al., 2008; Klinkert and Comans, 2020; Sjöstedt et al., 2018). Ces constantes de solubilité peuvent être modifiées dans le but d'optimiser la modélisation du relargage du fer et de l'aluminium. Dans ces conditions, la maitrise des conditions de pH-pE est fondamentale puisque ces oxydes sont rédox sensibles. Les conditions rédox, moins couramment mesurées que le pH, peuvent être fixées sur celles mesurées dans l'échantillon où, suivre la relation pH + pE = 10 ou 15 représentative de milieux naturels modérément oxydés (Dijkstra et al., 2009, 2004).

b. Méthode d'implémentation de la capacité de sorption de la matière organique

Les modèles de sorption par les matières organiques sont paramétrés pour les acides humiques et fulviques d'origines diverses, isolés et purifiés en laboratoires (Milne et al., 2001; Tipping et al., 2011). Malgré le caractère générique de Model VII et NICA-Donnan, les molécules organiques des échantillons présentés dans le tableau 3 peuvent, plus ou moins, s'éloigner des caractéristiques physico-chimiques et donc des capacités de sorptions des SH décrites dans ces modèles. Bien que ces deux familles regroupent une très grande variété de substances organiques, d'autres molécules aux affinités différentes pour les métaux, peuvent aussi composer les matières organiques naturelles. En plus des acides humiques et fulviques, les sols et solutions de sols peuvent, par exemple, contenir des acides organiques de faible poids moléculaire, inférieur à 1 kDa, notamment produit pendant la décomposition bactérienne des matières organiques (Fox and Comerford, 1990). De même, la fraction récalcitrante des matières organiques aussi appelées humines n'est pas décrite par ces modèles de sorptions aux substances humiques qui se focalisent sur les acides humiques et fulviques. C'est pourquoi, les mesures de matières organiques solides et dissoutes sont pondérées afin d'obtenir des concentrations « réactives » transposables aux capacités de sorption des acides humiques et fulviques développées au sein des modèles dédiés (voir tableau 3). L'important écart de pourcentage de MO active entre les différentes études référencées dans le tableau 3 met en évidence la variabilité de la réactivité de la MO en fonction de son origine. En effet, dans la table 3, le pourcentage de matière organique solide active oscille entre 17 (Tiberg et al., 2021) et 150 % (Fisher-Power et al., 2019) et celle de la matière organique dissoute entre 40 (Zhu et al., 2018) et 100 % (Sjöstedt et al., 2018). Bien que la quantité et la qualité des matières organiques solides ou en solution aient un impact important sur la complexation des métaux (Baken et *al.,* 2011), il n'existe pas de consensus, de prérequis minimum, entre les différentes études sur la manière de mesurer la fraction réactive de la matière organique.

Un processus expérimental de caractérisation de la matière organique solide et dissoute peut-être engagé. Des techniques de fractionnements chimiques, comme celle proposée par l'IHSS, permettent d'obtenir la fraction « active » de la MO solide (Martín-Torre et al., 2015; Van Eynde et al., 2020) et dissoute (Fang et al., 2016a; Klinkert and Comans, 2020; Ren et al., 2015). D'autres études, comme celle de Pourret et *al.* (2007), utilisent des techniques d'ultrafiltration afin de mieux comprendre les caractéristiques structurales de leur matière organique et d'ajuster la proportion d'acide humique et fulvique en conséquence. Dans cet exemple, les quantités d'acides humiques et fulviques ont été modélisées en utilisant les quantités mesurées dans les fractions 0,22 µm – 5 kDa et < 5kDa, respectivement. Des techniques spectrophotométriques ont aussi été utilisées afin de remonter

jusqu'à l'assemblage organique des échantillons. Parmi celles-ci, l'utilisation du SUVA comme indicateur de la capacité de sorption des matières organiques modélisées, développée par (Amery et al., 2008) est citée en exemple à plusieurs reprises (Baken et al., 2011; Laurent et al., 2020). L'équation développée par Amery et al. 2008 :

$$\%\ \text{AF actif} = 100 \times (\text{SUVA}_{\text{echantillon}}/\text{SUVA}_{\text{AF}}) \qquad 23$$

relie empiriquement les valeurs de SUVA mesurées à la quantité de matière organique dissoute active en se basant sur la valeur du SUVA d'acides fulviques purifiés ($SUVA_{AF}$).

L'implémentation des matières organiques peut aussi se faire via l'optimisation de la quantité de matières organiques actives et/ou des constantes de complexations établies au sein des bases de données. C'est le cas de l'étude de Zhu et al. (2018), dans laquelle la concentration en matière organique solide est modulée afin de minimiser au maximum l'écart entre les concentrations mesurées et calculées en Cd. Les résultats montrent que l'utilisation de 31 % de matière organique solide réactive est la meilleure option de modélisation. Par ailleurs, Laurent et al. (2020) ont modulé les constantes de complexations du modèle et, notamment, le Log K_{Cu} de Model VII.

Enfin, une dernière voie d'optimisation possible du ratio de matière organique active consiste à se baser sur des données déjà présentes dans la bibliographie sur des échantillons (Shi et *al.,* 2020 ; Sjöstedt et al., 2018 *;* Tiberg et al., 2021). Dwane and Tipping en 1998 après avoir optimisé la quantité d'AF actifs sur des données de titration d'eaux naturelles (les AF actifs représentant entre 30 et 130 % du total) recommandent de considérer un ratio de 50 % de la MO dissoute active dans des échantillons d'eau de surfaces en cas d'absence de données relatives à sa qualité.

Finalement, il semble cependant difficile de s'affranchir d'étapes de caractérisation des matières organiques solides et dissoutes en présence. Par exemple, la relation présentée par Amery et al. (2008) (eq. 24) n'est plus valable dans des milieux anthropisés. Matar et al. (2015) recommandent d'intégrer la fraction hydrophile en complément des plus classiques acides humiques et fulviques dans le cadre de modélisation de solutions impactées par les activités humaines.

c. Détermination de la quantité d'éléments actifs

Comme on peut l'observer dans le tableau 3, de nombreuses études utilisent la quantité d'éléments géochimiquement actifs comme données d'entrée. Cette fraction de la concentration totale représente la quantité d'éléments concernée par les différentes réactions chimiques à l'équilibre (Groenenberg et Loft, 2014). Les phases minérales cristallisées contenant des métaux d'intérêts, ainsi que les métaux complexés sur des matières organiques récalcitrantes, ne sont donc pas prises en compte dans ces calculs. La concentration en électrolytes des solutions pouvant largement impacter

les résultats de modélisation (Zhang et al., 2018) via des processus de compétitions par exemple, certaines études implémentent aussi, en plus de la quantité d'éléments réactifs ou disponibles, la concentration d'éléments majeurs mesurée en solution (Fisher-Power et al., 2019; Van Eynde et al., 2020).

D'autres facteurs peuvent, en revanche, motiver certaines études à préférer utiliser la quantité totale d'éléments d'intérêts dans leurs études de modélisation. De nombreux travaux de caractérisation d'échantillons solides s'appuient sur la modélisation géochimique afin de remonter jusqu'à un assemblage organo-minéral représentatif de l'échantillon étudié (Bisone et *al.,* 2016 ; Gonzalez et *al.,* 2019 ; Lupsea et *al.,* 2014). L'utilisation de la quantité totale en éléments est donc nécessaire afin de pouvoir observer les indices de saturations des différentes phases minérales cristallisées. Par ailleurs, dans le domaine des matrices environnementales anthropisées, la quantité totale est souvent mesurée en routine. Tester la capacité des modèles à répartir la quantité totale en élément entre phases solide et liquide peut être donc nécessaire afin de fournir des informations pour la gestion des risques associés à ces matrices environnementales anthropisées.

Tableau 3. Référencement des études ayant utilisées la modélisation géochimique au sein de milieu poreux. Le formalisme du tableau est inspiré de Di Bonito et al., 2018 mais toutes les études référencées ici en sont postérieures.

Surface réactive et modèles utilisés	**Echantillon modélisé (test+noms echantillon)**	**Eléments d'intérêt**	**Mesure [éléments d'intérêt]**	**Données d'entrée utilisées**	**Matière organique utilisée**	**Méthode définition MO**	**Mesure des surfaces minérales**	**Référence**
MOS/MOD: NICA-D Clay: CD-MUSIC Ferrihydrite: CD-MUSIC	Sol tropical relargage en fonction du pH	B	$CaCl_2$ extraction	pH, B, solubilisé CO_3^{2-}, Ca^{2+} et Cl^-	MOS: 100% AH MOD: 50% AH	HA/FA obtenu par extraction chimique	Al/Fe oxydes: ammonium-oxalate extraction Crist-oxydes : DCB-AO	(Van Eynde et al., 2020)
MOS/MOD: NICA-D; Amorphous HFO: GTLM; Crystalline Fe oxydes: CD-MUSIC; Clay: CCM	Biodisponibilité du Cd dans le sol	Cd	0,43 M HNO_3	pH, Cd, 0,01m $CaCl_2$	MOS: 31, 60 et 100 % reactive MOD: 40 % AF	Optimisé pour fiter Cd	HFO: Ox-Fe Crist-Fe : DCB-Ox-Fe	(Zhu et al., 2018)
MOS/MOD: SHM Ferrihydrite: CD-MUSIC	Expérience de spéciation en batch d'un spodosol	Cd, Co, Pb	EDTA, HNO3	pH, concentration active en Cd, Co, Pb solublisé Ca, Mg, K, SO4, Fe, Al	MOS: 50 % active with 50/50 AH /AF MOD: 100 % AF	Optimisé pour fiter et obtenu de Gustafsson et al., 2011	Ferrihydrite: Ox-Fe	(Tiberg et al., 2018)

MOS/MOD: SHM HFO: CD-MUSIC	Relargage pH-dépendent (pH 5-9) de déchet solide incinéré	Cu, Zn	Extracted at pH 12 for 32H	pH, élément majeur et trace dissout Actif Cu, Zn	MOS: 17 % active with 50/50 AH /AF MOD: 100 % AF	Depuis Zomeren and Comans (2009)	HFO: Al+ Fe extraction Ox	(Tiberg et al., 2021)
MOS/MOD: SHM +sites for Pb; Ferrihydrite + amorphous Al: CD-MUSIC	Expérimentation en batch d'un sol contaminé	Pb	0,1M HNO_3	pH, actif Pb, Cu, Zn, Ba, Cr; Dissout Ca, Mg, Fe, Al, S, P	MOS: 50 % active: 50/50 AH /AF. MOD 100 % AF	Depuis Almås et al. (2007); Gustafsson et al. (2003)	Al + Fe oxide calculés par indice saturation	(Sjöstedt et al., 2018)
MOS/MOD: SHM $Fe(OH)_3$(am):CD-music (ferrihydrite); Al(OH)3(am): DLM (gibbsite); Fe-crystalline: CD-MUSIC Clay: CCM	pH-edge adsorption d'un sediment	Zn, Cu	Spiked	pH, T, pCO2, Ajout total de Na, NO3-, Cu et Zn Solubilisé Ca, Mg, Al, Fe	MOS: entre 50 et 150% MOD: 100% AF	Optimisé pour Zn, Cu	Ferrihydrite: AOD-extractible Gibbsite: AOD-extractible Crystalline Fe: DCB-AOD extractible Fe	(Fisher-Power et al., 2019)
MOS/MOD: WHAM-ModelVII Fe-Al (hydr)oxides CCM	Relargage en batch d'un sol contaminé	Cu	0.43M HNO3	pH, solubilisé Ca et $NO3^-$	MOS: 60% active 84% AH et 16% AF MOD: 65% AF	Depuis Peng et al. (2018)	DCB-Fe Ox-Al Reactive cryst-Fe = 16% of total	(Shi et al., 2020)

MOS/MOD: NICA-D HFO: GTLM Clay: Donnan model	Speciation dans une solution de composte	Zn, Cu	0.43M HNO3	pH, actif Zn, Cu, Solubilisé Ca, Mg, Mn, P, S; Total Al, Fe	MOS: 100% AH/AF MOD:100% AH/AF	AH/AF: extraction au NaOH MOD: Dax-resine	HFO calculé par le modèle comme ferrihydrite + $Al(OH)_3$ Clay : XRD	(Klinkert and Comans, 2020)
MOS/MOD: NICA-D HFO: GTLM Geothite: CD-MUSIC Illite: two site model	19 extraits de solution de sol	Ni, Cd	Spiked Ni, Cd 0.43M HNO3	pH, ajout Ni, Cd, solubilisé K, Na, Ca, Mg, Al, Fe. pCO2 et concentration en électrolyte dans la solution	MOS: 31%AH MOD: 40% AF Reactive clay= 80% total clay	Depuis Bonten et al. (2008); Milne et al. (2001); Pan (2015)	DCB-Fe: HFO Cryst-Fe: Ox – DCB extractible	(Zhang et al., 2018)
MOS/MOD: WHAM-ModelVII; Fe-Al (hydr)oxides CCM; Clay: non-specific cation exchange model	Extraction en batch d'un sol et membrane de Donnan	Cd, Pb, Cu, Ni, Zn	Plusieurs techniques	pH, solubilisé Ca, Mg, Al, Fe actif Cd, Pb, Cu, Ni, Zn	MOS: 84% AH et 16% AF MOD: 65% AF	Depuis Tipping et al. (2003)	Plusieurs techniques Reactive cryst-Fe = 16% of total	(Peng et al., 2018)

AOD: ammonium oxalate under darkness méthode

AF et AH : Acide fulvique et acide humique

Asc: ascorbate/ascorbique acide

CCM : constant capacitance model (Lofts and Tipping, 1998)

CD-MUSIC : charge distribution and multisite surface complexation (Hiemstra and Van Riemsdijk, 1996)

Crist : cristallisé

DCB : dithionite-citrate bicarbonate Fe

Fh : ferrihydrite

HFO: hydrous ferric oxides

GTLM: generalized two-layer model (Dzombak and Morel, 1990)

MOD : matière organique dissoute

MOS : matière organique solide

Ox: oxalate extractable

III. Généralités sur le traitement des eaux usées et de ruissellement

Parmi les enjeux sociétaux du XXIe siècle, on retrouve la lutte contre le changement climatique, la gestion des risques naturels, la sécurisation de l'accès à l'eau potable, la santé, la sécurité alimentaire… En ce qui concerne plus spécifiquement les problématiques liées à la gestion de l'eau et notamment la gestion des eaux usées domestiques et des eaux de ruissellement, le plan stratégique européen pour la sauvegarde des ressources en eaux a établi en 2012 que les solutions fondées sur la nature ou infrastructures vertes devraient être adoptées, lorsque possible, comme mesures de mise en œuvre de la directive-cadre sur l'eau. Les solutions fondées sur la nature sont définies par l'union européenne comme étant l'ensemble des solutions inspirées, continuellement soutenues et utilisant la nature, conçues pour relever les défis sociétaux d'une manière efficace et adaptable sur le plan de la gestion des ressources afin d'apporter simultanément des avantages économiques, sociaux et environnementaux (Maes and Jacobs, 2017). Quelques années plus tard, un rapport de la commission européenne de 2019 (European Commission, 2019) prévoit le renforcement de la mise en œuvre de ces solutions fondées sur la nature en améliorant l'accès au financement, en augmentant le socle de connaissances et en contribuant au développement de projets à l'échelle de l'Union européenne. Un large panel de solutions fondées sur la nature a montré son efficacité comme outil de gestion des eaux (Cross et al., 2021). On peut notamment citer la réimplantation des mangroves permettant de limiter l'impact de la montée des eaux sur l'érosion des littoraux ou bien encore l'utilisation de toitures végétalisées et de noues afin de lutter contre l'imperméabilisation des zones urbaines. Dans la gestion plus spécifique des eaux usées domestiques et industrielles en petites collectivités et des eaux de ruissellement en milieu urbain, les filtres plantés de roseaux et les bassins d'infiltration sont deux solutions fondées sur la nature classiquement utilisées (Cross et al., 2021).

Récemment, le développement de solutions fondées sur la nature dédiées aux traitements des eaux usées et eaux de ruissellement a généré la production de dépôts fortement organiques issus de la rétention des particules contenues dans ces eaux. Ces dépôts ont déjà fait l'objet d'études ayant notamment permis d'accroitre nos connaissances sur leurs caractéristiques physico-chimique et leurs évolutions dans le temps (Drapeau et al., 2017; Kania et al., 2018a, 2017; Kim et al., 2015; Tedoldi et al., 2016). La participation active de ces dépôts dans la rétention des polluants des eaux a notamment pu être mise en évidence (Kim et al., 2015; Kim et al., 2014; Mermillod-Blondin et al., 2015; Walaszek et al., 2018). Cependant, les études dédiées à la compréhension des mécanismes de rétention/remobilisation des polluants retenus dans ces dépôts, comme cela a pu être fait sur des échantillons de sol naturels, sont plus rares (Drapeau et al., 2017; Kania et al., 2019; Peng et al., 2018).

Dans la suite de cette section, nous verrons les caractéristiques physico-chimiques des eaux usées et des eaux de ruissellement, les systèmes de traitement fondés sur la nature permettant de les traiter et les caractéristiques chimiques des résidus issus de ces traitements.

3.1 Caractéristiques physico-chimiques des eaux usées et des eaux de ruissellement

Les eaux usées et de ruissellement générent un large panel de polluants dont la spéciation et la distribution en taille des particules va largement impacter leur accumulation au sein des dépots des solutions de traitements fondées sur la nature. La littérature en lien avec la distribution de taille et la spéciation des polluants des eaux usées et de ruissellement sera donc décrite dans la prochaine section afin de mieux comprendre les caractéristiques des dépots engendrés par la rétention de ces particules.

a. Les matières en suspension.

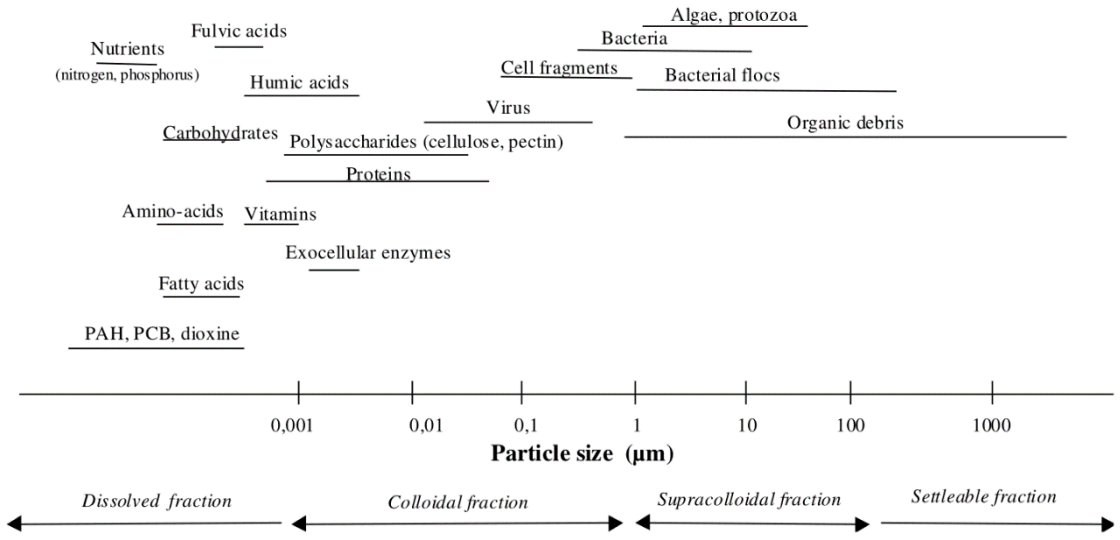

Fig.8. Description de la taille des principaux contaminants décrits par Azema et *al.* (2002)

Comme présenté sur la figure 8, les particules des eaux usées sont séparées en 4 classes, selon leur taille : la fraction dissoute (< 1nm), la fraction colloïdale (1nm – 0,45 µm), la fraction supra-colloïdale (0,45 µm – 100 µm) et enfin la fraction « sédimentable » (> 100 µm) (Azema et al., 2002; Dulekgurgen et al., 2006). La concentration en matières en suspension des eaux usées domestiques brutes peut être particulièrement conséquente avec en moyenne 300 mg.L^{-1} d'eaux usées (Gourlay-francé et al., 2011; B. Kim et al., 2015; Kim et al., 2014). Plus de 75 % du poids de ces particules en suspension est composé de matières organiques (Kania et al., 2018a). L'ajout de chlorure ferrique, un floculant couramment utilisé dans le cadre du traitement des eaux usées et, notamment, sur certaines stations à filtre planté (Kania et al., 2017; Kim et al., 2015; Kim et al., 2014), permet la précipitation d'hydroxydes de fer et la

sorption de matières organiques ou d'éléments très solubles comme le phosphore. La concentration en particule en suspension des eaux de ruissellement est quantitativement moins importante que celle des eaux usées domestiques avec approximativement 100 $mg.L^{-1}$ (Brezonik and Stadelmann, 2002). La matière organique représente approximativement 50 % du poids de ces particules en suspension (Baum et al., 2021; Sønderup et al., 2016).

b. Les polluants inorganiques.

Les nutriments. Au regard de leur impact sur l'eutrophisation des milieux, l'azote et le phosphore sont, avec le carbone, l'objet de toutes les attentions dans la filière du traitement des eaux. La concentration moyenne en azote total des eaux usées domestiques oscille autour de 40-50 $mg.L^{-1}$ (Kim et al., 2014; Tchobanoglous et al., 2011), avec approximativement 50 % du N total retrouvé sous forme organique. Les eaux usées domestiques concentrent comparativement moins de phosphore avec approximativement 10 $mg.L^{-1}$ de phosphore total (Tchobanoglous et al., 2011), majoritairement retrouvé sous forme inorganique (orthophosphate). L'abattement du phosphore peut se faire via (i) la précipitation des phosphates d'aluminium, de fer ou des apatites, (ii) la sorption sur les surfaces solides des particules en suspension et (iii) par assimilation biologique. L'ajout de chlorure ferrique aux eaux usées domestiques permet notamment la complexation du phosphore sur les oxydes de fer précipités (Kim et *al.,* 2014). La problématique liée à l'élimination des nutriments est moins importante pour les eaux de ruissellement où l'on retrouve des concentrations en phosphore et azote total respectivement comprises autour de 0,5 et 2,5 $mg.L^{-1}$ (Brezonik and Stadelmann, 2002). La majorité étant associée aux particules en suspension. Dans des eaux de ruissellement de zones urbaines, Vaze et Chiew en 2004 ont mesuré plus de 90 % de l'azote et du phosphore dans la fraction solide de ces eaux.

Les métaux et métalloïdes. La plus grande source de métaux et métalloïdes des eaux usées et des eaux de ruissellement provient des activités humaines. Les systèmes d'épuration représentent l'un des derniers lieux de transition des métaux traces produits par l'activité humaine et constituent donc le dernier lieu de récupération de ces métaux avant leur retour dans l'environnement.

Le cuivre, le plomb, le nickel et le zinc sont parmi les métaux traces divalents les plus concentrés dans les eaux usées domestiques avec des concentrations de l'ordre du $\mu g.L^{-1}$ (Hargreaves et al., 2018) (Vriens et al., 2017*)*. De larges différences de concentrations peuvent être observées dans la littérature (Carletti et al., 2008; Farkas et al., 2020; Soonthornnonda and Christensen, 2008), conséquence d'eaux usées de différentes origines. Parmi ces métaux, Cu, Pb et Zn sont principalement retrouvés associés aux matières en suspension (> 0,45 µm) alors que le Ni est majoritairement sous une forme dissoute (< 0,45 µm) (Choubert et al., 2011; Gardner et al., 2013; Hargreaves et al., 2018; Karvelas et al., 2003). Dans la fraction solide, ces éléments sont majoritairement complexés aux matières organiques solides

(Carletti et al., 2008). Des travaux d'ultrafiltration de la fraction dissoute d'eaux usées domestiques effectués par Hargreaves et al. (2018) ont permis de montrer que 20 % de ces éléments était présents dans la fraction < 1 kDa, probablement sous forme ionisée ou complexés à de petits ligands inorganiques. La pollution aux métaux et métalloïdes semble être la principale pollution des eaux de ruissellement. Dans de nombreuses zones urbaines, ces eaux concentrent d'importantes quantités en Zn et Pb, dont la concentration peut dépasser plusieurs centaines de $\mu g.L^{-1}$ en fonction de leur localisation (Brezonik and Stadelmann, 2002; Brown and Peake, 2006; Milik and Pasela, 2018). Alors que Zn et Cu sont principalement retrouvés dans la fraction dissoute, associés aux matières organiques dissoutes (Boulanger and Nikolaidis, 2003), le Pb est majoritairement retrouvé dans la fraction solide des eaux de ruissellement probablement associé à des particules organo-minérales solides (Herngren et al., 2005; Yousef et al., 1984). Ces informations sont cependant à considérer au regard de l'importante variabilité observée en fonction du lieu d'échantillonnage (Aryal et al., 2010). En effet, Lindfors et al (2020) ont montré l'affinité importante des métaux d'intérêts pour la phase particulaire des eaux de ruissellement d'une zone urbaine. Les études portant sur l'affinité de ces éléments pour les phases colloïdales des eaux de ruissellement sont rares. Cependant, Lindfors et al (2020) ont pu mettre en évidence que les éléments Zn, Cd, Cu, Ni et Cr mesurés dans la phase dissoute d'eaux urbaines sont majoritairement retrouvés dans la fraction réellement dissoute (*i.e* > 3 kDa dans cette étude).

La concentration en fer, aluminium et manganèse s'exprime, quant à elle, en $mg.L^{-1}$ dans les eaux usées et les eaux de ruissellement (Aryal et al., 2010; Yousef et al., 1984). Quel que soit le type d'eaux considéré, ces éléments sont très largement associés aux matières en suspension. Gardner et *al.* (2013) ont montré que plus de 90 % du fer et de l'aluminium est retrouvé dans la fraction > 0,45 µm dans des eaux usées domestiques provenant de 16 stations d'épuration différentes du Royaume-Uni. Ces éléments peuvent être associés à la matière organique et/ou précipités sous la forme d'oxy(hydro)oxides métalliques. Le chrome, un autre métal de transition souvent présent sous la forme de Cr(III) dans des conditions oxydantes, est retrouvé à plus de 80 % dans la phase particulaire des eaux usées (Choubert et al., 2011; Farkas et al., 2020) et des eaux de ruissellement (Lindfors et al., 2020).

Dans les eaux usées domestiques, les éléments de la classe des métalloïdes comme l'arsenic et l'antimoine sont retrouvés dans des concentrations inférieures à celles des métaux divalents, de l'ordre de quelques $\mu g.L^{-1}$ (Choubert et al., 2011; Du et al., 2020; Farkas et al., 2020). La distribution de ces éléments entre les phases solides et dissoutes n'est pas claire puisque Choubert et al. (2011)

montrent, par exemple, que 70 % de l'arsenic est retrouvé dans la fraction dissoute quand Carletti et al. (2008) n'en comptent que 45 %.

c. Les molécules organiques.

La matière organique. La concentration en matières organiques des eaux usées brutes varient largement selon les stations d'épuration considérées. Comme présenté en amont, une très large fraction de la concentration en particules en suspension est organique. La quantité de carbone organique dissout est comprise entre 40 et 90 $mg.L^{-1}$ (Hargreaves et al., 2017; Katsoyiannis and Samara, 2007). Ces molécules organiques dissoutes semblent équitablement distribuées entre la fraction colloïdale et la fraction réellement dissoute (*i.e. <1-3 kDa)* (Hargreaves et al., 2017). Comparativement, la concentration totale en carbone organique (*i.e.* prenant en compte les fractions solides et dissoutes) des eaux de ruissellement, bien que variant en fonction des études, reste globalement comprise autour de 10 $mg.L^{-1}$, le carbone organique dissout représentant plus de 90 % du carbone total mesuré dans des eaux de ruissellement de zones urbaines (Grout et al., 1999; Kalev and Toor, 2020).

Les micropolluants organiques synthétiques. Dans cette classe de molécule organique synthétique, on retrouve des polluants dont le suivi dans les eaux usées est relativement récent. Parmi ces contaminants dont le suivi est relativement récent, de nombreuses molécules médicamenteuses connues pour être d'important perturbateur du fonctionnement endocrinien chez l'être humain sont présentes (Kasonga et al., 2021). Les concentrations mesurées dans des eaux usées les plus élevées sont celles de l'acide salicylique et de l'ibuprofène avec des valeurs de concentrations moyennes de 48 et 15 $\mu g.L^{-1}$, respectivement, (Gardner et al., 2013). Pesticides et herbicides sont aussi suivis. Ces molécules ubiquitaires ne sont pas seulement retrouvées dans les eaux usées d'origine rurale, des concentrations non négligeables sont également mesurées en zone urbaine (Köck-Schulmeyer et al., 2013). La concentration de la majorité des pesticides ne dépasse pas 1 $\mu g.L^{-1}$ d'eaux usées (Gardner et al., 2013; Köck-Schulmeyer et al., 2013). Ces molécules et leurs métabolites sont également détectés dans les eaux de ruissellement rurales et urbaines (Chen et al., 2019a). Dans ces eaux aussi les concentrations ne dépassent pas quelques $\mu g.L^{-1}$ pour la plupart des pesticides et herbicides (Weston et al., 2009; Zhang et al., 2011).

Les hydrocarbures. La pollution aux hydrocarbures concerne principalement les eaux usées de ruissellement puisque cette pollution provient, en partie, de la circulation automobile. La concentration en hydrocarbure total peut se mesurer en $mg.l^{-1}$ dans des zones résidentielles et autoroutières (Gautier, 1998; Pagotto, 1999; Saget, 1994). D'après le guide technique des bassins de

retenue d'eaux pluviales réalisées par l'Agence de l'Eau Seine Normandie en 1994, les hydrocarbures sont à plus de 80 % retrouvés sous forme solide dans les eaux de ruissellement.

Les plastiques. En plus de la problématique de l'accumulation de plastique dans de nombreux écosystèmes, ces composés sont aussi des vecteurs de transport et d'accumulation de micropolluants dans l'environnement (Sarkar et al., 2021). La pollution plastique peut être découpée en deux familles en fonction de leur taille : (i) les microplastiques dont la taille globale peut atteindre plusieurs centaines de micromètres, et (ii) les nanoplastiques d'une taille équivalente à celle de colloïdes (1 nm – 0,45 µm). Récemment Liu et al. (2021) ont pu calculer une valeur moyenne de 1,9 x 10^3 particules plastiques par litre de solution dans une grande diversité d'eaux usées. L'agrégation de micro et nanoparticules avec les particules en suspension contenues dans les eaux et leur sédimentation est le principal processus à l'origine de leur élimination (Carr et al., 2016; Praetorius et al., 2012; Quik et al., 2015). La problématique des micro et nanoplasiques contenus dans les eaux de ruissellement reste encore assez peu explorée malgré le possible dépôts de composés plastiques issus de la dégradation des pneus notamment. La première mise en évidence de la présence de microplastiques dans ces eaux semble avoir été réalisée par Dris et al. (2018) sur la ville de Paris. L'étude de Treilles et al. (2021) à l'aide d'un travail bibliographique montre que la concentration en microplastiques varie entre 0,5 et 1050 particules par litre de solution. Cette variabilité pouvant provenir du lieu d'échantillonnage et de l'intensité de l'événement pluvieux.

3.2 Les solutions fondées sur la nature pour le traitement des eaux usées et de ruissellement

a. Traitement des eaux usées par filtres plantés de roseaux

Présentation de la structure. Les filtres plantés sont une solution extensive de traitement des eaux usées, s'inspirant des capacités épuratoires des zones humides naturelles. Ces solutions peuvent dans certains cas être utilisées dans la gestion des eaux de ruissellement. Bien que différentes familles de filtres plantés existent, tous reposent, en revanche, sur les mêmes principes de base : (i) une fosse imperméabilisée, remblayée à l'aide de substrats minéraux de différentes granulométries sur laquelle est plantée des espèces végétales adaptées aux conditions humides, (ii) un système d'approvisionnement en eaux permettant de saturer totalement ou partiellement le substrat et (iii) un système d'évacuation des eaux usées traitées vers les eaux de surface environnantes. Ces systèmes sont principalement utilisés pour le traitement des eaux usées domestiques de petites collectivités (< 2000 équivalents habitant). Ils sont aussi utilisés dans le traitement secondaire d'effluent de station d'épuration « classique » (Barber et al., 2001; Park et al., 2018), dans le traitement des eaux pluviales

urbaines (Walaszek et al., 2018), dans l'assainissement d'eaux industrielles principalement rejetées par l'industrie agroalimentaire (Kim et al., 2014; Serrano et al., 2011). La capacité épuratoire de ces systèmes repose sur une multitude de mécanismes physico-chimiques mais aussi biologiques (Brix, 1987).

Les filtres plantés de roseaux peuvent être subdivisés en deux sous-catégories en fonction du mode d'écoulement des eaux usées dans le bassin filtrant (fig. 6) :

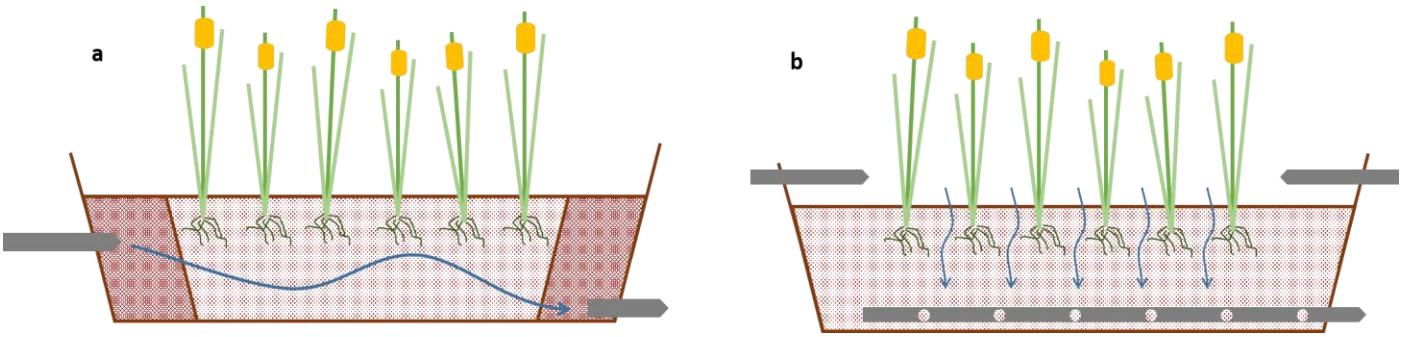

Fig.6. Représentation schématique des bassins en fonction de la direction du flux : a) filtre planté à écoulement horizontal et b) filtre planté à écoulement vertical.

- Les filtres à écoulement horizontal

Dans ces systèmes, des eaux usées non brutes, prétraitées mécaniquement, s'écoulent horizontalement sous la surface du filtre planté maintenu en permanence saturé en eau, afin de créer des conditions anoxiques dans la quasi-totalité du filtre (Vymazal, 2019). Ces systèmes sont, par exemple, particulièrement adaptés au traitement de l'ammonium. Le point d'entrée de l'eau est positionné en dessous de la surface des filtres. Afin de garantir une immersion constante, l'alimentation en eaux est continue.

- Les filtres à écoulement vertical

Au sein des systèmes à écoulement vertical « français », les eaux usées brutes sont déversées à la surface du filtre. Ces systèmes, subdivisés en plusieurs cellules, reçoivent alternativement de gros volumes d'eaux usées (appelés bâchées). Ces eaux vont ensuite pouvoir percoler à l'intérieur du massif filtrant. Ces filtres sont classiquement non saturés. Cependant, l'ajout d'une zone saturée en fond de filtre permet de créer des conditions anoxiques favorisant les processus de dénitrification et donc l'abattement en carbone et en azote du système. La rétention des particules en suspension contenues dans les eaux usées provoque la création d'un dépôt fortement chargé en matières organiques participant par la suite au processus de filtration (Molle 2014). Ce dépôt, appelé dépôt de boue a un

taux d'accumulation de 2-3 cm par an (Kania, 2018; Kim et al., 2014). La filière française classique est composée d'un second étage de filtration (fig. 7). Les eaux sont alors récupérées au fond du 1er étage par un système de drainage puis transmises, par bâchées, au second étage. Ce second étage permet d'augmenter l'abattement en demande chimique en oxygène (DCO) et en matières en suspension (MES) mais augmente également l'efficacité de la rétention de l'azote en favorisant des processus de nitrification/dénitrification non complètement remplis en 1er étage.

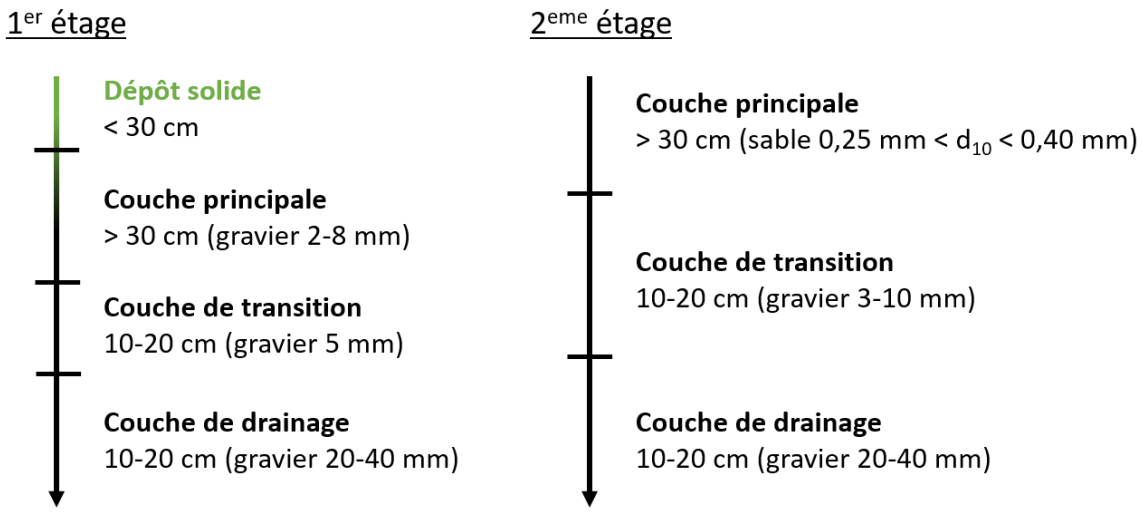

Fig.7. Profil et composition des différentes strates habituellement rencontrées dans un filtre planté à écoulement vertical (adapté de Molle et *al.,* 2005).

Mécanismes de rétention des polluants (filière FP à écoulement vertical). Comme évoqué précédemment, les eaux usées domestiques sont constituées d'une variété importante de polluants organiques et inorganiques associés à des risques environnementaux potentiellement importants. Leur rétention au sein des systèmes de traitement des eaux est un enjeu environnemental majeur. Le devenir de ces polluants est largement contrôlé par leur répartition entre phases liquides et solides (Dulekgurgen et al., 2006; Levine et al., 1991) à l'intérieur des eaux usées. Quand, associés aux particules en suspension, ces contaminants vont être éliminés de l'eau par un processus de sédimentation, ceux plus largement distribués dans la phase liquide vont être plus difficilement éliminés (Choubert et *al.,* 2011). Molle et al. (2005) ont par exemple montré sur une étude réalisée sur plus de 81 stations que plus de 95 % des particules en suspension et donc les polluants associés étaient éliminés sur le premier étage des filtres plantés à écoulement vertical. C'est l'accumulation de ces matières en suspension contenues dans les eaux usées qui induit la formation d'une couche à la surface du premier filtre appelée dépôt de boue. Des auteurs ont mis en évidence la participation active de cette couche aux performances épuratoires des filtres plantés (Kania, 2018; Boram Kim et al., 2015; Molle et al., 2005). Le développement d'une structure microporeuse à l'intérieur de ces dépôts permet

d'augmenter la rétention des particules en suspension, mais aussi celle des contaminants de la phase dissoute en favorisant leur complexation sur les surfaces solides sédimentées au sein du dépôt (Kania et al., 2018a; Kim et al., 2015; Molle, 2013). En condition aérobie, cette couche est aussi le lieu d'activité microbienne intense responsable de la transformation des composés organiques et des processus de nitrification (Chazarenc and Merlin, 2005; Morvannou et al., 2011). L'élimination de l'azote se fait principalement par une combinaison de processus physico-chimiques et biologiques. Succinctement, via des processus d'ammonification, l'azote organique est minéralisé. Les processus de nitrification/dénitrification, effectués par des bactéries autotrophes et hétérotrophes respectivement, nécessitent des conditions chimiques particulières. La dénitrification, étape finale de la transformation de l'azote, requière notamment des conditions anoxiques strictes, et une source de carbone organique facilement biodégradable pour les bactéries. Dans les filtres plantés, l'absorption d'azote dans le système racinaire des plantes est aussi un phénomène non négligeable (Grebenshchykova, 2021).

Globalement, les propriétés structurales de cette couche, la qualité et la quantité de matières organiques qu'elle contient et qu'elle émet, ainsi que son évolution dans le temps sont des facteurs d'influence importants des performances épuratoires du système dans son ensemble (Collard et al., 2017; Kania et al., 2017, 2018a, 2019; Kim et al., 2014; Kim et al., 2015; Kim et al., 2016; Peruzzi et al., 2013).

b. Traitement des eaux de ruissellement par bassins d'infiltrations.

Présentation de la structure. Les bassins d'infiltrations reçoivent les eaux de ruissellement pluviales provenant de bassins versants de taille variable. Le fonctionnement et la conception de ces ouvrages dépend des caractéristiques physico-chimiques du sous-sol (conductivité hydraulique…) et de la position de la nappe phréatique (Gonzalez-Merchan, 2012). Le bassin d'infiltration est souvent creusé sur le sol en place (fig. 8), l'ajout d'une couche de fond faite de matériaux drainant similaire au filtre planté de roseau est une option possible permettant notamment d'homogénéiser l'infiltration de l'eau. En règle générale, l'épaisseur de cette couche de fond n'est pas inférieure à 1 mètre de profondeur (Barraud, 2009). Une couche de géotextile peut être ajoutée entre le sous-sol naturel et les strates supérieures rapportées. Les eaux acheminées vers ces systèmes peuvent être prélevées par la végétation sur place ou être évacuées par percolation dans le sol sous-jacent. Avant d'être déversées sur ces bassins, les eaux de ruissellement peuvent subir une série de prétraitements permettant par exemple la rétention des flottants. Sur la couche de fond du bassin viennent se déposer les particules en suspension des eaux de ruissellement créant, à l'instar des filtres plantés, une nouvelle couche de dépôt appelé sédiment. Le Coutumer (2008) a pu estimer l'accumulation des particules en suspension

sur la couche de fond à 1-3,5 mm par an. Par ailleurs, après 20 ans de fonctionnement, l'épaisseur de ce sédiment peut atteindre des hauteurs variant de 5 à 30 cm (Cannavo et al., 2010).

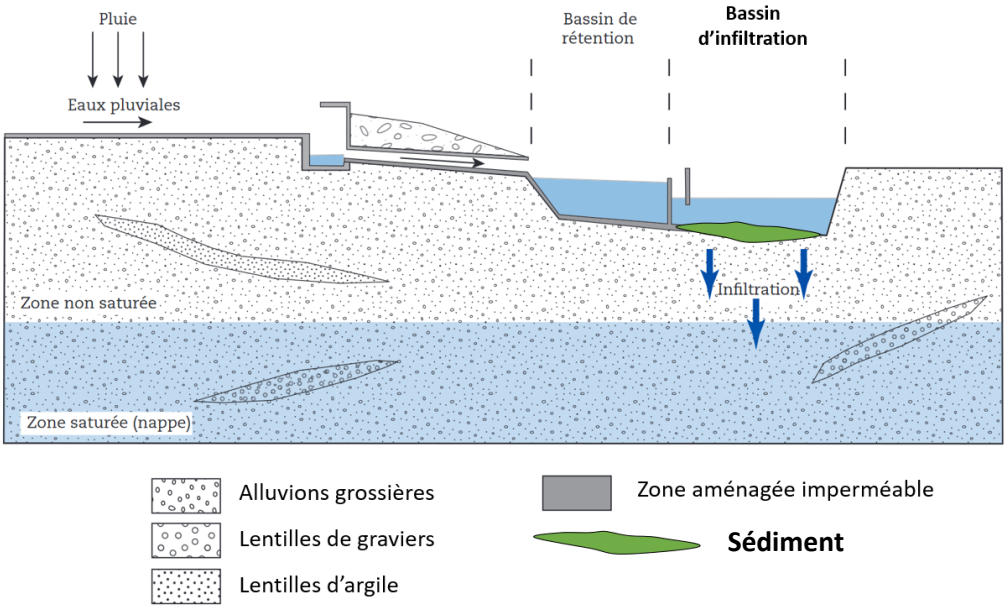

Fig.8. Représentation schématique d'un bassin d'infiltration précédé d'un bassin de rétention modifié depuis Winiarski (2014).

Mécanismes de rétention des polluants. L'ensemble regroupant la couche de fond et la couche de dépôt participe activement aux propriétés épuratoires des bassins d'infiltrations sur des principes relativement similaires à ceux développés pour les filtres plantés de roseaux. Ces principes reposent sur la rétention physique des particules en suspension (Martinelli, 1999), la sorption chimique des polluants sur les surfaces solides organiques et minérales constitutives de cette couche (Clozel et al., 2006b; Gautier, 1998; Martinelli, 1999; Tedoldi et al., 2016a), et l'activité microbienne responsable notamment de la minéralisation de la matière organique. Les performances de ces filtres sont liées à la nature des massifs filtrants (Lalire, 2010). On peut cependant noter des taux moyens d'abattement supérieurs à 90 % pour les matières en suspension , de 80 % pour les hydrocarbures, supérieurs à 60 % pour l'azote et le phosphore total (Landphair, 2001; Winer, 2000). La rétention des métaux traces semble elle aussi globalement importante puisque des taux d'abattement de plus de 80 % du Zn et du Pb ont été mesurés sur des bassins d'infiltration (Lalire, 2010; Landphair and Building, 2001).

3.3 Caractéristiques des dépôts des solutions fondées sur la nature : le cas des filtres plantés et des bassins d'infiltrations.

Comme présenté précédemment, une large fraction des particules en suspension des eaux usées et de ruissellement est retenue à la surface des filtres plantés et des bassins d'infiltrations. Les dépôts,

résultant de l'accumulation des particules en suspension, présentent des teneurs en matières organiques et en contaminants importantes. La Fig. 9, en se basant sur des résultats d'analyses élémentaires disponibles dans la littérature, a pour objectif de comparer les dépôts des deux types de système, de quantifier l'accumulation de contaminants inorganiques mais aussi le potentiel risque lié à la remobilisation de ces éléments.

a. Composition élémentaire des dépôts

Afin d'illustrer la composition élémentaire des dépôts, les résultats d'analyses de Kania, (2018) obtenus sur 7 boues d'âges matures ont été compilés dans la Fig. 9 où sont uniquement présentés les éléments les plus concentrés. Ces dépôts comprennent des taux de matières organiques généralement supérieurs à 50 % de leur poids en matière sèche (Boutin and Lienard, 2003; Kania et al., 2018a; Trein et al., 2020). Ce taux peut évoluer en fonction de l'âge du dépôt (Kania et al., 2018b) mais reste peu influencé par la nature des eaux usées. A titre de comparaison, ces taux de matières organiques sont comparables à ceux observés dans des tourbières (Negassa et al., 2019; Rodriguez et al., 2021). Un large travail de caractérisation de la matière organique solide constituant des boues d'âges différents a été effectué (Kania et al., 2018b, 2017; Kania et al., 2019). Parmi ces études, Kania et al. (2018b) a permis de mettre en évidence une stabilité des caractéristiques physico-chimiques de la matière organique des boues de plus de 3 ans. Les humines, les acides humiques et fulviques représentent approximativement et respectivement 60, 20 et 20 % du carbone organique total contenu dans ces boues matures. Le zinc et le cuivre sont les deux principaux métaux traces retrouvés au sein des dépôts solides de filtre planté avec 750 et 426 $mg.kg^{-1}$ de matière sèche, respectivement. Les contenus totaux en azote et phosphore dépassent les 10 $g.kg^{-1}$ de MS. Des travaux d'extractions séquentielles ont permis de mettre en évidence l'importance de la complexation de ces éléments majeurs et traces par les matières organiques et hydroxydes métalliques solides (Kania et al., 2019; Kim et al., 2016).

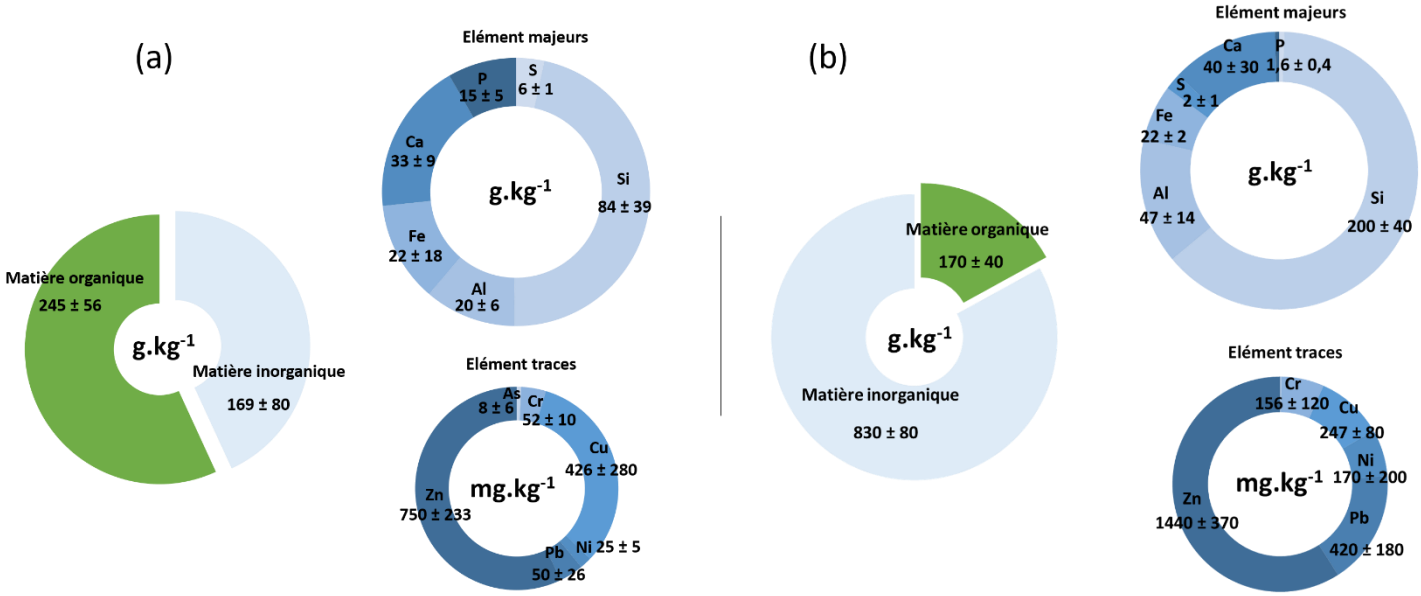

Fig.9. Moyennes et écart-types des contenus totaux en matières organiques et principaux éléments majeurs et traces mesurés sur (a) 7 dépôts matures de filtres plantés à écoulement vertical obtenus par Kania, 2018 et (b) 15 dépôts échantillonnés sur 4 bassins d'infiltrations de zone urbaines et d'axes autoroutier obtenu par Clozel et al (2006) (exprimé en g ou mg.kg^{-1} de matière sèche).

Les sédiments issus de l'infiltration des eaux de ruissellement montrent une signature géochimique bien particulière (Fig. 9b). La couche de dépôts affiche des contenus en matière organique élevée atteignant parfois plus de 30 % du poids en matière sèche dans les zones les plus sollicitées (Clozel et al., 2006; Gonzalez-Merchan, 2012). Ce taux a par exemple tendance à diminuer avec l'éloignement par rapport à la zone d'arrivée des eaux (Drapeau et al., 2017). Les données récoltées par Clozel et al (2006), sur 4 bassins d'infiltrations urbains différents, montrent des concentrations en métaux trace surpassant largement les concentrations relevées dans les dépôts de boue de filtres plantés de roseaux évoqués précédemment. Les teneurs en azote et phosphore sont en revanche inférieures (Drapeau et al., 2017). A l'aide de l'extraction séquentielle, Clozel et al. (2006) ont pu montrer l'affinité du cuivre, du zinc et du plomb pour les phases organiques et pour les oxydes présents dans les dépôts. Le chrome et le nickel semblent eux plus largement associés à la fraction résiduelle, sous forme précipité ou adsorbé sur des oxydes récalcitrants.

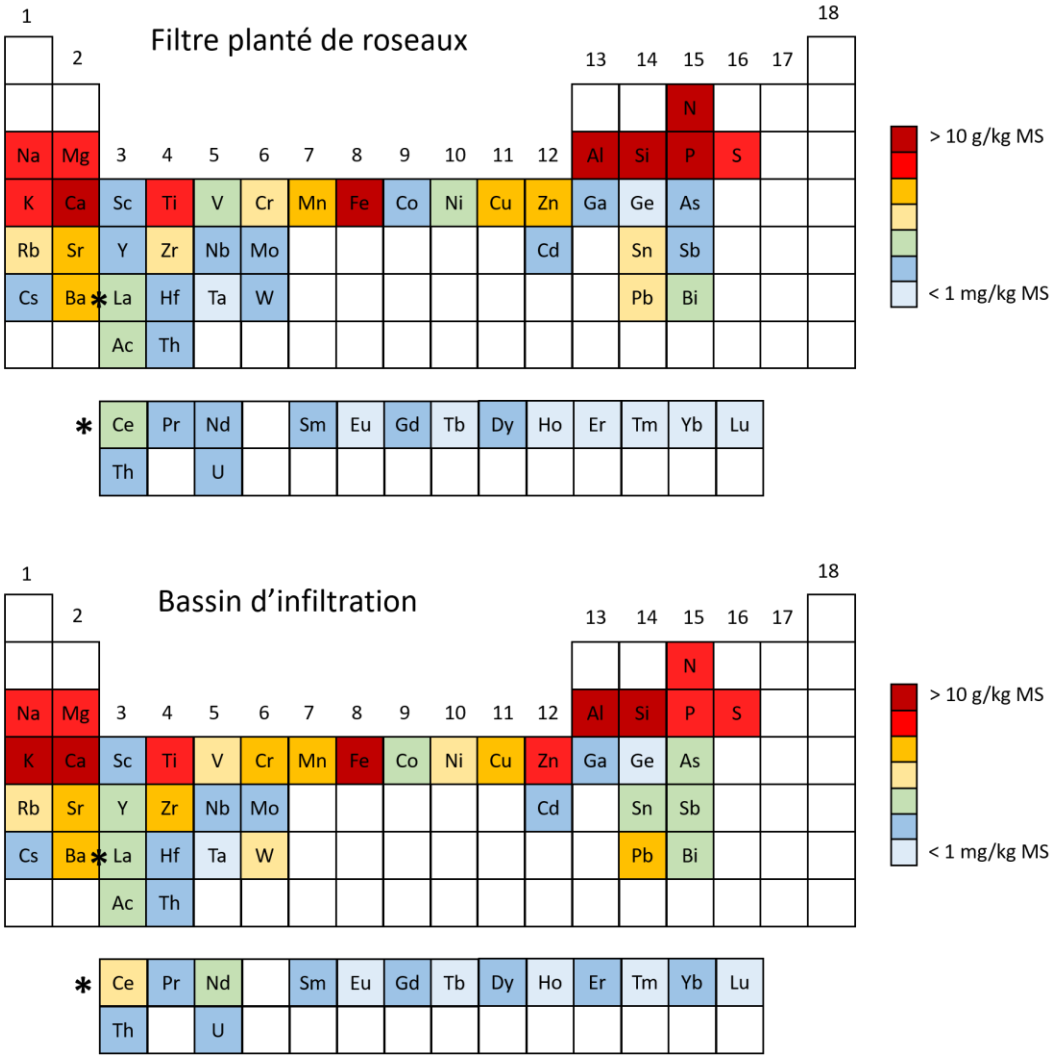

Fig.10. Présentation de la teneur de 56 éléments au sein des dépôts de filtres plantés à écoulement vertical (en haut) et de bassins d'infiltrations (en bas). Moyenne effectuée sur un panel supérieur à 7 dépôts de boue matures obtenues dans le cadre de la thèse de Manon Kania (2018) et sur des données de sédiments de bassins d'infiltrations provenant de différentes études (Clozel et al., 2006b; Drapeau, 2018) et du projet GEESOL.

Pour compléter la figure 9 et avoir une vue d'ensemble sur l'accumulation d'un large spectre d'éléments, les contenus totaux de 56 éléments mesurés sur des dépôts d'âges matures de filtres plantés (Kania, 2018) et de bassins d'infiltrations (Clozel et al., 2006b ; Drapeau, 2018 ; GEESOL) ont été compilés sur un tableau périodique des éléments (voir figure 10). Parmi les éléments les moins concentrés, on retrouve la classe des lanthanides et des actinides avec des contenus de quelques $mg.kg^{-1}$ de MS. Les dépôts de bassins d'infiltrations en contiennent globalement des quantités plus importantes comparativement aux dépôts de filtres plantés de roseaux. C'est d'ailleurs le cas pour la majorité des éléments de la figure 10 : la teneur en métaux et métalloïdes est plus importante au sein

des dépôts de bassins d'infiltrations. Seul les éléments non-métaux comme le phosphore et l'azote sont plus concentrés dans les dépôts de boue de filtres plantés.

b. Influence du pH sur la remobilisation des éléments

Ces résultats interrogent donc sur la possible remobilisation de ces éléments. A titre d'exemple, le dépôt de boue des filtres plantés peut être périodiquement traversé par des eaux usées dont les valeurs de pH varient entre 7 et 8,5 (Dulekgurgen et al., 2006; Kim et al., 2014). Mais ces valeurs peuvent atteindre des pH compris entre 5 et 7 (Serrano et al., 2011; Sheridan et al., 2011) dans le cas d'eaux usées d'origine vinicole. Or, comme évoqué précédemment, le pH contrôle le relargage de matières organiques et des éléments associés dans de nombreux environnements (Almas et al., 2007; Grybos et al., 2007a, 2009a). Ces interrogations sur la remobilisation de ces contaminants sont aussi à mettre en perspective des voies de réutilisation de ces dépôts. En effet, en France, 70 % des boues issues du traitement des eaux usées (toutes filières confondues) sont valorisées en épandage agricole. Ce chiffre grandit encore en regardant uniquement les dépôts issus des filtres plantés de roseaux. Une fois épandues, ces boues peuvent aussi être soumises à des conditions environnementales variables, dont les conséquences sur la remobilisation d'éléments contenus dans ces dépôts ont été peu étudiées (Fang et al., 2016a).

Afin de mieux comprendre les processus de remobilisation des dépôts issus de solutions de traitements des eaux fondées sur la nature, plusieurs études ont évalué l'influence des variations de pH, en conditions contrôlées, sur le relargage (Drapeau et al., 2017; Fang et al., 2016a; Kania et al., 2019; Kim et al., 2016). A l'instar des milieux poreux d'origine naturelle (Grybos et al., 2007a), les matières organiques des dépôts se sont révélées sensibles aux variations de pH. De même, les éléments traces et majeurs montrent des courbes de relargage en « V » entre pH 2 et 12 (Drapeau et al., 2017; Fang et al., 2016a; Kania et al., 2019) symptomatiques d'une forte sensibilité aux variations de pH. Kim et al. (2016) ont aussi pu mettre en évidence l'influence des oxydes métalliques solides et, plus précisément, l'influence de leur dissolution dans le relargage du phosphore contenu dans des dépôts de filtre planté.

Bien que prépondérante dans la compréhension des mécanismes géochimiques à l'origine de la remobilisation d'éléments contenus dans ces dépôts, les analyses précédemment évoquées apportent des données essentiellement quantitatives. Or, des informations sur la spéciation en solution peuvent permettre de mieux comprendre les mécanismes de relargage et de transport, mais aussi la biodisponibilité de ces éléments. Au sein de milieux poreux d'origine naturelle, la mobilité et le transfert des éléments traces et majeurs peuvent être, par exemple, fortement impactés par l'émission de phases colloïdales organiques et/ou organo-minérales (Pédrot et al., 2008; Pokrovsky et al., 2005; Raudina et al., 2021a). Comme démontré par Pédrot et al. (2008), la capacité de sorption de ces

colloïdes est dépendante des paramètres chimiques de la solution, des caractéristiques physico-chimiques des colloïdes et de l'élément chimique considéré.

Références :

Aiken, G.R., Hsu-Kim, H., Ryan, J.N., 2011. Influence of Dissolved Organic Matter on the Environmental Fate of Metals, Nanoparticles, and Colloids. Environ. Sci. Technol. 45, 3196–3201. https://doi.org/10.1021/es103992s

Almas, Å.R., Lofts, S., Mulder, J., Tipping, E., 2007. 2 Solubility of major cations and trace metals (Cu, Zn and Cd) in soil 3 extracts of some contaminated agricultural soils near a zinc smelter in 4 Norway: modelling with a multisurface extension of WHAM 41.

Almås, Å.R., Lofts, S., Mulder, J., Tipping, E., 2007. Solubility of major cations and Cu, Zn and Cd in soil extracts of some contaminated agricultural soils near a zinc smelter in Norway: modelling with a multisurface extension of WHAM. European Journal of Soil Science 58, 1074–1086. https://doi.org/10.1111/j.1365-2389.2007.00894.x

Amery, F., Degryse, F., Cheyns, K., Troyer, I.D., Mertens, J., Merckx, R., Smolders, E., 2008. The UV-absorbance of dissolved organic matter predicts the fivefold variation in its affinity for mobilizing Cu in an agricultural soil horizon. European Journal of Soil Science 59, 1087–1095. https://doi.org/10.1111/j.1365-2389.2008.01078.x

Aryal, R., Vigneswaran, S., Kandasamy, J., Naidu, R., 2010. Urban stormwater quality and treatment. Korean J. Chem. Eng. 27, 1343–1359. https://doi.org/10.1007/s11814-010-0387-0

Avena, M.J., Koopal, L.K., 1998. Desorption of Humic Acids from an Iron Oxide Surface. Environ. Sci. Technol. 32, 2572–2577. https://doi.org/10.1021/es980112e

Azema, N., Pouet, M.-F., Berho, C., Thomas, O., 2002. Wastewater suspended solids study by optical methods. Colloids and Surfaces A: Physicochemical and Engineering Aspects 204, 131–140. https://doi.org/10.1016/S0927-7757(02)00006-7

Baigorri, R., Fuentes, M., González-Gaitano, G., García-Mina, J.M., 2007. Analysis of molecular aggregation in humic substances in solution. Colloids and Surfaces A: Physicochemical and Engineering Aspects 302, 301–306. https://doi.org/10.1016/j.colsurfa.2007.02.048

Baken, S., Degryse, F., Verheyen, L., Merckx, R., Smolders, E., 2011. Metal Complexation Properties of Freshwater Dissolved Organic Matter Are Explained by Its Aromaticity and by Anthropogenic Ligands. Environ. Sci. Technol. 45, 2584–2590. https://doi.org/10.1021/es103532a

Barber, L.B., Leenheer, J.A., Noyes, T.I., Stiles, E.A., 2001. Nature and Transformation of Dissolved Organic Matter in Treatment Wetlands. Environ. Sci. Technol. 35, 4805–4816. https://doi.org/10.1021/es010518i

Batjes, N.H., 2016. Harmonized soil property values for broad-scale modelling (WISE30sec) with estimates of global soil carbon stocks. Geoderma 269, 61–68. https://doi.org/10.1016/j.geoderma.2016.01.034

Baum, P., Kuch, B., Dittmer, U., 2021. Adsorption of Metals to Particles in Urban Stormwater Runoff—Does Size Really Matter? Water 13, 309. https://doi.org/10.3390/w13030309

Benedetti, M.F., Van Riemsdijk, W.H., Koopal, L.K., 1996. Humic Substances Considered as a Heterogeneous Donnan Gel Phase. Environ. Sci. Technol. 30, 1805–1813. https://doi.org/10.1021/es950012y

Bongoua-Devisme, A.J., Cebron, A., Kassin, K.E., Yoro, G.R., Mustin, C., Berthelin, J., 2013. Microbial Communities Involved in Fe Reduction and Mobility During Soil Organic Matter (SOM)

Mineralization in Two Contrasted Paddy Soils. Geomicrobiology Journal 30, 347–361. https://doi.org/10.1080/01490451.2012.688928

Bonten, L.T.C., Groenenberg, J.E., Weng, L., van Riemsdijk, W.H., 2008. Use of speciation and complexation models to estimate heavy metal sorption in soils. Geoderma 146, 303–310. https://doi.org/10.1016/j.geoderma.2008.06.005

Boulanger, B., Nikolaidis, N.P., 2003. Mobility and Aquatic Toxicity of Copper in an Urban Watershed1. JAWRA Journal of the American Water Resources Association 39, 325–336. https://doi.org/10.1111/j.1752-1688.2003.tb04387.x

Boutin, C., Lienard, A., 2003. Constructed wetlands for wastewater treatment: the French experience, in: 1st International Seminar on the Use of Aquatic Macrophytes for Wastewater Treatment in Constructed Wetlands. Lisbonne, Portugal, pp. 437–466.

Brezonik, P.L., King, S.O., Mach, C.E., 1991. The Influence of Water Chemistry on Trace Metal Bioavailability and Toxicity to Aquatic Organisms, in: Metal Ecotoxicology. CRC Press.

Brezonik, P.L., Stadelmann, T.H., 2002. Analysis and predictive models of stormwater runoff volumes, loads, and pollutant concentrations from watersheds in the Twin Cities metropolitan area, Minnesota, USA. Water Research 36, 1743–1757. https://doi.org/10.1016/S0043-1354(01)00375-X

Brix, H., 1987. Treatment of Wastewater in the Rhizosphere of Wetland Plants – The Root-Zone Method. Water Science and Technology 19, 107–118. https://doi.org/10.2166/wst.1987.0193

Brown, J.N., Peake, B.M., 2006. Sources of heavy metals and polycyclic aromatic hydrocarbons in urban stormwater runoff. Science of The Total Environment 359, 145–155. https://doi.org/10.1016/j.scitotenv.2005.05.016

Cancès, B., Ponthieu, M., Castrec-Rouelle, M., Aubry, E., Benedetti, M.F., 2003. Metal ions speciation in a soil and its solution: experimental data and model results. Geoderma, Ecological aspects of dissolved organic matter in soils 113, 341–355. https://doi.org/10.1016/S0016-7061(02)00369-5

Cannavo, P., Vidal-Beaudet, L., Béchet, B., Lassabatère, L., Charpentier, S., 2010. Spatial distribution of sediments and transfer properties in soils in a stormwater infiltration basin. J Soils Sediments 10, 1499–1509. https://doi.org/10.1007/s11368-010-0258-7

Carletti, G., Fatone, F., Bolzonella, D., Cecchi, F., Carletti, G., 2008. Occurrence and fate of heavy metals in large wastewater treatment plants treating municipal and industrial wastewaters. Water Sci Technol 57, 1329–1336. https://doi.org/10.2166/wst.2008.230

Carr, S.A., Liu, J., Tesoro, A.G., 2016. Transport and fate of microplastic particles in wastewater treatment plants. Water Research 91, 174–182. https://doi.org/10.1016/j.watres.2016.01.002

Chazarenc, F., Merlin, G., 2005. Influence of surface layer on hydrology and biology of gravel bed vertical flow constructed wetlands. Water Science and Technology 51, 91–97. https://doi.org/10.2166/wst.2005.0295

Chen, C., Guo, W., Ngo, H.H., 2019. Pesticides in stormwater runoff—A mini review. Front. Environ. Sci. Eng. 13, 72. https://doi.org/10.1007/s11783-019-1150-3

Chen, C., Wang, X., Jiang, H., Hu, W., 2007. Direct observation of macromolecular structures of humic acid by AFM and SEM. Colloids and Surfaces A: Physicochemical and Engineering Aspects 302, 121–125. https://doi.org/10.1016/j.colsurfa.2007.02.014

Choubert, J.-M., Pomiès, M., Martin Ruel, S., Coquery, M., 2011. Influent concentrations and removal performances of metals through municipal wastewater treatment processes. Water Science and Technology 63, 1967–1973. https://doi.org/10.2166/wst.2011.126

Christl, I., 2012. Ionic strength-and pH-dependence of calcium binding by terrestrial humic acids. Environmental Chemistry 9, 89–96. https://doi.org/10.1071/EN11112

Christl, I., Metzger, A., Heidmann, I., Kretzschmar, R., 2005. Effect of Humic and Fulvic Acid Concentrations and Ionic Strength on Copper and Lead Binding. Environ. Sci. Technol. 39, 5319–5326. https://doi.org/10.1021/es050018f

Clapp, C.E., Hayes, M.H.B., Simpson, A.J., Kingery, W.L., 2005. Chemistry of Soil Organic Matter, in: Chemical Processes in Soils. John Wiley & Sons, Ltd, pp. 1–150. https://doi.org/10.2136/sssabookser8.c1

Clozel, B., Ruban, V., Durand, C., Conil, P., 2006. Origin and mobility of heavy metals in contaminated sediments from retention and infiltration ponds. Applied Geochemistry 21, 1781–1798. https://doi.org/10.1016/j.apgeochem.2006.06.017

Collard, M., Teychené, B., Lemée, L., 2017. Comparison of three different wastewater sludge and their respective drying processes: Solar, thermal and reed beds – Impact on organic matter characteristics. Journal of Environmental Management, Waste Management with emphasis on municipal waste, biowaste and industrial waste 203, 760–767. https://doi.org/10.1016/j.jenvman.2016.05.070

Cross, K., Tondera, K., Rizzo, A., Andrews, L., Pucher, B., Istenič, D., Karres, N., McDonald, R. (Eds.), 2021. Nature-Based Solutions for Wastewater Treatment: A Series of Factsheets and Case Studies. IWA Publishing. https://doi.org/10.2166/9781789062267

Demey, H., Vincent, T., Guibal, E., 2018. A novel algal-based sorbent for heavy metal removal. Chemical Engineering Journal 332, 582–595. https://doi.org/10.1016/j.cej.2017.09.083

Di Bonito, M., Lofts, S., Groenenberg, J.E., 2018. Chapter 11 - Models of Geochemical Speciation: Structure and Applications, in: De Vivo, B., Belkin, H.E., Lima, A. (Eds.), Environmental Geochemistry (Second Edition). Elsevier, pp. 237–305. https://doi.org/10.1016/B978-0-444-63763-5.00012-4

Dijkstra, J.J., Meeussen, J.C.L., Comans, R.N.J., 2009. Evaluation of a Generic Multisurface Sorption Model for Inorganic Soil Contaminants. Environ. Sci. Technol. 43, 6196–6201. https://doi.org/10.1021/es900555g

Dijkstra, J.J., Meeussen, J.C.L., Comans, R.N.J., 2004. Leaching of Heavy Metals from Contaminated Soils: An Experimental and Modeling Study. Environ. Sci. Technol. 38, 4390–4395. https://doi.org/10.1021/es049885v

Drapeau, C., 2018. Mesure et modélisation de la mobilité et de la spéciation des éléments majeurs et traces métalliques au sein de matrices complexes polluées en fonction du pH : application aux sédiments urbains et déchets miniers (These de doctorat). Lyon.

Drapeau, C., Delolme, C., Chatain, V., Gautier, M., Blanc, D., Benzaazoua, M., Lassabatère, L., 2017. Spatial and Temporal Stability of Major and Trace Element Leaching in Urban Stormwater Sediments. Open Journal of Soil Science 07, 347. https://doi.org/10.4236/ojss.2017.711025

Dris, R., Gasperi, J., Tassin, B., 2018. Sources and Fate of Microplastics in Urban Areas: A Focus on Paris Megacity, in: Wagner, M., Lambert, S. (Eds.), Freshwater Microplastics : Emerging Environmental Contaminants?, The Handbook of Environmental Chemistry. Springer International Publishing, Cham, pp. 69–83. https://doi.org/10.1007/978-3-319-61615-5_4

Du, P., Zhang, L., Ma, Y., Li, Xinyue, Wang, Z., Mao, K., Wang, N., Li, Y., He, J., Zhang, X., Hao, F., Li, Xiqing, Liu, M., Wang, X., 2020. Occurrence and Fate of Heavy Metals in Municipal Wastewater in Heilongjiang Province, China: A Monthly Reconnaissance from 2015 to 2017. Water 12, 728. https://doi.org/10.3390/w12030728

Duffus, J.H., 2002. “Heavy metals” a meaningless term? (IUPAC Technical Report). Pure and Applied Chemistry 74, 793–807. https://doi.org/10.1351/pac200274050793

Dulekgurgen, E., Doğruel, S., Karahan, Ö., Orhon, D., 2006. Size distribution of wastewater COD fractions as an index for biodegradability. Water Research 40, 273–282. https://doi.org/10.1016/j.watres.2005.10.032

Durce, D., Maes, N., Bruggeman, C., Van Ravestyn, L., 2016. Alteration of the molecular-size-distribution of Boom Clay dissolved organic matter induced by Na+ and Ca2+. Journal of Contaminant Hydrology 185–186, 14–27. https://doi.org/10.1016/j.jconhyd.2015.12.001

Dwane, Tipping, E., 1998. Testing a humic speciation model by titration of copper-amended natural waters. Environment International 24, 609–616. https://doi.org/10.1016/S0160-4120(98)00046-4

Dzombak, D.A., Morel, F.M.M., 1990. Surface Complexation Modeling: Hydrous Ferric Oxide. John Wiley & Sons.

El-sayed, M.E.A., Khalaf, M.M.R., Gibson, D., Rice, J.A., 2019. Assessment of clay mineral selectivity for adsorption of aliphatic/aromatic humic acid fraction. Chemical Geology 511, 21–27. https://doi.org/10.1016/j.chemgeo.2019.02.034

European Commission. Joint Research Centre., 2019. Strategic green infrastructure and ecosystem restoration :geospatial methods, data and tools. Publications Office, LU.

Evangelou, V.P., Marsi, M., 2001. Composition and metal ion complexation behavour of humic fractions derived from corn tissue. Plant and Soil 229, 13–24. https://doi.org/10.1023/A:1004862100925

Fang, W., Wei, Y., Liu, J., 2016. Comparative characterization of sewage sludge compost and soil: Heavy metal leaching characteristics. Journal of Hazardous Materials 310, 1–10. https://doi.org/10.1016/j.jhazmat.2016.02.025

FAO, 2017. Carbone organique du sol une richesse invisible 90.

Farkas, J., Polesel, F., Kjos, M., Carvalho, P.A., Ciesielski, T., Flores-Alsina, X., Hansen, S.F., Booth, A.M., 2020. Monitoring and modelling of influent patterns, phase distribution and removal of 20 elements in two primary wastewater treatment plants in Norway. Science of The Total Environment 725, 138420. https://doi.org/10.1016/j.scitotenv.2020.138420

Fernández-Calviño, D., Soler-Rovira, P., Polo, A., Arias-Estévez, M., Plaza, C., 2010. Influence of humified organic matter on copper behavior in acid polluted soils. Environmental Pollution 158, 3634–3641. https://doi.org/10.1016/j.envpol.2010.08.005

Fisher-Power, L.M., Shi, Z., Cheng, T., 2019. Testing the “component additivity” approach for modelling Cu and Zn adsorption to a natural sediment. Chemical Geology 512, 31–42. https://doi.org/10.1016/j.chemgeo.2019.02.038

Flaig, W., Beutelspacher, H., Rietz, E., 1975. Chemical Composition and Physical Properties of Humic Substances, in: Gieseking, J.E. (Ed.), Soil Components: Vol. 1: Organic Components. Springer, Berlin, Heidelberg, pp. 1–211. https://doi.org/10.1007/978-3-642-65915-7_1

Fox, T.R., Comerford, N.B., 1990. Low-Molecular-Weight Organic Acids in Selected Forest Soils of the Southeastern USA. Soil Science Society of America Journal 54, 1139–1144. https://doi.org/10.2136/sssaj1990.03615995005400040037x

Gardner, M., Jones, V., Comber, S., Scrimshaw, M.D., Coello - Garcia, T., Cartmell, E., Lester, J., Ellor, B., 2013. Performance of UK wastewater treatment works with respect to trace contaminants. Science of The Total Environment 456–457, 359–369. https://doi.org/10.1016/j.scitotenv.2013.03.088

Gautier, A., 1998. Contribution à la connaissance du fonctionnement d'ouvrages d'infiltration d'eau de ruissellement pluvial urbain (These de doctorat). Lyon, INSA.

Gonzalez-Merchan, C., n.d. Amélioration des connaissances sur le colmatage des systèmes d'infiltration d'eaux pluviales 299.

Gourlay-francé, C., Bressy, A., Uher, E., Lorgeoux, C., 2011. Labile, dissolved and particulate PAHs and trace metals in wastewater: passive sampling, occurrence, partitioning in treatment plants. undefined.

Grebenshchykova, Z., n.d. Optimisation de la filière de filtres plantés pour l'épuration d'eaux usées municipales en climat continental nordique 162.

Groenenberg, J.E., Dijkstra, J.J., Bonten, L.T.C., de Vries, W., Comans, R.N.J., 2012. Evaluation of the performance and limitations of empirical partition-relations and process based multisurface models to predict trace element solubility in soils. Environmental Pollution 166, 98–107. https://doi.org/10.1016/j.envpol.2012.03.011

Grout, H., Wiesner, M.R., Bottero, J.-Y., 1999. Analysis of Colloidal Phases in Urban Stormwater Runoff. Environ. Sci. Technol. 33, 831–839. https://doi.org/10.1021/es980195z

Grybos, M., Davranche, M., Gruau, G., Petitjean, P., 2007. Is trace metal release in wetland soils controlled by organic matter mobility or Fe-oxyhydroxides reduction? Journal of Colloid and Interface Science 314, 490–501. https://doi.org/10.1016/j.jcis.2007.04.062

Grybos, M., Davranche, M., Gruau, G., Petitjean, P., Pédrot, M., 2009. Increasing pH drives organic matter solubilization from wetland soils under reducing conditions. Geoderma 154, 13–19. https://doi.org/10.1016/j.geoderma.2009.09.001

Gu, B., Schmitt, J., Chen, Z., Liang, L., McCarthy, J.F., 1995. Adsorption and desorption of different organic matter fractions on iron oxide. Geochimica et Cosmochimica Acta 59, 219–229. https://doi.org/10.1016/0016-7037(94)00282-Q

Gu, Baohua., Schmitt, Juergen., Chen, Zhihong., Liang, Liyuan., McCarthy, J.F., 1994. Adsorption and desorption of natural organic matter on iron oxide: mechanisms and models. Environ. Sci. Technol. 28, 38–46. https://doi.org/10.1021/es00050a007

Gustafsson, J.P., Pechová, P., Berggren, D., 2003. Modeling Metal Binding to Soils: The Role of Natural Organic Matter. Environ. Sci. Technol. 37, 2767–2774. https://doi.org/10.1021/es026249t

Gustafsson, J.P., Tiberg, C., Edkymish, A., Kleja, D.B., Gustafsson, J.P., Tiberg, C., Edkymish, A., Kleja, D.B., 2011. Modelling lead(II) sorption to ferrihydrite and soil organic matter. Environ. Chem. 8, 485–492. https://doi.org/10.1071/EN11025

Hargreaves, A.J., Constantino, C., Dotro, G., Cartmell, E., Campo, P., 2018. Fate and removal of metals in municipal wastewater treatment: a review. Environmental Technology Reviews 7, 1–18. https://doi.org/10.1080/21622515.2017.1423398

Hargreaves, A.J., Vale, P., Whelan, J., Constantino, C., Dotro, G., Campo, P., Cartmell, E., 2017. Distribution of trace metals (Cu, Pb, Ni, Zn) between particulate, colloidal and truly dissolved fractions in wastewater treatment. Chemosphere 175, 239–246. https://doi.org/10.1016/j.chemosphere.2017.02.034

Havelcová, M., Mizera, J., Sýkorová, I., Pekař, M., 2009. Sorption of metal ions on lignite and the derived humic substances. Journal of Hazardous Materials 161, 559–564. https://doi.org/10.1016/j.jhazmat.2008.03.136

Hayes, M.H., Swift, R., 1978. The chemistry of soil organic colloids. The chemistry of soil constituents 179–320.

Herngren, L., Goonetilleke, A., Ayoko, G.A., 2005. Understanding heavy metal and suspended solids relationships in urban stormwater using simulated rainfall. Journal of Environmental Management 76, 149–158. https://doi.org/10.1016/j.jenvman.2005.01.013

Hiemstra, T., Van Riemsdijk, W.H., 1996. A Surface Structural Approach to Ion Adsorption: The Charge Distribution (CD) Model. Journal of Colloid and Interface Science 179, 488–508. https://doi.org/10.1006/jcis.1996.0242

Holguera, J.G., Etui, I.D., Jensen, L.H.S., Peña, J., 2018. Contaminant loading and competitive access of Pb, Zn and Mn(III) to vacancy sites in biogenic MnO2. Chemical Geology 502, 76–87. https://doi.org/10.1016/j.chemgeo.2018.10.020

Huang, X., Chen, T., Zou, X., Zhu, M., Chen, D., Pan, M., 2017. The Adsorption of Cd(II) on Manganese Oxide Investigated by Batch and Modeling Techniques. Int J Environ Res Public Health 14. https://doi.org/10.3390/ijerph14101145

Imoto, Y., Yasutaka, T., 2020. Comparison of the impacts of the experimental parameters and soil properties on the prediction of the soil sorption of Cd and Pb. Geoderma 376, 114538. https://doi.org/10.1016/j.geoderma.2020.114538

ISO 12782-2, 2012. ISO 12782-2:2012 [WWW Document]. ISO. URL https://www.iso.org/cms/render/live/en/sites/isoorg/contents/data/standard/05/16/51698.html (accessed 5.14.21).

Kaiser, K., Guggenberger, G., 2000. The role of DOM sorption to mineral surfaces in the preservation of organic matter in soils. Organic Geochemistry 31, 711–725. https://doi.org/10.1016/S0146-6380(00)00046-2

Kalev, S., Toor, G.S., 2020. Concentrations and Loads of Dissolved and Particulate Organic Carbon in Urban Stormwater Runoff. Water 12, 1031. https://doi.org/10.3390/w12041031

Kalinichev, A.G., Iskrenova-Tchoukova, E., Ahn, W.-Y., Clark, M.M., Kirkpatrick, R.J., 2011. Effects of Ca2+ on supramolecular aggregation of natural organic matter in aqueous solutions: A comparison of molecular modeling approaches. Geoderma, Advances of Molecular Modeling of Biogeochemical Interfaces in Soils 169, 27–32. https://doi.org/10.1016/j.geoderma.2010.09.002

Kania, Gautier, M., Blanc, D., Lupsea-Toader, M., Merlot, L., Quaresima, M.-C., Gourdon, R., 2019. Leaching behavior of major and trace elements from sludge deposits of a French vertical flow constructed wetland. Science of The Total Environment 649, 544–553. https://doi.org/10.1016/j.scitotenv.2018.08.364

Kania, M., 2018. Caractérisation des dépôts de surface des filtres plantés de roseaux à écoulement vertical. Rôle et évolution de la matière organique particulaire (These de doctorat). Lyon.

Kania, M., Gautier, M., Imig, A., Michel, P., Gourdon, R., 2019. Comparative characterization of surface sludge deposits from fourteen French Vertical Flow Constructed Wetlands sewage treatment plants using biological, chemical and thermal indices. Science of The Total Environment 647, 464–473. https://doi.org/10.1016/j.scitotenv.2018.07.440

Kania, M., Gautier, M., Michel, P., Gourdon, R., 2017. Study of aggregation in surface sludge deposits from 14 full-scale French constructed wetlands using particle size distribution and dynamic vapor sorption analyses. Water Science and Technology 77, 79–90. https://doi.org/10.2166/wst.2017.523

Kania, M., Gautier, M., Ni, Z., Bonjour, E., Guégan, R., Michel, P., Jame, P., Liu, J., Gourdon, R., 2018a. Analytical indicators to characterize Particulate Organic Matter (POM) and its evolution in French Vertical Flow Constructed Wetlands (VFCWs). Science of The Total Environment 622–623, 801–813. https://doi.org/10.1016/j.scitotenv.2017.11.357

Kania, M., Gautier, M., Ni, Z., Bonjour, E., Guégan, R., Michel, P., Jame, P., Liu, J., Gourdon, R., 2018b. Analytical indicators to characterize Particulate Organic Matter (POM) and its evolution in French Vertical Flow Constructed Wetlands (VFCWs). Science of The Total Environment 622–623, 801–813. https://doi.org/10.1016/j.scitotenv.2017.11.357

Karvelas, M., Katsoyiannis, A., Samara, C., 2003. Occurrence and fate of heavy metals in the wastewater treatment process. Chemosphere 53, 1201–1210. https://doi.org/10.1016/S0045-6535(03)00591-5

Kasonga, T.K., Coetzee, M.A.A., Kamika, I., Ngole-Jeme, V.M., Benteke Momba, M.N., 2021. Endocrine-disruptive chemicals as contaminants of emerging concern in wastewater and surface water: A review. Journal of Environmental Management 277, 111485. https://doi.org/10.1016/j.jenvman.2020.111485

Katsoyiannis, A., Samara, C., 2007. The fate of dissolved organic carbon (DOC) in the wastewater treatment process and its importance in the removal of wastewater contaminants. Env Sci Poll Res Int 14, 284–292. https://doi.org/10.1065/espr2006.05.302

Kim, B., Gautier, M., Olvera Palma, G., Molle, P., Michel, P., Gourdon, R., 2015. Pilot-scale study of vertical flow constructed wetland combined with trickling filter and ferric chloride coagulation: influence of irregular operational conditions. Water Science and Technology 71, 1088–1096. https://doi.org/10.2166/wst.2015.077

Kim, B., Gautier, M., Prost-Boucle, S., Molle, P., Michel, P., Gourdon, R., 2014. Performance evaluation of partially saturated vertical-flow constructed wetland with trickling filter and chemical precipitation for domestic and winery wastewaters treatment. Ecological Engineering 71, 41–47. https://doi.org/10.1016/j.ecoleng.2014.07.045

Kim, Boram, Gautier, M., Rivard, C., Sanglar, C., Michel, P., Gourdon, R., 2015. Effect of Aging on Phosphorus Speciation in Surface Deposit of a Vertical Flow Constructed Wetland. Environ. Sci. Technol. 49, 4903–4910. https://doi.org/10.1021/es506164v

Kim, B., Gautier, M., Simidoff, A., Sanglar, C., Chatain, V., Michel, P., Gourdon, R., 2016. pH and Eh effects on phosphorus fate in constructed wetland's sludge surface deposit. Journal of Environmental Management 183, 175–181. https://doi.org/10.1016/j.jenvman.2016.08.064

Kipton, H., Powell, J., Town, R.M., 1992. Solubility and fractionation of humic acid; effect of pH and ionic medium. Analytica Chimica Acta 267, 47–54. https://doi.org/10.1016/0003-2670(92)85005-Q

Klinkert, S., Comans, R.N.J., 2020. Geochemical Multisurface Modeling of Reactive Zinc Speciation in Compost as Influenced by Extraction Conditions. Environ. Sci. Technol. 54, 2467–2475. https://doi.org/10.1021/acs.est.9b04104

Köck-Schulmeyer, M., Villagrasa, M., López de Alda, M., Céspedes-Sánchez, R., Ventura, F., Barceló, D., 2013. Occurrence and behavior of pesticides in wastewater treatment plants and their environmental impact. Science of The Total Environment 458–460, 466–476. https://doi.org/10.1016/j.scitotenv.2013.04.010

Kononova, M.M., 2013. Soil Organic Matter: Its Nature, Its Role in Soil Formation and in Soil Fertility. Elsevier.

Koopal, L.K., Saito, T., Pinheiro, J.P., Riemsdijk, W.H. van, 2005. Ion binding to natural organic matter: General considerations and the NICA–Donnan model. Colloids and Surfaces A: Physicochemical and Engineering Aspects, A Selection of Papers from the Third International Conference “Interfaces against Pollutions” (IAP 2004), May 24-27, Jülich, Germany 265, 40–54. https://doi.org/10.1016/j.colsurfa.2004.11.050

Koopal, L.K., van Riemsdijk, W.H., de Wit, J.C.M., Benedetti, M.F., 1994. Analytical Isotherm Equations for Multicomponent Adsorption to Heterogeneous Surfaces. Journal of Colloid and Interface Science 166, 51–60. https://doi.org/10.1006/jcis.1994.1270

Lalire, E., 2010. Efficacité des systèmes de dépollution des eaux pluviales 56.

Landphair, H.C., Building, G., 2001. COST TO PERFORMANCE ANALYSIS OF SELECTED STORMWATER QUALITY BEST MANAGEMENT PRACTICES 15.

Laurent, C., Bravin, M.N., Crouzet, O., Pelosi, C., Tillard, E., Lecomte, P., Lamy, I., 2020. Increased soil pH and dissolved organic matter after a decade of organic fertilizer application mitigates copper and zinc availability despite contamination. Science of The Total Environment 709, 135927. https://doi.org/10.1016/j.scitotenv.2019.135927

LE COUSTUMER, S.-M., 2008. Colmatage et rétention des éléments traces métalliques dans les systèmes d’infiltration des eaux pluviales [WWW Document].

Levine, A.D., Tchobanoglous, G., Asano, T., 1991. Size distributions of particulate contaminants in wastewater and their impact on treatability. Water Research 25, 911–922. https://doi.org/10.1016/0043-1354(91)90138-G

Li, X., Guo, H., Zheng, H., Xiu, W., He, W., Ding, Q., 2019. Roles of different molecular weights of dissolved organic matter in arsenic enrichment in groundwater: Evidences from ultrafiltration and EEM-PARAFAC. Applied Geochemistry 104, 124–134. https://doi.org/10.1016/j.apgeochem.2019.03.024

Lindfors, S., Österlund, H., Lundy, L., Viklander, M., 2020. Metal size distribution in rainfall and snowmelt-induced runoff from three urban catchments. Science of The Total Environment 743, 140813. https://doi.org/10.1016/j.scitotenv.2020.140813

Liu, A., Gonzalez, R.D., 2000. Modeling Adsorption of Copper(II), Cadmium(II) and Lead(II) on Purified Humic Acid. Langmuir 16, 3902–3909. https://doi.org/10.1021/la990607x

Liu, W., Zhang, J., Liu, H., Guo, X., Zhang, X., Yao, X., Cao, Z., Zhang, T., 2021. A review of the removal of microplastics in global wastewater treatment plants: Characteristics and mechanisms. Environment International 146, 106277. https://doi.org/10.1016/j.envint.2020.106277

Lofts, S., Tipping, E., 1998. An assemblage model for cation binding by natural particulate matter. Geochimica et Cosmochimica Acta 62, 2609–2625. https://doi.org/10.1016/S0016-7037(98)00183-5

Maes, J., Jacobs, S., 2017. Nature-Based Solutions for Europe's Sustainable Development: Europe's sustainable development. CONSERVATION LETTERS 10, 121–124. https://doi.org/10.1111/conl.12216

Manceau, A., Marcus, M.A., Tamura, N., 2002. Quantitative Speciation of Heavy Metals in Soils and Sediments by Synchrotron X-ray Techniques. Reviews in Mineralogy and Geochemistry 49, 341–428. https://doi.org/10.2138/gsrmg.49.1.341

Marang, L., 2007. Influence de la matière organique sur la spéciation des radionucléides en contexte géochimique (phdthesis). Université Paris-Diderot - Paris VII ; Institut de physique du globe de paris - IPGP.

Martinelli, I., 1999. Infiltration des eaux de ruissellement pluvial et transfert de polluants associés dans un sol urbain : Vers une approche globale et pluridisciplinaire (These de doctorat). Lyon, INSA.

Martín-Torre, M.C., Payán, M.C., Verbinnen, B., Coz, A., Ruiz, G., Vandecasteele, C., Viguri, J.R., 2015. Metal Release from Contaminated Estuarine Sediment under pH Changes in the Marine Environment. Archives of Environmental Contamination and Toxicology 68, 577–587. https://doi.org/10.1007/s00244-015-0133-z

Marzouk, E.R., Chenery, S.R., Young, S.D., 2013a. Predicting the solubility and lability of Zn, Cd, and Pb in soils from a minespoil-contaminated catchment by stable isotopic exchange. Geochimica et Cosmochimica Acta 123, 1–16. https://doi.org/10.1016/j.gca.2013.09.004

Marzouk, E.R., Chenery, S.R., Young, S.D., 2013b. Measuring reactive metal in soil: a comparison of multi-element isotopic dilution and chemical extraction. European Journal of Soil Science 64, 526–536. https://doi.org/10.1111/ejss.12043

Matar, Z., Soares Pereira, C., Chebbo, G., Uher, E., Troupel, M., Boudahmane, L., Saad, M., Gourlay-France, C., Rocher, V., Varrault, G., 2015. Influence of effluent organic matter on copper speciation and bioavailability in rivers under strong urban pressure. Environ Sci Pollut Res Int 22, 19461–19472. https://doi.org/10.1007/s11356-015-5110-6

McKenzie, R.M., 1981. The surface charge on manganese dioxides. Soil Res. 19, 41–50. https://doi.org/10.1071/sr9810041

Meier, M., Namjesnik-Dejanovic, K., Maurice, P.A., Chin, Y.-P., Aiken, G.R., 1999. Fractionation of aquatic natural organic matter upon sorption to goethite and kaolinite. Chemical Geology 157, 275–284. https://doi.org/10.1016/S0009-2541(99)00006-6

Mermillod-Blondin, F., Simon, L., Maazouzi, C., Foulquier, A., Delolme, C., Marmonier, P., 2015. Dynamics of dissolved organic carbon (DOC) through stormwater basins designed for groundwater recharge in urban area: Assessment of retention efficiency. Water Research 81, 27–37. https://doi.org/10.1016/j.watres.2015.05.031

Milik, J., Pasela, R., 2018. Analysis of concentration trends and origins of heavy metal loads in stormwater runoff in selected cities: A review. E3S Web Conf. 44, 00111. https://doi.org/10.1051/e3sconf/20184400111

Milne, C.J., Kinniburgh, D.G., Tipping, E., 2001. Generic NICA-Donnan model parameters for proton binding by humic substances. Environ Sci Technol 35, 2049–2059. https://doi.org/10.1021/es000123j

Molina, F.V., 2016. Soil Colloids: Properties and Ion Binding. CRC Press.

Molle, P., 2013. French vertical flow constructed wetlands: a need of a better understanding of the role of the deposit layer. Water Science and Technology 69, 106–112. https://doi.org/10.2166/wst.2013.561

Molle, P., Liénard, A., Boutin, C., Merlin, G., Iwema, A., 2005. How to treat raw sewage with constructed wetlands: an overview of the French systems. Water Science and Technology 51, 11–21. https://doi.org/10.2166/wst.2005.0277

Morvannou, A., Choubert, J.-M., Vanclooster, M., Molle, P., 2011. Solid respirometry to characterize nitrification kinetics: A better insight for modelling nitrogen conversion in vertical flow constructed wetlands. Water Research 45, 4995–5004. https://doi.org/10.1016/j.watres.2011.07.004

Murphy, Zachara, 1995. The role of sorbed humic substances on the distribution of organic and inorganic contaminants in groundwater. Geoderma 67, 103–124. https://doi.org/10.1016/0016-7061(94)00055-F

Negassa, W., Acksel, A., Eckhardt, K.-U., Regier, T., Leinweber, P., 2019. Soil organic matter characteristics in drained and rewetted peatlands of northern Germany: Chemical and spectroscopic analyses. Geoderma 353, 468–481. https://doi.org/10.1016/j.geoderma.2019.07.002

Nieboer, E., Richardson, D.H.S., 1980. The replacement of the nondescript term 'heavy metals' by a biologically and chemically significant classification of metal ions. Environmental Pollution Series B, Chemical and Physical 1, 3–26. https://doi.org/10.1016/0143-148X(80)90017-8

Pagotto, C., 1999. Etude sur l'émission et le transfert dans les eaux et les sols des éléments traces métalliques et des hydrocarbures en domaine routier (These de doctorat). Poitiers.

Pan, Y., 2015. Speciation of trace metals and their uptake by rice in paddy soils.

Paquin, P.R., Gorsuch, J.W., Apte, S., Batley, G.E., Bowles, K.C., Campbell, P.G.C., Delos, C.G., Di Toro, D.M., Dwyer, R.L., Galvez, F., Gensemer, R.W., Goss, G.G., Hogstrand, C., Janssen, C.R., McGeer, J.C., Naddy, R.B., Playle, R.C., Santore, R.C., Schneider, U., Stubblefield, W.A., Wood, C.M., Wu, K.B., 2002. The biotic ligand model: a historical overview. Comparative Biochemistry and Physiology Part C: Toxicology & Pharmacology 133, 3–35. https://doi.org/10.1016/S1532-0456(02)00112-6

Park, J., Choi, M., Cho, J., Chon, K., 2018. Transformation of dissolved organic matter in a constructed wetland: A molecular-level composition analysis using pyrolysis-gas chromatography mass spectrometry. Environmental Engineering Research 23, 390–396. https://doi.org/10.4491/eer.2018.043

Pédrot, M., Dia, A., Davranche, M., 2010. Dynamic structure of humic substances: Rare earth elements as a fingerprint. Journal of Colloid and Interface Science 345, 206–213. https://doi.org/10.1016/j.jcis.2010.01.069

Pédrot, M., Dia, A., Davranche, M., 2009. Double pH control on humic substance-borne trace elements distribution in soil waters as inferred from ultrafiltration. Journal of Colloid and Interface Science 339, 390–403. https://doi.org/10.1016/j.jcis.2009.07.046

Pédrot, M., Dia, A., Davranche, M., Bouhnik-Le Coz, M., Henin, O., Gruau, G., 2008. Insights into colloid-mediated trace element release at the soil/water interface. Journal of Colloid and Interface Science 325, 187–197. https://doi.org/10.1016/j.jcis.2008.05.019

Peng, S., Wang, P., Peng, L., Cheng, T., Sun, W., Shi, Z., 2018. Predicting Heavy Metal Partition Equilibrium in Soils: Roles of Soil Components and Binding Sites. Soil Science Society of America Journal 82, 839–849. https://doi.org/10.2136/sssaj2018.03.0104

Peruzzi, E., Nielsen, S., Macci, C., Doni, S., Iannelli, R., Chiarugi, M., Masciandaro, G., 2013. Organic matter stabilization in reed bed systems: Danish and Italian examples. undefined.

Piccolo, A., 2001. THE SUPRAMOLECULAR STRUCTURE OF HUMIC SUBSTANCES. Soil Science 166, 810–832.

Plaza, C., Senesi, N., Polo, A., Brunetti, G., 2005. Acid−Base Properties of Humic and Fulvic Acids Formed during Composting. Environ. Sci. Technol. 39, 7141–7146. https://doi.org/10.1021/es050613h

Pokrovsky, O.S., Dupré, B., Schott, J., 2005. Fe–Al–organic Colloids Control of Trace Elements in Peat Soil Solutions: Results of Ultrafiltration and Dialysis. Aquat Geochem 11, 241–278. https://doi.org/10.1007/s10498-004-4765-2

Pokrovsky, O.S., Schott, J., 2002. Iron colloids/organic matter associated transport of major and trace elements in small boreal rivers and their estuaries (NW Russia). Chemical Geology 190, 141–179. https://doi.org/10.1016/S0009-2541(02)00115-8

Pourret, O., Dia, A., Davranche, M., Gruau, G., Hénin, O., Angée, M., 2007. Organo-colloidal control on major- and trace-element partitioning in shallow groundwaters: Confronting ultrafiltration and modelling. Applied Geochemistry, Metal interactions with natural organic matter and Watershed-scale geochemistry 22, 1568–1582. https://doi.org/10.1016/j.apgeochem.2007.03.022

Praetorius, A., Scheringer, M., Hungerbühler, K., 2012. Development of Environmental Fate Models for Engineered Nanoparticles—A Case Study of TiO2 Nanoparticles in the Rhine River. Environ. Sci. Technol. 46, 6705–6713. https://doi.org/10.1021/es204530n

Quantin, C., Becquer, T., Rouiller, J.H., Berthelin, J., 2001. Oxide weathering and trace metal release by bacterial reduction in a New Caledonia Ferralsol. Biogeochemistry 53, 323–340. https://doi.org/10.1023/A:1010680531328

Quik, J.T.K., de Klein, J.J.M., Koelmans, A.A., 2015. Spatially explicit fate modelling of nanomaterials in natural waters. Water Research 80, 200–208. https://doi.org/10.1016/j.watres.2015.05.025

Raudina, T.V., Loiko, S.V., Kuzmina, D.M., Shirokova, L.S., Kulizhskiy, S.P., Golovatskaya, E.A., Pokrovsky, O.S., 2021. Colloidal organic carbon and trace elements in peat porewaters across a permafrost gradient in Western Siberia. Geoderma 390, 114971. https://doi.org/10.1016/j.geoderma.2021.114971

Ren, Z.-L., Tella, M., Bravin, M.N., Comans, R.N.J., Dai, J., Garnier, J.-M., Sivry, Y., Doelsch, E., Straathof, A., Benedetti, M.F., 2015. Effect of dissolved organic matter composition on metal speciation in soil solutions. Chemical Geology 398, 61–69. https://doi.org/10.1016/j.chemgeo.2015.01.020

Rodriguez, A.F., Gerber, S., Inglett, P.W., Tran, N.T., Long, J.R., Daroub, S.H., 2021. Soil carbon characterization in a subtropical drained peatland. Geoderma 382, 114758. https://doi.org/10.1016/j.geoderma.2020.114758

Saget, A., 1994. Base de données sur la qualité des rejets urbains de temps de pluie : distribution de la pollution rejetée, dimensions des ouvrages d'interception (phdthesis). Ecole nationale des ponts et chaussées - ENPC PARIS / MARNE LA VALLEE.

Sarkar, D.J., Das Sarkar, S., Das, B.K., Sahoo, B.K., Das, A., Nag, S.K., Manna, R.K., Behera, B.K., Samanta, S., 2021. Occurrence, fate and removal of microplastics as heavy metal vector in natural wastewater treatment wetland system. Water Research 192, 116853. https://doi.org/10.1016/j.watres.2021.116853

SCHULTEN, H.-R., SCHNITZER, M., 1993. A state of the art structural concept for humic substances. Naturwissenschaften 80, 29–30.

Senesi, N., Plaza, C., Brunetti, G., Polo, A., 2007. A comparative survey of recent results on humic-like fractions in organic amendments and effects on native soil humic substances. Soil Biology and Biochemistry, Organic Wastes in Soils: Biochemical and Environmental Aspects 39, 1244–1262. https://doi.org/10.1016/j.soilbio.2006.12.002

Serrano, L., de la Varga, D., Ruiz, I., Soto, M., 2011. Winery wastewater treatment in a hybrid constructed wetland. Ecological Engineering, Advances in pollutant removal processes and fate in natural and constructed wetlands 37, 744–753. https://doi.org/10.1016/j.ecoleng.2010.06.038

Shaheen, S.M., Alessi, D.S., Tack, F.M.G., Ok, Y.S., Kim, K.-H., Gustafsson, J.P., Sparks, D.L., Rinklebe, J., 2019. Redox chemistry of vanadium in soils and sediments: Interactions with colloidal materials, mobilization, speciation, and relevant environmental implications- A review. Advances in Colloid and Interface Science 265, 1–13. https://doi.org/10.1016/j.cis.2019.01.002

Sheridan, C.M., Glasser, D., Hildebrandt, D., Petersen, J., Rohwer, J., 2011. An Annual and Seasonal Characterisation of Winery Effluent in South Africa. South African Journal of Enology and Viticulture.

Shi, Z., Allen, H.E., Di Toro, D.M., Lee, S.-Z., Harsh, J.B., 2013. Predicting PbII adsorption on soils: the roles of soil organic matter, cation competition and iron (hydr)oxides. Environ. Chem. 10, 465. https://doi.org/10.1071/EN13153

Shi, Z., Yang, Y., Liu, F., Lu, Y., Ye, Q., Lin, X., Feng, C., Liang, Y., Dang, Z., 2020. Effect of soil particle size on the kinetics of Cu release from field-contaminated soils: Experiments and a quantitative model. Chemical Geology 552, 119780. https://doi.org/10.1016/j.chemgeo.2020.119780

Simpson, A.J., Kingery, W.L., Hayes, M.H., Spraul, M., Humpfer, E., Dvortsak, P., Kerssebaum, R., Godejohann, M., Hofmann, M., 2002. Molecular structures and associations of humic substances in the terrestrial environment. Naturwissenschaften 89, 84–88. https://doi.org/10.1007/s00114-001-0293-8

Sips, R., 1948. On the Structure of a Catalyst Surface. J. Chem. Phys. 16, 490–495. https://doi.org/10.1063/1.1746922

Sjöstedt, C., Löv, Å., Olivecrona, Z., Boye, K., Kleja, D.B., 2018. Improved geochemical modeling of lead solubility in contaminated soils by considering colloidal fractions and solid phase EXAFS

speciation. Applied Geochemistry 92, 110–120. https://doi.org/10.1016/j.apgeochem.2018.01.014

Sønderup, M.J., Egemose, S., Hansen, A.S., Grudinina, A., Madsen, M.H., Flindt, M.R., 2016. Factors affecting retention of nutrients and organic matter in stormwater ponds: Nutrients and Organic Matter in Stormwater Ponds. Ecohydrol. 9, 796–806. https://doi.org/10.1002/eco.1683

Soonthornnonda, P., Christensen, E.R., 2008. Source apportionment of pollutants and flows of combined sewer wastewater. Water Research 42, 1989–1998. https://doi.org/10.1016/j.watres.2007.11.034

Specht, C.H., Kumke, M.U., Frimmel, F.H., 2000. Characterization of NOM adsorption to clay minerals by size exclusion chromatography. Water Research 34, 4063–4069. https://doi.org/10.1016/S0043-1354(00)00148-2

Stevenson, F.J., 1994. Humus Chemistry: Genesis, Composition, Reactions. John Wiley & Sons.

Suteerapataranon, S., Bouby, M., Geckeis, H., Fanghänel, T., Grudpan, K., 2006. Interaction of trace elements in acid mine drainage solution with humic acid. Water Research 40, 2044–2054. https://doi.org/10.1016/j.watres.2006.03.009

Swift, R., 1999. Macromolecular Properties of Soil Humic Substances: Fact, Fiction, and Opinion. Soil Science 164, 790–802. https://doi.org/10.1097/00010694-199911000-00003

Tang, J., Li, X., Luo, Y., Li, G., Khan, S., 2016. Spectroscopic characterization of dissolved organic matter derived from different biochars and their polycylic aromatic hydrocarbons (PAHs) binding affinity. Chemosphere 152, 399–406. https://doi.org/10.1016/j.chemosphere.2016.03.016

Tanneberger, F., Moen, A., Joosten, H., Nilsen, N., 2017. The peatland map of Europe. 1-17. https://doi.org/10.19189/MaP.2016.OMB.264

Tchobanoglous, G., Franklin, L.M., Burton, E., Stensel, H.D., 2011. Wastewater Engineering Treatment and Reuse (Fourth Edition) [WWW Document]. URL /paper/Wastewater-Engineering-Treatment-and-Reuse-(-Fourth-Tchobanoglous-Franklin/f65f8e459abc86496e7658ee7e7203855c159ea3 (accessed 5.24.21).

Tedoldi, D., Chebbo, G., Pierlot, D., Kovacs, Y., Gromaire, M.-C., 2016. Impact of runoff infiltration on contaminant accumulation and transport in the soil/filter media of Sustainable Urban Drainage Systems: A literature review. Science of The Total Environment 569–570, 904–926. https://doi.org/10.1016/j.scitotenv.2016.04.215

Tiberg, C., Sjöstedt, C., Gustafsson, J.P., 2018. Metal sorption to Spodosol Bs horizons: Organic matter complexes predominate. Chemosphere 196, 556–565. https://doi.org/10.1016/j.chemosphere.2018.01.004

Tiberg, C., Sjöstedt, C., Karlfeldt Fedje, K., 2021. Speciation of Cu and Zn in bottom ash from solid waste incineration studied by XAS, XRD, and geochemical modelling. Waste Management 119, 389–398. https://doi.org/10.1016/j.wasman.2020.10.023

Tipping, E., Lofts, S., Sonke, J.E., 2011. Humic Ion-Binding Model VII: a revised parameterisation of cation-binding by humic substances. Environ. Chem. 8, 225. https://doi.org/10.1071/EN11016

Tipping, E., Rieuwerts, J., Pan, G., Ashmore, M.R., Lofts, S., Hill, M.T.R., Farago, M.E., Thornton, I., 2003. The solid–solution partitioning of heavy metals (Cu, Zn, Cd, Pb) in upland soils of

England and Wales. Environmental Pollution 125, 213–225. https://doi.org/10.1016/S0269-7491(03)00058-7

Tonkin, J.W., Balistrieri, L.S., Murray, J.W., 2004. Modeling sorption of divalent metal cations on hydrous manganese oxide using the diffuse double layer model. Applied Geochemistry 19, 29–53. https://doi.org/10.1016/S0883-2927(03)00115-X

Town, R.M., van Leeuwen, H.P., Duval, J.F.L., 2019. Rigorous Physicochemical Framework for Metal Ion Binding by Aqueous Nanoparticulate Humic Substances: Implications for Speciation Modeling by the NICA-Donnan and WHAM Codes. Environ. Sci. Technol. 53, 8516–8532. https://doi.org/10.1021/acs.est.9b00624

Treilles, R., Gasperi, J., Gallard, A., Saad, M., Dris, R., Partibane, C., Breton, J., Tassin, B., 2021. Microplastics and microfibers in urban runoff from a suburban catchment of Greater Paris. Environmental Pollution 287, 117352. https://doi.org/10.1016/j.envpol.2021.117352

Trein, C.M., Banc, C., Maciejewski, K., de Moraes Motta, A., Gourdon, R., Molle, P., Gautier, M., von Sperling, M., 2020. French vertical flow treatment wetlands in a subtropical climate: Characterization of the organic deposit layer and comparison with systems in France. Science of The Total Environment 742, 140608. https://doi.org/10.1016/j.scitotenv.2020.140608

Van Eynde, E., Weng, L., Comans, R.N.J., 2020. Boron speciation and extractability in temperate and tropical soils: A multi-surface modeling approach. Applied Geochemistry 123, 104797. https://doi.org/10.1016/j.apgeochem.2020.104797

Vaze, J., Chiew, F.H.S., 2004. Nutrient Loads Associated with Different Sediment Sizes in Urban Stormwater and Surface Pollutants. Journal of Environmental Engineering 130, 391–396. https://doi.org/10.1061/(ASCE)0733-9372(2004)130:4(391)

Vymazal, J., 2019. Is removal of organics and suspended solids in horizontal sub-surface flow constructed wetlands sustainable for twenty and more years? Chemical Engineering Journal 378, 122117. https://doi.org/10.1016/j.cej.2019.122117

Waksman, S.A., 1931. Principles of soil microbiology. Principles of soil microbiology.

Walaszek, M., Del Nero, M., Bois, P., Ribstein, L., Courson, O., Wanko, A., Laurent, J., 2018. Sorption behavior of copper, lead and zinc by a constructed wetland treating urban stormwater. Applied Geochemistry 97, 167–180. https://doi.org/10.1016/j.apgeochem.2018.08.019

Wang, M., Lu, T., Chen, W., Zhang, H., Qi, W., Song, Y., Qi, Z., 2020. Enhanced role of humic acid on the transport of iron oxide colloids in saturated porous media under various solution chemistry conditions. Colloids and Surfaces A: Physicochemical and Engineering Aspects 607, 125486. https://doi.org/10.1016/j.colsurfa.2020.125486

Weissert, L.F., Salmond, J.A., Schwendenmann, L., 2016. Variability of soil organic carbon stocks and soil CO2 efflux across urban land use and soil cover types. Geoderma 271, 80–90. https://doi.org/10.1016/j.geoderma.2016.02.014

Weston, D.P., Holmes, R.W., Lydy, M.J., 2009. Residential runoff as a source of pyrethroid pesticides to urban creeks. Environmental Pollution 157, 287–294. https://doi.org/10.1016/j.envpol.2008.06.037

Winer, R., 2000. National Pollutant Removal Performance Database for Stormwater Treatment Practices. Center for Watershed Protection.

Winiarski, T., 2014. Fonction filtration d'un ouvrage urbain - consequence sur la formation d'un anthroposol 199.

Wiseman, C.L.S., Püttmann, W., 2006. Interactions between mineral phases in the preservation of soil organic matter. Geoderma 134, 109–118. https://doi.org/10.1016/j.geoderma.2005.09.001

Worms, I.A.M., Chmiel, H.E., Traber, J., Tofield-Pasche, N., Slaveykova, V.I., 2019. Dissolved Organic Matter and Associated Trace Metal Dynamics from River to Lake, Under Ice-Covered and Ice-Free Conditions. Environ. Sci. Technol. 53, 14134–14143. https://doi.org/10.1021/acs.est.9b02184

Xu, H., Ji, L., Kong, M., Jiang, H., Chen, J., 2019a. Molecular weight-dependent adsorption fractionation of natural organic matter on ferrihydrite colloids in aquatic environment. Chemical Engineering Journal 363, 356–364. https://doi.org/10.1016/j.cej.2019.01.154

Xu, H., Lin, H., Jiang, H., Guo, L., 2018. Dynamic molecular size transformation of aquatic colloidal organic matter as a function of pH and cations. Water Research 144, 543–552. https://doi.org/10.1016/j.watres.2018.07.075

Xu, H., Zou, L., Guan, D., Li, W., Jiang, H., 2019b. Molecular weight-dependent spectral and metal binding properties of sediment dissolved organic matter from different origins. Science of The Total Environment 665, 828–835. https://doi.org/10.1016/j.scitotenv.2019.02.186

Yang, K., Miao, G., Wu, W., Lin, D., Pan, B., Wu, F., Xing, B., 2015. Sorption of Cu2+ on humic acids sequentially extracted from a sediment. Chemosphere 138, 657–663. https://doi.org/10.1016/j.chemosphere.2015.07.061

You, S.-J., Thakali, S., Allen, H.E., 2006. Characteristics of soil organic matter (SOM) extracted using base with subsequent pH lowering and sequential pH extraction. Environment International 32, 101–105. https://doi.org/10.1016/j.envint.2005.07.003

Yousef, Y.A., Wanielista, M.P., Hvitved-Jacobsen, T., Harper, H.H., 1984. Fate of heavy metals in stormwater runoff from highway bridges. Science of The Total Environment, Highway Pollution 33, 233–244. https://doi.org/10.1016/0048-9697(84)90397-8

Zhang, C., Gu, X., Gu, C., Evans, L.J., 2018. Multi-surface modeling of Ni(II) and Cd(II) partitioning in soils: Effects of salts and solid/liquid ratios. Science of The Total Environment 635, 859–866. https://doi.org/10.1016/j.scitotenv.2018.04.191

Zhang, W., Ye, Y., Tong, Y., Ou, L., Hu, D., Wang, X., 2011. Contribution and loading estimation of organochlorine pesticides from rain and canopy throughfall to runoff in an urban environment. Journal of Hazardous Materials 185, 801–806. https://doi.org/10.1016/j.jhazmat.2010.09.091

Zhou, P., Yan, H., Gu, B., 2005. Competitive complexation of metal ions with humic substances. Chemosphere 58, 1327–1337. https://doi.org/10.1016/j.chemosphere.2004.10.017

Zhu, B., Liao, Q., Zhao, X., Gu, X., Gu, C., 2018. A multi-surface model to predict Cd phytoavailability to wheat (Triticum aestivum L.). Science of The Total Environment 630, 1374–1380. https://doi.org/10.1016/j.scitotenv.2018.03.002

Zomeren, A. van, Comans, R.N.J., 2009. Carbon speciation in municipal solid waste incinerator (MSWI) bottom ash in relation to facilitated metal leaching. Waste Management 29, 2059–2064. https://doi.org/10.1016/j.wasman.2009.01.005

OBJECTIFS DE RECHERCHES

L'activité humaine génère de nombreux polluants organiques et inorganiques se retrouvant dans l'atmosphère, l'eau et le sol. Les eaux usées et les eaux de ruissellement sont des voies convergentes de ces polluants, faisant des zones de traitements des eaux, la dernière zone tampon entre les milieux anthropisés et l'environnement. Au sein des systèmes de traitements fondés sur la nature, la sédimentation des particules en suspension des eaux permet la rétention d'une large fraction de polluants associés. Ce processus de rétention aboutit à la formation d'un dépôt fortement chargé en matières organiques, en nutriments et en polluants. Souvent considéré comme une source de polluants, l'amélioration des connaissances sur la spéciation des polluants et leur mécanisme de remobilisation, ainsi que la calibration de modèle géochimique pourront permettre de prédire la spéciation et la biodisponibilité des éléments remobilisés depuis ces dépôts. Pouvant aussi être considéré comme des sources de nutriment notamment, les connaissances précédemment évoquées pourraient permettre d'améliorer ou d'envisager de nouvelles voies de réutilisation et/ou de récupération des dépôts et des éléments qu'elles renferment.

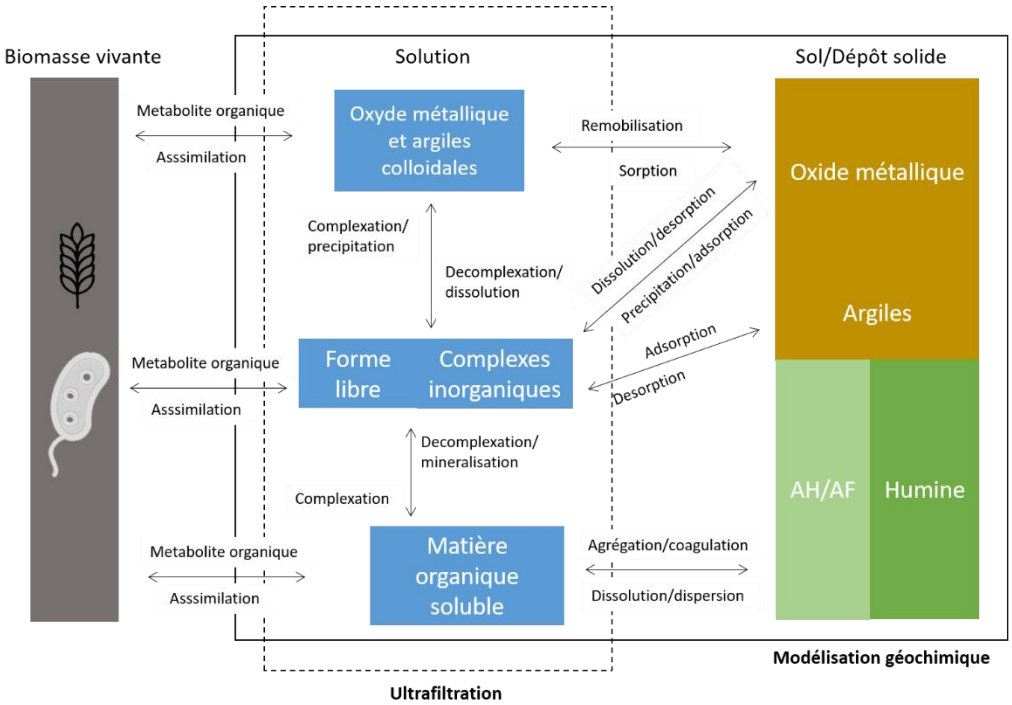

Fig.1. Diagramme simplifié des sources et transfert des métaux traces dans l'environnement, modifié de Bonito et al., 2018.

Dans ce contexte, cette thèse combine des études de caractérisations du relargage de colloïdes et la modélisation géochimique afin de :

a. Evaluer l'influence des variations de pH sur l'émission des phases et le relargage associé d'éléments majeurs et traces métalliques accumulés au sein des boues de filtres plantés de roseaux (Chapitre III) ;

b. En se basant sur les connaissances obtenues précédemment, calibrer puis tester l'applicabilité et l'efficacité d'un modèle multi-surfacique intégrant la sorption sur la matière organique et les oxydes métalliques dans le calcul du relargage d'éléments traces et majeurs d'un dépôt de boue de filtres plantés de roseaux soumis à une large gamme de pH (Chapitre IV) ;

c. Evaluer la robustesse de la méthode de modélisation sur des dépôts issus d'autres systèmes de traitements des eaux inspirées par la nature présentant des caractéristiques physico-chimiques différentes (Chapitre IV).

CHAPITRE II. MATERIELS ET METHODES

I. Origine des dépôts et échantillonnage

Deux différents types de dépôts ont été étudiés dans cette thèse :

- Des dépôts provenant d'une station de filtre planté de roseaux à écoulement vertical destiné à la filtration des eaux usées domestiques de la commune de Vercia (Jura). Dans ce document les dépôts provenant du filtre planté de roseaux sont appelés **dépôt de boue** (sludge deposit). La station Vercia fait partie de la filière AZOE-NP® développée et brevetée par la société SCIRPE (brevets : FR2900921A1 ; EP1857419A1 ; WO201215026A2). Le fonctionnement de ces stations a été largement décrit lors de thèses précédentes (Kania, 2018; Kim, 2014). Les eaux usées brutes sont préalablement dégrillée puis pompée dans un lit bactérien permettant notamment de débuter l'abattement de l'azote et du carbone. Les eaux sortant de ce lit bactérien sont mélangées avec une solution aqueuse de $FeCl_3$ dont l'objectif est de provoquer la précipitation du phosphore. Ces eaux sont ensuite déversées par bâchés sur le premier étage du filtre. Les eaux sortant de ce premier étage sont collectées et déversées sur un deuxième filtre. Les eaux sont ensuite évacuées dans les eaux de surface environnantes.
- Des dépôts du bassin d'infiltration Django Reinhardt de la banlieue Est de Lyon. Dans ce document, les dépôts résidu de l'infiltration des eaux dans un bassin d'infiltration sont appelés **sédiment**. Le bassin s'étend sur 2 hectares et draine une zone industrielle de 185 hectares (Drapeau, 2018). Dans un premier temps les eaux sont acheminées jusqu'à un bassin de décantation non perméable permettant la sédimentation d'une partie des particules en suspension. Les eaux sont ensuite déversées dans le bassin d'infiltration perméable permettant l'infiltration des eaux vers la nappe phréatique. C'est dans ce bassin d'infiltration que les 2 sédiments étudiés ont été prélevés (Tableau 1).

Deux dépôts de boue et deux sédiments ont fait l'objet de travaux dans cette étude (Tableau 1). Un dépôt de boue a été échantillonné durant cette thèse en octobre 2018. Une analyse élémentaire de ce dépôt de boue a été effectuée. En plus de la teneur en carbone organique totale, le taux d'humification a aussi été mesuré. Ce dépôt de boue a fait l'objet d'un test de lixiviation en batch suivant la norme CENTS/TS 14429 European standard. Les solutions ainsi obtenues ont été ultrafiltrées suivant le protocole présenté dans la section suivante. Des mesures de concentrations en carbone organique, en éléments majeurs et traces ainsi que des mesures en UV-vis ont été menées sur chacun des ultrafiltrats. Les résultats de l'ultrafiltration des solutions sont discutés dans le chapitre III. Les modélisations du relargage d'éléments majeurs et traces depuis ces dépôts sont discutées dans le chapitre IV.

Le dépôt de boue prélevé lors de cette étude a été enlevé par pelletage en différents points et sur toute leur épaisseur. Les rhizomes et graviers éventuellement présent ont été retirés manuellement des échantillons. L'ensemble des différents points de prélèvement a été homogénéisé et mélangé sur place. Dans la journée les échantillons ont été séchés en laboratoire à 35°C puis lyophilisés et conservés dans au congélateur à - 20 °C avant d'effectuer d'autres analyses. Cette méthode d'échantillonnage est très similaire à celle utilisée pour les autres dépôts utilisés dans cette thèse (Drapeau et al., 2017; Kania et al., 2019).

Tableau 1. Référencement des différents dépôts utilisés et provenance des jeux de données.

Nature du dépôt (Provenance data)	Station (date)	Jeux de données		
		Mesure	**Principe de la mesure**	**Appareillage**
Dépôt de boue 1 (Cette étude)	Vercia AOZE-NP **(2018)**	Analyse élémentaire majeurs	Mesure par spectrométrie par torche à plasma d'émission optique (ICP-AES ou ICP-OES)	IRIS Advantage ERS à torche radiale, Thermo Scientific
		Analyse élémentaire traces	Fusion au LiBO2 à 980°C Mesure par spectrométrie de masse à plasma à couplage inductif (ICP-MS)	Sciex Perkin Elmer ELAN 5000a
		Teneur en carbone organique	Digestion à chaud a HCl	Carbon sulfur analyzer EMIA-320 V2, Horiba Scientific Co., Ltd
		Taux d'humification	Extraction des substances humiques : AH+AF par NaOH (0,1 N) et AF par H_2SO_4 (Serra-Wittling et al., 1996)	
		Tests de lixiviation	Lixiviation (HCl, KOH) CENTS/TS 14429	
		Ultrafiltration	Précédemment décrit dans ce chapitre	
		Majeurs et traces relargué	Dilution dans une solution à 2% HNO_3	ICP-OES iCap6500 ThermoFisher et ICP-MS iCapQ ThermoFisher
		Mesure DOC		Shimadzu TOC-V CSH
		UV-vis		Perkin-Elmer Lambda 25 spectrophotometer
Dépôt de boue 2 (Kania, 2018)	Vercia AOZE-NP **(2011)**	Analyse élémentaire majeurs	Mesure par spectrométrie par torche à plasma d'émission optique (ICP-AES ou ICP-OES)	IRIS Advantage ERS à torche radiale, Thermo Scientific
		Analyse élémentaire traces	Fusion au LiBO2 à 980°C Mesure par spectrométrie de masse à plasma à couplage inductif (ICP-MS)	Sciex Perkin Elmer ELAN 5000a
		Teneur en carbone organique	Digestion à chaud a HCl	Carbon sulfur analyzer EMIA-320 V2, Horiba Scientific Co., Ltd
		Taux d'humification	Extraction des substances humiques : AH+AF par NaOH (0,1 N) et AF par H_2SO_4 (Serra-Wittling et al., 1996)	
		Tests de lixiviation	Lixiviation (HNO_3, KOH) CENTS/TS 14429	
		Majeurs et traces relargué	ICP-AES Dilution préalable avec solutions HNO_3	Ultima 2; Horiba Jobin Yvon SAS
		Mesure DOC		Shimadzu 505A Carbon analyzer
		UV-vis		Shimadzu UV-2450 spectrophotometer

Sédiment 1 (Drapeau, 2018)	Django Reinhardt (**2017)**	Analyse elementaire majeurs	Mesure par spectrométrie par torche à plasma d'émission optique (ICP-AES ou ICP-OES)	IRIS Advantage ERS à torche radiale, Thermo Scientific
		Analyse elementaire traces	Fusion au LiBO2 à 980°C Mesure par spectrométrie de masse à plasma à couplage inductif (ICP-MS)	Sciex Perkin Elmer ELAN 5000a
		Tests de lixiviation	Lixiviation (HNO_3, KOH) CENTS/TS 14429	
		Majeurs et traces relargué	ICP-AES	Ultima 2; Horiba Jobin Yvon SAS
		Mesure DOC		Shimadzu, TOC model 5050A
Sédiment 2	Django Reinhardt (**2020)**	Analyse elementaire majeurs	Mesure par spectrométrie par torche à plasma d'émission optique (ICP-AES ou ICP-OES)	IRIS Advantage ERS à torche radiale, Thermo Scientific
		Analyse elementaire traces	Fusion au LiBO2 à 980°C Mesure par spectrométrie de masse à plasma à couplage inductif (ICP-MS)	Sciex Perkin Elmer ELAN 5000a
		Tests de lixiviation	Lixiviation (HNO_3, KOH) CENTS/TS 14429	
		Teneur en carbone organique	Digestion à chaud avec HCl	Carbon sulfur analyzer EMIA-320 V2, Horiba Scientific Co., Ltd
		Majeurs et traces relargué	ICP-AES Dilution préalable avec solutions HNO_3	Ultima 2; Horiba Jobin Yvon SAS
		Mesure DOC		Shimadzu 505A Carbon analyzer

II. Expérimentations et modélisation

2.1 Dosage de la capacité de neutralisation acido-basique

Afin d'évaluer l'influence des conditions de pH sur la remobilisation de colloides et des éléments majeurs et traces associés, le dépôt de boue 1 a été soumis à un test de lixiviation. Le protocole utilisé est issu d'un standard européen (CENTS/TS 14429 European standard) largement référéncé, pour évaluer le potentiel relargage de polluants inorganique contenus dans des déchets ou des sols (Chatain et al., 2013; Drapeau et al., 2017; Gonzalez et al., 2019; Kania et al., 2019). Dans ce protocole, la matière solide est mélangée avec de l'eau et des quantités croissantes d'acide et de base afin de balayer toute la gamme de pH. La matière séche est introduite à un ratio liquide/solide de 10, identique pour chaque solution. S'en suit une phase d'agitation de 48H ou l'état d'équilibre sera considéré comme atteint si la mesure du pH de la solution reste stable entre 44H et 48H d'agitation. Après agitation, les batchs sont centrifugés à 5000 tours par minute pendant 20 minutes. Le lixiviat est ensuite filtré à 0.45 µm et la concentration en éléments majeurs et traces est mesurée. Nos matrices spécifiques nous ont conduit à moduler ce protocole largement établit en intégrant des mesures de caractérisation physico-chimique des matières organiques relarguées. Notamment, en ajoutant des techniques de fractionnement comme l'ultrafiltration, et des mesures de concentration en carbone organique dissout et de spectrophotométrie en UV-vis.

2.2 Ultrafiltration des solutions

Les solutions de lixiviations en fonction du pH obtenues sur le dépôt de boue 1 ont été ultrafiltrées au laboratoire Géoscience Rennes. Les 12 solutions de différents pH ont été ultrafiltrées en parallèle à 30, 10 et 3 kDa à l'aide de cellules d'ultrafiltration par centrifugation Sartorius en acétate de cellulose. 15 mL de solution préalablement filtrés à 0,45 µm (CENTS/TS 14429 European standard) sont ajoutés dans la cellule. Les solutions sont alors centrifugées pendant 30 min à 3000 g à l'aide d'une centrifugeuse équipée de rotor à godets oscillants.

Au préalable les cellules d'ultrafiltration ont été lavées à l'aide d'une solution de soude à 0,1M. Cette solution de rinçage a été préparé à l'aide d'une solution mère de soude à 19,8M et de l'eau ultrapure. Les cellules sont considérées « rincées » lorsque la solution de rinçage contient moins de 0,2 $mg.L^{-1}$ de carbone organique dissout. Pour atteindre cette valeur une dizaine de rinçages successifs par cellule ont été nécessaires.

Dans cette thèse les colloïdes sont définis comme étant des particules en suspension dont la taille est comprise entre 0,45 µm et 3 kDa. Différentes fractions de poids moléculaire ont pu être mise en

évidence dans le chapitre III. Le calcul des concentrations en carbone organique, éléments majeurs et traces ainsi que le SUVA de chacune des différentes fractions sont détaillés dans le tableau 2.

Tableau 2. Description des gammes de poids moléculaire des molécules remobilisées depuis le dépôt de boue de FPR.

Dénomination/Acronym	Poids moléculaire	Concentration	$SUVA_{254}$
Gros colloids *Large Colloid (LC)*	30 kDa - 0.45 µm	$[M]_{0.45\ \mu m} - [M]_{30\ kDa}$	$\frac{Abs^{254}_{0.45\ \mu m} - Abs^{254}_{30\ kDa}}{[OC]_{0.45\ \mu m} - [OC]_{30\ kDa}}$
Petits colloids *Small Colloids (SC)*	3 kDa - 30 kDa	$[M]_{30\ kDa} - [M]_{3\ kDa}$	$\frac{Abs^{254}_{30\ kDa} - Abs^{254}_{3\ kDa}}{[OC]_{30\ kDa} - [OC]_{3\ kDa}}$
Réellement dissout *Truly Dissolved (TD)*	< 3 kDa	$[M]_{3\ kDa}$	$\frac{Abs^{254}_{3\ kDa}}{[OC]_{3\ kDa}}$

2.3 Modélisation géochimique

L'intégralité des calculs de spéciation géochimique ont été effectués sur l'interface PHREEQC. PHREEQC version 2 permet le calcul de la répartition des éléments entre les phases solide, liquide et gazeuse (Parkhurst and Appelo, 1999). Dans cette étude la base de données thermodynamique « llnl.dat » a été utilisée. La modélisation de la capacité de sorption de la matière organique décrite dans Model VII (Tipping et al., 2011) a été intégrée à PHREEQC en suivant la méthodologie développée par Marsac et al. (2017). Succinctement, les 50 sites de sorption des acides humiques et fulviques ont été définis dans SURFACE_MASTER_SPECIES ainsi que leur constante de complexation à l'aide de SURFACE_SPECIES dans la base de données llnl.dat. Les acides humiques et fulviques de la fraction solide (*i.e* fraction > 0,45 µm) ont été référencés comme des HAS (Humic acid solid) et des FAS (Fulvic acid solid), respectivement. Dans la fraction relarguée les sites de sorption organique sont dénommés HAC (Humic acid colloidal) et FAC (Fulvic acid colloidal). Comme évoqué dans le chapitre I, les constantes de complexation entre les sites de sorptions organique et les cations sont corrigées par un facteur électrostatique similaire au facteur de Boltzmann. Cependant l'application de cette correction n'est pas possible dans PHREEQC. Marsac et al. (2017) ont montré que l'utilisation du Constant Capacitance Model (CCM) pouvait se substituer à l'équation de Boltzmann décrite dans Model VII. L'utilisation du CCM passe par la modulation du Three Plane Model (TPM) disponible via le terme « CD-

MUSIC » de PHREEQC. La modulation du TPM pour obtenir le CCM est précisément décrite par Marsac et al. (2017). La même méthodologie a été utilisée durant les travaux de modélisation.

Références :

Chatain, V., Blanc, D., Borschneck, D., Delolme, C., 2013. Determining the experimental leachability of copper, lead, and zinc in a harbor sediment and modeling. Environ Sci Pollut Res 20, 66–74. https://doi.org/10.1007/s11356-012-1233-1

Drapeau, C., 2018. Mesure et modélisation de la mobilité et de la spéciation des éléments majeurs et traces métalliques au sein de matrices complexes polluées en fonction du pH : application aux sédiments urbains et déchets miniers (These de doctorat). Lyon.

Drapeau, C., Delolme, C., Chatain, V., Gautier, M., Blanc, D., Benzaazoua, M., Lassabatère, L., 2017. Spatial and Temporal Stability of Major and Trace Element Leaching in Urban Stormwater Sediments. Open Journal of Soil Science 07, 347. https://doi.org/10.4236/ojss.2017.711025

Gonzalez, M.L., Blanc, D., de Brauer, C., 2019. Multi-Analytical Approach and Geochemical Modeling for Mineral Trace Element Speciation in MSWI Bottom-Ash. Waste Biomass Valor 10, 547–560. https://doi.org/10.1007/s12649-017-0075-y

Kania, Gautier, M., Blanc, D., Lupsea-Toader, M., Merlot, L., Quaresima, M.-C., Gourdon, R., 2019. Leaching behavior of major and trace elements from sludge deposits of a French vertical flow constructed wetland. Science of The Total Environment 649, 544–553. https://doi.org/10.1016/j.scitotenv.2018.08.364

Kania, M., 2018. Caractérisation des dépôts de surface des filtres plantés de roseaux à écoulement vertical. Rôle et évolution de la matière organique particulaire (These de doctorat). Lyon.

Kim, B., 2014. Devenir du phosphore dans les filtres plantés de roseaux : Etude de sa rétention / libération et des facteurs d'influence (These de doctorat). Lyon, INSA.

Marsac, R., Banik, N.L., Lützenkirchen, J., Catrouillet, C., Marquardt, C.M., Johannesson, K.H., 2017. Modeling metal ion-humic substances complexation in highly saline conditions. Applied Geochemistry 79, 52–64. https://doi.org/10.1016/j.apgeochem.2017.02.004

Parkhurst, Appelo, 1999. User's guide to PHREEQC (Version 2) : a computer program for speciation, batch-reaction, one-dimensional transport, and inverse geochemical calculations. https://doi.org/10.3133/wri994259

Serra-Wittling, C., Barriuso, E., Houot, S., 1996. Impact of Composting Type on Composts Organic Matter Characteristics, in: de Bertoldi, M., Sequi, P., Lemmes, B., Papi, T. (Eds.), The Science of Composting. Springer Netherlands, Dordrecht, pp. 262–273. https://doi.org/10.1007/978-94-009-1569-5_26

Tipping, E., Lofts, S., Sonke, J.E., 2011. Humic Ion-Binding Model VII: a revised parameterisation of cation-binding by humic substances. Environ. Chem. 8, 225. https://doi.org/10.1071/EN11016

CHAPITRE III. ROLE DES COLLOÏDES DANS LA REMOBILISATION D'ELEMENTS MAJEURS ET TRACES

PREAMBULE

Cette section s'interroge sur les mécanismes de remobilisation des phases colloïdales, leurs natures et leurs impacts sur le relargage de polluants retenus au sein des dépôts de boue de filtres plantés de roseaux. Etant soumis à l'influence de conditions de pH variable tout le long de leur cycle de vie, il était essentiel de tester l'influence des conditions de pH sur le dépôt solide.

Un dépôt solide a été échantillonné sur une station de filtre planté de roseaux en fonctionnement depuis 14 ans. Passé 3 ans d'accumulation, les caractéristiques physico-chimique des dépôts restent stable dans le temps (Kania, 2018). Ces dépôts ont été échantillonnés juste avant le curage de la station, ils sont donc représentatifs de dépôts en fin de vie, pouvant potentiellement être réutilisés en agriculture par exemple. Les échantillons ont d'abord fait l'objet de caractérisation de la matière organique solide qu'ils contiennent et d'une analyse élémentaire. Afin de tester l'influence des conditions de pH sur l'émission de phases colloïdales, un test de lixiviation en batch a été mis en place. Ce test suit un protocole standardisé européen (CENTS/TS 14429) largement utilisé dans la caractérisation des déchets et autres échantillons solides. Chacunes des différentes solutions ont ensuite été (ultra)filtrées à différents seuils de coupure puis la concentration totale en carbone organique, la réponse en UV-vis et la concentration en éléments majeurs et traces a été mesurée dans chacun des (ultra)filtrats.

Les résultats de la caractérisation de la matière organique solide et de l'influence du pH sur la taille et l'aromaticité des colloïdes organiques remobilisés depuis le dépôt solide sont synthétisés et discutés dans un 1er article intitulé : « Influence of pH on the release of colloidal and dissolved organic matter from Vertical Flow Constructed Wetland surface sludge deposits » publié en aout 2021 dans Chemical Engineering Journal. L'influence du pH sur la remobilisation des colloïdes et sur le relargage d'éléments majeurs et traces seront quant à eux discutés dans un 2ème article intitulé «Organic and organo-mineral colloids control of major and trace elements leached from treatment wetland sludge deposits. Influence of pH conditions» qui est en cours de soumission.

ARTICLE 1

Influence of pH on the release of colloidal and dissolved organic matter from Vertical Flow Constructed Wetland surface sludge deposits.

Banc, C. *, Gautier, M. *, Blanc, D. *, Lupsea-Toader, M. *, Marsac, R., Gourdon, R. ***

* Univ Lyon, INSA Lyon, DEEP, EA7429, 69621 Villeurbanne, France.

** Univ Rennes, CNRS, Géosciences Rennes, UMR **6118**, 35000 Rennes, France.

Publié sous une forme similaire:

Banc, C., Gautier, M., Blanc, D., Lupsea-Toader, M., Marsac, R., & Gourdon, R. (2021). Influence of pH on the release of colloidal and dissolved organic matter from Vertical Flow Constructed Wetland surface sludge deposits. *Chemical Engineering Journal*, *418*, 129353.

Abstract

The very rapid development of vertical flow constructed wetlands (VFCW) in Europe and throughout the world has induced a growing concern on the conditions of management of their surface sludge deposits (SD). The leaching of organic components from SD was explored in this study with respect to their potential impact on biochemical oxygen demand (BOD) and their role as complexing agents in the release of trace contaminants. The aromaticity and molecular size of leached organic compounds was investigated over a large range of pHs. Experimental results showed that the pH of the leaching aqueous solution influenced the concentration and characteristics of leached OC. Around the natural pH of SD aqueous suspensions (6 to 8), truly dissolved organics (<3 kDa) exhibited high aromatic content. Under alkaline conditions (pH >8), large organic colloids (>30 kDa) were found predominant, exhibiting a low aromaticity growing with pH. Under acidic conditions (pH<6), hydrophilic truly dissolved organics were leached. Comparison of concentration, aromaticity and molecular size of OC leached from 14-year and 7-year SD suggested that ageing of SD reduced their sensitivity to pH conditions and may improve their agronomic properties.

Keywords

Lixiviation; Organic carbon; Molecular weight; Ultrafiltration; Aromaticity; pH variations.

Abbreviations

BOD: Biochemical Oxygen Demand

LOC: Large Organic Colloids

MW: Molecular Weight

OC: Organic Carbon

SD: Sludge Deposit

SOC: Small Organic Colloids

SOM: Solid Organic Matter

SUVA: Specific Ultra Violet Absorbance

tDOC: Truly Dissolved Organic Carbons

TOC: Total Organic Carbon

VFCW: Vertical Flow Constructed Wetlands

1. Introduction

In porous media such as soil, sediment and sludge, the partition of organic molecules between solid and dissolved states controls the fate of many trace contaminants (Pédrot et al., 2009a; Pokrovsky et al., 2005; Sauvé et al., 2000). The presence of complexing groups in solid organic matter (SOM) contributes to the retention of trace metals within the solid fraction. The solubilization of organic molecules through SOM hydrolysis thereby induces the release and transport of associated pollutants (Kikuchi et al., 2017; Pearson et al., 2017) which may alter the quality of the receiving water bodies.

A large variety of organic molecules may be leached in the dissolved form. Depending of the SOM of origin, these molecules may exhibit different molecular sizes and chemical compositions, particularly with regards to their functional groups (aromatic rings, carboxylic acids, N-containing groups, etc.). Molecular fractionation using ultrafiltration (El-sayed et al., 2019; Pokrovsky et al., 2016) and UV-visible spectroscopy (Peacock et al., 2014; Wang et al., 2013) have been used extensively to characterize the molecular weight (MW) and aromaticity of DOM. $SUVA_{254}$, defined as the ratio between absorbance at a wavelength of 254 nm and dissolved organic carbon concentration, is a well-known indicator of DOM aromaticity. It has also been reported to be a good indicator of DOM capacity to sorb trace metals in organic rich water (Kikuchi et al., 2017; Yan et al., 2020) or organic-rich soil solutions (Araújo et al., 2019). Moreover, the chemical speciation of associated trace metals has been shown to be largely affected by the molecular weight of organic ligands in natural water samples (Gangloff et al., 2016; Pokrovsky et al., 2016). Finally, the aromaticity of DOM, estimated by $SUVA_{254}$ or other parameters, has also been shown to play a role in biodegradabily as shown by the anti-correlation observed between the biological oxygen demand BOD and the aromaticity of dissolved organic compounds (Marschner and Kalbitz, 2003).

The release of DOM from SOM may occur by different mechanisms, such as the hydrolysis of macromolecular structures (Durce et al., 2016; Piccolo, 2001) or the desorption of organic molecules attached to solid mineral phases (Chen et al., 2018; Gao et al., 2018). The extent to which each mechanism may contribute to the overall leaching phenomenon is dictated by the physico-chemical characteristics of the solid matter of origin (Kalbitz et al., 2000) and the environmental conditions of the medium. pH conditions appears to be a key factor of influence (Grybos et al., 2009b; Pédrot et al., 2009a). Several studies have reported that dissolved organics with high MW and aromaticity were preferentially aggregated by solid mineral phases (Kalbitz et al., 2000; Xu et al., 2019b), resulting in a poor solubilization of these molecules. Alkaline pHs were reported to destabilize organo-mineral associations via the deprotonation of the ligands in both phases inducing anionic electrostatic

repulsion (Avena and Koopal, 1998; Avena and Wilkinson, 2002). Pédrot et al. (Pédrot et al., 2010) reported that low pHs could also induces the disaggregation of supramolecular assemblies of humic substances, leading to the release of low molecular weight organic molecules.

Constructed wetlands are engineered nature-based systems designed to treat domestic wastewaters and similar effluents (Vymazal, 2019). So-called “Classical French” vertical flow constructed wetlands (VFCWs) are based on the percolation of unsettled wastewaters through 2 successive stages of filters filled with gravels or sand and planted with reeds. This process induces the formation of a sludge deposit (SD) layer at the surface of the first-stage filter which has been shown to play a major role in the retention and degradation of a large variety of contaminants during regular conditions of operation (Kania et al., 2019, 2018a). Organic matter in SD is mostly present in the solid form and its concentration ranges between 40% and 90% of dry mass (Kania et al., 2019). It originates predominantly from anthropic sources (wastewaters), but may also be autochtonous (*e.g.* biofilms, plants and microbial cells fractions; (GARCÍA et al., 2010)) or allochtonous (*e.g.* terrestrial organic residues from the catchment area). The surface sludge layer is the siege of numerous reactions which induce the evolution of organic matter (Kania et al., 2018a; Kim et al., 2016) that could in turn influence the quantity and the chemical nature of the DOM.

Some studies have already monitored the concentration of DOM in VFCW systems, from inflow to outflow (Barber et al., 2001; Clark et al., 2020; Park et al., 2018). Kania et al.(Kania et al., 2019) showed that SDs were sources of DOM and reported a pH-dependent leaching pattern. However, despite the significant scientific and operational implications this observation may have during the operation of VFCW systems or for the use of the sludge outside the system, little is known on the influence of pH on the fluxes, molecular weight and other characteristics of DOM leached from the SDs. Yet, by controlling the quantities, nature, and molecular size of DOM, the pH conditions could strongly influence the associated release of contaminants from the SDs (Kania et al., 2019; Pédrot et al., 2009a). During the operation of a wastewater treatment plant unit, the SD layer is usually submitted to pHs ranging between 6 and 9 (Park et al., 2018; Yu et al., 2008); However, more acidic conditions (pH below 6) can be observed with winery effluents for example (Rodríguez-Chueca et al., 2017). A better description of the leaching of organic compounds from the SDs may also provide useful information regarding the final use of the sludge material in land applications where it would be submitted to pHs ranging from 5 to 9 (Gao et al., 2017).

The general objective of this study was thus to generate scientific knowledge on the release of organic colloids from the SOM of VFCW surface sludge deposits, and more specifically on the effects of pH on the quantities and physical–chemical characteristics of the leached organic compounds. Previous work from our group compared the characteristics of 14 SDs samples from different origins and identified 2 typologies of samples according to their age, namely the older SDs group beyond 3 years of age, and the younger SDs group of 1 year or less (Kania et al., 2018a). The present study focused on sludge deposits of the older SDs group (beyond 3 years of age) which was considered as representative of a steady state mode of operation of the VFCW unit. The work was therefore done using SD samples taken from a same plant at different ages above 3 years, respectively 7 and 14 years, in order to investigate the influence of ageing on the leaching properties. SD samples were leached under controlled conditions over a wide pH range to generate information which would not be accessible in field studies. The aqueous extracts were fractionated by ultrafiltration and then analyzed for DOC concentration. Each ultrafiltrate was then further analyzed to evaluate the chemical nature of the organic compounds.

2. Materials and methods

2.1. Sampling

SD were sampled from the Vertical Flow Constructed Wetland (VFCW) treatment plant of Vercia (FRANCE) already described in details by Kim et al.(Boram Kim et al., 2015). This plant is designed according to the AZOE-NP patented process (EP1857419A1). It is considered as a “French system” because it receives unsettled wastewater. It differs from the so-called “classical French system” by some additional operations, in particular the implementation of a trickling filter before the first filter stage and the presence of a water-saturated zone in the lower part of the first stage filter, providing anoxic conditions to allow partial denitrification. SD samples were taken from the surface sludge layer of the first-stage filter which had been left in place since the first day of operation of the treatment plant following the protocol reported by Kania et al.(Kania et al., 2019). The 7-year samples were taken by Kania et al.(Kania et al., 2019), freeze-dried for conservation and stored at 4 °C The 14-year samples were taken specifically for the present study following the same protocol. All samplings were done in winter time for the good accessibility to the sludge layer due to the absence of the reeds. Several kg of SD were collected over the whole depth of the sludge layer (>15 cm) from 8 different spots at the surface of the first-stage filter. All samples were sorted manually on site to remove reeds rhizomes and gravels, and subsequently mixed together by shoveling. A representative sample of a few kg was then prepared by quartering, refrigerated and transported to the laboratory within a maximum of 4 hours.

Then, aliquot fractions were prepared, crushed and sieved at 1 mm, freeze-dried and stored at 4 °C for further analyses and assays.

2.2. Analysis of particulate matter

Organic carbon contents of the two SD samples were determined by a carbon sulfur analyzer (EMIA-320V2, Horiba Scientific Co., Ltd) previously decarbonized by hot digestion with diluted HCl. The precision of the analysis for carbon is ±2 mg/kg.

The freeze-dried SD samples were analyzed in duplicates for humic-like, fulvic-like and humin-like components, following a protocol adapted from Serra-Wittling et *al.* (Serra-Wittling et al., 1996). To obtain humic and fulvic-like content, a dry mass of 1g of SD was suspended and mixed for 2 hours in 50 mL of a 0.1 M sodium hydroxide aqueous solution. The suspension was then centrifuged at 10 000 g for 15 min and filtered at 0.45 µm using Sartorius acetate cellulose filters. The solutions, containing humic- and fulvic-like substances, were analyzed for OC using a Shimadzu TOC-L analyzer with an uncertainty of ± 5%. The residual solids contained all the SD constituents which were not extracted under the alkaline conditions used. Their OC content, representing the humin-like fraction, was calculated as the difference between the total organic carbon (TOC) content of the initial SD sample and the OC content of the filtered solution. To obtain fulvic-like content, SD solutions were acidified to pH 1.5 with 1 M sulfuric acid aqueous solution and kept overnight at +4°C to allow precipitation of humic-like substances. Fulvic-like substances were collected in the solutions by centrifugation at 6000 g for 15 min followed by filtration at 0.45µm. The filtered solutions were analyzed for OC concentration.

The SD samples were also analyzed by thermogravimetry (TGA) coupled to differential scanning calorimetry (DSC) using a METTLER TOLEDO TGA /DSC analyzer. Analyses were done in duplicates. Aliquote sub-samples of 20 mg dry mass (DM) were heated from 35 to 900 °C at a rate of 10 °C.min^{-1} under an airflow of 50 NmL.min^{-1}. Blanks were run under the same conditions without any samples. Mass losses obtained from TGA and heat fluxes obtained from DSC were monitored as a function of the temperature. The data were used to calculate R_{TGA} and R_{DSC} indexes as indicators of the stability of the organic matter as described previously (Kania et al., 2018a). These indexes were respectively calculated as the ratios between the mass loss (R_{TGA}) and the heat release (R_{DSC}) recorded between 400 and 600°C to those recorded between 200 and 400 °C. They were shown to increase with the contents in complex organic compounds such as lignin, poly aromatic structures of high MW and O-containing functional groups in the solid organic matter SOM (Kania et al., 2019).

2.2. pH-dependent leaching test

A batch leaching test, based on the CENTS/TS 14429 European standard, was used to evaluate the effect of pH on the release of organic components from the sludge deposits (SD) samples. The assays were performed in Nalgene® polypropylene centrifuge tubes, at a solid-to-liquid ratio of 100 g of SD dry matter per liter of leaching solution. Prior to the tests, all tubes were soaked in 1M HCl aqueous solution overnight and then rinsed with deionized water. All assays were duplicated.

The SD samples were contacted with: (i) deionized water for natural pH conditions (blank), (ii) 0.022, 0.08, 0.13, 0.25, 0.35 M nitric acid aqueous solutions for acidic conditions and (iii) 0.02, 0.03, 0.06, 0.1, 0.15, 0.20 M potassium hydroxide aqueous solution for alkaline conditions. The number of moles of protons (acidic solutions) or hydroxide ions (alkaline solutions) in each leaching solution was calculated as the product of HNO_3 or KOH concentrations by the volumes of solution used in each assay**.** Altogether, 5 acidic and 6 alkaline leaching solutions were used, in addition to the blank at natural pH. All assays and blank were stirred at room temperature in a rotary shaker set at 9 rpm until an apparent steady state was reached, which was observed within 48 hours in preliminary experiments.

2.3. Fractionation of leached compounds

The suspensions obtained from the batch leaching experiments described above with the two SD samples at the different pHs tested were centrifuged at 4000 rpm (2400 g) and the supernatants were filtered at 0.45 µm using Sartorius cellulose acetate filters to separate SOM from truly dissolved or colloidal forms. The solutions filtered at 0.45µm were analyzed for OC concentration and the results expressed as $[OC]_{0.45\ \mu m}$ corresponding to the colloidal and truly dissolved compounds leached. They were then further filtered at 0.22 µm on Sartorius microporous cellulose acetate.

Then, ultracentrifugation tubes equipped with Sartorius Vivaspin cellulose acetate ultrafiltration membranes of 30 kDa, 10 kDa and 3 kDa were used to fractionate the soluble components according to their MW. Centrifuge ultrafiltrations were performed at 3000g for 30 min using a swinging bucket rotor. Ultracentrifugation cells were previously rinsed with a 0.1M NaOH solution followed by de-ionized ultrapure water to guarantee initial concentrations of dissolved organic carbon (DOC) below 0.1 $mg.L^{-1}$ in the ultrafiltrate.

2.4. Analyses of suspensions and solutions

The suspensions obtained from the leaching experiments were analyzed for pH and conductivity before being filtered. A Consort C3020 meter equipped with Bioblock 11706358 and Consort SK10T electrodes was used for pH and conductivity.

Organic carbon (OC) concentrations were measured in solid, colloidal and truly dissolved fractions using a Shimadzu TOC-V CSH analyzer previously calibrated with a standard solution of potassium hydrogen phthalate. The uncertainty of the analysis was estimated to ± 5%. OC concentrations in blanks at natural pH (leaching in de-ionized ultrapure water) were found to be systematically below 0.2 $mgC.L^{-1}$.

The colloidal and truly dissolved fractions were further analyzed for UV-visible absorbance using a Perkin-Elmer Lambda 25 spectrophotometer to record UV-visible spectra from 800 to 220 nm with 0.5 nm increments. Analyses were done in duplicates at room temperature in 1-cm light-path quartz cells. The ratio of the absorbances measured at 250 and 365 nm (referred to as E_2:E_3) was calculated as an indicator of the size of the UV-absorbing organic molecules present in the solutions (Peacock et al., 2014). It was considered that an increase of the ratio revealed a decrease of the average molecular size of the UV-absorbing molecules in solution (Helms et al., 2008). The specific ultraviolet absorbance at 254 nm ($SUVA_{254}$, $L.mgOC^{-1}.m^{-1}$), defined as the ratio of the absorbance at 254 nm to the organic carbon concentration was used as an indicator of the degree of aromaticity of the molecules (Helms et al., 2008; Weishaar et al., 2003). Values of $SUVA_{254}$ above 4 and below 2 were considered to reveal highly aromatic and poorly aromatic molecules, respectively (Park et al., 2018).

3. Results and discussion

3.1. Comparison of the SDs physicochemical properties

a. General characteristics of the SDs

Table 1- Analyses of surface sludge deposits (SD) from Vercia VFCW wastewater treatment plant sampled after 7 and 14 years of operation

Sample	TOC [1] (g TOC/g DM)	Humic-like[2] (% of TOC)	Fulvic-like[2] (% of TOC)	Humin-like[2] (% of TOC)	R_{DSC}	R_{TGA}	N_{tot}[2] (% of DM)	P_{tot}[2] (% of DM)
14-year SD	0.17	13.0	12.7	74.3	2.14	0.84	2.45	2.11
7-year SD	0.23	18.0	12.6	69.5	1.90	0.76	3.78	2.04

TOC: total organic carbon (in dry solids); DM: dry matter; R_{DSC}: calorimetric index; R_{TGA}: thermogravimetric index.

[1] Uncertainty of ± 2%; [2] Uncertainty of ± 5%

The results of the characterization tests of our samples including the total amount of organic carbon (TOC), the extractions of humic and fulvic-like compounds and thermogravimetric indexes are shown in Table 1. TOC contents in both SD samples (0.17 and 0.23 g TOC/g DM, for 14-years and 7-years SD respectively) were far above the concentrations reported in literature for natural systems like natural wetlands sediments in which TOC rarely exceeds 10% (Guénet et al., 2016; Yin et al., 2019). TOC content in SD samples are closer to the 30-45% of TOC content generally observed in the first peatland soil profiles of temperate climate (Chen et al., 2018; Hong et al., 2019). The rest of the sludge deposits' matter is composed of inorganic matter such as Fe-oxyhydroxydes, carbonates, silica and clays (Boram Kim et al., 2015). The lower TOC content in 14-year, compared to 7-year SD, was assigned to the mineralization of organic matter which was reported in several studies (Boram Kim et al., 2015; Sellami et al., 2008).

About 70 to 75% of the TOC was present in the humin-like fraction in both samples (Table 1). Fulvic- and humic-like compounds were found to account for approximately 31% and 25% of the TOC content in the 7-year and 14-year samples, respectively. Previous studies from literature showed that the humin fraction's OC exhibited a higher concentration in aromatic and polyhydroxy aromatic compounds than the humic and fulvic-like fraction (Weishaar et al., 2003; Yao et al., 2019). This observation was confirmed here by TGA-DSC analyses that revealed higher values of R_{TGA} and R_{DSC} indexes for the 14 years old sludge deposit (Table 1). These results indicate that with aging, the sludge deposits' concentrates more and more aromatic and O-containing functional groups despite the continuous input of low aromatic organic matter from wastewater (Kania et al., 2019).

b. Acid-base buffering capacity of SDs

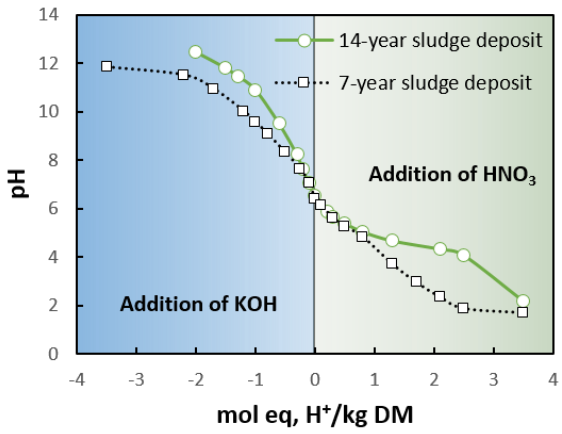

Fig. 1: Acid and basic titration curves of the 14-year and 7-year SD. The error bars, comprised within the symbols, represent the standard deviation of two measurements.

Fig 1a shows the acid-base buffering capacity of the two SD samples over the whole pH range tested. The x-axis shows the number of moles of protons (positive values, acidic solutions) or hydroxide ions (negative values, alkaline solutions) in each leaching solution, expressed per g of SD dry matter. The pH buffering capacity of solid samples such as soils, sediments or composts is largely influenced by the density of functional groups of OM (Nelson and Su, 2010; Plaza et al., 2005). Plaza et *al.* (Plaza et al., 2005) evidenced that OM enrichment in carboxyl and phenolic groups, occurring with composting process of various sludge residue, increase their acid buffering capacity. The buffer capacity of the two SDs were similar over most of the pH range but, with respect to 7-year SD, the 14-year SD shows a greater buffering capacity for acidic conditions (pH~5). Thus, this was probably due to the enrichment of the 14-year SD in aromatic and O-containing functional groups as observed in the previous section. This change in acid-base proprieties occurring with aging could improve the SD's resistance to acidic rain or acidic agricultural soils.

3.2. Characterization of the conventionally dissolved fraction (<0.45µm)

a. Evolution of the OC concentration

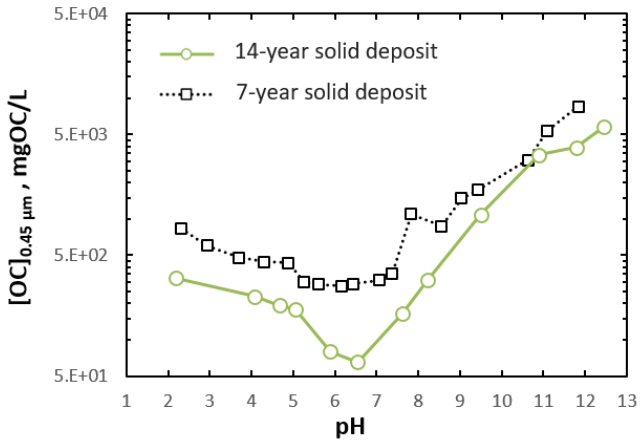

Fig. 2: Effect of pH on the leaching of OC from 7-year and 14-year solid deposits sampled from the same wastewater treatment plant. The size of the dots includes the 5% experimental uncertainty.

Fig. 2 shows the concentration of organic carbon measured at equilibrium in the 7-year and 14-year SD leachates after filtration at 0.45 µm ($[OC]_{0.45\ \mu m}$). The lowest extraction was observed at neutral pH (*i.e* pH 6.5), where only 0.4% and 1.6% of the TOC content was leached for 14-year and 7-year SD, respectively. These leaching values are similar to those reported in literature for agricultural soils with pH close to 7 and much lower TOC contents (Corvasce et al., 2006; Fang et al., 2016b). Under these circum-neutral pH conditions, the conformational structures of the organic matter and organo-mineral

aggregates are less impacted than under more acidic conditions (Pédrot et al., 2010) resulting in a lower leaching.

For both samples, leaching of organic compounds increased below pH 5 and above pH 7. Leaching at neutral to acidic pH affected only a very small proportion (less than 5%) of TOC present in the samples: the highest release under acidic conditions was obtained at pH 2.2 with 323 mg/L for the 14-year and 830 mg/L of OC for the 7-year SD, corresponding to 1.8% and 4.8% of the TOC respectively. The increased release of OC observed, for both SD samples, under acidic conditions is the net effect of several phenomena (Kalbitz et al., 2000). For example, under acidic conditions, protonation of hydroxyl groups and the development of a positive surface charge at mineral surfaces favored the adsorption of negatively charged organic molecules, thereby limiting the transfer of OC into the aqueous solution (Kalbitz et al., 2000; Tipping et al., 2011). But, the increase of protons competition under acidic conditions reduce cation bridging of organic molecules and could induce the release of OC (Guggenberger and Zech, 1993; Kalbitz et al., 2000). The sum of these phenomenon produces a net increase of the OC leached concentration observed under acidic conditions as compared to circum-neutral pH conditions.

The effect of pH on the leaching of soluble compounds was much stronger over the alkaline range (Fig. 2). For the 14-year SD, leaching was increased by a factor 4 from pH 6.5 to 8.0 (from 65 mg/L to more than 300 mg/L of OC), and by a factor 20 from pH 8 to 12 (6000 mg/L of OC at pH 12, Fig. 2). At pH 12, more than 33% of the overall TOC content of the sludge deposits was leached into the solution. For the 7-year SD, the maximum release, obtained at pH 12, was around 8000 mg/L, corresponding to 48% of the overall TOC content. The increasing solubilization of organic molecules with increasing pH could be attributed to the deprotonation of SD's mineral surfaces (e.g. Fe-oxyhydroxydes, clays…) occurring with increasing pH conditions which would disrupt organo-mineral association (Avena and Koopal, 1999, 1998) and lead to the solubilization of organic molecules associated to these mineral surfaces.

The chemical structure of organic functional groups was also reported as a factor controlling the solubilization of organic molecules (Matiasek and Hernes, 2019). This factor may explain the differences observed in the leaching behavior of the 7-year and 14-year samples (Fig.2), which cannot be attributed only to their different TOC contents. Over the entire pH range, released OC concentrations were higher for the 7-year SD but the largest gap was observed close to neutral pH (*i.e* pH 6.5) where 14-year SD released about 4 times less OC than the 7-year SD. This result emphasized that the 7-year SD contained more easily leachable organic molecules than the 14-year sample. This observation was attributed to the higher aromaticity of the 14-year sample and its higher content in

oxygenated functional groups (Table 1), which increased the proportion of OC trapped in organo-mineral aggregates (Bhattacharyya et al., 2018) and thus OC stability.

b. pH-dependent characteristics of soluble organic compounds

Figure *3a* shows the $SUVA_{254}$ values of the soluble organic compounds leached over the tested pH range for the 7-year and 14-year after filtration at 0.45 µm. At neutral pH (*i.e.* pH 6.5), SUVA values around 1 $L.mgOC^{-1}.m^{-1}$ were recorded for both 7-year and 14-year SD, suggesting a low aromaticity and high proportion of proteins, lipids and carbohydrates. Aromatic compounds were reported to have a higher affinity with mineral phases (Gao et al., 2018; Kramer et al., 2012) and were therefore probably sorbed under these pH conditions. The SUVA measured here were similar to those obtained by other authors on natural wetlands (Wang et al., 2014), sediments (He et al., 2016) and various agricultural soils with pH varying from pH 8 to pH 5 (Gao et al., 2017).

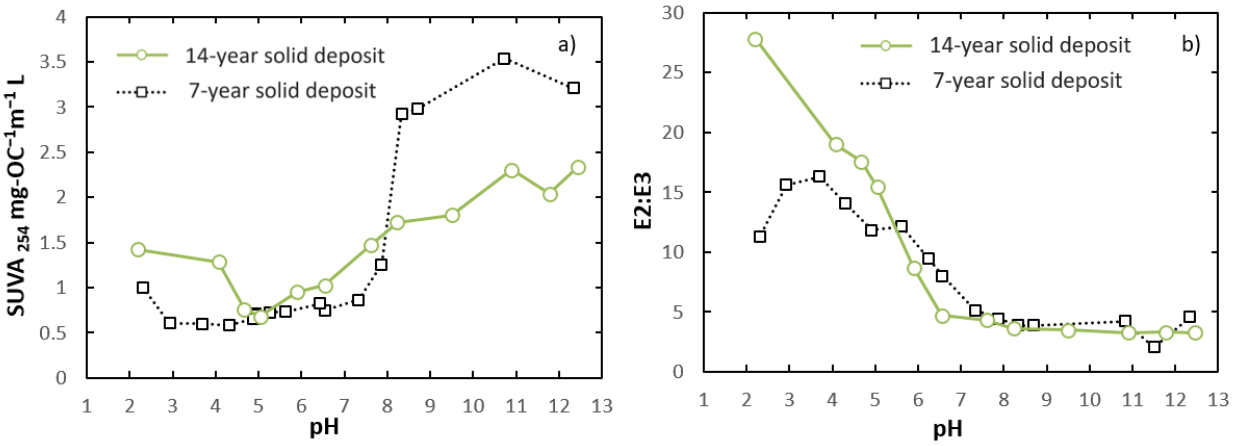

Fig. 3: Effect of pH on a) the SUVA and b) E2:E3 ratio of the soluble organic compounds leached at equilibrium from each sludge deposit. The size of the dots includes the 5% experimental uncertainty.

Under alkaline conditions, an increase of $SUVA_{254}$ values was observed, up to 2.5 $L.mgOC^{-1}.m^{-1}$ (14-years SD) and 3.5 $L.mgOC^{-1}.m^{-1}$ (7-years SD) at pH 12, suggesting the release of more aromatic organic compounds. The higher aromaticity of the compounds leached at increasingly alkaline pHs was attributed to the desorption of fulvic and humic-like compounds. Above pH 8 or so, $SUVA_{254}$ values were higher for the 7-year SD than the 14-year sample (Fig. 3a) despite the aromatic content deduced from table 1, which were lower in the 7-year SD. This observation could be attributed to a stronger stability in the 14-year SD as compared to the 7-year sample of the complexes between organic compounds and clay (El-sayed et al., 2019) or metal-oxyhydroxides (Kaiser and Guggenberger, 2000) within the SD particles. Under very acidic conditions, the SUVA of the leached compounds was slightly higher than under natural pH conditions (around 1.5 and 0.5-1.0 respectively). This result may be

explained by the possible dissolution of carrier mineral phases (Kögel-Knabner et al., 2008) at very acidic pH leading to the release of associated organic compounds.

Figure 3b shows the evolution of E2:E3 values of the soluble organic compounds leached over the tested pH range for the 7-year and 14-year after filtration at 0.45 µm. For both samples, higher E2:E3 are observed below pH 7 compared to pH above 7. This result suggests that the SD release smaller UV-absorbing organic compounds at acidic pHs. In addition, the constant increase in E2:E3 values from pH 7 to pH 2 suggests a gradual decrease in the size of the UV-absorbing released molecules as the solutions become more acidic. At pH values below 5, the 14-year SD soluble organic compounds induced a higher proportion of small size organic components assimilated to fulvic acids. Between pH 7 and pH 12, for both samples, E2:E3 remains stable in the range of 4.5 to 3.5. These values were similar to those obtained for pore water of peatland that fluctuate around 4 (Peacock et al., 2014; Strack et al., 2015) and for agricultural soil solution (Tiefenbacher et al., 2020). Finally, the evolution of SD characteristics with ageing seemed to affect only partially the molecular size of UV-absorbing leached organic molecules as shown by the similar E2:E3 between the two SDs.

3.3. Ultrafiltration of the leached organic compounds from the 14-year SD

a. Assessment of the molecular size of emitted organics compound at various pH from SD

The OC concentration measured in each filtrates (0.45 and 0.22 µm) and ultrafiltrates (30, 10 and 3 kDa) depending on pH conditions is presented in Figure 4a. The OC concentrations were very similar in the 0.45 µm and 0.22 µm filtrates regardless of pH conditions, indicating that only a very small quantity of compounds were leached in the size range comprised between 0.22 and 0.45 µm. The same was observed for 30 kDa and 10 kDa filtrates over the whole pH range, indicating that very few molecules are comprised between 10 and 30 kDa. At acidic pH, the comparison of the different curves indicated that a large proportion of organic molecules exhibited a molecular size below 3 kDa. At neutral and alkaline pH's, it was observed that the $OC_{<0.45\mu m}$ curve differed from the others indicating a large proportion of molecules with a molecular size higher than 30 kDa.

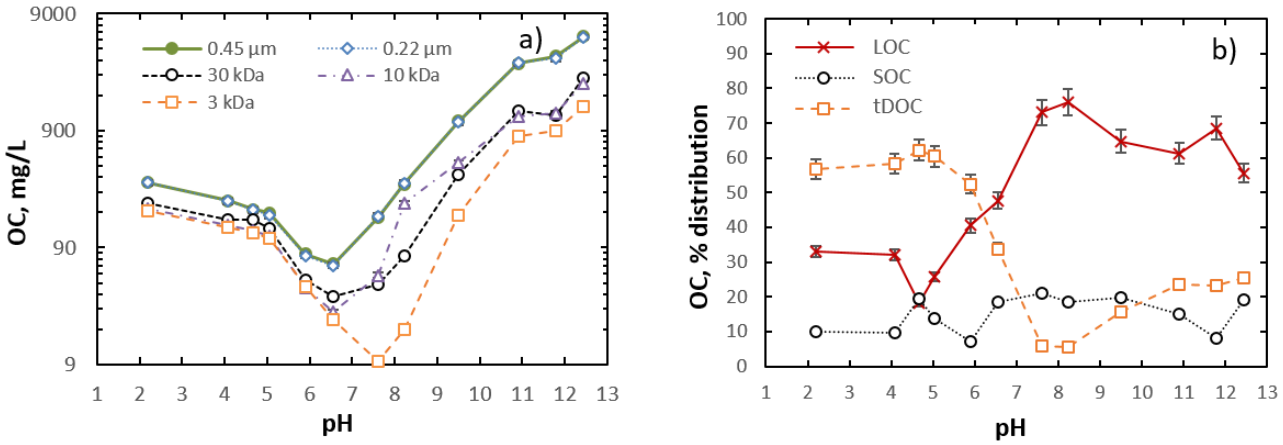

Fig. 4: Effect of pH on a) the size distribution of the leached organic compounds and b) the distribution of OC in 3 different MW fractions previously defined. The size of the dots includes the 5% experimental uncertainty.

The pH-dependent molecular size of organic compounds released from the 14-year SD can be simplified by grouping the results within different molecular size classes (Durce et al., 2016; Xu et al., 2018). The size of the leached organic compounds was therefore described here in a simplified manner according to the following classes: (i) Large Organic Colloid (LOC) between 30 kDa and 0.45 µm, (ii) Small Organic Colloid (SOC) between 3 kDa and 10 kDa and (iii) "truly" Dissolved Organic Carbon (tDOC), smaller than 3 kDa. All designations and acronyms, along with the equations used for the calculations, are gathered in supplementary data in Table S1.

The relative abundance of leached organic compounds in each molecular-size fraction, expressed in % of total released OC concentration, is shown in Figure 4b. Over the whole pH range, the percentage of small colloids remained relatively constant (between 5 and 20%), but the proportions of LOC and truly dissolved compounds varied considerably with the pH. Under acidic conditions, truly dissolved compounds were predominantly leached (about 60% of overall leached OC), whereas large colloids were predominant above pH 7. This observation was in agreement with the increase of E_2:E_3 measured on the $OC_{<0.45\mu m}$, observed from pH 6.5 to 2 (Fig.3 b.) confirmed that the size of the leached organic compounds was smaller as the pH was decreased. The size distribution of leached organic compounds remained relatively stable below pH 6 (tDOC predominant) and above pH 8 (LOC predominant). However, the E2:E3 suggests a progressive decrease in the MW of leached organic compounds with acidification, which cannot be detected with the 3 kDa cut-off. Thus, the proportion of molecules <3 kDa remains constant but within this class, the released molecules are increasingly smaller with acidification. The strongest variations in the size distributions were observed between pH 6 and 8 that is, naturally occurring pH conditions. An increase of one pH unit (from pH 6 to pH 7) was found to

divide by 2.5 the proportion of truly dissolved compounds (from more than 50% to less than 20% of overall of leached OC).

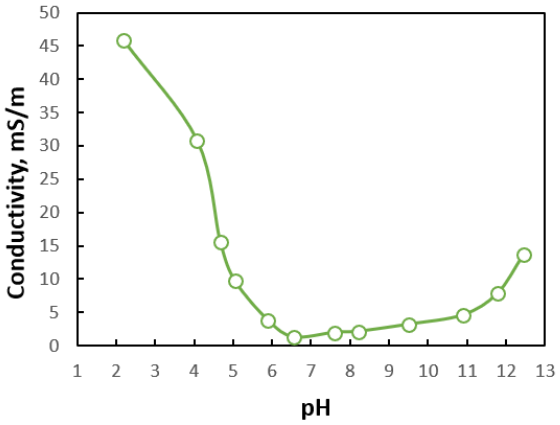

Fig. 5: Conductivity of the 14-year SD sample recorded at equilibrium in the batch leaching assays.

Mineral phases preferentially sorb high MW OC with higher content in aromatic and O-containing polar groups (Specht et al., 2000; Xu et al., 2019b), thus the desorption of OC from these phases occurring with alkalization of the solution conditions could both explain the increasing of OC MW and the relative aromaticity of released OC described in further details in the following paragraph. The preferential solubilization of small MW organic matter under acidic conditions have been previously observed on soils batch experiments (Pédrot et al., 2009a) and in acidic soil solutions (Pokrovsky et al., 2005). This phenomenon could be explained by both pH and conductivity of the SD solutions. Under acidic pH conditions, organic molecules with higher net surface charge are preferentially solubilized (Tipping and Woof, 1991). Fulvic acids, which MW is smaller than humic acids, have stronger total charge per gram of carbon and higher proportion in weak proton affinity sites compare to humic acids (Weng et al., 2006). These proprieties of small organic molecules assimilated to fulvic acids could explain the release of tDOC from the SD submitted to acidic conditions. Besides pH conditions, the size of the released OC could be affected by the conductivity of the solution which is described in Figure 5. The dissociation of metal oxides and the important release of multivalent cation showed via ICP-MS analysis by Kania et *al.* (Kania et al., 2019) on the 7-year SD sample could explain the significant increase in conductivity observed under acidic conditions for the 14-year SD. This phenomenon occurring with the acidification of the solutions may promote the aggregation of large macromolecules (>20 kDa) into solid OM >0.45 µm (Durce et al., 2016; Sillanpää et al., 2018). Smaller molecules were not affected resulting in an increase of the proportion of dissolved compounds with the acidification.

b. Aromaticity of the leached organic compounds in the different size ranges and effect of pH

Figure 6 shows the $SUVA_{254}$ values of the leached compounds in each size range at the different pHs of equilibrium. Over the entire pH range, the SUVA of large and small colloids (LOC and SOC) were very similar, increasing with the pH from 0.4 at pH 6.5 to 3 $L.mgOC^{-1}.m^{-1}$ at pH 12. The $SUVA_{254}$ was however always below 3, suggesting a high proportion in hydrophilic molecules. Several factors may explain the relative low aromaticity measured for large and small colloidal fractions, such as the preferential sequestration of aromatic compounds by minerals (Specht et al., 2000) present in the solid phases. Moreover, it has been shown that weak acids groups and aliphatic structure can be linked via hydrogen, hydrophobic or cation bonding to aromatics rings of the large and small colloidal fraction (Kipton et al., 1992; Piccolo, 2001) thus decreasing the aromaticity of the supramolecular assemblies observed in these size fraction.

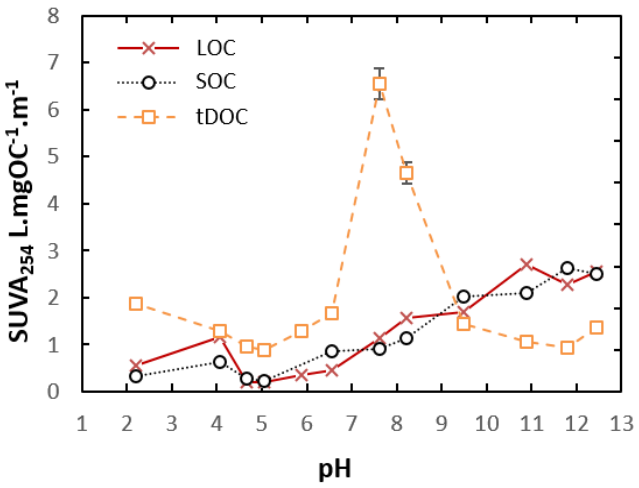

Fig. 6: $SUVA_{254}$ values of leached organic compounds as a function of pH and MW fractions. (Bars represent the analytical uncertainty).

The $SUVA_{254}$ of the tDOC fraction remained close to 1 $L.mgOC^{-1}.m^{-1}$ over the acidic and alkaline pH ranges, but fluctuated greatly around the neutral pH (6.5) from 1.4 $L.mgOC^{-1}.m^{-1}$ at pH 6 to 7 $L.mgOC^{-1}.m^{-1}$ at pH 8. These high $SUVA_{254}$ values suggested that truly dissolved organic matter contained a high proportion of aromatic molecules like phenols, phenolic acids and flavonoids (Klotzbücher et al., 2013). This near-neutral pH range is also the range with the lowest conductivity (Fig. 5) and the smallest amount of tDOC released (Fig. 6). The important tDOC aromaticity could be reasonably explained by the low conductivity suggesting low cations release and thus low quantity of cationic bridging between low MW aromatic structure and other low MW hydrophilic compounds decreasing the aromaticity

such as polysaccharides. The major results of this section (*i.e* transition between a release of LOC versus a release of tDOC and the release of highly aromatic truly dissolved molecules) are obtained in a pH range ranging from 5.5 to 8. These results were even more important as the sensitivity of SD is manifested in a critical pH range that SD may encounter during regular conditions of operation with environmental implications described in the following section.

4. Environmental significance

The results presented in this study contribute to a better description of the mechanisms of retention and release of organic compounds during the contact between aqueous solutions and sludge deposits solid organic matter. The experimental conditions used allow potential applications to various conditions that the sludge may encounter either in the VCFW during its operation or outside during its reuse in agriculture for example. The pH range tested in this study by far encompasses the possible situations that may be encountered in practice. Results show the effects of pH on the quantities, nature and molecular size of leached organics, and provide indications on the retention or co-transport of pollutants with organic carriers and the potential associated environmental impacts.

SD layer play a major role in the performance of VFCW systems (Molle, 2013). By reducing the release and transfer of OC and associated contaminants from the SD solid organic matter, ageing may improve the performance in carbon removal. However, for the same reason, SD ageing may be unfavorable to denitrification which requires sufficient quantities of bioavailable OM (Grießmeier and Gescher, 2018).

At the end of their operational life, SD may be reused as soil applications to increase or restore organic matter content of the receiving soils (Senesi et al., 2007). This study suggests the importance of the SD ageing process to improve the environmental safety and agronomic performance of this practice. The main benefits of soil application of organic amendments such as compost [51,54] or related materials is in the formation of soil organo-mineral aggregates which reduce the erosion phenomena and contribute to the improvement of the agronomic properties of the soil such as its porous structure and water retention capacity. However, application of readily biodegradable matter (as in younger SDs) would cause a series of undesired phenomena such as oxygen depletion due to its rapid aerobic mineralization. Improving the agronomic properties of the soil while reducing the potential environmental impacts is achievable by applying stable forms of organic matter (Senesi et al., 2007) such as in older SDs. 14-year sludge deposits were also shown in this study to reduce the release of soluble organic compounds regardless of pH conditions, thereby limiting carbon loss in the receiving soil and increasing the residence time of solid organic matter.

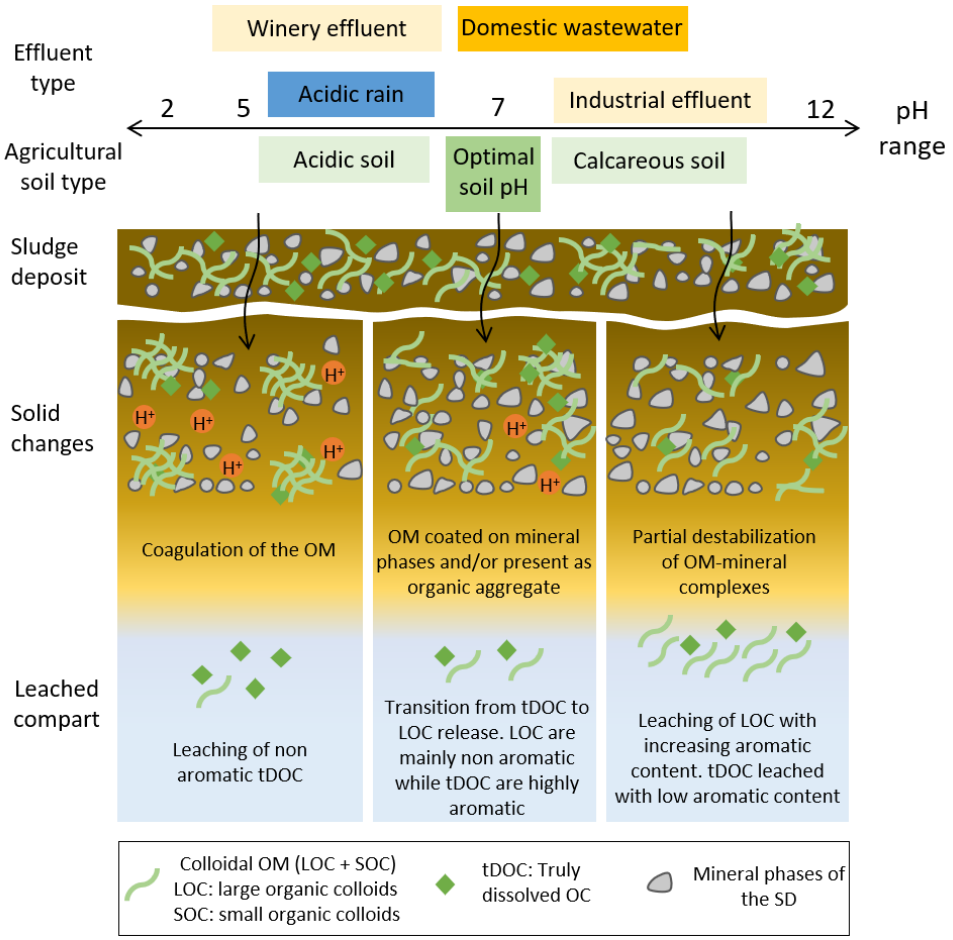

Fig. 7: Conceptual solid-solution partition of organic matter and evolution of the quality of the released organic molecules from SD under various pH conditions corresponding to different operational and reuse conditions SD might undergo.

Under regular operating conditions, the deposits in the surface sludge layer of VFCWs would be in contact with close to neutral to slightly alkaline solution (Fig.7). This study showed that small pH variations in this range would strongly affect the leaching of organic matter, both quantitatively and qualitatively (size and aromaticity). In this pH range, the colloidal fraction was found to contain mostly hydrophilic compounds. The low $SUVA_{254}$ values (Hansen et al., 2016) as well as, in a less extent, the molecular weight (Amon and Benner, 1996) of this colloidal pool are indicators of a high biodegradability of these molecules. Indeed, molecular weight and $SUVA_{254}$ are positively and negatively, correlated to the biodegradability of natural organic molecules, respectively. Thus, the leaching of this colloidal fraction could negatively influence water quality indicator such as the Biochemical Oxygen Demand (BOD) of the treated water. The “truly” dissolved fractions containing a high proportion of aromatic compounds could have strong interactions with the micropollutants

possibly present in the SD. However, the high aromaticity, and consequently the probable low biodegradability of these molecules, limits their contribution to the BOD of the leachates.

Under alkaline conditions, the leached organics were predominantly in the form of large colloids, containing aromatic compounds. These pH conditions would increase the interactions between the leached organic molecules and trace metals thus enhancing the mobility of such pollutants from the SD to the receiving environment.

Under conditions of flooding for example, anoxic to anaerobic conditions may cause the installation of reductive conditions associated with possible acidification due to the formation of volatile fatty acids (Robles-Martínez and Gourdon, 1999). SD would then leach poorly aromatics molecules of small molecular size (<3 kDa), probably composed by low-molecular weight organic acids, carbohydrates and small amino-acids, having the capacities to sorb heavy metals contaminants (Pokrovsky et al., 2005) and would be more bio-available (Marschner and Kalbitz, 2003).

5. Conclusion

The nature of the organic compounds leached from the SD under a wide range of pH was approached here through their size distribution using (ultra)filtration and their aromaticity using UV-visible spectroscopy indicators. Under acidic conditions, leached organics were predominantly (more than 50%) in the form of truly dissolved compounds tDOC made of poorly aromatic molecules. Under alkaline conditions however, tDOC was less than 20% of leached organics which were associated to large colloids for more than 70%. The release of OC trapped in solid organo-mineral association increased the overall aromaticity and molecular size of the leachates. This study clearly demonstrated important changes in the nature of the leaching molecules in the natural range of pH (*i.e.* pH 5 to pH 8). These results showed that a small variation in pH could induce strong effects on the characteristics of the released organic matter. The organic components in the large colloids were mostly carbohydrates, proteins, and aliphatic molecules, whereas the truly dissolved components were predominantly aromatic molecules.

The transformation of the SD occurring with ageing increased their acid-base buffering capacity, reduced the amount and aromaticity of the leached organic molecules without changing the molecular size of UV-absorbing molecules. These effects of ageing may be seen as improving the capacity of the SD surface layer to retain pollutants during the operation of a VFCW unit, and also the suitability for land applications of sludge deposits dredged from French VFCW.

Acknowledgments

This work was supported by the C-FACTOR project funded by ANR (project number ANR-18-CE01-0008). Through the support of the GeOHeLiS analytical platform of Rennes University, this publication is also supported by the European Union through the European Regional Development Fund (FEDER), the French ministry of Higher Education and Research, the French Region of Brittany and Rennes Metropole.

This work was realized within the Graduate School H2O'Lyon (ANR-17-EURE-0018) and Université de Lyon (UdL), as part of the programme "Investissements d'Avenir " run by Agence Nationale de la Recherche (ANR).

The authors would like to thank the "Bonus Qualité Recherche" of INSA Lyon for funding part of this research project.

Literature cited

Amon, R.M.W., Benner, R., 1996. Bacterial utilization of different size classes of dissolved organic matter. Limnology and Oceanography 41, 41–51. https://doi.org/10.4319/lo.1996.41.1.0041

Araújo, E., Strawn, D.G., Morra, M., Moore, A., Ferracciú Alleoni, L.R., 2019. Association between extracted copper and dissolved organic matter in dairy-manure amended soils. Environmental Pollution 246, 1020–1026. https://doi.org/10.1016/j.envpol.2018.12.070

Avena, M.J., Koopal, L.K., 1999. Kinetics of Humic Acid Adsorption at Solid-Water Interfaces. Environ. Sci. Technol. 33, 2739–2744. https://doi.org/10.1021/es981236u

Avena, M.J., Koopal, L.K., 1998. Desorption of Humic Acids from an Iron Oxide Surface. Environ. Sci. Technol. 32, 2572–2577. https://doi.org/10.1021/es980112e

Avena, M.J., Wilkinson, K.J., 2002. Disaggregation Kinetics of a Peat Humic Acid: Mechanism and pH Effects. Environ. Sci. Technol. 36, 5100–5105. https://doi.org/10.1021/es025582u

Barber, L.B., Leenheer, J.A., Noyes, T.I., Stiles, E.A., 2001. Nature and Transformation of Dissolved Organic Matter in Treatment Wetlands. Environ. Sci. Technol. 35, 4805–4816. https://doi.org/10.1021/es010518i

Bhattacharyya, A., Schmidt, M.P., Stavitski, E., Martínez, C.E., 2018. Iron speciation in peats: Chemical and spectroscopic evidence for the co-occurrence of ferric and ferrous iron in organic complexes and mineral precipitates. Organic Geochemistry 115, 124–137. https://doi.org/10.1016/j.orggeochem.2017.10.012

Chen, S., Hong, H., Huang, X., Fang, Q., Yin, K., Wang, C., Zhang, Y., Cheng, L., Algeo, T.J., 2018. The role of organo-clay associations in limiting organic matter decay: Insights from the Dajiuhu peat soil, central China. Geoderma 320, 149–160. https://doi.org/10.1016/j.geoderma.2018.01.013

Clark, C.D., De Bruyn, W.J., Brahm, B., Aiona, P., 2020. Optical properties of chromophoric dissolved organic matter (CDOM) and dissolved organic carbon (DOC) levels in constructed water treatment wetland systems in southern California, USA. Chemosphere 247, 125906. https://doi.org/10.1016/j.chemosphere.2020.125906

Corvasce, M., Zsolnay, A., D'Orazio, V., Lopez, R., Miano, T.M., 2006. Characterization of water extractable organic matter in a deep soil profile. Chemosphere 62, 1583–1590. https://doi.org/10.1016/j.chemosphere.2005.07.065

Durce, D., Maes, N., Bruggeman, C., Van Ravestyn, L., 2016. Alteration of the molecular-size-distribution of Boom Clay dissolved organic matter induced by Na+ and Ca2+. Journal of Contaminant Hydrology 185–186, 14–27. https://doi.org/10.1016/j.jconhyd.2015.12.001

El-sayed, M.E.A., Khalaf, M.M.R., Gibson, D., Rice, J.A., 2019. Assessment of clay mineral selectivity for adsorption of aliphatic/aromatic humic acid fraction. Chemical Geology 511, 21–27. https://doi.org/10.1016/j.chemgeo.2019.02.034

Fang, W., Wei, Y., Liu, J., 2016. Comparative characterization of sewage sludge compost and soil: Heavy metal leaching characteristics. Journal of Hazardous Materials 310, 1–10. https://doi.org/10.1016/j.jhazmat.2016.02.025

Gangloff, S., Stille, P., Schmitt, A.-D., Chabaux, F., 2016. Factors controlling the chemical composition of colloidal and dissolved fractions in soil solutions and the mobility of trace elements in soils. Geochimica et Cosmochimica Acta 189, 37–57. https://doi.org/10.1016/j.gca.2016.06.009

Gao, J., Jansen, B., Cerli, C., Helmus, R., Mikutta, R., Dultz, S., Guggenberger, G., Vogel, C., Kalbitz, K., 2018. Organic matter coatings of soil minerals affect adsorptive interactions with phenolic and amino acids. European Journal of Soil Science 69, 613–624. https://doi.org/10.1111/ejss.12562

Gao, J., Liang, C., Shen, G., Lv, J., Wu, H., 2017. Spectral characteristics of dissolved organic matter in various agricultural soils throughout China. Chemosphere 176, 108–116. https://doi.org/10.1016/j.chemosphere.2017.02.104

GARCÍA, J., ROUSSEAU, D.P.L., MORATÓ, J., LESAGE, E., MATAMOROS, V., BAYONA, J.M., 2010. Contaminant Removal Processes in Subsurface-Flow Constructed Wetlands: A Review. Critical Reviews in Environmental Science and Technology 40, 561–661. https://doi.org/10.1080/10643380802471076

Grießmeier, V., Gescher, J., 2018. Influence of the Potential Carbon Sources for Field Denitrification Beds on Their Microbial Diversity and the Fate of Carbon and Nitrate. Front. Microbiol. 9. https://doi.org/10.3389/fmicb.2018.01313

Grybos, M., Davranche, M., Gruau, G., Petitjean, P., Pédrot, M., 2009. Increasing pH drives organic matter solubilization from wetland soils under reducing conditions. Geoderma 154, 13–19. https://doi.org/10.1016/j.geoderma.2009.09.001

Guénet, H., Davranche, M., Vantelon, D., Pédrot, M., Al-Sid-Cheikh, M., Dia, A., Jestin, J., 2016. Evidence of organic matter control on As oxidation by iron oxides in riparian wetlands. Chemical Geology 439, 161–172. https://doi.org/10.1016/j.chemgeo.2016.06.023

Guggenberger, G., Zech, W., 1993. Dissolved organic carbon control in acid forest soils of the Fichtelgebirge (Germany) as revealed by distribution patterns and structural composition analyses. Geoderma 59, 109–129. https://doi.org/10.1016/0016-7061(93)90065-S

Hansen, A.M., Kraus, T.E.C., Pellerin, B.A., Fleck, J.A., Downing, B.D., Bergamaschi, B.A., 2016. Optical properties of dissolved organic matter (DOM): Effects of biological and photolytic degradation. Limnology and Oceanography 61, 1015–1032. https://doi.org/10.1002/lno.10270

He, W., Jung, H., Lee, J.-H., Hur, J., 2016. Differences in spectroscopic characteristics between dissolved and particulate organic matters in sediments: Insight into distribution behavior of sediment organic matter. Science of The Total Environment 547, 1–8. https://doi.org/10.1016/j.scitotenv.2015.12.146

Helms, J.R., Stubbins, A., Ritchie, J.D., Minor, E.C., Kieber, D.J., Mopper, K., 2008. Absorption spectral slopes and slope ratios as indicators of molecular weight, source, and photobleaching of chromophoric dissolved organic matter. Limnology and Oceanography 53, 955–969. https://doi.org/10.4319/lo.2008.53.3.0955

Hong, H., Chen, S., Fang, Q., Algeo, T.J., Zhao, L., 2019. Adsorption of organic matter on clay minerals in the Dajiuhu peat soil chronosequence, South China. Applied Clay Science 178, 105125. https://doi.org/10.1016/j.clay.2019.105125

Kaiser, K., Guggenberger, G., 2000. The role of DOM sorption to mineral surfaces in the preservation of organic matter in soils. Organic Geochemistry 31, 711–725. https://doi.org/10.1016/S0146-6380(00)00046-2

Kalbitz, K., Solinger, S., Park, J.-H., Michalzik, B., Matzner, E., 2000. CONTROLS ON THE DYNAMICS OF DISSOLVED ORGANIC MATTER IN SOILS: A REVIEW. Soil Science 165, 277.

Kania, M., Gautier, M., Blanc, D., Lupsea-Toader, M., Merlot, L., Quaresima, M.-C., Gourdon, R., 2019. Leaching behavior of major and trace elements from sludge deposits of a French vertical flow constructed wetland. Science of The Total Environment 649, 544–553. https://doi.org/10.1016/j.scitotenv.2018.08.364

Kania, M., Gautier, M., Ni, Z., Bonjour, E., Guégan, R., Michel, P., Jame, P., Liu, J., Gourdon, R., 2018. Analytical indicators to characterize Particulate Organic Matter (POM) and its evolution in French Vertical Flow Constructed Wetlands (VFCWs). Science of The Total Environment 622–623, 801–813. https://doi.org/10.1016/j.scitotenv.2017.11.357

Kikuchi, T., Fujii, M., Terao, K., Jiwei, R., Lee, Y.P., Yoshimura, C., 2017. Correlations between aromaticity of dissolved organic matter and trace metal concentrations in natural and effluent waters: A case study in the Sagami River Basin, Japan. Science of The Total Environment 576, 36–45. https://doi.org/10.1016/j.scitotenv.2016.10.068

Kim, B., Gautier, M., Rivard, C., Sanglar, C., Michel, P., Gourdon, R., 2015. Effect of Aging on Phosphorus Speciation in Surface Deposit of a Vertical Flow Constructed Wetland. Environ. Sci. Technol. 49, 4903–4910. https://doi.org/10.1021/es506164v

Kim, B., Gautier, M., Simidoff, A., Sanglar, C., Chatain, V., Michel, P., Gourdon, R., 2016. pH and Eh effects on phosphorus fate in constructed wetland's sludge surface deposit. Journal of Environmental Management 183, 175–181. https://doi.org/10.1016/j.jenvman.2016.08.064

Kipton, H., Powell, J., Town, R.M., 1992. Solubility and fractionation of humic acid; effect of pH and ionic medium. Analytica Chimica Acta 267, 47–54. https://doi.org/10.1016/0003-2670(92)85005-Q

Klotzbücher, T., Kaiser, K., Filley, T.R., Kalbitz, K., 2013. Processes controlling the production of aromatic water-soluble organic matter during litter decomposition. Soil Biology and Biochemistry 67, 133–139. https://doi.org/10.1016/j.soilbio.2013.08.003

Kögel-Knabner, I., Guggenberger, G., Kleber, M., Kandeler, E., Kalbitz, K., Scheu, S., Eusterhues, K., Leinweber, P., 2008. Organo-mineral associations in temperate soils: Integrating biology, mineralogy, and organic matter chemistry. Journal of Plant Nutrition and Soil Science 171, 61–82. https://doi.org/10.1002/jpln.200700048

Kramer, M.G., Sanderman, J., Chadwick, O.A., Chorover, J., Vitousek, P.M., 2012. Long-term carbon storage through retention of dissolved aromatic acids by reactive particles in soil. Global Change Biology 18, 2594–2605. https://doi.org/10.1111/j.1365-2486.2012.02681.x

Marschner, B., Kalbitz, K., 2003. Controls of bioavailability and biodegradability of dissolved organic matter in soils. Geoderma, Ecological aspects of dissolved organic matter in soils 113, 211–235. https://doi.org/10.1016/S0016-7061(02)00362-2

Matiasek, S.J., Hernes, P.J., 2019. The chemical fingerprint of solubilized organic matter from eroded soils and sediments. Geochimica et Cosmochimica Acta 267, 92–112. https://doi.org/10.1016/j.gca.2019.09.016

Molle, P., 2013. French vertical flow constructed wetlands: a need of a better understanding of the role of the deposit layer. Water Science and Technology 69, 106–112. https://doi.org/10.2166/wst.2013.561

Nelson, P.N., Su, N., 2010. Soil pH buffering capacity: a descriptive function and its application to some acidic tropical soils. Soil Res. 48, 201–207. https://doi.org/10.1071/SR09150

Park, J., Choi, M., Cho, J., Chon, K., 2018. Transformation of dissolved organic matter in a constructed wetland: A molecular-level composition analysis using pyrolysis-gas chromatography mass

spectrometry. Environmental Engineering Research 23, 390–396. https://doi.org/10.4491/eer.2018.043

Peacock, M., Evans, C.D., Fenner, N., Freeman, C., Gough, R., Jones, T.G., Lebron, I., 2014. UV-visible absorbance spectroscopy as a proxy for peatland dissolved organic carbon (DOC) quantity and quality: considerations on wavelength and absorbance degradation. Environ Sci Process Impacts 16, 1445–1461. https://doi.org/10.1039/c4em00108g

Pearson, H.B.C., Comber, S.D.W., Braungardt, C., Worsfold, P.J., 2017. Predicting Copper Speciation in Estuarine Waters—Is Dissolved Organic Carbon a Good Proxy for the Presence of Organic Ligands? Environ. Sci. Technol. 51, 2206–2216. https://doi.org/10.1021/acs.est.6b05510

Pédrot, M., Dia, A., Davranche, M., 2010. Dynamic structure of humic substances: Rare earth elements as a fingerprint. Journal of Colloid and Interface Science 345, 206–213. https://doi.org/10.1016/j.jcis.2010.01.069

Pédrot, M., Dia, A., Davranche, M., 2009. Double pH control on humic substance-borne trace elements distribution in soil waters as inferred from ultrafiltration. Journal of Colloid and Interface Science 339, 390–403. https://doi.org/10.1016/j.jcis.2009.07.046

Piccolo, A., 2001. THE SUPRAMOLECULAR STRUCTURE OF HUMIC SUBSTANCES. Soil Science 166, 810–832.

Plaza, C., Senesi, N., Polo, A., Brunetti, G., 2005. Acid−Base Properties of Humic and Fulvic Acids Formed during Composting. Environ. Sci. Technol. 39, 7141–7146. https://doi.org/10.1021/es050613h

Pokrovsky, O.S., Dupré, B., Schott, J., 2005. Fe–Al–organic Colloids Control of Trace Elements in Peat Soil Solutions: Results of Ultrafiltration and Dialysis. Aquat Geochem 11, 241–278. https://doi.org/10.1007/s10498-004-4765-2

Pokrovsky, O.S., Manasypov, R.M., Loiko, S.V., Shirokova, L.S., 2016. Organic and organo-mineral colloids in discontinuous permafrost zone. Geochimica et Cosmochimica Acta 188, 1–20. https://doi.org/10.1016/j.gca.2016.05.035

Robles-Martínez, F., Gourdon, R., 1999. Effect of baling on the behaviour of domestic wastes: laboratory study on the role of pH in biodegradation. Bioresource Technology 69, 15–22. https://doi.org/10.1016/S0960-8524(98)00176-X

Rodríguez-Chueca, J., Amor, C., Silva, T., Dionysiou, D.D., Li Puma, G., Lucas, M.S., Peres, J.A., 2017. Treatment of winery wastewater by sulphate radicals: HSO5−/transition metal/UV-A LEDs. Chemical Engineering Journal, Intensification of Photocatalytic Processes for Niche Applications in the Area of Water, Wastewater and Air Treatment 310, 473–483. https://doi.org/10.1016/j.cej.2016.04.135

Sauvé, S., Hendershot, W., Allen, H.E., 2000. Solid-Solution Partitioning of Metals in Contaminated Soils: Dependence on pH, Total Metal Burden, and Organic Matter. Environ. Sci. Technol. 34, 1125–1131. https://doi.org/10.1021/es9907764

Sellami, F., Hachicha, S., Chtourou, M., Medhioub, K., Ammar, E., 2008. Maturity assessment of composted olive mill wastes using UV spectra and humification parameters. Bioresource Technology 99, 6900–6907. https://doi.org/10.1016/j.biortech.2008.01.055

Senesi, N., Plaza, C., Brunetti, G., Polo, A., 2007. A comparative survey of recent results on humic-like fractions in organic amendments and effects on native soil humic substances. Soil Biology

and Biochemistry, Organic Wastes in Soils: Biochemical and Environmental Aspects 39, 1244–1262. https://doi.org/10.1016/j.soilbio.2006.12.002

Serra-Wittling, C., Barriuso, E., Houot, S., 1996. Impact of Composting Type on Composts Organic Matter Characteristics, in: de Bertoldi, M., Sequi, P., Lemmes, B., Papi, T. (Eds.), The Science of Composting. Springer Netherlands, Dordrecht, pp. 262–273. https://doi.org/10.1007/978-94-009-1569-5_26

Sillanpää, M., Ncibi, M.C., Matilainen, A., Vepsäläinen, M., 2018. Removal of natural organic matter in drinking water treatment by coagulation: A comprehensive review. Chemosphere 190, 54–71. https://doi.org/10.1016/j.chemosphere.2017.09.113

Specht, C.H., Kumke, M.U., Frimmel, F.H., 2000. Characterization of NOM adsorption to clay minerals by size exclusion chromatography. Water Research 34, 4063–4069. https://doi.org/10.1016/S0043-1354(00)00148-2

Strack, M., Zuback, Y., McCarter, C., Price, J., 2015. Changes in dissolved organic carbon quality in soils and discharge 10years after peatland restoration. Journal of Hydrology 527, 345–354. https://doi.org/10.1016/j.jhydrol.2015.04.061

Tiefenbacher, A., Weigelhofer, G., Klik, A., Pucher, M., Santner, J., Wenzel, W., Eder, A., Strauss, P., 2020. Short-term effects of fertilization on dissolved organic matter (DOM) in soil leachate (preprint). Soils and biogeochemical cycling. https://doi.org/10.5194/soil-2019-97

Tipping, E., Lofts, S., Sonke, J.E., 2011. Humic Ion-Binding Model VII: a revised parameterisation of cation-binding by humic substances. Environ. Chem. 8, 225. https://doi.org/10.1071/EN11016

Tipping, E., Woof, C., 1991. The distribution of humic substances between the solid and aqueous phases of acid organic soils; a description based on humic heterogeneity and charge-dependent sorption equilibria. Journal of Soil Science 42, 437–448. https://doi.org/10.1111/j.1365-2389.1991.tb00421.x

Vymazal, J., 2019. Is removal of organics and suspended solids in horizontal sub-surface flow constructed wetlands sustainable for twenty and more years? Chemical Engineering Journal 378, 122117. https://doi.org/10.1016/j.cej.2019.122117

Wang, H., Holden, J., Zhang, Z., Li, M., Li, X., 2014. Concentration dynamics and biodegradability of dissolved organic matter in wetland soils subjected to experimental warming. Science of The Total Environment 470–471, 907–916. https://doi.org/10.1016/j.scitotenv.2013.10.049

Wang, L.-F., Wang, L.-L., Ye, X.-D., Li, W.-W., Ren, X.-M., Sheng, G.-P., Yu, H.-Q., Wang, X.-K., 2013. Coagulation Kinetics of Humic Aggregates in Mono- and Di-Valent Electrolyte Solutions. Environ. Sci. Technol. 47, 5042–5049. https://doi.org/10.1021/es304993j

Weishaar, J.L., Aiken, G.R., Bergamaschi, B.A., Fram, M.S., Fujii, R., Mopper, K., 2003. Evaluation of Specific Ultraviolet Absorbance as an Indicator of the Chemical Composition and Reactivity of Dissolved Organic Carbon. Environmental Science & Technology 37, 4702–4708. https://doi.org/10.1021/es030360x

Weng, Van Riemsdijk, W.H., Koopal, L.K., Hiemstra, T., 2006. Adsorption of Humic Substances on Goethite: Comparison between Humic Acids and Fulvic Acids. Environ. Sci. Technol. 40, 7494–7500. https://doi.org/10.1021/es060777d

Xu, H., Ji, L., Kong, M., Jiang, H., Chen, J., 2019. Molecular weight-dependent adsorption fractionation of natural organic matter on ferrihydrite colloids in aquatic environment. Chemical Engineering Journal 363, 356–364. https://doi.org/10.1016/j.cej.2019.01.154

Xu, H., Lin, H., Jiang, H., Guo, L., 2018. Dynamic molecular size transformation of aquatic colloidal organic matter as a function of pH and cations. Water Research 144, 543–552. https://doi.org/10.1016/j.watres.2018.07.075

Yan, C., Sheng, Y., Ju, M., Ding, C., Li, Q., Luo, Z., Ding, M., Nie, M., 2020. Relationship between the characterization of natural colloids and metal elements in surface waters. Environmental Science and Pollution Research 27, 31872–31883. https://doi.org/10.1007/s11356-020-09500-x

Yao, S.-H., Zhang, Y.-L., Han, Y., Han, X.-Z., Mao, J.-D., Zhang, B., 2019. Labile and recalcitrant components of organic matter of a Mollisol changed with land use and plant litter management: An advanced 13C NMR study. Science of The Total Environment 660, 1–10. https://doi.org/10.1016/j.scitotenv.2018.12.403

Yin, S., Bai, J., Wang, W., Zhang, G., Jia, J., Cui, B., Liu, X., 2019. Effects of soil moisture on carbon mineralization in floodplain wetlands with different flooding frequencies. Journal of Hydrology 574, 1074–1084. https://doi.org/10.1016/j.jhydrol.2019.05.007

Yu, R.-F., Chen, H.-W., Cheng, W.-P., Shen, Y.-C., 2008. Dynamic control of disinfection for wastewater reuse applying ORP/pH monitoring and artificial neural networks. Resources, Conservation and Recycling 52, 1015–1021. https://doi.org/10.1016/j.resconrec.2008.03.007

ARTICLE 2

Organo-mineral colloids control of major and trace elements leached from treatment wetland sludge deposits. Influence of pH conditions.

Banc, C. *, Gautier, M. *, Blanc, D. *, Lupsea-Toader, M. *, Marsac, R., Gourdon, R. ***

* Univ Lyon, INSA Lyon, DEEP (Déchets Eaux Environnement Pollutions), EA 7429, 69621 Villeurbanne Cedex, France.

** Univ Rennes, CNRS, Géosciences Rennes, UMR **6118**, 35000 Rennes, France.

Abbreviation

TD: truly dissolved

SD: Sludge Deposit

OC: Organic Carbon

SC: Small Colloids

LC: large colloids

tDOC: truly dissolved organic carbon

1. Introduction

In natural soil system, the mobility of inorganic species is strongly controlled by the dynamics of soluble colloidal species (Gangloff et al., 2016; Gu et al., 2020; Riise et al., 2000; van Hees et al., 2001). Due to their high specific surface, colloids exhibit a high complexation capacity of various inorganic species whose solubilization may thereby be strongly increased. Colloidal detachment is influenced by the nature of the colloids, the properties of the considered media but also by biological, chemical and hydrological factors (Gangloff et al., 2016; Grybos et al., 2009a; Pédrot et al., 2009a; Zhuang et al., 2009). Among the chemical factors, pH is probably the most important parameter controlling major and trace elements speciation in soil solution. By disturbing the organic supramolecular assemblies and organo-mineral association, pH change could induce the detachment of organic colloids in soil samples (Chen et al., 2018; Grybos et al., 2009a; Xu et al., 2018) and the release of associated elements. The remobilization of such organic molecules is known to promote the remobilization of colloidal metal-oxides in various natural soil samples (Pédrot et al., 2009a; Pokrovsky et al., 2005; Raudina et al., 2021a). pH also controls the sorption capacity of the colloidal phases by affecting the dissociation of functional groups.

Vertical Flow Constructed Wetlands (VFCW) are a nature-based system (NBS) where domestic wastewaters are treated by percolation through successive stages of filters planted with reeds. In so-called “French systems”, the influent wastewater is not settled and a solid layer accumulates progressively at the surface of the first filter due to the retention of the solid particles present in wastewater (Kania et al., 2017; B. Kim et al., 2015). This layer is well oxygenated by contact with the atmosphere and percolation of water flows through the rhizosphere of the reeds. Intense aerobic microbial activities thereby occurs and play a major role in the overall treatment performance (Kania et al., 2017; Kim et al., 2013a; B. Kim et al., 2015; Morvannou et al., 2011).

The surface sludge deposit (SD) are made by the aggregation of organic and inorganic matter interacting with various elements, nutrients and contaminants (Kania et al., 2019; Kim et al., 2016). This SD is known to actively contribute to the performance of the treatment by favoring the retention of wastewaters' pollutants (Kania et al., 2017, 2019; Kim et al., 2015, 2013). If the contaminants are not degraded as in the case of trace metals for example, they accumulate progressively within the SD. This accumulation induces a potential risk of remobilization of the contaminants either under the effect of possible variations in the treatment operating conditions (*e.g* periods of flooding, pH variations…), or when the sludge is extracted to maintain the good permeability of the filter and then disposed on soils in the purpose of using their potential fertilizing and agronomic properties.

In our previous work (Banc et al., 2021) we investigated the remobilization of organic colloids and looked at their molecular size and their aromaticity. The nature of the organic molecules generated by the SD were highly dependent of the pH conditions. Under alkaline conditions, the destabilization of particulate organo-mineral complexes causes the detachment of aromatic and large organic molecules comprised between 0.45 µm and 30 kDa. Acidic conditions however were found to generate the remobilization of low molecular weight organic molecules (*i.e* < 3kDa) with low aromatic content. The possible detachment of metal oxides with organic matter and the impact of such colloidal production on the release of trace elements were not investigated. Questioning the role of the detachment of colloids in the release of trace metals retained in the solid fraction is of major interest for SD originating from VFCW. Indeed, the colloidal detachment could promote the release of trace metals and reduce the treatment performance of these systems. Moreover, when reused in agricultural soil, the remobilization of colloids and associated pollutants could disturb the geochemical cycle of the considered soil. Globally, the detachment of colloids could induce the release of pollutants retained in the SD with possible important environmental consequences.

To identify the influence of pH on the detachment of colloids and their impact on the release of trace elements retained in the SD, pH leaching experiments were conducted on VFCW SD. Ultrafiltration experiments were performed on the leached solutions to identify the association between colloidal phases and a large variety of major and trace elements contained in the SD.

2. Materials and methods

2.1. Sampling and chemical analysis of sludge deposits (SD)

SD samples sampled by Banc et al. (2021) were used in this study. The sampling procedure is summarized above. SD were sampled in winter time from the surface sludge layer of the first-stage filter of the Vertical Flow Constructed Wetland (VFCW) treatment plant of Vercia (FRANCE). The sludge layer had been staying in place from the first day of operation of the treatment plant, i.e. 14 years.

Samples were collected and processed following the protocol reported by Kania *et al.* (2019) and summarized below. Several kg of SD were collected over the whole depth (>15 cm) of the sludge layer from 8 different spots at the surface of the first-stage filter. All samples were sorted manually on-site to remove reeds rhizomes and gravels, and subsequently mixed by shoveling. A representative sample of a few kg was then prepared by quartering, refrigerated and transported to the laboratory within a maximum of 4 hours. Then, representative sub-samples were prepared, crushed and sieved at 1 mm, freeze-dried and stored at 4 °C for further analyses assays.

The SD freeze-dried powders thus prepared were analyzed for their total contents in a series of elements. The powdered samples (200 mg) were suspended through alkaline fusion with $LiBO_2$ in a tunnel oven at 980 °C. After cooling, the sample was dissolved in a 0.5N HNO_3 solution. Major elements analysis was performed using ICP-OES iCap6500 ThermoFisher after 2-fold dilution in 2% HNO_3 aqueous solution. Trace elements were quantified with ICP-MS iCapQ ThermoFisher after 2-fold dilution in 2% HNO_3 aqueous solution. Results are given in Table 1.

Table 1: Total content of trace elements and major elements in dried sludge deposit.

Major elements	C_{org}	Al	Ca	Fe	Mg	Mn	Na	P	S
g/kgDM	166	21.3	62.9	34.3	2.9	0.26	1.7	21.1	5.5

Trace elements	As	Ba	Cd	Co	Cr	Cu	Ni	Pb	Rb	Sb	Sr	V	Y
mg/kgDM	6.61	274	1.1	6.6	54.8	584	28.4	67.5	30.5	2.35	157	33.0	11.0

DM: dry matter

2.2. Leaching protocol

A batch leaching protocol, based on the European standard method CENTS/TS 14429, was used to evaluate the effects of pH on the release of organic and inorganic compounds from the SD samples. The assays were performed in batch, using Nalgene® polypropylene centrifuge tubes in which SD were contacted with aqueous leaching solutions. Before the tests, all tubes were soaked in a 1M HCl aqueous solution overnight and then rinsed with deionized water.

Leaching assays were done at a solid-to-liquid ratio of 10 g of SD dry matter per liter of the leaching solution. The following leaching solutions were used: (i) ultrapure deionized water for natural pH conditions, (ii) nitric acid aqueous solutions for acidic conditions and (iii) potassium hydroxide aqueous solutions for alkaline conditions. Altogether, 5 acidic and 6 alkaline leaching solutions were used in addition to the use of ultrapure deionized water for the natural pH condition. All assays were stirred

at room temperature in a rotary shaker set at 9 rpm until an apparent steady-state was reached, which was observed within 48 hours in preliminary experiments. All assays were duplicated.

2.3. Filtration and ultrafiltration of eluates

The suspensions obtained from the batch leaching assays were centrifuged at 10000 rpm for 10 min and the supernatants were filtered at 0.45µm using Sartorius cellulose acetate filters to separate particulate organic matter (POM) in the filtrate above 0.45 µm from dissolved organic matter below 0.45 µm. The 0.45 µm was further treated to separate the dissolved forms according to their molecular weight (MW) using a Jouan G4.12 centrifuge equipped with a swinging bucket rotor. Centrifugations were done at 3000 g and room temperature for 20 min in tubes equipped with Sartorius Vivaspin cellulose acetate ultrafiltration membranes of 30 kDa, 10 kDa and 3 kDa cutoff limits. Ultracentrifugation tubes were previously rinsed with a 0.1M NaOH solution followed by Milli-Q water to guarantee background concentrations of dissolved organic carbon (DOC) below 0.1 $mg.L^{-1}$ in the ultrafiltrate. The ultrafiltrates collected from the ultrafiltration of all the leachates obtained from the leaching assays were analyzed for organic carbon and inorganic major and trace elements concentrations.

This protocol allowed to separate the soluble compounds into 3 fractions, namely large colloids LC above 30 kDa (with one sub-fractions between 0.45 and 30 kDa µm), small colloids SC between 30 kDa and 3 kDa (with 2 sub-fractions 30 to 10 kDa and 10 to 3 kDa), and truly dissolved TD constituents below 3 kDa. The proportions of the leached organic and inorganic compounds in each respective fraction was calculated at each pH tested as the ratio between the amounts leached in each fraction and the overall amount leached in the whole of the fractions. Results were expressed in mass %.

2.4. Analysis of leached fractions

After the completion of the leaching experiments, the suspensions were analyzed for pH, using a Consort C3020 meter equipped with Bioblock 11706358 pH probes calibrated with certified pH buffer solutions (pH 4.01, 7.00 and 10.00 at 25 °C).

Major and trace element concentrations previously identified in the solid matrix (see Table 1) were measured in all permeates obtained by filtration and ultrafiltration operations. Al, S and P concentration were determined by ICP-AES (Ultima2; Horiba Jobin Yvon SAS) with an uncertainty below 10%. The concentrations of the rest of the elements were measured using a 7700x Agilent ICP-MS analyzer with uncertainty below 5%.

2.5. Thermodynamic modeling

Predominance pH-Eh diagrams were obtained using PhreePlot (Kinniburgh and Cooper, 2011), which contains an embedded version of the geochemical speciation program PHREEQC (Parkhurst and Appelo, 1999). The “minteq.v4” database provided with this code was used.

3. Results and discussion

3.1. Leaching of organic species

The remobilization of organic colloids induced by pH variations have been already measured in the same leaching sample by Banc et al. (2021) and printed in Fig. 1. The quantity and the molecular size of the leached organic molecules was strongly affected by the pH (Fig. 1). Below pH 6, close to 60% of the dissolved OC leached was found in the TD fraction, whereas under alkaline conditions large colloids LC were predominantly remobilized, corresponding to up to 70% of the leached dissolved OC. Under alkaline conditions, the destabilization of organo-mineral aggregates due to electrostatic repulsion lead to the remobilization of large organic molecules. However, under acidic conditions, the release of TD molecules was attributed to the preferential remobilization of molecules with higher surface charge characterized by low molecular weight as observed by Pédrot et al. (2009). The proportion of small colloids SC was found relatively stable (around 10%) over the whole pH range

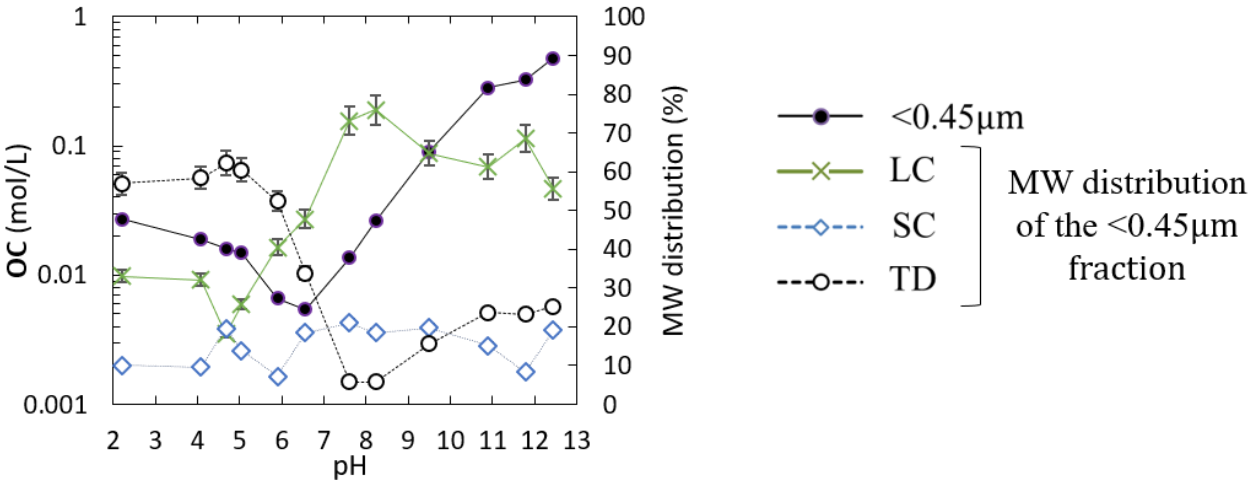

Fig. 1: Effect of pH on the overall concentration and the MW of leaching of organic compounds from VFCW sludge deposits obtained from Banc et al. (2021). Large colloids (LC) (x), small colloids (SC) (◇) and truly dissolved constituents (TD) (o), expressed in % of the overall OC leached at each pH.

3.2. Leaching of major trivalent metals (Fe, Al)

In addition to organic colloidal carriers, Fe and Al-oxides are known to control the solubility and mobility of numerous species (Kretzschmar and Schäfer, 2005; Plathe et al., 2010; Theng and Yuan, 2008). It can be seen in Fig. 2 that the evolutions with pH of Al and Fe concentrations in the <0.45µm fraction were similar. Leached concentrations ranged between 0.003-9 mmol/L for Al and 0.009-1

mmol/L for Fe, respectively. Only small proportions, less than 12% (Al) and 3% (Fe) of the total content in the sludge deposits (see Table 1) were leached over the whole pH range tested. This observation revealed the stability of the Fe-Al phases of the SD. Increasing the pH of the solutions from ca. 5 up to pH 12 progressively increased the proportion of leached Al and Fe. This can be attributed to the remobilization of monomeric Fe/Al forms bound to organic molecules or to Fe/Al oxides released from the SD as observed in natural samples (Pokrovsky et al., 2005; Pourret et al., 2007a). An even more drastic increase was observed in the acidic range between pH 5 and pH 2, which was attributed to the dissolution of Al-Fe oxides under acidic conditions.

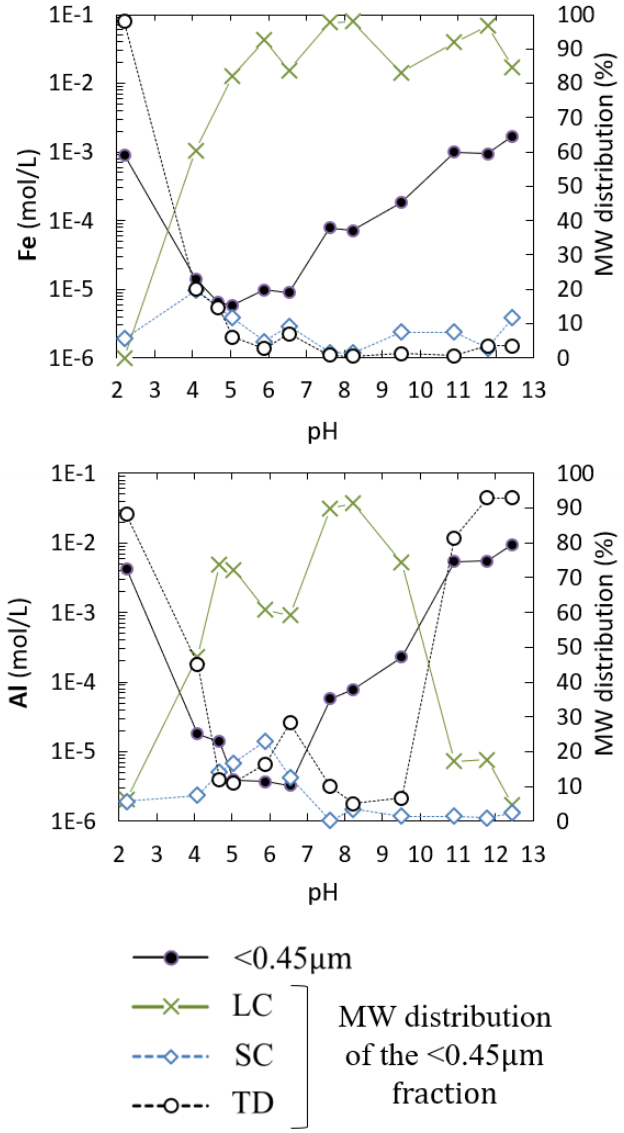

Fig. 2: Effect of pH on: (i) the overall release of Fe (a) and Al (b) expressed mol/L (●) ; (ii) the proportions of leached Fe (a) and Al (b) species in the forms of large colloids (x), small colloids (◇) and truly dissolved constituents (O).

For both Al and Fe, the increased leaching observed at acidic pH was predominantly observed in the TD fraction (<3kDa) where 90% of Fe and Al were analyzed. Under strongly acidic conditions, pH-Eh diagram (plotted in the supporting information section) suggests that Fe was mainly released as Fe(II) while for the rest of the pH range, Fe(III) was probably predominant in solution. Interestingly, the pH value corresponding to the estimated Fe(II)-Fe(III) transition suggested by the pH-Eh diagram, was also the pH point corresponding to the transition of the predominant fraction from the TD fraction to the LC fraction. It was observed that when pH increased the proportion of TD species decreased while LC fraction increased up to 90 % and more at neutral to alkaline pH. By contrast with Fe, for pH >10, Al was mainly found in the TD fraction. These results are not specific to constructed wetlands sludge deposits. Similar observations were reported during leaching column experiments of natural wetlands soils at pH~6 (Pédrot et al., 2008, 2009a). The specific pH-dependent MW distribution of Al and Fe did not strictly follow OC MW distribution. The MW of Fe and Al species in LC fraction matched well with their oxyhydroxides forms (Pédrot et al., 2008; Vermöhlen et al., 2000). Moreover studies showed that Fe/Al oxides were stabilized in the aqueous phase by dissolved organic matter (Guénet et al., 2017; Li et al., 2020). Various studies on wetlands soil solution highlighted the presence of mixed Fe/Al oxyhydroxides in the LC fraction (Pédrot et al., 2009a; Pokrovsky et al., 2005; Pourret et al., 2007a).

3.3 Leaching of trace elements

3.3.1 Leaching of alkali and alkaline earth metals (Li, Na, Rb, Mg, Ca, Sr, Ba)

The concentrations of alkali and alkaline earth metals in the different MW fractions of the leachates collected over the tested pH range are shown in Fig. 3. The alkaline metals analyzed (Li, Na and Rb) showed different solubility patterns. While Rb was rather leached under alkaline conditions, up to a maximum of ~ 5.5 µmol/L at pH 12, Li was preferentially leached under acidic conditions with a maximal concentration of ~ 5.2 µmol/L at pH 2. Na leaching was only slightly affected by pH with concentrations comprised between 2 mmol/L at pH 8.2 and 3 mmol/L at pH 2.2. Na and Rb were mostly present in the TD fraction. Although proportions of large and small colloidal increased with pH, LC and SC fractions remained below 25% of overall leached quantities. On the contrary, the MW of leached Li species was much more affected by the pH. Below pH 7.5, more than 80% of leached Li was measured in the TD fraction while above pH >8 more than 90% of leached Li was in the LC fraction while the overall leaching of Li was relatively stable. The distribution of the MW of leached Li species was similar to that observed with the alkaline-earth metals discussed above. This observation was attributed to the similar ionic properties of Li and alkaline-earth metals species (Barshad, 1950). The molecular weight distribution of Na, Rb and Li leached species was consistent with observations reported by

other in acidic wetlands soil solution (Pédrot et al., 2008; Pokrovsky et al., 2005, 2006; Raudina et al., 2021a). However, Pédrot et al. 2009, working on natural wetland soils, reported that at pH 7.2 leached Rb species exhibited sizes above 30kDa (corresponding to the LC fraction in the present study). The authors suggested associations of Rb with Fe-Al oxides. The high OC content of the SD solutions however could reduce the availability of Al-Fe-oxides sites as organic matter is a competitor for soil mineral surface sites (Staunton et *al.,*2008, Verbeeck et *al.,* 2017).

All alkaline-earth metals followed in this study (Ca, Mg, Sr, Ba) exhibited similar pH-dependent leaching patterns with similar MW distribution of the leached species (Fig. 3). These elements were globally more sensitive to acidic conditions. Leaching of Ca, Mg and Sr were found minimal at slightly alkaline pH (pH~8). Slightly different patterns were observed however for Ba which exhibited a V-shaped profile of leached concentration vs. pH with a minimal leaching observed under natural pH conditions (pH 6.5). For these four elements, the pH of minimal leaching was also the pH of transition of the leached species MW from TD species the LC fraction. If Ca, Mg and Sr showed similar MW distributions of the leached species according to pH, the situation was slightly different with Ba. Whereas leached species of Ca, Mg and Sr were increasingly observed in the large colloids LC fraction with increasing pH (up to more than 90% at pH 12), Ba species were in the large colloidal fraction at pH 7.6. The MW distribution of these alkaline earth elements was consistent with results obtained on slightly acidic wetlands (Pédrot et al., 2008) and peat (Pokrovsky et al., 2005) soil solution. However, Raudina et al. 2021, measured more than 50% of these elements in the LC fraction in peat soil solution despite very acidic conditions with a pH of 3.3. In the latter study, Mg, Ca, Sr and Ba measured in the colloidal fraction (> 3kDa) were suspected to be electrostatically bond to organic molecules. In our study, the high concentration in background electrolytes measured in acidic conditions, responsible for the shrinkage of the electric double layer of the organic molecules (Milne et al., 2001), could explain the very low sorption of alkaline and alkaline earth metals to organic molecules measured under acidic conditions. Moreover, the important competition with other metals for organic and/or oxides surface binding sites could also explain these results.

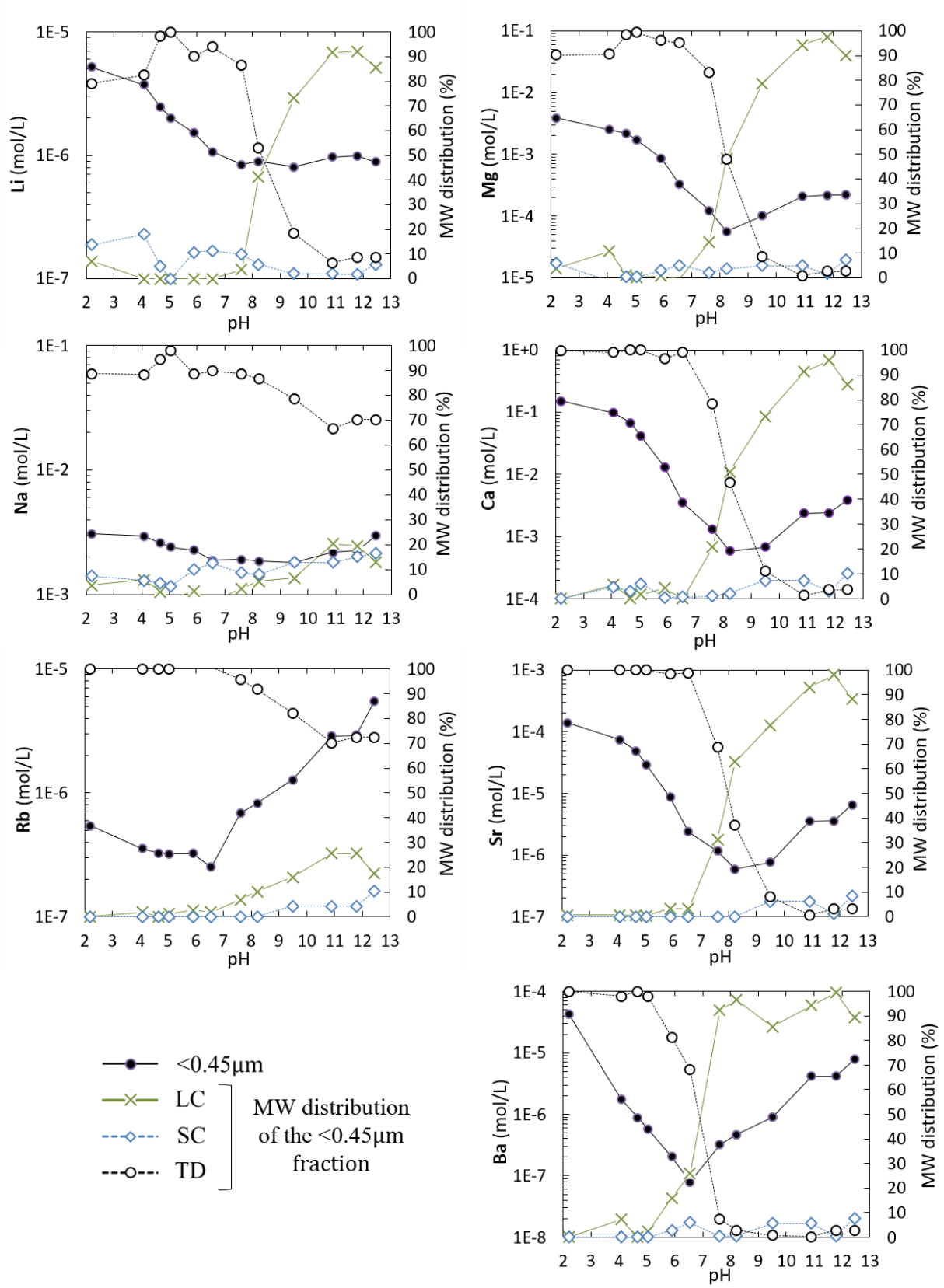

Fig. 3: Effect of pH on: (i) the overall release alkaline and alkaline-earth metals expressed in mol.L^{-1} (●); (ii) the proportions of leached alkaline and alkaline-earth metals in the forms of large colloids (x), small colloids (◇) and truly dissolved constituents (O).

3.3.2 Leaching of divalent metals (Mn, Co, Ni, Cu, Zn, Cd, Pb)

It can be seen in Fig. 4 that these elements exhibited similar profiles with respect to the effect of pH on their solubilization. The lowest leaching was globally observed at pHs around neutrality (6.5 to 8.2). Only very small fractions of the total contents of the considered elements in the SD were leached under these conditions (below 1 % regardless on the element). A very sharp increase was observed in the leaching of all the considered elements when the medium was acidified. At pH 2, the leached concentrations were 2 to 3 orders of magnitude higher than observed close to neutrality, corresponding to the solubilization of 20 to 80% of the total contents depending on the considered element. Increasing pH also enhanced leaching but in proportions which were not the same for all the elements. In most cases, the pH increases from close to neutrality up to 12 enhanced leaching to a similar extent as observed by acidification to pH 2 (same order of magnitude for Ni and Cd, slightly smaller for Co and Zn, slightly higher for Cu and Pb). In contrast, in the case of Mn, increasing pH enhanced leaching only in a marginal proportion.

Fig. 4 also showed that all the considered elements were leached predominantly in the TD fraction under acidic conditions. Under neutral to alkaline conditions however, the distribution was not the same for all the elements. Mn and Zn were leached mostly in the form of large colloids (LC fraction). Co, Ni, Cu and Cd were found in similar proportions in all the size fractions. Enrichment of the TD fraction in these trace metals has been also observed in organic-rich wetlands (Pédrot et al., 2008) and peat pore waters (Pokrovsky et al., 2005). Finally, in the case of Pb, the large colloids were predominant over almost the entire pH range (4 to 12). Truly dissolved species were found predominant only at pH below 4. The affinity of Pb for large colloids has been already reported in rich organic soils (Gangloff et al., 2016; Pédrot et al., 2009a; Pokrovsky et al., 2005).

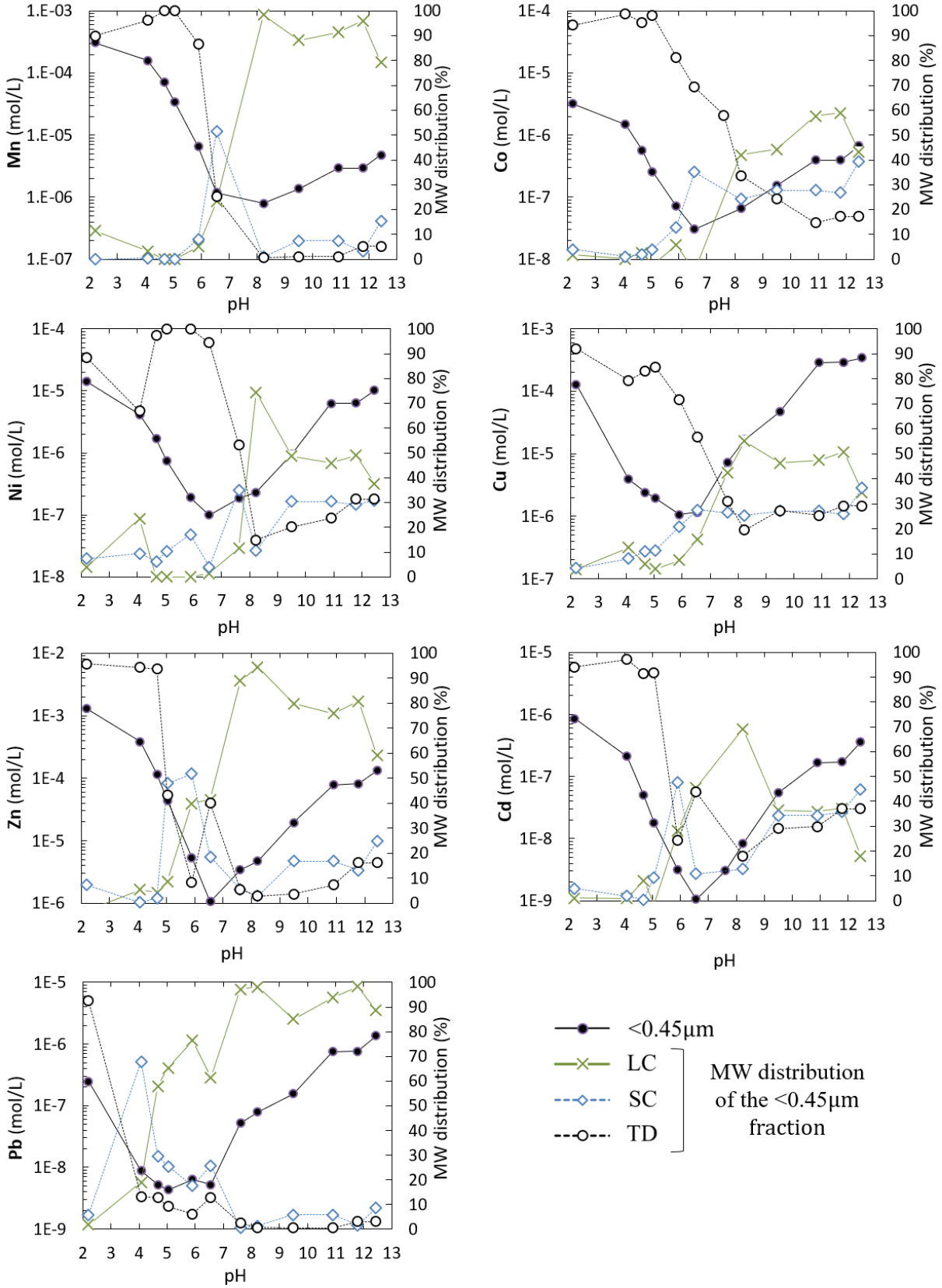

Fig. 4: Effect of pH on: (i) the overall release divalent metals expressed in mol.L^{-1} (●); (ii) the proportions of leached trace metals in the forms of large colloids (x), small colloids (◇) and truly dissolved constituents (O).

3.3.3 Leaching of trivalent elements (Cr, Sc, Y)

Three of the elements monitored in this study are trivalent (ScIII and YIII) or likely to occur in a trivalent form in the conditions of the study (CrIII). The pH-dependent leaching profiles of these elements were found similar as shown in Fig. 5. The lowest leaching was recorded under close to neutral pH conditions (pH 6.5) with leached concentrations of 20, 1 and 2 nmol/L for Cr, Sc and Y, respectively. Solubilization was enhanced in similar proportions by decreasing or increasing pH. However, less than 5% of the total contents in Cr, Sc and Y were leached, even under extreme acidic (pH 2) or alkaline (pH 12) conditions, revealing the high stability of the bearing phases in the sludge deposits.

The MW distributions of the leached species were also very similar for the 3 elements. Large colloids were largely predominant (50% to more than 90%) at pH above 5-6 and truly dissolved species below pH 5. Small colloids were present in significant proportions (30-60%) only between pH 5 and 7 or so.

While Sc and Y may only occur under a trivalent from, Cr may be commonly observed under hexavalent or trivalent forms. The hexavalent form Cr(VI) is described as much more soluble and toxic than the trivalent form Cr(III) (Fan et al., 2019; Gorny et al., 2016; Kotaś and Stasicka, 2000). It occurs mostly under the form of the oxyanion CrO_4^{2-}. Results obtained here suggested that Cr was released in its trivalent form since the pH dependent MW distribution of leached Cr species was the same as to those observed for cationic species and more precisely to trivalent species Y(III) and Sc(III). Moreover, the pH-Eh diagram (see supporting information) suggest that the present experimental conditions, Cr is mainly released as Cr(III). This observation was consistent with other published studies on natural peat soil solution where the presence of trivalent elements in the colloidal fraction (>3kDa) was also reported (Pokrovsky et al., 2005; Raudina et al., 2021a).

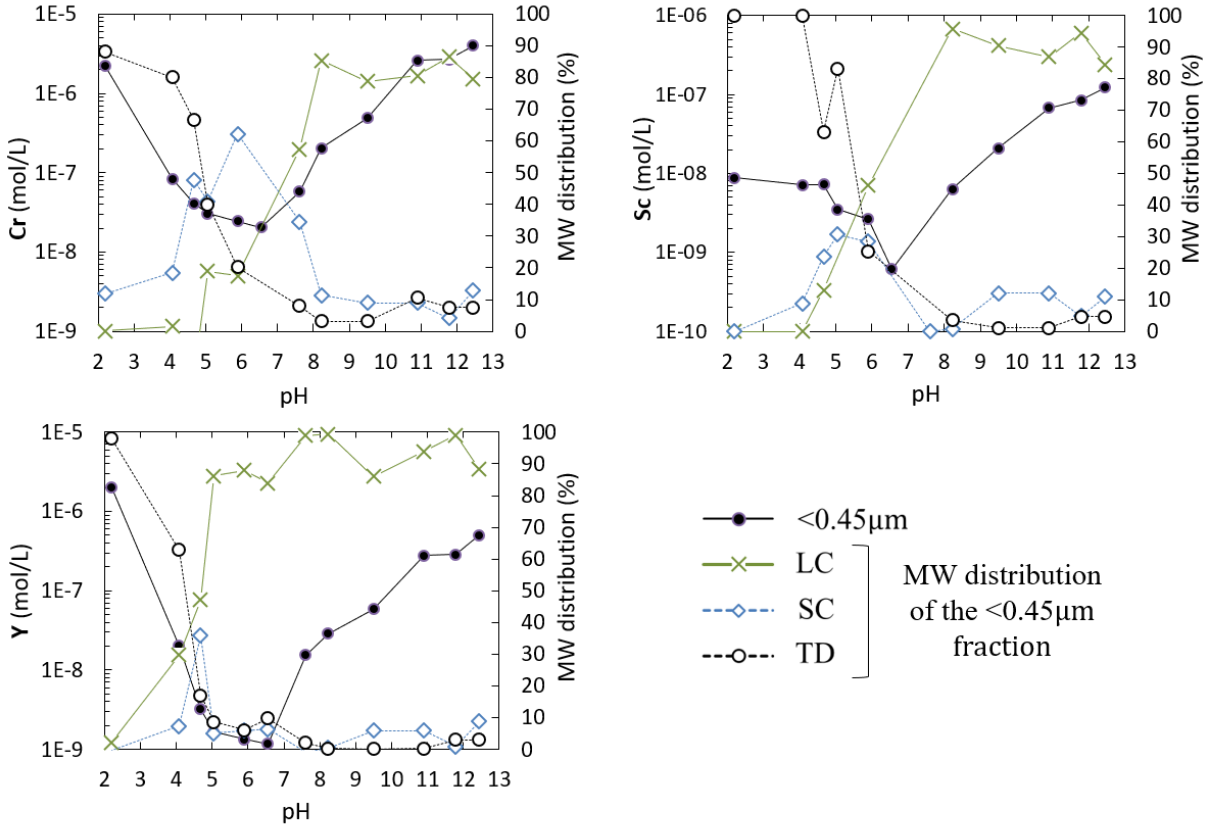

Fig. 5: Effect of pH on: (i) the overall release trivalent species expressed in mol.L^{-1} (●); (ii) the proportions of leached trace metals in the forms of large colloids (x), small colloids (◇) and truly dissolved constituents (O).

3.4 Leaching of anionic species (V, As, Sb, S, P)

Several elements are known to occur in the form of (oxy)anions in aqueous solutions. This is the case for *V, As, Sb, S, P* in the present study. Cr may also occur in the form of oxyanions in its hexavalent state, but it was not the case here as discussed above.

Results of V, As, Sb, S and P leaching gathered in Fig. 6 showed that these elements were quite soluble since 20 % of their total contents were leached depending on the pH. Their lowest solubilization was recorded at pH close to neutrality as it was also observed for the other elements discussed in the sections above. The effect of pH on leaching was however relatively specific to the considered elements. As and P showed a classical profile, observed for most elements, where decreasing or increasing pH induced a similar increase of their leaching. For S, Sb and V however, acidification had a low (Sb) to very low effect (S and V except at pH 2 where leaching of V was strongly increased), whereas increasing pH from 6-7 to 12 increased leaching in a regular manner. The leaching of V was particularly affected by pH, with an increase by more than 2 orders of magnitude between pH 4-5 and pH 12-13.

Fig. 6 also showed that the pH-dependent MW distributions of leached species were very similar for all these elements, which can be explained by the fact that they are known to compete for the same binding sites (Arco-Lázaro et al., 2016; Darland and Inskeep, 1997). Especially As and Sb expected to be mainly released as As(V) and Sb(V), pentavalent forms being less toxic compare to trivalent ones (Jain and Ali, 2000). Over the entire pH range, all the elements considered here were predominantly released in the form of truly dissolved species. The proportion of large colloids increased however at alkaline pH, but decreased in most cases at extreme alkaline pH. The proportion of small colloids was in all cases marginal, except for P species at pH 6-9. These observations suggested the remobilization of organic and/or mineral colloidal carrier phases played a role in the leaching of the considered elements. In other natural systems, such as in agricultural soil solutions (Gu et *al.*, 2020) or solutions extracted from forest soil samples (Missong et *al.,* 2018), the remobilization of colloidal fraction was for exemple responsible for the release of P species and their mobility was reported as a major source of P losses.

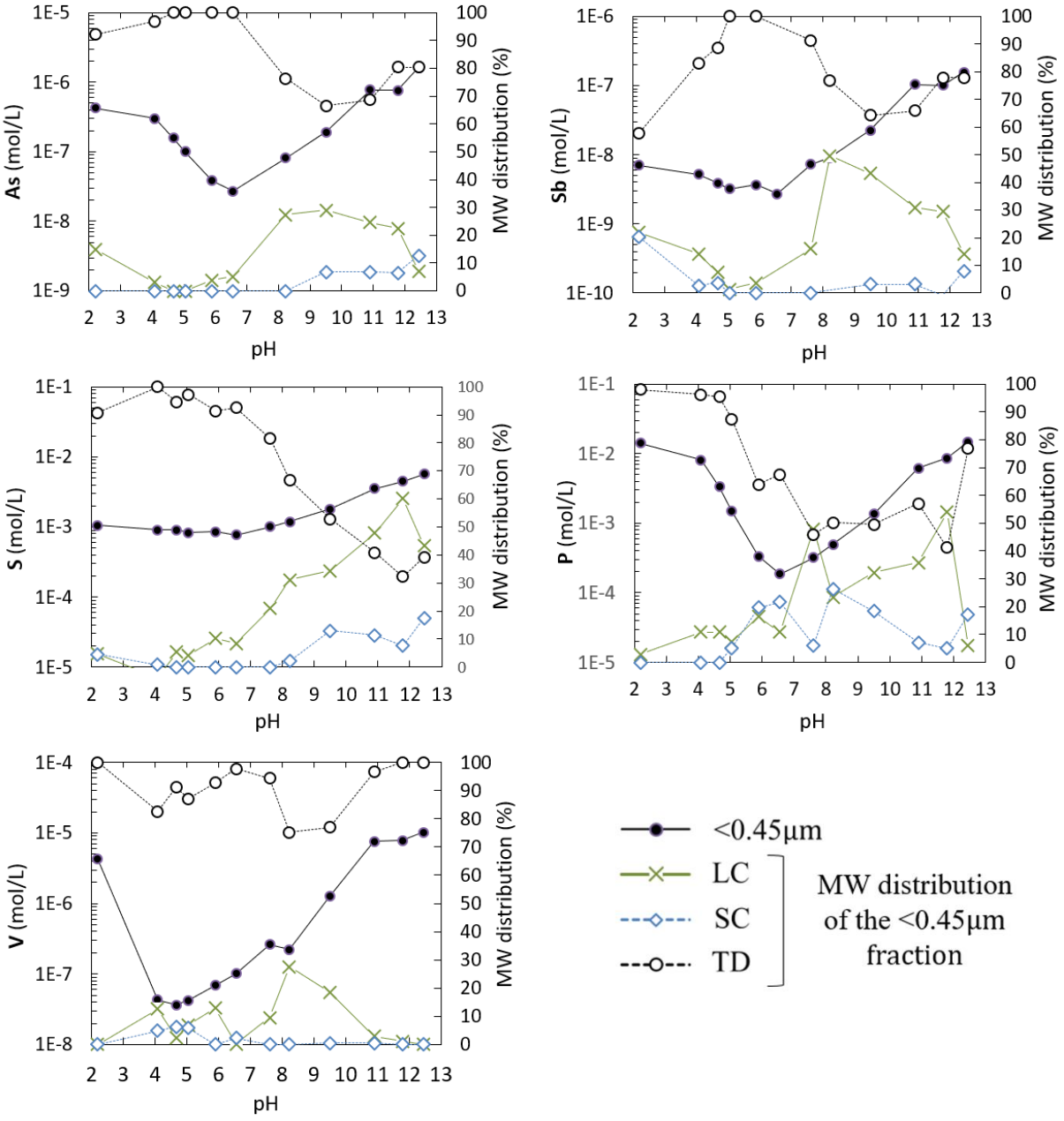

Fig. 6: Effect of pH on the leaching gahaviors of As, Sb, S, P expressed in mol.L^{-1} (●) and their proportions of leached species in the forms of large colloids (x), small colloids (◇) and truly dissolved constituents (O).

In natural soil system Vanadium mainly occurs as V(III), V(IV) and V(V) (Wu et al., 2020). According to the pH-Eh diagram of equilibrium (Fig S1), V was probably released mainly as V(V) in the experimental conditions of the present study. This form is the most mobile and toxic (Shaheen et al., 2019). This speciation was confirmed by the fact that more than 80% of leached V was solubilized in the form of truly dissolved species (Fig. 6) as observed for anionic species. V(V) has been reported to have a strong affinity for complexation with mineral surfaces (Peacock and Sherman, 2004). Published studies

conducted on natural soil solution reported that V was solubilized by organic and/or inorganic colloids to a higher extent than observed here (Pédrot et al., 2008; Pokrovsky et al., 2005; Raudina et al., 2021a). This could be attributed to a lower availability of binding sites in our study due to competition with organic molecules or inorganic elements such as phosphorus.

3.5 Determination of the colloidal carrier phases and elements association

In all the MW fractions obtained by filtration or ultrafiltration of the leachates collected at the different pHs tested, predominant major elements were firstly organic carbon, followed by Fe and Al. The molar ratios of these elements were therefore calculated to assess, in a first approach, the possible nature of the phases constituting the colloids in LC an SC fractions. Results are shown in Fig. 7. It was observed that Fe/OC and Fe/Al ratios fluctuated with pH in each respective MW fraction. However, excluding some of the results obtained at the most extreme pH values, the fluctuations within each MW fraction followed horizontal lines, suggesting that pH in the range of 4 to 12 did not profoundly modify the nature of the phases. As already discussed before, the enrichment of the LC in Fe and Al could be explained by the remobilization of Fe and Al oxides from the SD. However, the concomitant released of OC, Fe and Al suggest that organic molecules and Fe/Al oxides are closely related thus forming possible large organo-mineral colloids as reported in many published studies (Guénet et al., 2017; Pédrot et al., 2008; Pokrovsky et al., 2005; Pourret et al., 2007a; Ratié et al., 2019; Vantelon et al., 2019). These results, therefore, require a more precise investigation of the specific role of organic and/or inorganic colloidal phases in the remobilization of the elements studied here. Moreover, numerous elements are only weakly (P, As, Sb, S, Na, Rb, V) or partly (Cu, Co, Ni, Cd) associated with released colloids and need further consideration to understand if the measured elements in the TD fraction is mainly composed by aqueous species forms (comprising free ionic forms and inorganic complex) or composed by an element associated to TD organic molecules. Classically, a plot of the element concentration as a function of OC, Fe and Al is used to distinguish between the main trace element carrier (Krickov et al., 2019; Pédrot et al., 2008; Pokrovsky et al., 2005). In this study, a plot of the percentage of each element versus OC and Fe percentage remaining in each ultrafiltrate and for each pH are shown in Figs. 8 to 10.

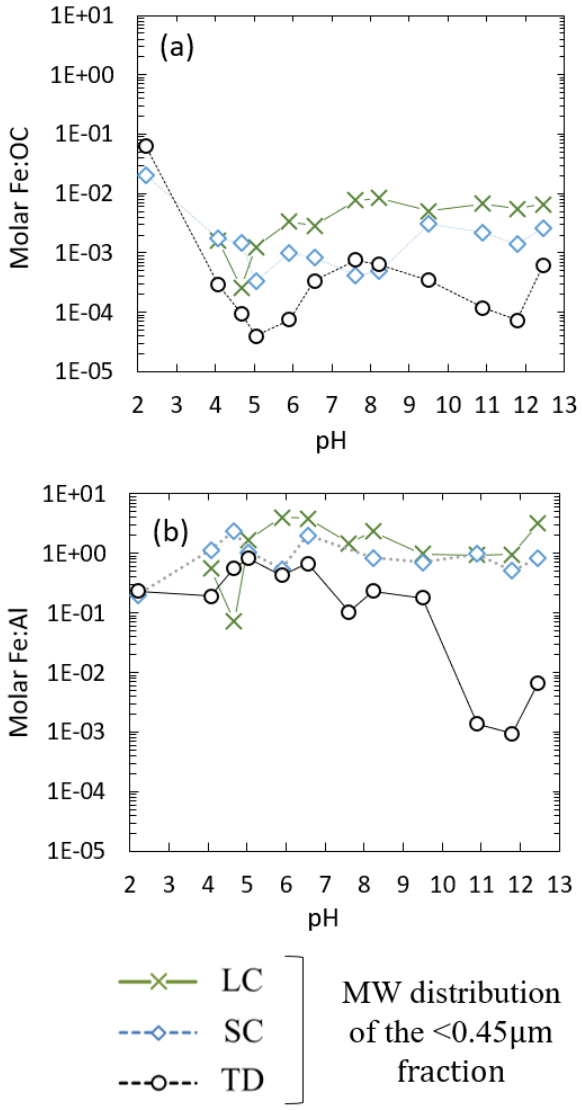

Fig. 7: Evolution of the molar ratios of (a) Fe:OC and (b) Al:Fe over the pH range in the large colloidal fraction (x), small colloidal fraction (◇) and truly dissolved fraction (O).

Co, Ni, Cu and Cd concentrations significantly change with the ultrafiltration cut-off but, as shown previously, even at neutral to alkaline pHs, more than 20% of these elements were released in the TD fraction. Fig. 8a. shows that the variations with pH of OC and Cu concentrations in each ultrafiltrates were positively correlated to each other from near neutral to alkaline pH conditions. The same behavior was observed with Co, Ni, and Cd (results not shown). This result shows that for pH values above 5-6, the release of these elements is strongly controlled by the remobilization of colloidal but also TD organic molecules. Co, Ni, Cu and Cd are classically classified as “borderline” cations which means that they can form strong covalent binding with all organic ligands (Duffus, 2002; Nieboer and Richardson, 1980) and thus, small organic ligands remobilized from the sludge deposit layer. The high

affinity of these divalent metals for low MW organic compounds from natural origins has been documented (Pokrovsky et *al.,* 2005; Pourret *al.,* 2007). However, the correlation between Cu and OC was degraded under acidic conditions which could be explained by the increased protonic competition for organic binding sites. Affinity of these elements for LC sorption sites decreases to a greater extent with acidification. A higher site density and a more important fraction in weak acid groups, still deprotonated in acidic conditions, is generally found in small organic molecules (fulvic acids with MW = 1.5 kDa) compare to large organics molecules (humic acids with MW > 15kDa) (Milne et al., 2001; Ritchie and Perdue, 2003; Tipping et al., 2011). These properties give TD organic molecules remobilized from SD the ability to increase the solubilization of these divalent transition metals even under relatively acidic conditions. Thus, part of the TD divalent metals should be associated with organic molecules in slightly acidic conditions. As observed previously, the MW distribution of Co, Ni, Cu and Cd slightly contrasts with those of divalent (Zn, Mn, Pb) and trivalent (Y, Cr, Sc) metals strongly associated with large colloidal fraction.

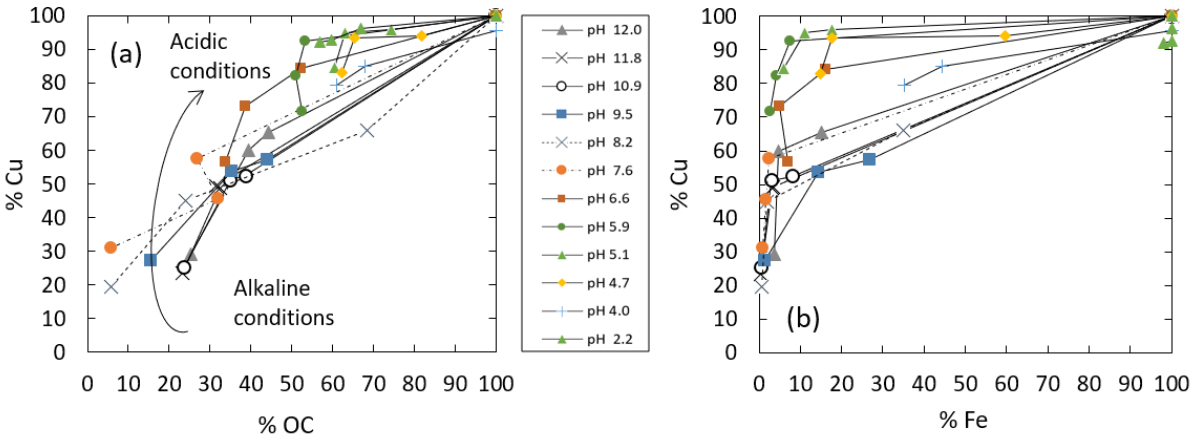

Fig. 8: Percentage of Cu leached in the different (ultra)filtrates (30, 10 and 3 kDa) over the pH range as a function of (a) OC and (b) Fe concentrations remaining in solution. Concentration measured in the 0.45µm solutions containing 100% of the considered element.

Compare to other divalent transition metals, Zn and Mn are more largely associated to the large colloidal fraction (Fig. 4). Fig. 9 evidenced a clear positive correlation between OC and Fe and these elements suggesting their sorption to large Fe/Al-organic colloids. Differences with other divalent transition metals could be explained reasonably well by the Irving-Williams series which describe the complex stability among the first transition metals: $Mn^{2+} < Fe^{2+} < Co^{2+} < Ni^{2+} < Cu^{2+} > Zn^{2+}$. In this series, ionic contribution in the Zn and Mn bonding to ligands is more important (Sajadi, 2010). This property relates them to the so-called “hard” cations having the properties to interact mainly electrostatically with “hard” organic ligands. Alkaline and alkaline earth metals, considered as “hard” cations, are also

mainly associated to large organic molecules in this study. The molecular weight and polyelectrolyte properties (Milne et al., 2001) give to the large organic molecules remobilized from solid deposit an important ability to electrostatically sorb and solubilized Mn, Zn, Ca, Mg, Sr and Ba.

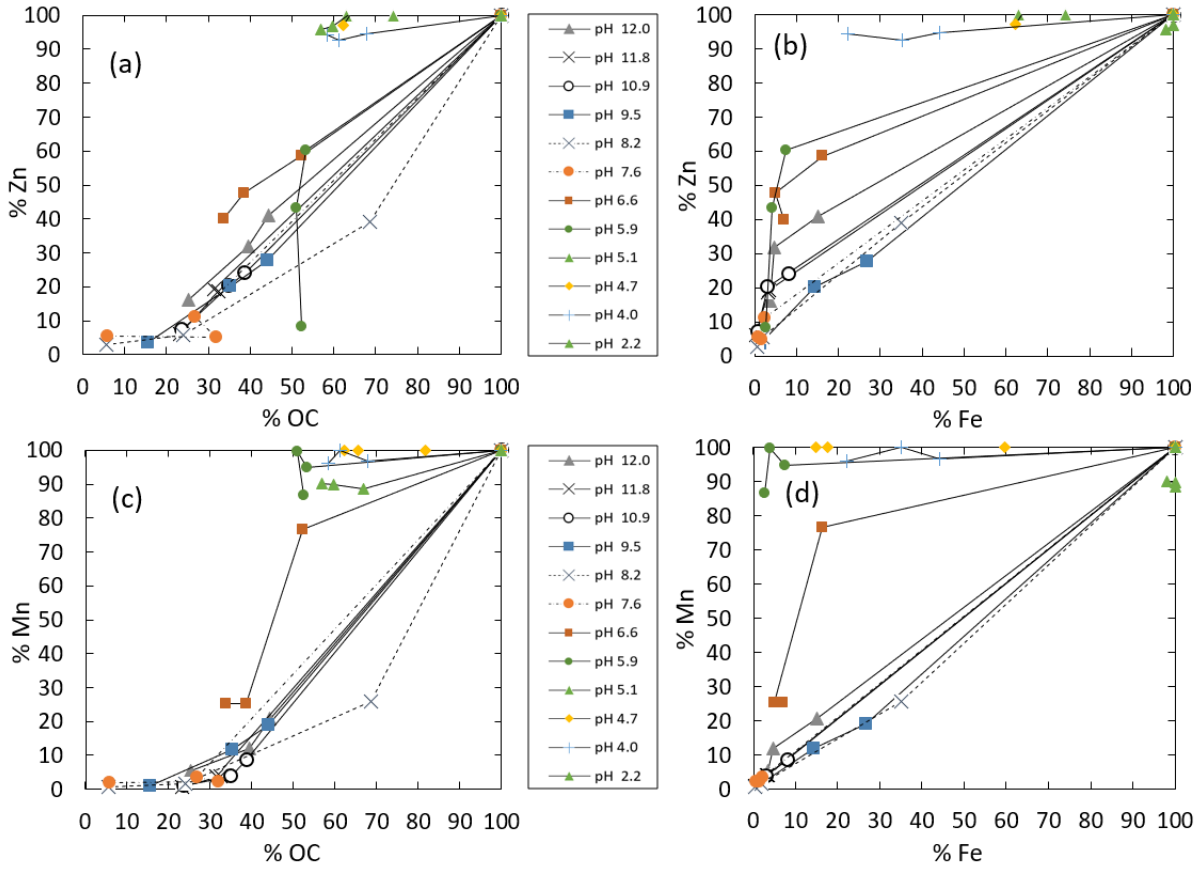

Fig. 9: Evolution of leached Zn (a,b) and Mn (c,d) percentage versus (a,c) OC and (b,d) Fe remaining in solution after each ultrafiltration (30, 10, 3 kDa) of the various solutions. Concentration measured in the 0.45µm solutions containing 100% of the considered element.

Pb, Y, Sc, and to a lesser extent Cr, are largely associated with LC fractions for a large pH range (Fig.4 and 5). This leaching pattern is similar to that observed for Fe and differs from that of OC suggesting their preferential bounding with large oxides colloids. Pb (Fig 10. a and b) but also Cr, Y and Sc concentrations is positively correlated to OC and Fe concentrations. Finally, iron oxides and iron oxides-organic particles (Fig 10. a and b) could be Cr, Pb, Y and Sc carriers and remobilizing phases in the SD. This result is supported by studies having demonstrated their affinity for iron oxides and organo-mineral colloids (Bau et *al.,* 1999; Fan et *al.,* 2005; Grybos et *al.,* 2007; Schijft and Marshall, 2011).

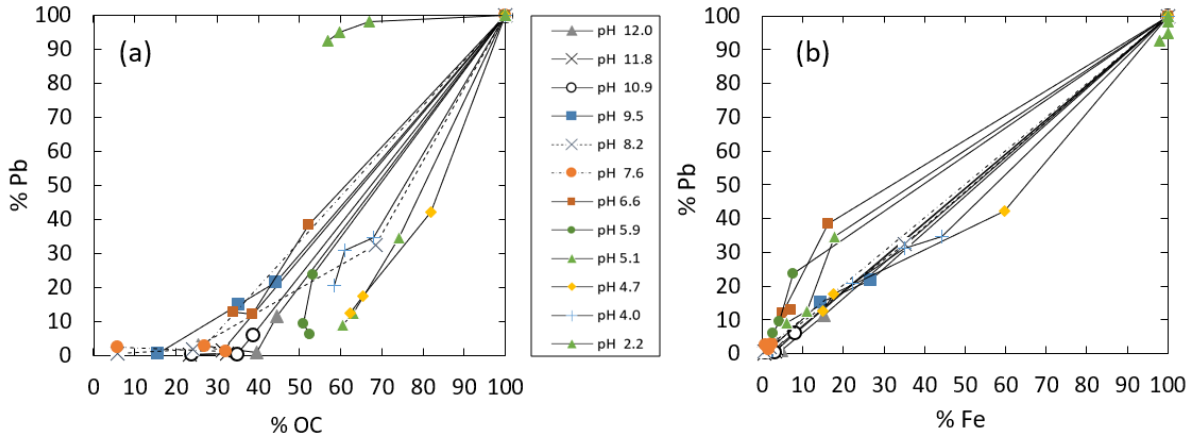

Fig. 10: Percentage of Pb leached in the different (ultra)filtrates (30, 10 and 3 kDa) over the pH range as a function of (a) OC and (b) Fe concentrations remaining in solution. Concentration measured in the 0.45µm solutions containing 100% of the considered element.

Surprisingly, phosphorus, whose important affinity for Fe-oxides is often used to quantify the amount of available sites on these surfaces (Hiemstra et al., 2010; Koopmans et al., 2020), as well as Sb(V) and As(V) who tend to behave similarly to P (Antelo et al., 2005), are preferentially released in the TD fraction (Fig.6). The low sorption rates of these elements to the Fe/Al-oxides could be due to the important adsorption competition with organic molecules for the oxides binding sites (Borggaard et al., 1990; Verbeeck et al., 2017; Wu et al., 2019). P, As and Sb measured in the LC could be associated with Fe-oxides but large organic molecules could also influence their lixiviation through ternary complexes involving either Fe/Al oxides-OM complex (Sharma et al., 2010) or cationic bridging (Sharma et al., 2010; Stachowicz et al., 2008; Wang and Mulligan, 2006). The proportion of P, As and Sb located in the TD fraction could be considered as inorganic complex or complexed by Fe-oxides organized as primary beads with a MW< 3kDa (Guénet et al., 2017).

3.6 Environmental implication

Constructed wetlands sludge deposits are known to concentrate high amounts of trace elements, organic micropollutants and nutrients (Kania et al., 2019). Understanding the possible mechanisms of remobilization of these constituents is therefore needed to assess the environmental and sanitary risks both during the wastewater treatment process operations and the disposal of the sludge after excavation.

In their life cycle, VFCW sludge deposits, may be exposed to variable geochemical, biological and hydrological factors which may affect the release of organic and inorganic colloids and associated trace

elements. pH is one of the key factors of influence. The experimental results obtained from this study showed the necessity to limit the mobilization of organic and/or inorganic colloids as these carrier phases promote the remobilization of inorganic pollutants. The release of such colloidal carrier phases would be minimal at pHs around neutrality while remobilization of organo-mineral colloids increase with alkalinization. The installation of acidic conditions should be avoided as they would enhance the release of most trace metals in the form of small inorganic complexes (Fig.11) known to be more toxic and bioavailable than the organic complexes (Aiken et al., 2011; Balistrieri and Blank, 2008).

In addition to pH, the leaching of redox-sensitive elements (Cr, V, As, Sb) will be controlled by their oxidation states and by the Eh of the medium as shown in natural wetland soils (Al-Sid-Cheikh et al., 2015; Pédrot et al., 2015). This study has experimentally conducted under oxidative conditions which prevail within the surface sludge deposits under regular conditions of operation. However, technical problems encountered in practice may induce anoxic conditions to install, for example during flooding periods due to clogging of the filters. This situation would drastically change the geochemical cycle of these elements and affect their remobilization from the sludge deposit by affecting their affinity for colloidal carrier phases.

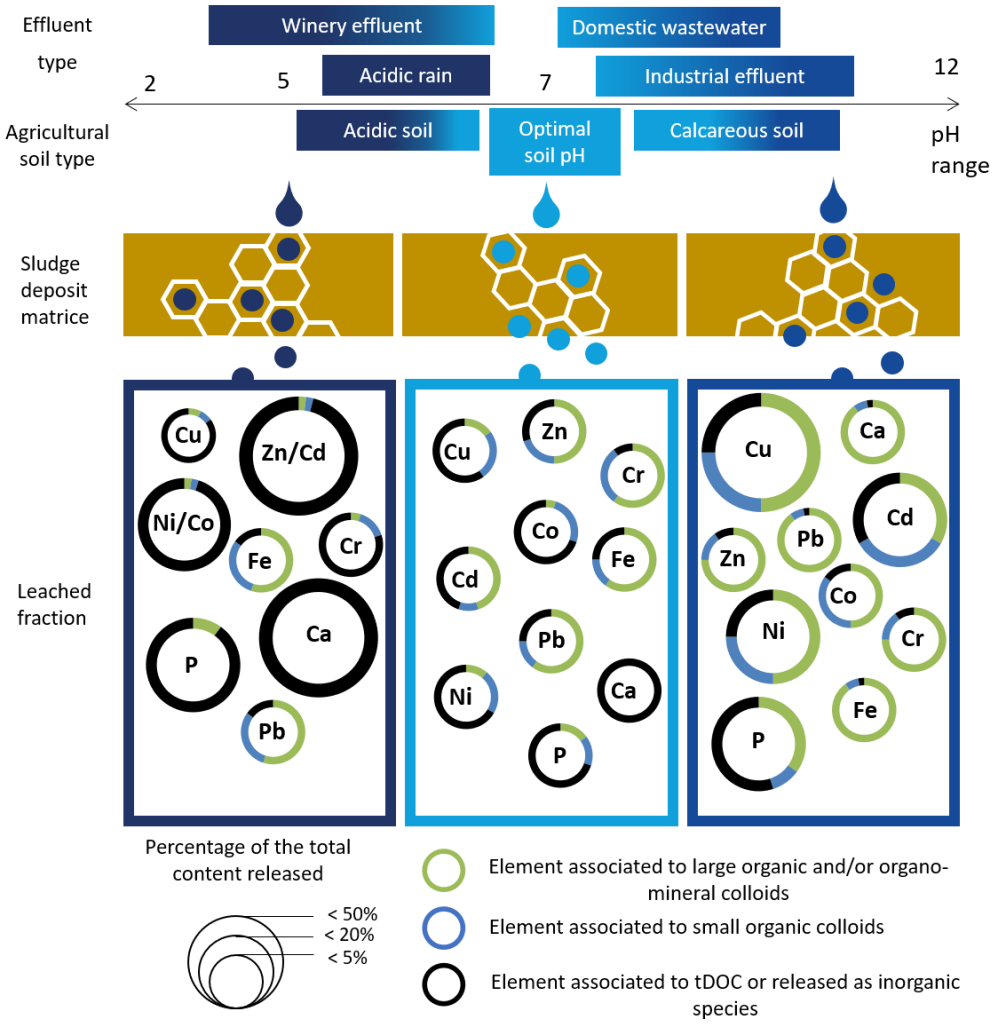

Fig. 11: Schematic representation of the possible effects of pH on the release of major and trace elements from VFW sludge deposits either *in situ* at the surface of the CW filter or *ex situ* at the surface of r soils receiving applications of dredged sludge.

Organic sludge from intensive or extensive domestic wastewater treatment plants may be used as organic amendment by spreading them onto agricultural soil (Fytili and Zabaniotou, 2008; Gherghel et al., 2019; Uggetti et al., 2011). Currently, only trace metals total content is regulated (Directive 1986/278/EEC). The solid-solution distribution and the speciation of the pollutants contained in the released fraction, will govern the bioavailability and possible toxicity of the sludge micropollutants (Aiken et al., 2011; Allen et al., 2001; Paquin et al., 2002). These parameters may be controlled by pH conditions and the colloidal mobility of the sludge deposit, as demonstrated in this study. The assessment of trace contaminants total content is therefore not sufficient to guarantee safe applications. Experimentally evaluation of the leaching behavior is necessary.

4 Conclusion

In this study, ultrafiltration technics usually used for geochemical studies on natural soil solution or water samples were applied on solid deposit leaching solution extracted using various pH conditions that sludge deposits may encounter. In addition to the expected release of an important amount of organic matter, this study evidenced the important control exerted by organo-mineral colloids on various inorganic contaminants from the solid deposit. The pH variations and the nature of colloidal phases control the remobilization of major and trace elements released from the sludge deposit. The colloidal phase reactivity toward elements is also strongly dependent on the element considered.

Depending on their affinity for colloids and their sensibility to pH variations, the element released from the SD could be assigned to three different leaching patterns. The first leaching pattern is characterized by a strong influence of large Fe/Al-organic colloids. Under near neutral to alkaline conditions divalent metals (Mg, Ca, Sr, Ba, Mn, Zn, Pb) and trivalent elements (Sc, Y, Cr) exhibit this leaching pattern. The second leaching pattern is composed of divalent metals (Co, Ni, Cu, Cd) with a high affinity for colloidal organic matter but also for small organics leached in the TD fraction. For these two first groups, the pH drastically influences the distribution of these elements as small acidifications of the solution could considerably increase the proportion of elements released as “truly” dissolved species. Finally, the third leaching pattern is composed of elements mainly released in the “truly” dissolved fraction regardless of pH conditions. This group is composed of metalloids (As, Sb), non-metals elements (P, S), alkaline (Na, Rb) and transition metals (V).

This study on the influence of pH on the distribution of major and trace elements, considered as pollutants or not, has shown the strong similarities existing between natural soils (wetland soils, peat soils) and the sludge deposit often considered as a technosoil. But the important amount of organic matter and contaminants retained in the solid deposit and the various pH conditions they could encounter increase the potential environmental impact of contaminant remobilization. By complexing trace contaminants, stabilizing Fe-Al oxides and competing for their binding sites, organic molecules exert a more important control on the geochemical fate of all the constituents of the solid deposit layer.

Acknowledgments

This work was supported by the C-FACTOR project funded by ANR (project number ANR-18-CE01-0008). Through the support of the GeOHeLiS analytical platform of Rennes University, this publication is also supported by the European Union through the European Regional Development Fund (FEDER), the French ministry of Higher Education and Research, the French Region of Brittany and Rennes Metropole.

Literature cited

Aiken, G.R., Hsu-Kim, H., Ryan, J.N., 2011. Influence of Dissolved Organic Matter on the Environmental Fate of Metals, Nanoparticles, and Colloids. Environ. Sci. Technol. 45, 3196–3201. https://doi.org/10.1021/es103992s

Allen, H.E., McGrath, S.P., McLaughlin, M.J., Peijnenburg, W.J.G.M., Sauvé, S., Lee, C., 2001. Bioavailability of metals in terrestrial ecosystems: importance of partitioning for bioavailability to invertebrates, microbes, and plants. Bioavailability of metals in terrestrial ecosystems: importance of partitioning for bioavailability to invertebrates, microbes, and plants.

Al-Sid-Cheikh, M., Pédrot, M., Dia, A., Guenet, H., Vantelon, D., Davranche, M., Gruau, G., Delhaye, T., 2015. Interactions between natural organic matter, sulfur, arsenic and iron oxides in re-oxidation compounds within riparian wetlands: NanoSIMS and X-ray adsorption spectroscopy evidences. Science of The Total Environment 515–516, 118–128. https://doi.org/10.1016/j.scitotenv.2015.02.047

Antelo, J., Avena, M., Fiol, S., López, R., Arce, F., 2005. Effects of pH and ionic strength on the adsorption of phosphate and arsenate at the goethite–water interface. Journal of Colloid and Interface Science 285, 476–486. https://doi.org/10.1016/j.jcis.2004.12.032

Arco-Lázaro, E., Agudo, I., Clemente, R., Bernal, M.P., 2016. Arsenic(V) adsorption-desorption in agricultural and mine soils: Effects of organic matter addition and phosphate competition. Environmental Pollution 216, 71–79. https://doi.org/10.1016/j.envpol.2016.05.054

Balistrieri, L.S., Blank, R.G., 2008. Dissolved and labile concentrations of Cd, Cu, Pb, and Zn in the South Fork Coeur d'Alene River, Idaho: Comparisons among chemical equilibrium models and implications for biotic ligand models. Applied Geochemistry 23, 3355–3371. https://doi.org/10.1016/j.apgeochem.2008.06.031

Banc, C., Gautier, M., Blanc, D., Lupsea-Toader, M., Marsac, R., Gourdon, R., 2021. Influence of pH on the release of colloidal and dissolved organic matter from vertical flow constructed wetland surface sludge deposits. Chemical Engineering Journal 418, 129353. https://doi.org/10.1016/j.cej.2021.129353

Borggaard, O.K., Jdrgensen, S.S., Moberg, J.P., Raben-Lange, B., 1990. Influence of organic matter on phosphate adsorption by aluminium and iron oxides in sandy soils. Journal of Soil Science 41, 443–449. https://doi.org/10.1111/j.1365-2389.1990.tb00078.x

Chen, S., Hong, H., Huang, X., Fang, Q., Yin, K., Wang, C., Zhang, Y., Cheng, L., Algeo, T.J., 2018. The role of organo-clay associations in limiting organic matter decay: Insights from the Dajiuhu peat soil, central China. Geoderma 320, 149–160. https://doi.org/10.1016/j.geoderma.2018.01.013

Darland, J.E., Inskeep, W.P., 1997. Effects of pH and Phosphate Competition on the Transport of Arsenate. Journal of Environmental Quality 26, 1133–1139. https://doi.org/10.2134/jeq1997.00472425002600040027x

Dixit, S., Hering, J.G., 2003. Comparison of Arsenic(V) and Arsenic(III) Sorption onto Iron Oxide Minerals: Implications for Arsenic Mobility. Environ. Sci. Technol. 37, 4182–4189. https://doi.org/10.1021/es030309t

Du, W., Parker, W., 2013. Characterization of Sulfur in Raw and Anaerobically Digested Municipal Wastewater Treatment Sludges. Water Environment Research 85, 124–132. https://doi.org/10.2175/106143012X13407275694671

Duffus, J.H., 2002. “Heavy metals” a meaningless term? (IUPAC Technical Report). Pure and Applied Chemistry 74, 793–807. https://doi.org/10.1351/pac200274050793

Fan, X., Ding, S., Chen, M., Gao, S., Fu, Z., Gong, M., Tsang, D.C.W., Wang, Y., Zhang, C., 2019. Peak Chromium Pollution in Summer and Winter Caused by High Mobility of Chromium in Sediment of a Eutrophic Lake: In Situ Evidence from High Spatiotemporal Sampling. Environ. Sci. Technol. 53, 4755–4764. https://doi.org/10.1021/acs.est.8b07060

Fytili, D., Zabaniotou, A., 2008. Utilization of sewage sludge in EU application of old and new methods—A review. Renewable and Sustainable Energy Reviews 12, 116–140. https://doi.org/10.1016/j.rser.2006.05.014

Gangloff, S., Stille, P., Schmitt, A.-D., Chabaux, F., 2016. Factors controlling the chemical composition of colloidal and dissolved fractions in soil solutions and the mobility of trace elements in soils. Geochimica et Cosmochimica Acta 189, 37–57. https://doi.org/10.1016/j.gca.2016.06.009

Gherghel, A., Teodosiu, C., De Gisi, S., 2019. A review on wastewater sludge valorisation and its challenges in the context of circular economy. Journal of Cleaner Production 228, 244–263. https://doi.org/10.1016/j.jclepro.2019.04.240

Gorny, J., Billon, G., Noiriel, C., Dumoulin, D., Lesven, L., Madé, B., 2016. Chromium behavior in aquatic environments: a review. Environ. Rev. 24, 503–516. https://doi.org/10.1139/er-2016-0012

Grybos, M., Davranche, M., Gruau, G., Petitjean, P., Pédrot, M., 2009. Increasing pH drives organic matter solubilization from wetland soils under reducing conditions. Geoderma 154, 13–19. https://doi.org/10.1016/j.geoderma.2009.09.001

Gu, S., Gruau, G., Dupas, R., Jeanneau, L., 2020. Evidence of colloids as important phosphorus carriers in natural soil and stream waters in an agricultural catchment. Journal of Environmental Quality 49, 921–932. https://doi.org/10.1002/jeq2.20090

Guénet, H., Davranche, M., Vantelon, D., Gigault, J., Prévost, S., Taché, O., Jaksch, S., Pédrot, M., Dorcet, V., Boutier, A., Jestin, J., 2017. Characterization of iron–organic matter nano-aggregate networks through a combination of SAXS/SANS and XAS analyses: impact on As binding. Environ. Sci.: Nano 4, 938–954. https://doi.org/10.1039/C6EN00589F

Hiemstra, T., Antelo, J., Rahnemaie, R., Riemsdijk, W.H. van, 2010. Nanoparticles in natural systems I: The effective reactive surface area of the natural oxide fraction in field samples. Geochimica et Cosmochimica Acta 74, 41–58. https://doi.org/10.1016/j.gca.2009.10.018

Jain, C.K., Ali, I., 2000. Arsenic: occurrence, toxicity and speciation techniques. Water Research 34, 4304–4312. https://doi.org/10.1016/S0043-1354(00)00182-2

Kania, Manon, Gautier, M., Blanc, D., Lupsea-Toader, M., Merlot, L., Quaresima, M.-C., Gourdon, R., 2019. Leaching behavior of major and trace elements from sludge deposits of a French vertical flow constructed wetland. Science of The Total Environment 649, 544–553. https://doi.org/10.1016/j.scitotenv.2018.08.364

Kania, M., Gautier, M., Imig, A., Michel, P., Gourdon, R., 2019. Comparative characterization of surface sludge deposits from fourteen French Vertical Flow Constructed Wetlands sewage treatment plants using biological, chemical and thermal indices. Science of The Total Environment 647, 464–473. https://doi.org/10.1016/j.scitotenv.2018.07.440

Kania, M., Gautier, M., Michel, P., Gourdon, R., 2017. Study of aggregation in surface sludge deposits from 14 full-scale French constructed wetlands using particle size distribution and dynamic

vapor sorption analyses. Water Science and Technology 77, 79–90. https://doi.org/10.2166/wst.2017.523

Kim, B., Gautier, M., Michel, P., Gourdon, R., 2013. Physical–chemical characterization of sludge and granular materials from a vertical flow constructed wetland for municipal wastewater treatment. Water Science and Technology 68, 2257–2263. https://doi.org/10.2166/wst.2013.485

Kim, B., Gautier, M., Olvera Palma, G., Molle, P., Michel, P., Gourdon, R., 2015. Pilot-scale study of vertical flow constructed wetland combined with trickling filter and ferric chloride coagulation: influence of irregular operational conditions. Water Science and Technology 71, 1088–1096. https://doi.org/10.2166/wst.2015.077

Kim, B., Gautier, M., Simidoff, A., Sanglar, C., Chatain, V., Michel, P., Gourdon, R., 2016. pH and Eh effects on phosphorus fate in constructed wetland's sludge surface deposit. Journal of Environmental Management 183, 175–181. https://doi.org/10.1016/j.jenvman.2016.08.064

Kinniburgh, D., Cooper, D., 2011. PhreePlot: Creating graphical output with PHREEQC. undefined.

Koopmans, G.F., Hiemstra, T., Vaseur, C., Chardon, W.J., Voegelin, A., Groenenberg, J.E., 2020. Use of iron oxide nanoparticles for immobilizing phosphorus in-situ: Increase in soil reactive surface area and effect on soluble phosphorus. Science of The Total Environment 711, 135220. https://doi.org/10.1016/j.scitotenv.2019.135220

Kotaś, J., Stasicka, Z., 2000. Chromium occurrence in the environment and methods of its speciation. Environmental Pollution 107, 263–283. https://doi.org/10.1016/S0269-7491(99)00168-2

Kretzschmar, R., Schäfer, T., 2005. Metal Retention and Transport on Colloidal Particles in the Environment. Elements 1, 205–210. https://doi.org/10.2113/gselements.1.4.205

Krickov, I.V., Pokrovsky, O.S., Manasypov, R.M., Lim, A.G., Shirokova, L.S., Viers, J., 2019. Colloidal transport of carbon and metals by western Siberian rivers during different seasons across a permafrost gradient. Geochimica et Cosmochimica Acta 265, 221–241. https://doi.org/10.1016/j.gca.2019.08.041

Li, Z., Shakiba, S., Deng, N., Chen, J., Louie, S.M., Hu, Y., 2020. Natural Organic Matter (NOM) Imparts Molecular-Weight-Dependent Steric Stabilization or Electrostatic Destabilization to Ferrihydrite Nanoparticles. Environ. Sci. Technol. 54, 6761–6770. https://doi.org/10.1021/acs.est.0c01189

Milne, C.J., Kinniburgh, D.G., Tipping, E., 2001. Generic NICA-Donnan model parameters for proton binding by humic substances. Environ Sci Technol 35, 2049–2059. https://doi.org/10.1021/es000123j

Morvannou, A., Choubert, J.-M., Vanclooster, M., Molle, P., 2011. Solid respirometry to characterize nitrification kinetics: A better insight for modelling nitrogen conversion in vertical flow constructed wetlands. Water Research 45, 4995–5004. https://doi.org/10.1016/j.watres.2011.07.004

Nieboer, E., Richardson, D.H.S., 1980. The replacement of the nondescript term 'heavy metals' by a biologically and chemically significant classification of metal ions. Environmental Pollution Series B, Chemical and Physical 1, 3–26. https://doi.org/10.1016/0143-148X(80)90017-8

Paquin, P.R., Gorsuch, J.W., Apte, S., Batley, G.E., Bowles, K.C., Campbell, P.G.C., Delos, C.G., Di Toro, D.M., Dwyer, R.L., Galvez, F., Gensemer, R.W., Goss, G.G., Hogstrand, C., Janssen, C.R., McGeer, J.C., Naddy, R.B., Playle, R.C., Santore, R.C., Schneider, U., Stubblefield, W.A., Wood,

C.M., Wu, K.B., 2002. The biotic ligand model: a historical overview. Comparative Biochemistry and Physiology Part C: Toxicology & Pharmacology 133, 3–35. https://doi.org/10.1016/S1532-0456(02)00112-6

Parkhurst, Appelo, 1999. User's guide to PHREEQC (Version 2) : a computer program for speciation, batch-reaction, one-dimensional transport, and inverse geochemical calculations. https://doi.org/10.3133/wri994259

Peacock, C.L., Sherman, D.M., 2004. Vanadium(V) adsorption onto goethite (α-FeOOH) at pH 1.5 to 12: a surface complexation model based on ab initio molecular geometries and EXAFS spectroscopy. Geochimica et Cosmochimica Acta 68, 1723–1733. https://doi.org/10.1016/j.gca.2003.10.018

Pédrot, M., Dia, A., Davranche, M., 2009. Double pH control on humic substance-borne trace elements distribution in soil waters as inferred from ultrafiltration. Journal of Colloid and Interface Science 339, 390–403. https://doi.org/10.1016/j.jcis.2009.07.046

Pédrot, M., Dia, A., Davranche, M., Bouhnik-Le Coz, M., Henin, O., Gruau, G., 2008. Insights into colloid-mediated trace element release at the soil/water interface. Journal of Colloid and Interface Science 325, 187–197. https://doi.org/10.1016/j.jcis.2008.05.019

Pédrot, M., Dia, A., Davranche, M., Martin, S., Al-Sid-Cheikh, M., Gruau, G., 2015. Unravelling the fate of arsenic during re-oxidation of reduced wetland waters: Experimental constraints and environmental consequences. Comptes Rendus Geoscience, Geochemical and isotopic record of anthropogenic activities (Part 1) 347, 304–314. https://doi.org/10.1016/j.crte.2015.03.002

Plathe, K.L., Kammer, F. von der, Hassellöv, M., Moore, J., Murayama, M., Hofmann, T., Hochella, M.F., Plathe, K.L., Kammer, F. von der, Hassellöv, M., Moore, J., Murayama, M., Hofmann, T., Hochella, M.F., 2010. Using FlFFF and aTEM to determine trace metal–nanoparticle associations in riverbed sediment. Environ. Chem. 7, 82–93. https://doi.org/10.1071/EN09111

Pokrovsky, O.S., Dupré, B., Schott, J., 2005. Fe–Al–organic Colloids Control of Trace Elements in Peat Soil Solutions: Results of Ultrafiltration and Dialysis. Aquat Geochem 11, 241–278. https://doi.org/10.1007/s10498-004-4765-2

Pokrovsky, O.S., Schott, J., Dupré, B., 2006. Trace element fractionation and transport in boreal rivers and soil porewaters of permafrost-dominated basaltic terrain in Central Siberia. Geochimica et Cosmochimica Acta 70, 3239–3260. https://doi.org/10.1016/j.gca.2006.04.008

Pourret, O., Dia, A., Davranche, M., Gruau, G., Hénin, O., Angée, M., 2007. Organo-colloidal control on major- and trace-element partitioning in shallow groundwaters: Confronting ultrafiltration and modelling. Applied Geochemistry, Metal interactions with natural organic matter and Watershed-scale geochemistry 22, 1568–1582. https://doi.org/10.1016/j.apgeochem.2007.03.022

Ratié, G., Vantelon, D., Lotfi Kalahroodi, E., Bihannic, I., Pierson-Wickmann, A.C., Davranche, M., 2019. Iron speciation at the riverbank surface in wetland and potential impact on the mobility of trace metals. Science of The Total Environment 651, 443–455. https://doi.org/10.1016/j.scitotenv.2018.09.143

Raudina, T.V., Loiko, S.V., Kuzmina, D.M., Shirokova, L.S., Kulizhskiy, S.P., Golovatskaya, E.A., Pokrovsky, O.S., 2021. Colloidal organic carbon and trace elements in peat porewaters across a permafrost gradient in Western Siberia. Geoderma 390, 114971. https://doi.org/10.1016/j.geoderma.2021.114971

Riise, G., Van Hees, P., Lundström, U., Tau Strand, L., 2000. Mobility of different size fractions of organic carbon, Al, Fe, Mn and Si in podzols. Geoderma 94, 237–247. https://doi.org/10.1016/S0016-7061(99)00044-0

Ritchie, J.D., Perdue, E.M., 2003. Proton-binding study of standard and reference fulvic acids, humic acids, and natural organic matter. Geochimica et Cosmochimica Acta 67, 85–96. https://doi.org/10.1016/S0016-7037(02)01044-X

Sajadi, S. a. A., 2010. Metal ion-binding properties of L-glutamic acid and L-aspartic acid, a comparative investigation. Natural Science 02, 85. https://doi.org/10.4236/ns.2010.22013

Shaheen, S.M., Alessi, D.S., Tack, F.M.G., Ok, Y.S., Kim, K.-H., Gustafsson, J.P., Sparks, D.L., Rinklebe, J., 2019. Redox chemistry of vanadium in soils and sediments: Interactions with colloidal materials, mobilization, speciation, and relevant environmental implications- A review. Advances in Colloid and Interface Science 265, 1–13. https://doi.org/10.1016/j.cis.2019.01.002

Sharma, P., Ofner, J., Kappler, A., 2010. Formation of Binary and Ternary Colloids and Dissolved Complexes of Organic Matter, Fe and As. Environ. Sci. Technol. 44, 4479–4485. https://doi.org/10.1021/es100066s

Stachowicz, M., Hiemstra, T., van Riemsdijk, W.H., 2008. Multi-competitive interaction of As(III) and As(V) oxyanions with Ca2+, Mg2+, PO3−4, and CO2−3 ions on goethite. Journal of Colloid and Interface Science 320, 400–414. https://doi.org/10.1016/j.jcis.2008.01.007

Theng, B.K.G., Yuan, G., 2008. Nanoparticles in the Soil Environment. Elements 4, 395–399. https://doi.org/10.2113/gselements.4.6.395

Tipping, E., Lofts, S., Sonke, J.E., 2011. Humic Ion-Binding Model VII: a revised parameterisation of cation-binding by humic substances. Environ. Chem. 8, 225. https://doi.org/10.1071/EN11016

Uggetti, E., Ferrer, I., Molist, J., García, J., 2011. Technical, economic and environmental assessment of sludge treatment wetlands. Water Research 45, 573–582. https://doi.org/10.1016/j.watres.2010.09.019

van Hees, P.A.W., van Hees, A.-M.T., Lundström, U.S., 2001. Determination of aluminium complexes of low molecular organic acids in soil solution from forest soils using ultrafiltration. Soil Biology and Biochemistry 33, 867–874. https://doi.org/10.1016/S0038-0717(00)00232-7

Vantelon, D., Davranche, M., Marsac, R., Fontaine, C.L., Guénet, H., Jestin, J., Campaore, G., Beauvois, A., Briois, V., 2019. Iron speciation in iron–organic matter nanoaggregates: a kinetic approach coupling Quick-EXAFS and MCR-ALS chemometrics. Environ. Sci.: Nano 6, 2641–2651. https://doi.org/10.1039/C9EN00210C

Verbeeck, M., Hiemstra, T., Thiry, Y., Smolders, E., 2017. Soil organic matter reduces the sorption of arsenate and phosphate: a soil profile study and geochemical modelling. European Journal of Soil Science 68, 678–688. https://doi.org/10.1111/ejss.12447

Vermöhlen, K., Lewandowski, H., Narres, H.-D., Koglin, E., 2000. Adsorption of polyacrylic acid on aluminium oxide: DRIFT spectroscopy and ab initio calculations. Colloids and Surfaces A: Physicochemical and Engineering Aspects 170, 181–189. https://doi.org/10.1016/S0927-7757(00)00408-8

Wang, S., Mulligan, C., 2006. Effect of Natural Organic Matter on Arsenic Release from Soils and Sediments into Groundwater. Environmental geochemistry and health 28, 197–214. https://doi.org/10.1007/s10653-005-9032-y

Wu, C.-Y., Asano, M., Hashimoto, Y., Rinklebe, J., Shaheen, S.M., Wang, S.-L., Hseu, Z.-Y., 2020. Evaluating vanadium bioavailability to cabbage in rural soils using geochemical and micro-spectroscopic techniques. Environmental Pollution 258, 113699. https://doi.org/10.1016/j.envpol.2019.113699

Wu, X., Bowers, B., Kim, D., Lee, B., Jun, Y.-S., 2019. Dissolved Organic Matter Affects Arsenic Mobility and Iron(III) (hydr)oxide Formation: Implications for Managed Aquifer Recharge. Environ. Sci. Technol. 53, 14357–14367. https://doi.org/10.1021/acs.est.9b04873

Xu, H., Lin, H., Jiang, H., Guo, L., 2018. Dynamic molecular size transformation of aquatic colloidal organic matter as a function of pH and cations. Water Research 144, 543–552. https://doi.org/10.1016/j.watres.2018.07.075

Zhuang, J., Tyner, J.S., Perfect, E., 2009. Colloid transport and remobilization in porous media during infiltration and drainage. Journal of Hydrology 377, 112–119. https://doi.org/10.1016/j.jhydrol.2

A RETENIR

L'ultrafiltration est une méthode de fractionnement très largement utilisée dans la caractérisation de la fraction colloidale de solutions de sols ou encore d'eaux naturelles. Couplé à des mesures en ICP et en spectrophotométrie UV-vis, ces analyses permettent de montrer la présence de colloïdes, d'évaluer leur taille et leur nature mais aussi leur impact sur la dynamique d'éléments chimique associés. La spécificité de ce travail a été d'appliquer pour la première fois cette méthodologie aux solutions issues des tests de neutralisation acido-basique d'une boue de FPR. Ces boues concentrant une importante quantité de matière organique, une première phase du travail a permis d'évaluer l'influence du pH sur la remobilisation de colloïdes organiques. L'émission de colloïdes organiques des dépôts de FPR et leur poids moléculaire sont largement influencés par les variations de pH mais aussi par les caractéristiques physico-chimiques initiales du dépôt solide. L'émission de trois principales fractions de molécules organiques ont pu être mises en évidence : (i) l'émission de gros colloïdes organiques (0,45 µm – 30 kDa) aux pH basiques, (ii) l'émission de petit colloïdes organiques (30 kDa – 3 kDa) sur toute la gamme de pH, et (iii) l'émission de petite molécules organiques (< 3 kDa) aux pH acides. A l'origine des phénomènes observés, on retrouve des processus d'adsorption/désorption de molécules organiques sur des minéraux (argile, oxyde de fer…), mais aussi, l'évolution de la conformation des molécules organiques via l'agrégation ou la désagrégation des structures supramoléculaires des matières organiques elles-mêmes.

A l'instar de solutions de sol naturel, les dépôts de boue produisent des oxydes de fer et d'aluminium retrouvés dans la fraction supérieure à 30 kDa en association avec la matière organique. Le relargage de matière organique semble donc favoriser la remobilisation de ces oxydes métalliques. En fonction de leur répartition au sein des différentes fraction de poids moléculaire et de leur affinité pour les différentes phases colloïdales, les éléments analysés peuvent être séparés en 3 catégories : (i) les éléments largement (> 50%) retrouvés dans la fraction < 3kDa sur toute la gamme de pH (Na, Rb, As, Sb, S, P, V) dont une portion est relarguée associée à des colloïdes organo-minéraux (0,45 µm – 30 kDa) avec l'augmentation du pH, (ii) les éléments largement (> 50%) associés aux gros colloïdes organiques (0,45 µm – 30 kDa) et aux petites molécules organiques avec plus de 20% mesuré dans la fraction < 3 kDa (Co, Cu, Ni, Cd) et (iii) les éléments très largement (>80%) associés aux colloïdes organo- minéraux remobilisés dans la grosse fraction colloïdale (Mg, Ca, Sr, Ba, Mn, Zn, Pb, Sc, Y, Cr). Pour ces deux derniers groupes, le pH influence drastiquement l'affinité des éléments pour les phases colloïdales. De petites acidifications de la solution peuvent augmenter considérablement la proportion d'éléments relargué dans la fraction < 3 kDa, sous la forme d'espèce inorganique dissoutes. Au-delà de l'émission de phases porteuses colloïdales et de leur nature, le pH de la solution, le degré d'oxydation et la classe

chimique des éléments étudiés sont donc d'importants paramètres régissant la spéciation des éléments au sein des solutions relarguées par ces dépôts.

Finalement, la nature des colloïdes remobilisés par ces dépôts de boue prélevés sur un filtre planté de roseaux et leur influence sur le relargage des métaux traces sont qualitativement similaires aux résultats obtenus par de précédentes études portant sur des échantillons de zones humides naturelles. La génération des données précédemment décrites va permettre dans la suite de ce document de calibrer des modèles de prédiction géochimiques dédiés aux matrices anthropisées comme les boues de filtres plantés de roseaux.

CHAPITRE IV. UTILISATION DE MODELES MULTISURFACIQUE POUR PREDIRE LE RELARGAGE ET LA SPECIATION D'ELEMENTS MAJEURS ET TRACES CONTENUS DANS DES DEPOTS

PREAMBULE

Les polluants inorganiques (métaux traces, nutriments) contenus dans les dépôts, résidu du traitement des eaux par solutions fondées sur la nature, peuvent présenter un risque environnemental majeur pour les eaux de surfaces et souterraines. Dans la gestion du risque liée à la remobilisation de polluants retenus dans des matrices poreuses, les modèles de prédiction géochimiques sont souvent utilisés. Ces modèles permettent notamment le calcul de la distribution entre phase solide et liquide des polluants mais aussi leur spéciation, deux paramètres fondamentaux pour évaluer la toxicité d'un relargage. Cependant, au sein de matrice complexe comme les dépôts, le devenir de ces polluants est contrôlé par de nombreux processus géochimiques. Les modèles multisurfaciques permettent de décrire ces milieux complexes. Ils sont composés de plusieurs sous-modèles génériques ayant pour objectif de calculer la sorption des ions sur les surfaces réactives de la matrice.

Dans ce chapitre, les données relatives à la nature des phases colloïdales et à l'influence de ces dernières sur la spéciation des éléments majeurs et traces relargués par les dépots de boue de filtre planté vont être utilisées afin de calibrer des modèles de spéciations géochimiques dédiés aux dépôts issus de solutions fondées sur la nature à écoulement vertical de l'eau. Les capacités de sorption des principales surfaces réactives composant un sol ont été intégrées dans le programme de spéciation PHREEQC. On retrouve la capacité de sorption de la matière organique avec Model VII (Tipping et al., 2011) et la capacité de sorption des oxydes de fer et d'aluminium avec le GTLM de Dzombak et Morel (1990). Les phénomènes de précipitation/dissolution de phases minérales sont aussi intégrés suivant les constantes thermodynamiques spécifiées dans la base de données llnl.dat.

Dans un premier temps, les prédictions d'un modèle multisurfacique seront testées, calibrées et comparées aux résultats expérimentaux précédemment obtenus sur la boue d'un filtre planté de roseaux. Les résultats de cette modélisation sont discutés dans l'article : « Use of multisurface sorption model to estimate major and trace elements speciation and distribution in solid sludge deposit solution ».

Dans un second temps, la méthodologie utilisée pour modéliser l'échantillon de boue de filtre planté de roseaux a été réutilisé afin de modéliser le relargage et la spéciation d'éléments provenant d'un sédiment de bassin d'infiltration des eaux pluviales. Les résultats obtenus sont discutés dans l'article « Coupled organic-mineral geochemical modelling of the leaching behaviour of major and trace metals from stormwater infiltration basin sediment ». Enfin, dans une dernière partie, les performances et limites de la méthodologie de modélisation employée seront évaluées. Pour ce faire, les résultats de

modélisation précédemment obtenus seront comparés à deux nouveaux travaux de modélisations effectués sur une autre boue de filtre planté de roseaux et un autre sédiment de bassin d'infiltration.

ARTICLE 3

Multi-surface sorption modelling of major and trace elements leaching from vertical flow constructed wetlands surface sludge deposits.

Banc, C. *, Gautier, M. *, Blanc, D. *, Lupsea-Toader, M. *, Marsac, R., Gourdon, R. ***

* Univ Lyon, INSA Lyon, DEEP (Déchets Eaux Environnement Pollutions), EA 7429, 69621 Villeurbanne Cedex, France.

** Univ Rennes, CNRS, Géosciences Rennes, UMR **6118**, 35000 Rennes, France.

1. Introduction

The fate and transfer of inorganic contaminants in soil/sediment-water systems is particularly complex due the large variety of chemical forms they can take from their reactions and interactions with the environment (Di Bonito et al., 2018). Inorganic contaminants can be complexed, adsorbed and/or exchanged with particulate matter, or co-precipitated with mineral and organic solid phases (Manceau et al., 2002). In the liquid phase they can form various complexes with organic and inorganic ligands as well as aquo and hydroxo complexes. These interactions are dictated by the biotic and abiotic conditions of the local environment (pH, Eh, ionic strength, temperature, etc.) (Christl, 2012; Dijkstra et al., 2004; Qu et al., 2019), which also influence the release of various species from solid matter to dissolved or colloidal fractions (Aiken et al., 2011; Durce et al., 2016; Grybos et al., 2007b, 2007a). Organic matter (OM), metal oxides and clays are the main interactive constituents in environmental porous media (Di Bonito et al., 2018; Fisher-Power et al., 2019). Among them, OM distribution between solid and dissolved phases is a driver for the mobility of contaminants (Audette et al., 2020; Grybos et al., 2007a; Pokrovsky et al., 2005). Despite this apparent complexity, modeling can provide a description of the processes regulating trace metal release, speciation, and bioavailability (Di Bonito et al., 2018). Multisurface modeling has been used as a tool for a better understanding of the geochemical processes occurring in porous matrices and for the study of speciation, solid-solution partition and bioavailability of trace metals (Dijkstra et al., 2004; Fisher-Power et al., 2019; Klinkert and Comans, 2020; Paquin et al., 2002). A multisurface model can be defined as an assemblage of generic models using thermodynamic constants to describe ion-binding capacity of the various surfaces composing porous matrices (Molina, 2016).

Several authors (Almas et al., 2007; Dijkstra et al., 2004; Fisher-Power et al., 2019; Golui et al., 2020a) have used the non-ideal competitive adsorption (NICA-Donnan) model (Milne et al., 2001) and the Humic Ion bindings (Model VII) model (Tipping et al., 2011) to describe ion-binding to fulvic and humic acids. The parameters of these models are usually determined from laboratory experiments using isolated and purified humic (HA) and fulvic acids (FA) mainly from natural waters. Since the sorption capacity of the organic binders varies with their nature and origin, the OM content in the particulate matter must be modulated in the models to express the effective relative sorption capacity. This approach, developed for soils or sediments, has been applied in systems where OM is present at relatively low concentrations (a few % w/w) from natural origins whereas much fewer studies have considered systems with high concentrations of organic matter from anthropogenic origins (Fang et al., 2016b; Klinkert and Comans, 2020). Yet, these conditions are met in several applications such as in vertical flow treatment wetlands (VFCW) where anthropogenic organic matter accumulates as a sludge

deposit (SD) at the surface of the filters and plays a major role in the treatment of the wastewater which is percolated through it (Kania et al., 2019; Kim et al., 2014). The SD solution are a complex mixture of colloidal OM of various molecular size associated with colloidal Fe-oxides with strong influence on the remobilization of major and trace elements retained in the SD (Banc et *al.,* 2021). The pollutant remobilization processes are therefore particularly complex to predict.

The objective of the present study was to develop and calibrate a multisurface models dedicated to SD generated by VFCW. The high contents in OM, trace metals and other inorganic constituents in the SD impose to control the operating conditions to avoid the release of contaminants into the aqueous phase (Drapeau et al., 2017; Kim et al., 2016; Molle, 2013; Tedoldi et al., 2016a). Existing models used in soil sciences for example may be useful in this objective, provided the multi-surface organic ion-binding approach is applicable to systems with high organic contents from anthropogenic origins. Compared to natural or polluted soils (Dijkstra et al., 2004; Fisher-Power et al., 2019; Golui et al., 2020a), surface sludge deposits (SD) from vertical flow treatment wetlands (VFTW) exhibit high organic matter contents (> 45%) from natural and anthropogenic origins with a large variety of pollutants associated to organic matter and/or metal oxides depending on the element considered (Kania et al., 2019).

2. Materials and methods

2.1. Sludge deposits (SD) samples and pH-leaching experiments

SD were sampled from the surface solid layer of the first-stage filter of the Vertical Flow Constructed Wetland (VFCW) treatment plant of Vercia (FRANCE). The sludge layer had been formed from the first day of operation of the treatment plant, i.e. 14 years ago. The total content in major and trace elements, the general characteristics of the organic matter contained in the SD sample (Table 1) as well as the pH-dependent leaching experiments were performed by Banc et al., 2021.

Table 1. General characteristics of the SD organic matter (Banc et *al.,* 2021).

Natural pH	Total OC gC/kg SD dm	Loss on ignition %	Humic-like gC/kg SD dm	Fulvic-like gC/kg SD dm	Humin-like gC/kg SD dm
6.5	166.6	42.6	21.6	21.1	123.3

2.2. Model description

The pH-dependent distribution between particulate and soluble fraction, for major elements (Ca, Mg, Fe, Al, P) and trace metal(loid)s (Zn, Cu, Ni, Cd, Pb, Cr, As) were modelled using the model multi-surface assemblage composed of well accepted "mechanistic" surface complexation models described below.

2.2.1. Ion binding to organic matter

The sorption capacity of Dissolved and Solid Organic Matter (DOM and SOM, respectively) was modeled using Humic Ion-Binding Model VII described by Tipping et al, 2011. Model VII considers two types of cation binding to humic acids (HA) and fulvic acids (FA): (i) a specific binding involving a discrete binding sites distribution and (ii) a non-specific binding considered to occur through electrostatic accumulation of counter-ion in a Donnan volume surrounding the molecular surface and inversely proportional to the ionic strength of the solution. A total of 50 binding sites are described in Model VII, allowing to consider the heterogeneity of humic substances binding capacity. These sites were described as composed of 4 carboxylic (type A sites) and 4 phenolic (type B sites) sites allowing them to form bidentate and tridentate recombination. Only the aqueous cations and their first hydrolysis product are likely to bind to HA and FA. The intrinsic equilibrium constants for cations binding to monodentate type A or B sites are described by two parameters log K_{MA} and log K_{MB}, respectively. These parameters are calculated as follow:

$$\log K_{MB} = \log K_{MA} \times \frac{pK_B}{pK_A}$$

In the previous equation pK_A and pK_B describe the intrinsic protonation constants for type A and type B sites, respectively.

Equilibrium constants for cations binding to bidentate or tridentate sites are defined as the sum of the log K of the monodentate sites constituting the multidentate site considered. The range of the metal binding strengths is also modulated by an empirical parameter called ΔLK_2 generating moderate and strong binding sites and by an electrostatic correction of charge development resulting from ion binding and release (Almas et al., 2007; Tipping et al., 2011). Non-specific ions accumulation in the Donnan volume surrounding humic molecules was neglected here, considering the high OM content and high concentration in background electrolyte (Bonten et al., 2008). The default binding constants from (Tipping et al, 2011) were not adjusted.

2.2.2. Ion binding to mineral surfaces

In this study, sorption of ions was considered to occur only on amorphous iron and aluminum oxides. Indeed, in natural conditions the presence of high content in organic matter limits oxides crystallization

but promotes the formation of amorphous forms (Guénet et al., 2017; Pédrot et al., 2011). Clay was not considered in order to simplify the approach. Cation binding to amorphous hydrous ferric oxides (HFO) and hydrous aluminum oxides (HAO) was modeled using the generalized two-layer model (GTLM) with generic parameters described by Dzombak and Morel, 1990. In this model, oxides binding capacity is also described by specific and non-specific binding. The default value of 600 $m^2.g^{-1}$ was used for the specific surface area of HFO/HAO. The oxides surface is composed of strong and weak monodentate amphoteric hydroxyl groups able to bind cations and anions. Relationship between precipitate amorphous Al and Fe-oxides and, the amount of chemically reactive surface is set as define by Dzombak and Morel (1990): 0.2 mol of weak and 0.005 mol of strong binding sites per mol of precipitated HFO/HAO. The electrostatic fields around the charged oxides affect the intrinsic ionic sorption capacity and also the non-specific interaction within a diffuse Gouy-Chapman layer.

2.2.3. Modelling approach, parameters and model inputs

All the aqueous geochemical calculations were performed with PHREEQC-V3 software. The thermodynamic data used for the simulations were taken from Lawrence Livermore National Laboratory (LLNL database). The input parameters consisted in the physico-chemical characteristics of the SD and the physico-chemical conditions of the aqueous solution, as follows:

1. pH and pE as measured in each of the solutions;
2. total contents in Zn, Cu, Cr, Ni, Cd, Pb and As in the SD, as determined by alkaline fusion (see § 2.1);
3. leached concentrations in S and Si to account for anionic competition;
4. natures of the mineral phases controlling the solubility of the major elements Fe, Al, Ca, P, i.e. calcite, amorphous $Fe(OH)_3$, strengite, $Al(OH)_3$, and hydroxyapatite ($Ca_5(OH)(PO_4)_3$). These phases were already observed in SD samples according to XRD results (Kim et al., 2015; Kim et al., 2013). We assume that magnesium carbonate ($MgCO_3$) controls the solubility of Mg;
5. the sorption proprieties of amorphous $Fe(OH)_3$ and $Al(OH)_3$;
6. the cations binding capacity of the organic matter described in Model VII. This parameter was implemented in PHREEQC using the constant capacitance model (CCM) and following the methodology developed by Marsac et al, 2017. The relationships between measured OC and reactive OC in the solid and soluble fractions were modulated according to the modelling scenario. Three scenarios were considered and two ways to consider organic matter sorption capacity were tested in this study (see Table 2).

Table 2. Description of the organic parameters applied in the 3 different scenarios tested.

	Active OM $gOC.L^{-1}$	Ratio HA:FA solid fraction	Active DOM	Ratio HA:FA released fraction	Released Fe-oxides
Scenario A	0	Ø	0	Ø	Not considered
Scenario B	4.27	1	100% measured DOM	From ultrafiltration data obtained by Banc et al., 2021	Not considered
Scenario C	16.6	7	Optimized	Optimized	Considered

- **Scenario A**: Absence of OM – SD modelled only by mineral phases and HFO/HAO sorption capacity. Mineral phases used as input were previously described. The main objective of this model was to test the ability of the model to predict element concentration without considering ion-binding to organic matter.
- **Scenario B**: In this scenario, organic matter sorption capacity was expressed from the physicochemical characteristics of solid and dissolved organic matter (SOM and DOM). Fractionation of SD SOM revealed that Humin, Humic and Fulvic-like fractions represented respectively 74%, 13% and 13% of the organic matter contents of the overall sample (Banc et al., 2021). In this scenario, only the solid Humic and Fulvic like fraction were considered corresponding to 26% of the total content in organic matter. The DOM of each pH-leaching tests were fractionated according to their apparent molecular weight; results were presented in Banc et al. 2021. Leached organic molecules with molecular weight below 3 kDa were considered as FA while leached organic molecules with molecular weight >3 kDa were modeled HA. The pH-dependent quantity of SOM is calculated as the difference between active SOM and active DOM. For all the pH conditions, quantity of active OM, corresponding to solid and dissolved organic matter in Scenario B is constant and equal to 4.27 g of OC. Mineral phases precipitation and ion binding to HFO/HAO is implemented as presented in Scenario A.
- **Scenario C**: based on the results obtained in Scenario B and described later (see § 3.1.2), the reactive fraction of POM and DOM were optimized. In Scenario C, 100% of the SOM content was considered as active with 87% of HA (corresponding to humin and humic acid fraction) and 13% of FA. The reactive fraction of DOM was modulated for acidic conditions according to results obtained on Scenario B and on ultrafiltration experiments (Banc et al., 2021). The pH-

dependent modulation of the reactive fraction of DOM depending of the considered scenario is represented in Fig 1 b. Moreover, as discuss further in this paper (see § 3.1.3), release of HFO colloids in suspension was also considered in this scenario as already observed by Almas et al, 2007. Mineral phases precipitation and ion binding to precipitated Al and Fe-oxides is implemented as described in Scenario A.

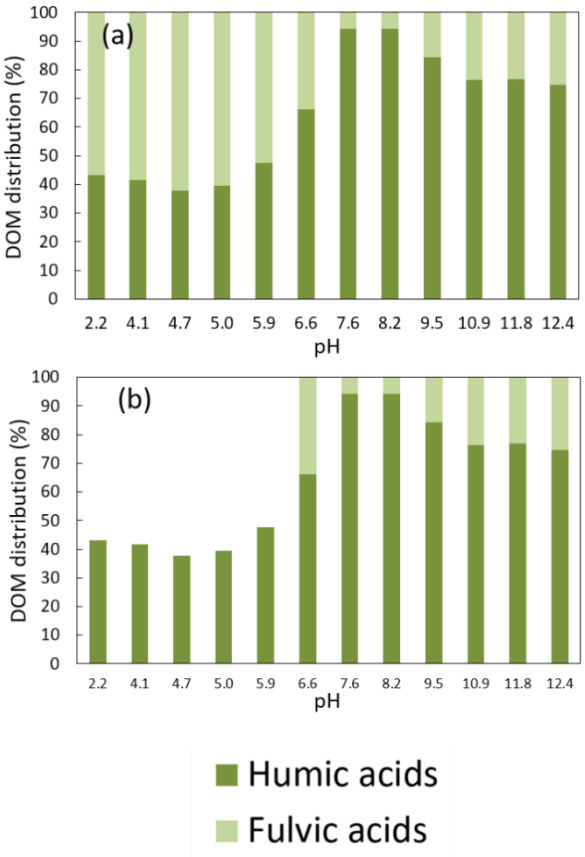

Fig. 1: Modulation of the reactive fraction of measured DOM and the distribution between humic and fulvic acids according to ultrafiltration experiments performed by Banc et al. (2021). In Scenario B (a), 100% of the measured DOM is considered active while in Scenario C (b), reactive DOM was reduced in acidic conditions.

3. Results and discussion

3.1. Modelling results of the release of major and trace elements according to the scenarios

3.1.1. Modelling of the release of major elements

Fig. 2 describes the results obtained from the pH-dependent leaching experiments for Al, Ca, Fe, Mg, and P, and the simulated release obtained with the three modelling scenarios described above. The experimental evolution of DOC is also presented in this figure.

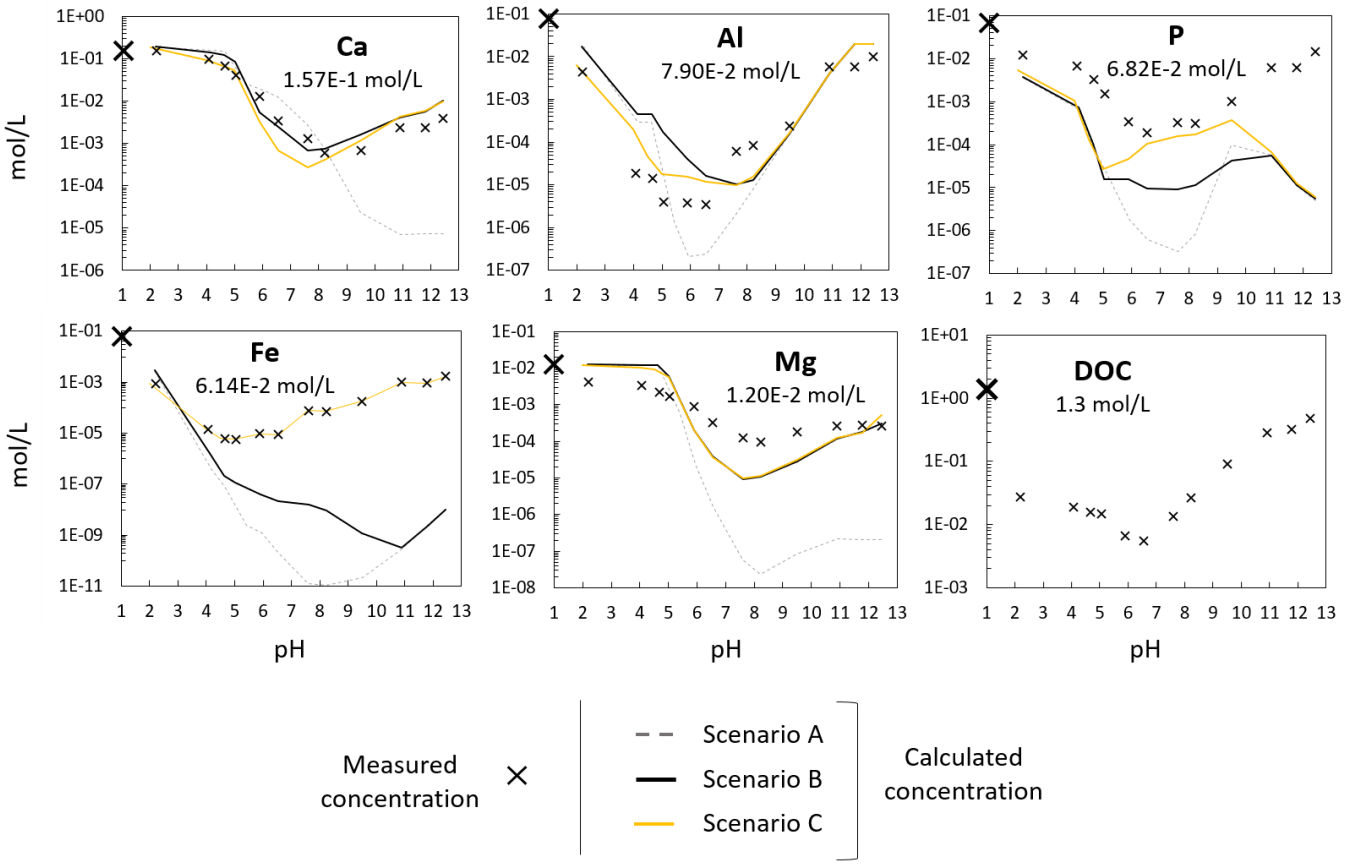

Fig. 2: Released concentrations and different model calculations as function of pH for major elements (Ca, Al, P, Fe, Mg). Total content measured in the SD are displayed below the various elements names and are also reported at pH 1.

Dissolved OC strongly varied within the tested pH range. The minimum concentration is observed at pH 6.5 and strongly increased up to two orders of magnitude with the progressive alkalization of the solution. This has been previously ascribed to the solubilization of high molecular weight organic matter (>30kDa) due to destabilization of solid organo-mineral association (Banc et al., 2021; Grybos et al., 2009a). Acid addition also increases DOC release, consequence of the solubilization of low molecular weight organic matter (<3kda) (Banc et al., 2021). The pH-dependent leaching concentration of Fe and Al are very similar. Minimum leaching concentration is measured at pH~5, but varies up to three orders of magnitude with under acidic and alkaline conditions. The maximum leaching content observed at pH 12 represents only a small proportion of the total content in Al and Fe (*i.e* less than 10% of the total content). The low solubility of Fe and Al could be attributed to low solubility of Fe and Al

mineral phases contained in the SD. Ca and Mg pH-dependent solubility also varied up to three orders of magnitude. However, the maximum leaching concentration measured at very acidic pH are closer to the total content measured in the solid deposit. This phenomenon could be attributed to dissolution of mineral phases containing Ca and Mg. Protonic competition for organic and inorganic binding sites could also contribute to increase the concentration of Ca and Mg release in acidic pH range. The leaching concentration of P varies up to one order of magnitude along the pH-range with a maximum of 20% of the total P content leached for very alkaline pH conditions.

Scenario A globally overestimates the release of major elements under acidic conditions, while under alkaline conditions concentrations are largely overestimated. For part of the pH range (pH<4), Ca and Mg concentrations are adequately predicted suggesting low influence of organic matter for the considered pH range. To better predict solubility of major elements, especially under alkaline conditions, sorption to solid and dissolved organic matter needs to be considered. As shown in Fig 2, Scenario B, largely improves model prediction for Ca and Mg. Increasing amount of DOM increased the solubilization of Ca and Mg complexed to DOM. For Al, the presence of organic matter slightly improves modelling prediction in the acidic pH range, by reducing the calculated leached concentration, thanks to Al complexation with SOM.

Despite the OM sorption capacity, Fe concentrations remain largely underestimated for the entire pH range due to low solubility of Fe-oxides. However, as observed in various soil solutions (Pédrot et al., 2009a; Pokrovsky et al., 2005; Pourret et al., 2007b), Banc et al, 2021 suggested the remobilization of colloidal Fe-oxides from the SD, possibly stabilized by organic coating, for pH>2. Thus, large underestimation of the Fe concentration in Scenario B could be reasonably explain by the lack Fe-oxides colloids in aqueous suspension in the model. Hence, in Scenario C, the amount of HFO remobilized from solid to release fraction is calculated as the difference between measured and calculated Fe concentration.

3.1.2. Modelling of the release of trace elements

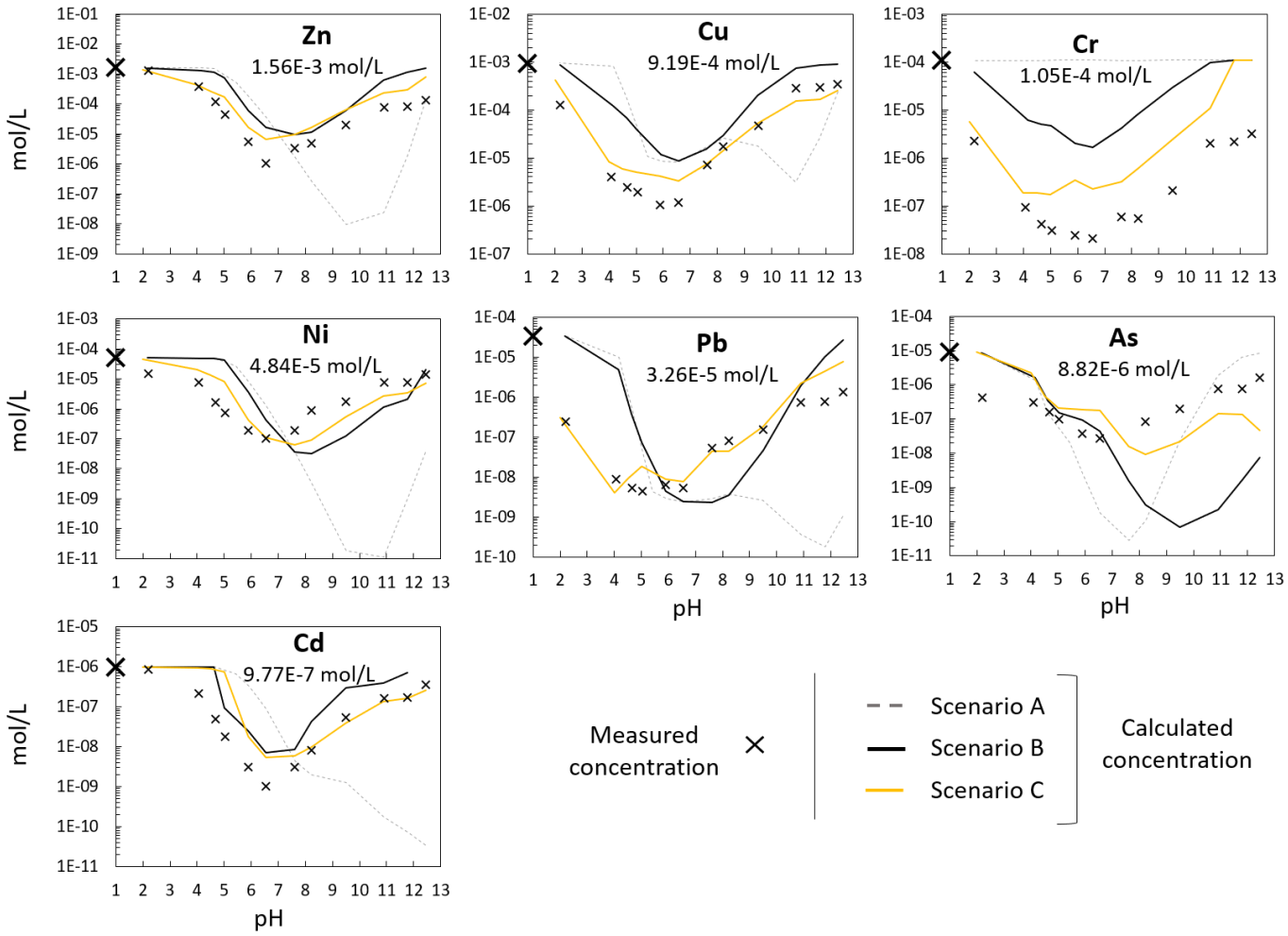

Fig. 3: Released concentrations and different model calculations as function of pH for trace elements (Zn, Cu, Cr, Ni, Pb, As and Cd). Total content measured in the SD are displayed below the various elements names and are also reported at pH 1.

The sludge deposit layer retains important amounts of trace metal(loids) (As, Cu, Cd, Cr, Ni, Pb, Zn) due to their presence in wastewaters. All these elements exhibit similar pH-dependent leaching pattern with increased solubilization with acidification or alkalization of the solutions. Globally, metal(loids) concentrations vary up to three orders of magnitudes, some elements being preferentially solubilized under acidic conditions (Co, Ni, Zn, Cd), while others are more sensible to alkalization (Cu, As, Cr). Among these metal(loids), Cr and As are poorly soluble elements as maximum leaching content is approximately of 3 and 15%, respectively. On the other hand, Cu, Cd, Co, Ni and Zn are more soluble elements as their leaching concentration exceed 30% of their total content in the solid deposit. For instance, 80% of solid deposit content in Zn and Cd is released at pH~2.

As observed for the major elements considered in this study, the simple consideration of trace metals sorption to Fe and Al-oxides binding sites, proposed in Scenario A, is not sufficient to adequately

predict their leaching. Indeed, Scenario A calculations overestimate the concentration of trace elements from the most acidic pH up to pH 6.55 where sorption on oxides starts. At pH above 6.55 adsorption becomes too important, leading Scenario A to underestimate the concentration of these elements in solution. For Cr, calculated concentration obtained with Scenario A are constant within the entire pH-range due to its low affinity for Fe and Al-oxides binding sites (Dzombak and Morel, 1990). The addition of dissolved and solid organic matter within Scenario B significantly improves predicted concentration for most of these trace elements. However, over the entire pH range, Scenario B largely overestimates the release of divalent transition metals. In other modelling studies of soil/sediment systems (Bonten et al., 2008; Fang et al., 2016b; Fisher-Power et al., 2019; Rennert et al., 2017), these elements such as Cu and Zn, are largely associated to OM suggesting that the reactive fraction of DOM and SOM used in scenario B is not adequate. The use of another scenario in which the fraction of reactive DOM and SOM will be adjusted is essential to improve model prediction.

3.1.3. Optimization of the description of solid and dissolved organic matter

As previously discussed, a given amount of organic binders of different natures and characteristics will develop different sorption capacities. Models must therefore modulate the OM concentration input data to express the corresponding effective sorption capacity based on the analyzed nature and characteristics of the organic matter (Amery et al., 2008; Pourret et al., 2007b), or by fitting experimental results and the predicted curves calculated with different input values for the sorption capacity (Bonten et al., 2008; Fisher-Power et al., 2019; Zhu et al., 2018). In this study, the quantity of reactive POM and DOM was modulated in Scenario C to improve the modeling performance on the basis of the physico-chemical characterization performed on the SD sample. Two modifications of the organic parameters of Scenario B have been made. First, it appears that the solid active fraction measured as HA and FA (~ 30% of the total organic content) used in Scenario B is not sufficient to sorb and immobilize enough elements in the solid fraction. In Scenario C, the humin fraction, representing ~70% of the total organic content, was added to the humic and fulvic fraction already considered in Scenario B. Because (i) no Model VII parameters are available for the humin fraction and (ii) it is generally less reactive than the humic one, it was assumed to have binding properties identical to fulvic fraction. However, the simulated release form SD remains overestimated at acidic pH. Thus, in Scenario C, the quantity of reactive DOM was reduced for pH<6. At these pHs, OC remobilized from SD is largely composed of molecules below 3 kDa with low aromatic content (Banc et al., 2021) modeled as fulvic acids in scenario B. Ion binding capacity for fulvic acids described by Tipping et al. 2011 encompass the ion binding capacity of the small organic molecules remobilized under acidic conditions leading to the overestimation of trace metals concentrations for pH<6. Considering these analytical results, we

assumed that, active DOM for pH<6 is only composed by the humic fraction. In Scenario C, the release of colloidal amorphous Fe-oxides was also considered as previously described.

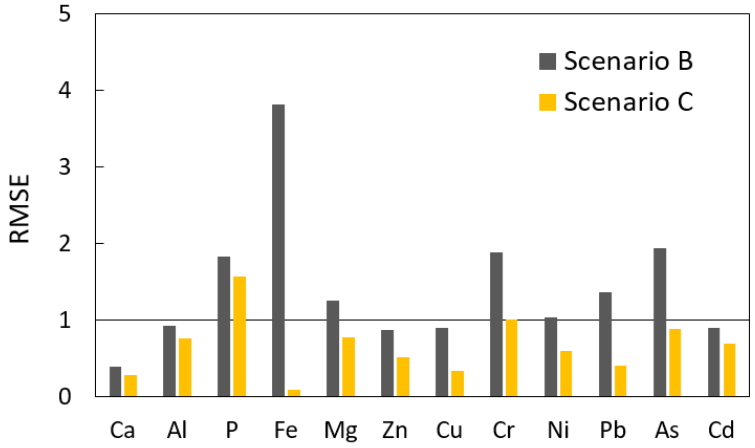

Fig. 4: Root mean squared errors (RMSEs) between calculated and measured major and trace elements concentration in solution (logarithm) as function of modeling scenario.

To evaluate the efficacity of such modifications, the logarithmic root mean squared errors ($RMSE_{log}$), a measure of absolute error between calculated and measured values, for scenario B and C and for major and trace elements have been calculated according to the protocol form Bonten et al. 2008 and provided in Fig 4. Scenario C globally reduces the discrepancy between calculated and measured concentration for most trace elements. Scenario C only slightly improves modelling performances for Ca, Al and Mg suggesting that these elements are less sensitive to OM. For most elements, $RMSE_{log}$ remains below 1. However, it should be noted that the performance of the model fluctuates depending on the considered element. Good adequation between calculated and measured concentrations are obtained on divalent transition metals (Cu, Cd, Zn, Ni), known to be largely controlled by OM. However, calculated $RMSE_{log}$ for Cr, P and As are higher compared to other elements studied here. Interestingly, Fe-oxides-OM aggregates largely contribute to the geochemical cycle of these elements in natural soil samples such as wetland soil solution (Beauvois et al., 2021; Krickov et al., 2019; Pédrot et al., 2009a; Pokrovsky et al., 2005; Xia et al., 2020; Yang et al., 2020). In this study, the binding capacity of Fe-oxides-OM complex is modeled by additive modelling, considering the sorption capacity of these complex as the sum of organic and oxide sorption capacity. This methodology does not take into account competition between organic matter and ions for oxides binding sites and have been shown, in some cases, to be inadequate to describe binding capacity of such organo-mineral particles (Christl and Kretzschmar, 2001; Janot et al., 2013). Moreover, even if the sorption of As and P to organic matter is not described in Model VII, As and P could bound organic matter directly or through ternary complex

with metals or Fe-oxides (Audette et al., 2020; Mikutta and Kretzschmar, 2011; Sharma et al., 2010). These processes, not described in Model VII, might explain the discrepancy between calculated and measured concentration for P, for instance.

The total measured content of elements used as input for the model proposed in this study is the sum of elements relatively easily accessible such as elements complexed to various surfaces and elements barely accessible, possibly precipitated or coprecipitated. While in the “available” elements fraction used in numerous studies (Dijkstra et al., 2004; Groenenberg et al., 2012; Klinkert and Comans, 2020), element in the recalcitrant fraction are not measured and not included in modeling calculations, in the total element content used in this study all the various form of the elements are measured. Thus, by using total content instead of the available content (Dijkstra et al., 2004; Fisher-Power et al., 2019) model prediction could largely overestimate the released concentration if the potential mineral phases are not included in the modelling calculation. But for trace elements modeled in this study, no overestimation of the leached content over the entire pH range is evidenced, suggesting that trace elements are largely associated to OM or Fe-Al oxides in the SD. Under highly acidic conditions however, elements such as Cd and As are overestimated. Mineral phases precipitation incorporating trace elements have been used in previous studies (Dijkstra et al., 2004; Fang et al., 2016b). However, no mineral phases available in the database used in this study were able to improve modelling results.

3.2 Influence of pH on the chemical speciation

In this section, the pH-dependent speciation of major and trace elements calculated with Scenario C will be analyzed. In the solid fraction, these elements might be complexed on solid organic matter and oxides or precipitated as mineral phases. In the soluble fraction, elements could be either associated to DOM and colloidal Fe-oxide or released as small inorganic species, comprising free ionic forms plus inorganic complex.

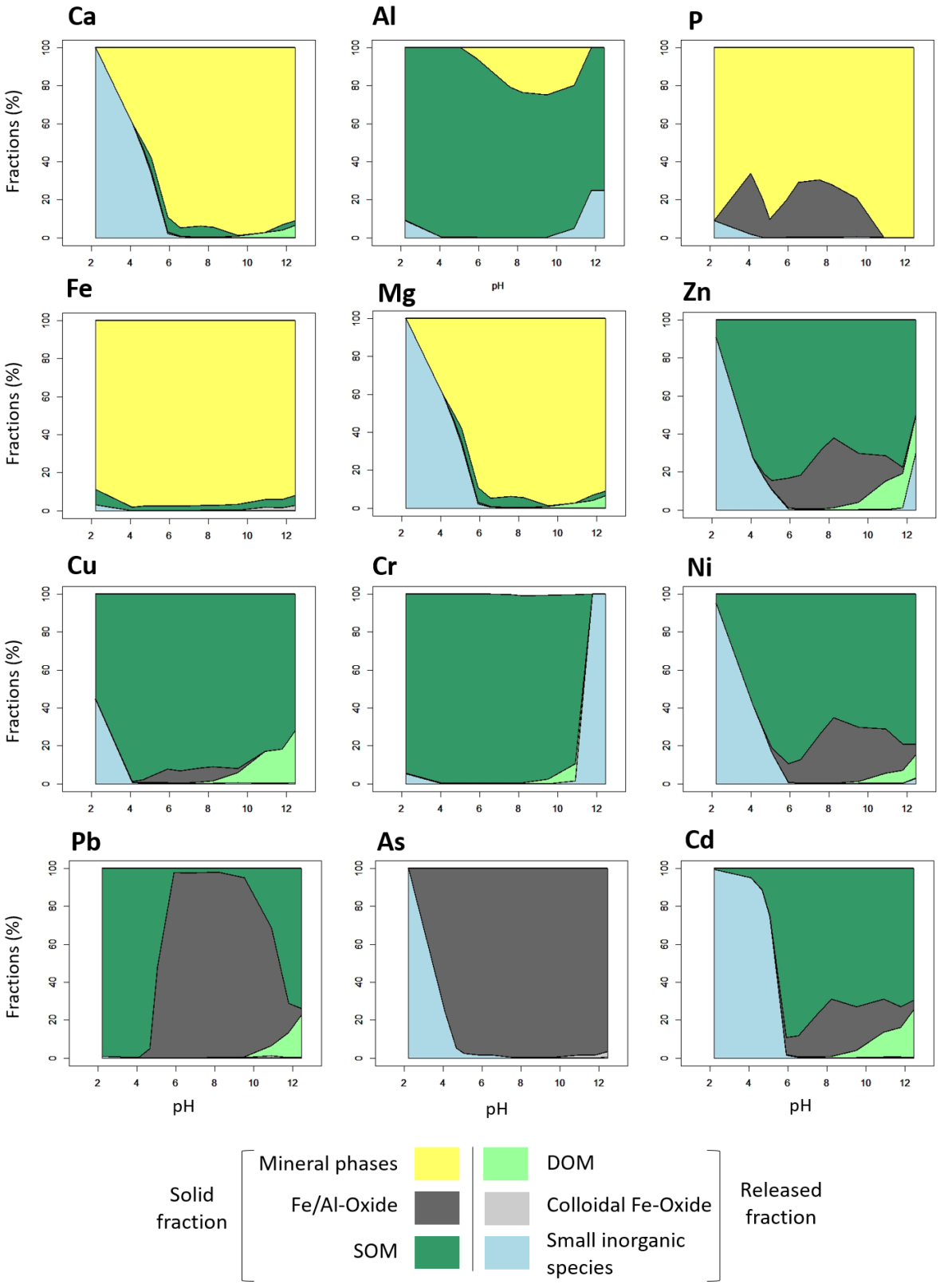

Fig.5: Distribution of major and trace elements in the particulate and released fractions. In the solid fraction elements could be precipitated (mineral phases such as $CaCO_3(s)$) or complexed to oxides (Fe/Al-oxides) and organic matter (SOM). In the released fraction, elements could be complexed to released organics (DOM) and colloidal oxides (Fe-oxides) or present as inorganic complex such as OH species and free ions such as Cu^{2+}, Pb^{2+} (Small inorganic species).

3.2.1 Role of SOM and oxides in the retention of trace elements

As presented in Fig. 5, SOM is calculated to be the main adsorbent phases for Cu, Zn, Cd and Cr in the solid deposit. In the acidic pH range, approximately 100% of major and trace metals are retained by SOM. In this pH range, the high quantity of SOM increases their ability to sorb elements. Previous modelling studies also reported the preponderance of SOM adsorption under acidic conditions in natural soils (Dijkstra et al., 2004; Fisher-Power et al., 2019; Groenenberg and Lofts, 2014; Shi et al., 2013a) or composted sewage sludge (Fang et al., 2016b). With the progressive alkalization of the solution, the proportion of elements complexed to SOM decreases due to competition to HFO/HAO. Indeed, for pH>6.5, Fe-oxides becomes negatively charged, increasing its capacity to sorb cationic elements. It should be noted that Pb and As are largely complexed by solid oxides as previously observed in natural soil samples (Bonten et al., 2008; Dijkstra et al., 2004).

The precipitation of mineral phases has an important contribution to the retention of major elements in the solid fraction. Precipitated amorphous Fe and, in a lesser extent, Al-oxides, strongly control the solubilization of Fe and Al. Ca and Mg are also mainly precipitated, as calcium and magnesium carbonate. Thus, the high proportion of Ca and Mg released (~ 90 and 30% for Ca and Mg, respectively), is calculated to originate from the acidic dissolution of these carbonates. Phosphorus is also mainly precipitated as apatite over the entire pH range, complexation to oxides contributing to 20% of the P form in the solid fraction in good agreement with previous results obtain by Kim et al. 2013 on the characterization of the P form in various SD samples.

3.2.2 Role of released OM and Fe-oxides in the remobilization of elements from SD

Fig.6 shows the distribution of elements in the leached fraction. Elements could be associated to DOM or released Fe-oxides, and released as small inorganic forms representing the sum of free ions (*e.g.* Ca^{2+}, Cu^{2+}…) and small inorganic complexes such as OH^- species. Under near neutral to alkaline conditions, released major and trace elements are complexed by DOM, while under more acidic conditions, these elements are released as small inorganic species, as observed in previous studies on soil (Dijkstra et al., 2004; Fisher-Power et al., 2019; Groenenberg and Lofts, 2014). Lower content in DOM and strong protonic competition for DOM binding sites could explain the decreasing fraction of elements complexed to DOM under acidic conditions. It should be noted that even under these acidic conditions, Cu and Cr remain largely complexed to DOM. Banc et al. 2021, evidenced by ultrafiltration, the complexation of Cu and Cr to released organic colloids, even under acidic conditions.

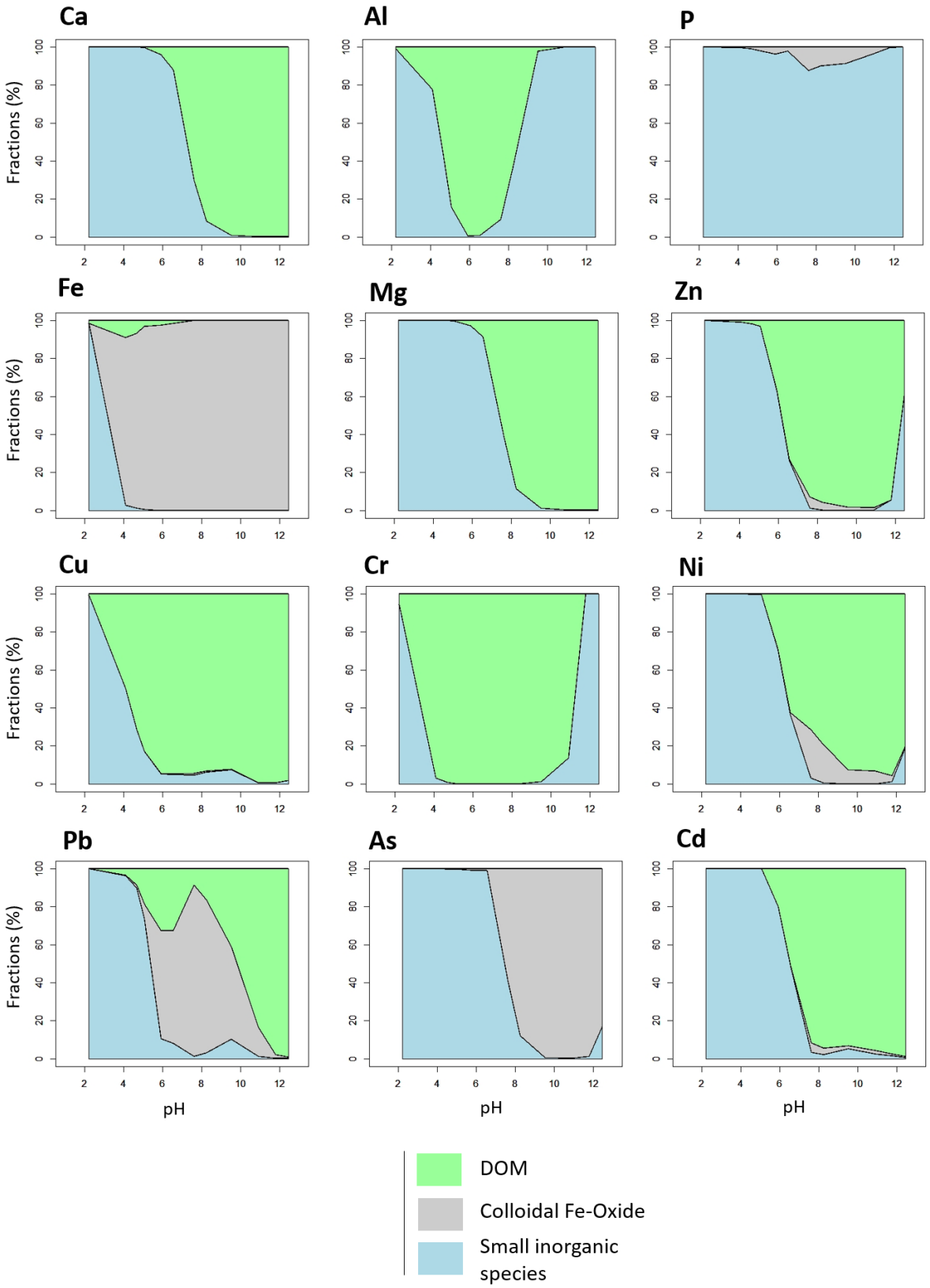

Fig.6: Focus on the major and trace elements speciation in the released fractions. In the released fraction, elements could be complexed to released organics (DOM) and colloidal oxides (Fe-oxides) or present as inorganic complex such as OH species and free ions such as Cu^{2+}, Pb^{2+} (Small inorganic species).

According to the modelling results, the remobilization of Fe-oxides also contributes to the remobilization of As, P and Pb. These results are in good agreement with ultrafiltration studies, which evidenced the fundamental role played by the remobilization of Fe-oxides in the geochemical cycle of these elements in natural soils (Gu et al., 2020; Hens and Merckx, 2002; Pédrot et al., 2009a; Pokrovsky et al., 2005) and solid deposit samples (Banc et al., 2021).

Globally, the good agreement between ultrafiltration results obtained by Banc et al, 2021 and the calculated speciation suggest that this model is also able to reproduce qualitatively the remobilization of elements from the SD samples.

4. Applicability of the model to constructed wetlands solid deposit

As mentioned earlier, Model VII had already shown good performances in predicting the release of many trace and major elements from soils (Dijkstra et al., 2004; Golui et al., 2020a; Groenenberg and Lofts, 2014). In this study, the presence of organic matter in important quantities, its anthropic origin and the use of total element content instead of the more largely used "available content" were challenging. Overall, the developed model (*i.e* with scenario C) gives a satisfying prediction of the pH-dependent release of several major and trace elements, without any extra optimization steps, only using intrinsic parameters developed in Model VII. The use of OM characterization results (Banc et al., 2021; Kania et al., 2019) has allowed the modulation of the reactive fraction of SOM and DOM in coherence with the quality of the organic molecules. In addition to solid-solution partitioning, the model also adequately predicts the speciation of major and trace elements. Distinction between the different forms of released elements is important to evaluate risks of varying pH conditions for aquatic systems or microorganism of soil amended with solid deposit (Aiken et al., 2011; Allen et al., 2001). For instance, modelling results emphasis that acidic conditions should be avoided as most major and trace metals are released as small inorganic species with high mobility and high biodisponiblity (Aiken et al., 2011; Paquin et al., 2002). Moreover, modeling calculation also evidenced the important role of Fe and Al-oxides in the retention of trace elements, whose reductive dissolution under anaerobic conditions and remobilization could enhance the release of associated pollutants.

In this study, the total content in major elements has been used as this measure is more largely used to characterize nature-based matrices compared to reactive or accessible content (Kania et al., 2019; Kim et al., 2013b; Tedoldi et al., 2016a). The dissolution of SD's precipitates including trace elements could contribute significantly in the total measured content and might lead to major overestimation of leached concentration, if the mineral phases concerned are not included in the modelling calculation (Bonten et al., 2008). But for high organic matter content solid deposit as studied here, sorption to organic matter and Fe-oxides is sufficient to globally adequately predict most trace elements

concentration. As described by Bonten et al., 2008, the prerequisite for using process-based modelling is the incorporation of all relevant chemical process driving element behavior. Especially in our highly organic sample, modeling results emphasis the need to integrate the possible sorption of anionic elements (*e.g* P, As) directly to organic matter or through tertiary complex with cationic bridge or Fe-oxides.

Globally, total content in OM contained in the SD is a good proxy of its binding capacity. Once adjusted to the physcio-chemical characteristics of the solid and dissolved OM from solid deposit, process-based models used in this study allows adequate calculation of solid-solution distribution of most major and trace elements without fitting any parameter. Considering the remobilization of Fe-oxides colloids was necessary to improve calculation for elements with high affinity for these surfaces. To fully describe geochemical processes occurring in the SD with pH-variation, the multisurface should integrate OM ion-binding capacity toward anionic elements such as P and As. The inputs of this model can be based on easily accessible simple standard soil analysis increasing their practical applicability. The quantity of DOM is not routinely measured but in studies using different SD the DOM pH-dependent leaching exhibit very similar leaching pattern (Banc et al., 2021; Kania et al., 2019; Kim et al., 2016) largely dependent of the total organic matter content.

Literature cited

Aiken, G.R., Hsu-Kim, H., Ryan, J.N., 2011. Influence of Dissolved Organic Matter on the Environmental Fate of Metals, Nanoparticles, and Colloids. Environ. Sci. Technol. 45, 3196–3201. https://doi.org/10.1021/es103992s

Allen, H.E., McGrath, S.P., McLaughlin, M.J., Peijnenburg, W.J.G.M., Sauvé, S., Lee, C., 2001. Bioavailability of metals in terrestrial ecosystems: importance of partitioning for bioavailability to invertebrates, microbes, and plants. Bioavailability of metals in terrestrial ecosystems: importance of partitioning for bioavailability to invertebrates, microbes, and plants.

Almas, Å.R., Lofts, S., Mulder, J., Tipping, E., 2007. 2 Solubility of major cations and trace metals (Cu, Zn and Cd) in soil 3 extracts of some contaminated agricultural soils near a zinc smelter in 4 Norway: modelling with a multisurface extension of WHAM 41.

Amery, F., Degryse, F., Cheyns, K., Troyer, I.D., Mertens, J., Merckx, R., Smolders, E., 2008. The UV-absorbance of dissolved organic matter predicts the fivefold variation in its affinity for mobilizing Cu in an agricultural soil horizon. European Journal of Soil Science 59, 1087–1095. https://doi.org/10.1111/j.1365-2389.2008.01078.x

Audette, Y., Smith, D.S., Parsons, C.T., Chen, W., Rezanezhad, F., Van Cappellen, P., 2020. Phosphorus binding to soil organic matter via ternary complexes with calcium. Chemosphere 260, 127624. https://doi.org/10.1016/j.chemosphere.2020.127624

Banc, C., Gautier, M., Blanc, D., Lupsea-Toader, M., Marsac, R., Gourdon, R., 2021. Influence of pH on the release of colloidal and dissolved organic matter from vertical flow constructed wetland surface sludge deposits. Chemical Engineering Journal 418, 129353. https://doi.org/10.1016/j.cej.2021.129353

Beauvois, A., Vantelon, D., Jestin, J., Bouhnik-Le Coz, M., Catrouillet, C., Briois, V., Bizien, T., Davranche, M., 2021. How crucial is the impact of calcium on the reactivity of iron-organic matter aggregates? Insights from arsenic. Journal of Hazardous Materials 404, 124127. https://doi.org/10.1016/j.jhazmat.2020.124127

Bonten, L.T.C., Groenenberg, J.E., Weng, L., van Riemsdijk, W.H., 2008. Use of speciation and complexation models to estimate heavy metal sorption in soils. Geoderma 146, 303–310. https://doi.org/10.1016/j.geoderma.2008.06.005

Christl, I., 2012. Ionic strength-and pH-dependence of calcium binding by terrestrial humic acids. Environmental Chemistry 9, 89–96. https://doi.org/10.1071/EN11112

Christl, I., Kretzschmar, R., 2001. Interaction of copper and fulvic acid at the hematite-water interface. Geochimica et Cosmochimica Acta 65, 3435–3442. https://doi.org/10.1016/S0016-7037(01)00695-0

Di Bonito, M., Lofts, S., Groenenberg, J.E., 2018. Chapter 11 - Models of Geochemical Speciation: Structure and Applications, in: De Vivo, B., Belkin, H.E., Lima, A. (Eds.), Environmental Geochemistry (Second Edition). Elsevier, pp. 237–305. https://doi.org/10.1016/B978-0-444-63763-5.00012-4

Dijkstra, J.J., Meeussen, J.C.L., Comans, R.N.J., 2004. Leaching of Heavy Metals from Contaminated Soils: An Experimental and Modeling Study. Environ. Sci. Technol. 38, 4390–4395. https://doi.org/10.1021/es049885v

Drapeau, C., Delolme, C., Chatain, V., Gautier, M., Blanc, D., Benzaazoua, M., Lassabatère, L., 2017. Spatial and Temporal Stability of Major and Trace Element Leaching in Urban Stormwater Sediments. Open Journal of Soil Science 07, 347. https://doi.org/10.4236/ojss.2017.711025

Durce, D., Maes, N., Bruggeman, C., Van Ravestyn, L., 2016. Alteration of the molecular-size-distribution of Boom Clay dissolved organic matter induced by Na+ and Ca2+. Journal of Contaminant Hydrology 185–186, 14–27. https://doi.org/10.1016/j.jconhyd.2015.12.001

Dzombak, D.A., Morel, F.M.M., 1990. Surface Complexation Modeling: Hydrous Ferric Oxide. John Wiley & Sons.

Fang, W., Wei, Y., Liu, J., 2016. Comparative characterization of sewage sludge compost and soil: Heavy metal leaching characteristics. Journal of Hazardous Materials 310, 1–10. https://doi.org/10.1016/j.jhazmat.2016.02.025

Fisher-Power, L.M., Shi, Z., Cheng, T., 2019. Testing the “component additivity” approach for modelling Cu and Zn adsorption to a natural sediment. Chemical Geology 512, 31–42. https://doi.org/10.1016/j.chemgeo.2019.02.038

Golui, D., Datta, S.P., Dwivedi, B.S., Meena, M.C., Trivedi, V.K., 2020. Prediction of free metal ion activity in contaminated soils using WHAM VII, baker soil test and solubility model. Chemosphere 243, 125408. https://doi.org/10.1016/j.chemosphere.2019.125408

Groenenberg, J.E., Dijkstra, J.J., Bonten, L.T.C., de Vries, W., Comans, R.N.J., 2012. Evaluation of the performance and limitations of empirical partition-relations and process based multisurface models to predict trace element solubility in soils. Environmental Pollution 166, 98–107. https://doi.org/10.1016/j.envpol.2012.03.011

Groenenberg, J.E., Lofts, S., 2014. The use of assemblage models to describe trace element partitioning, speciation, and fate: A review. Environmental Toxicology and Chemistry 33, 2181–2196. https://doi.org/10.1002/etc.2642

Grybos, M., Davranche, M., Gruau, G., Petitjean, P., 2007a. Is trace metal release in wetland soils controlled by organic matter mobility or Fe-oxyhydroxides reduction? Journal of Colloid and Interface Science 314, 490–501. https://doi.org/10.1016/j.jcis.2007.04.062

Grybos, M., Davranche, M., Gruau, G., Petitjean, P., 2007b. Is trace metal release in wetland soils controlled by organic matter mobility or Fe-oxyhydroxides reduction? Journal of Colloid and Interface Science 314, 490–501. https://doi.org/10.1016/j.jcis.2007.04.062

Grybos, M., Davranche, M., Gruau, G., Petitjean, P., Pédrot, M., 2009. Increasing pH drives organic matter solubilization from wetland soils under reducing conditions. Geoderma 154, 13–19. https://doi.org/10.1016/j.geoderma.2009.09.001

Gu, S., Gruau, G., Dupas, R., Jeanneau, L., 2020. Evidence of colloids as important phosphorus carriers in natural soil and stream waters in an agricultural catchment. Journal of Environmental Quality 49, 921–932. https://doi.org/10.1002/jeq2.20090

Guénet, H., Davranche, M., Vantelon, D., Gigault, J., Prévost, S., Taché, O., Jaksch, S., Pédrot, M., Dorcet, V., Boutier, A., Jestin, J., 2017. Characterization of iron–organic matter nano-aggregate networks through a combination of SAXS/SANS and XAS analyses: impact on As binding. Environ. Sci.: Nano 4, 938–954. https://doi.org/10.1039/C6EN00589F

Hens, M., Merckx, R., 2002. The role of colloidal particles in the speciation and analysis of “dissolved” phosphorus. Water Research 36, 1483–1492. https://doi.org/10.1016/S0043-1354(01)00349-9

Janot, N., Reiller, P.E., Benedetti, M.F., 2013. Modelling Eu(III) speciation in a Eu(III)/PAHA/α-Al2O3 ternary system. Colloids and Surfaces A: Physicochemical and Engineering Aspects, Special Issue : IAP 2012 435, 9–15. https://doi.org/10.1016/j.colsurfa.2013.02.052

Kania, Manon, Gautier, M., Blanc, D., Lupsea-Toader, M., Merlot, L., Quaresima, M.-C., Gourdon, R., 2019. Leaching behavior of major and trace elements from sludge deposits of a French vertical flow constructed wetland. Science of The Total Environment 649, 544–553. https://doi.org/10.1016/j.scitotenv.2018.08.364

Kania, M., Gautier, M., Imig, A., Michel, P., Gourdon, R., 2019. Comparative characterization of surface sludge deposits from fourteen French Vertical Flow Constructed Wetlands sewage treatment plants using biological, chemical and thermal indices. Science of The Total Environment 647, 464–473. https://doi.org/10.1016/j.scitotenv.2018.07.440

Kim, B., Gautier, M., Michel, P., Gourdon, R., 2013. Physical–chemical characterization of sludge and granular materials from a vertical flow constructed wetland for municipal wastewater treatment. Water Science and Technology 68, 2257–2263. https://doi.org/10.2166/wst.2013.485

Kim, B., Gautier, M., Prost-Boucle, S., Molle, P., Michel, P., Gourdon, R., 2014. Performance evaluation of partially saturated vertical-flow constructed wetland with trickling filter and chemical precipitation for domestic and winery wastewaters treatment. Ecological Engineering 71, 41–47. https://doi.org/10.1016/j.ecoleng.2014.07.045

Kim, B., Gautier, M., Rivard, C., Sanglar, C., Michel, P., Gourdon, R., 2015. Effect of Aging on Phosphorus Speciation in Surface Deposit of a Vertical Flow Constructed Wetland. Environ. Sci. Technol. 49, 4903–4910. https://doi.org/10.1021/es506164v

Kim, B., Gautier, M., Simidoff, A., Sanglar, C., Chatain, V., Michel, P., Gourdon, R., 2016. pH and Eh effects on phosphorus fate in constructed wetland's sludge surface deposit. Journal of Environmental Management 183, 175–181. https://doi.org/10.1016/j.jenvman.2016.08.064

Klinkert, S., Comans, R.N.J., 2020. Geochemical Multisurface Modeling of Reactive Zinc Speciation in Compost as Influenced by Extraction Conditions. Environ. Sci. Technol. 54, 2467–2475. https://doi.org/10.1021/acs.est.9b04104

Krickov, I.V., Pokrovsky, O.S., Manasypov, R.M., Lim, A.G., Shirokova, L.S., Viers, J., 2019. Colloidal transport of carbon and metals by western Siberian rivers during different seasons across a permafrost gradient. Geochimica et Cosmochimica Acta 265, 221–241. https://doi.org/10.1016/j.gca.2019.08.041

Manceau, A., Marcus, M.A., Tamura, N., 2002. Quantitative Speciation of Heavy Metals in Soils and Sediments by Synchrotron X-ray Techniques. Reviews in Mineralogy and Geochemistry 49, 341–428. https://doi.org/10.2138/gsrmg.49.1.341

Marsac, R., Banik, N.L., Lützenkirchen, J., Catrouillet, C., Marquardt, C.M., Johannesson, K.H., 2017. Modeling metal ion-humic substances complexation in highly saline conditions. Applied Geochemistry 79, 52–64. https://doi.org/10.1016/j.apgeochem.2017.02.004

Mikutta, C., Kretzschmar, R., 2011. Spectroscopic Evidence for Ternary Complex Formation between Arsenate and Ferric Iron Complexes of Humic Substances. Environ. Sci. Technol. 45, 9550–9557. https://doi.org/10.1021/es202300w

Milne, C.J., Kinniburgh, D.G., Tipping, E., 2001. Generic NICA-Donnan model parameters for proton binding by humic substances. Environ Sci Technol 35, 2049–2059. https://doi.org/10.1021/es000123j

Molina, F.V., 2016. Soil Colloids: Properties and Ion Binding. CRC Press.

Molle, P., 2013. French vertical flow constructed wetlands: a need of a better understanding of the role of the deposit layer. Water Science and Technology 69, 106–112. https://doi.org/10.2166/wst.2013.561

Paquin, P.R., Gorsuch, J.W., Apte, S., Batley, G.E., Bowles, K.C., Campbell, P.G.C., Delos, C.G., Di Toro, D.M., Dwyer, R.L., Galvez, F., Gensemer, R.W., Goss, G.G., Hogstrand, C., Janssen, C.R., McGeer, J.C., Naddy, R.B., Playle, R.C., Santore, R.C., Schneider, U., Stubblefield, W.A., Wood, C.M., Wu, K.B., 2002. The biotic ligand model: a historical overview. Comparative Biochemistry and Physiology Part C: Toxicology & Pharmacology 133, 3–35. https://doi.org/10.1016/S1532-0456(02)00112-6

Pédrot, M., Boudec, A.L., Davranche, M., Dia, A., Henin, O., 2011. How does organic matter constrain the nature, size and availability of Fe nanoparticles for biological reduction? Journal of Colloid and Interface Science 359, 75–85. https://doi.org/10.1016/j.jcis.2011.03.067

Pédrot, M., Dia, A., Davranche, M., 2009. Double pH control on humic substance-borne trace elements distribution in soil waters as inferred from ultrafiltration. Journal of Colloid and Interface Science 339, 390–403. https://doi.org/10.1016/j.jcis.2009.07.046

Pokrovsky, O.S., Dupré, B., Schott, J., 2005. Fe–Al–organic Colloids Control of Trace Elements in Peat Soil Solutions: Results of Ultrafiltration and Dialysis. Aquat Geochem 11, 241–278. https://doi.org/10.1007/s10498-004-4765-2

Pourret, O., Dia, A., Davranche, M., Gruau, G., Hénin, O., Angée, M., 2007. Organo-colloidal control on major- and trace-element partitioning in shallow groundwaters: Confronting ultrafiltration and modelling. Applied Geochemistry 22, 1568–1582. https://doi.org/10.1016/j.apgeochem.2007.03.022

Qu, C., Chen, W., Hu, X., Cai, P., Chen, C., Yu, X.-Y., Huang, Q., 2019. Heavy metal behaviour at mineral-organo interfaces: Mechanisms, modelling and influence factors. Environment International 131, 104995. https://doi.org/10.1016/j.envint.2019.104995

Rennert, T., Rabus, W., Rinklebe, J., 2017. Modelling the concentrations of dissolved contaminants (Cd, Cu, Ni, Pb, Zn) in floodplain soils. Environ Geochem Health 39, 331–344. https://doi.org/10.1007/s10653-016-9859-4

Sharma, P., Ofner, J., Kappler, A., 2010. Formation of Binary and Ternary Colloids and Dissolved Complexes of Organic Matter, Fe and As. Environ. Sci. Technol. 44, 4479–4485. https://doi.org/10.1021/es100066s

Shi, Z., Allen, H.E., Di Toro, D.M., Lee, S.-Z., Harsh, J.B., 2013. Predicting PbII adsorption on soils: the roles of soil organic matter, cation competition and iron (hydr)oxides. Environ. Chem. 10, 465. https://doi.org/10.1071/EN13153

Tedoldi, D., Chebbo, G., Pierlot, D., Kovacs, Y., Gromaire, M.-C., 2016. Impact of runoff infiltration on contaminant accumulation and transport in the soil/filter media of Sustainable Urban Drainage Systems: A literature review. Science of The Total Environment 569–570, 904–926. https://doi.org/10.1016/j.scitotenv.2016.04.215

Tipping, E., Lofts, S., Sonke, J.E., 2011. Humic Ion-Binding Model VII: a revised parameterisation of cation-binding by humic substances. Environ. Chem. 8, 225. https://doi.org/10.1071/EN11016

Xia, X., Yang, J., Yan, Y., Wang, J., Hu, Y., Zeng, X., 2020. Molecular Sorption Mechanisms of Cr(III) to Organo-Ferrihydrite Coprecipitates Using Synchrotron-Based EXAFS and STXM Techniques. Environ. Sci. Technol. 54, 12989–12997. https://doi.org/10.1021/acs.est.0c02872

Yang, J., Xia, X., Liu, J., Wang, J., Hu, Y., 2020. Molecular Mechanisms of Chromium(III) Immobilization by Organo–Ferrihydrite Co-precipitates: The Significant Roles of Ferrihydrite and Carboxyl. Environ. Sci. Technol. 54, 4820–4828. https://doi.org/10.1021/acs.est.9b06510

Zhu, B., Liao, Q., Zhao, X., Gu, X., Gu, C., 2018. A multi-surface model to predict Cd phytoavailability to wheat (Triticum aestivum L.). Science of The Total Environment 630, 1374–1380. https://doi.org/10.1016/j.scitotenv.2018.03.002

ARTICLE 4

Coupled organic-mineral geochemical modelling of the leaching behaviour of major and trace metals from stormwater infiltration basin sediments.

Banc, C. [*], Gautier, M. [*], Blanc, D. [*], Lupsea-Toader, M. [*], Drapeau, C[***]., Zhan, Q. [*], Lassabatère, L. [**], Delolme, C.[**], Chatain V. [*], Gourdon, R. [*]

[*] Univ Lyon, INSA Lyon, DEEP, EA7429, 69621 Villeurbanne, France.

[**] Univ Lyon, ENTPE, LEHNA, 69120 Vaulx-en-Velin, France.

[***] Direction Régionale de L'environnement, de L'aménagement et du Logement (DREAL), Auvergne Rhône-Alpes, Unité Départementale du Rhône, 63 Avenue Roger Salengro, 69100 Villeurbanne, France

Abbreviation

IB: infiltration basin

NBS: nature-based solution

DOM: dissolved organic matter

SOM: solid organic matter

1. Introduction

The progressive urbanization of the landscape in response to the increase of human population induces the growing of impervious surface cover (Gong et al., 2019; Trusilova et al., 2009). Consequently, stormwater infiltration in soils is affected and increases surface runoff. It is well known that during its runoff, stormwater is a vector of accumulation and transport of pollutants, such as trace metals, pesticides, organic residues, and nutrients produce by human activities (Aryal et al., 2010; Chen et al., 2019b; Hallberg et al., 2007; Treilles et al., 2021; Zhang et al., 2011). Nature Based Solutions (NBS) are promoted as an effective approach for urban runoff or stormwater sustainable management (Faivre et al., 2017; Maes and Jacobs, 2017). Among these technics, infiltration basins (IB) can provide several ecosystem services such as buffer the flow of stormwater discharge, improve water quality discharge into groundwater and also promote the development of fauna and flora in urbanized area (Bonneau et al., 2017; Natarajan and Davis, 2015; Tedoldi et al., 2016b). Improving water quality implies to retain a maximum of pollutants in the NBS and then to also control the fate of retained pollutants in the structure. The retention of suspended solids and potentially associated pollutants transported with stormwater generates the formation of a sediment known to concentrate organic matter and important content in pollutants such as trace metals (Clozel et al., 2006b; Drapeau et al., 2017; Zhu et al., 2020). Among trace metals, because of their important concentration in the SD and their potential toxicity, Cr, Cu, Zn and Pb are more largely monitored (Clozel et al., 2006b; Drapeau et al., 2017; Tedoldi et al., 2016b). The remobilization of trace metals through the sediment, associated or not with organic/mineral carrier phases is a major threat for the released water quality (Mermillod-Blondin et al., 2015; Tedoldi et al., 2016b).

The risk assessment of polluted porous media such as sediment or soil is more complex than a unique measure of the total content in a pollutant. The influence of some chemical parameters (*i.e.* pH, pE, conductivity) on the distribution of pollutants between dissolved and solid phases and their speciation are important parameters to evaluate the potential release, transport and biodisponibility of a pollutant (Allen et al., 2001; Sauvé et al., 2003; Sigg, 2014). In porous media, the remobilization of

organic matter and metal oxides, retained in the solid fraction, is known to promote the release of element usually hardly soluble (Gangloff et al., 2016; Pokrovsky et al., 2005; Pourret et al., 2007a). To better describe, understand and predict the geochemical remobilization and speciation of pollutants in porous media, geochemical multisurface model have been used in numerous studies (Almås et al., 2007b; Dijkstra et al., 2009; Fang et al., 2016b; Klinkert and Comans, 2020).

Geochemical multisurface models are a combination of "mechanistic" models describing the different chemical interactions that inorganic contaminants may encounter in its environment such as sorption to metal oxides and organic matter (Dijkstra et al., 2009). Some of these mechanistic models integrate generic complexation parameters (*e.g.* Dzombak and Morel, 1990; Tipping et al., 2011) derived for large environmental conditions like pH conditions and various loading in major and trace elements.

So far multisurface model dedicated to IB sediment mainly focus on precipitates and ion-binding to oxides (Drapeau, 2018) without incorporating generic model to model ion-binding to OM. In this study, a multisurface model dedicated to stormwater IB sediment was developed in order to predict the pH-dependent solubilization and speciation of major (Al, Ca, Fe, P, S, Si) and trace elements (Cu, Cr, Pb, Zn). This multisurface model integrates all the relevant geochemical process controlling the release of ions to solution such as complexation to organic matter and oxides, and also includes ion precipitation. The sediment has been submitted to a wide range of pH conditions using batch-titration process. Calculated and measured concentration were compared as a function of pH conditions. The results obtained from the optimized model will be used to discuss the influence of pH on the solid-solution distribution and speciation of trace contaminants presented above.

2. Materials and methods

2.1. Sediment characterization

The sample were collected in the Django Reinhardt infiltration basin located in the East suburb of Lyon. Stormwaters collected over an industrial catchment of 185 hectares are discharged in a previous settling basin designed to retain as much as possible suspended solids before routing the stormwater to the infiltration basin (Drapeau et al., 2017). Since 2012, infiltration of the stormwater generated a sediment of several centimeters whose whole thickness have been collected in several representative spot. The samples were manually sorted in order to remove stones and roots, homogenized, lyophilized and then stored at 4 °C before experiments.

The lyophilized sediment thus prepared were analyzed for their total contents in a series of elements. The powdered samples (200 mg) were suspended through alkaline fusion with $LiBO_2$ in a tunnel oven

at 980 °C. After cooling, the sample was dissolved in a 0.5N HNO3 solution. Major elements analysis was performed using ICP-OES iCap6500 ThermoFisher after 2-fold dilution in 2% HNO3 aqueous solution. Trace elements were quantified with ICP-MS iCapQ ThermoFisher after 2-fold dilution in 2% HNO3 aqueous solution. Results are given in Table 1.

Table 1. Elemental composition of the IB sediment.

OM	Ca	Al	Fe	Si	S	P	Zn	Cu	Cr	Pb
%	$g.kg^{-1}$						$mg.kg^{-1}$			
26.5	54.3	42.3	32.9	201.3	2.2	2.3	1975	286	178	162

2.2. pH-dependency leaching test

A batch leaching test, based on the CENTS/TS 14429 European standard, was conducted to evaluate the effect of pH on the release major and trace elements, and OM from the IB sediment. All assays were duplicated and performed in Nalgene® polypropylene centrifuge tubes, at a solid-to-liquid ratio of 100 g of SD dry matter per liter of leaching solution. Prior to the tests, all tubes were soaked in 1 M HCl aqueous solution overnight and then rinsed with deionized water. The SD samples were stirred with: (i) deionized water for natural pH conditions, (ii) nitric acid aqueous solutions for acidic conditions and (iii) potassium hydroxide aqueous solution for alkaline conditions. The number of moles of protons (acidic solutions) or hydroxide ions (alkaline solutions) in each leaching solution was calculated as the product of HNO3 or KOH concentrations by the volumes of solution used in each assay. All assays and blank were stirred at room temperature in a rotary shaker set at 9 rpm for 48H. pH and pE were measured before being filtred with Consort C3020 equipped with Bioblock 11706358 and Metlerlabo PAM202 equipped with Ag/AgCl electrode, respectively.

The suspensions obtained from the batch leaching experiments described above at the different pHs tested were centrifuged at 4000 rpm (2400 g) and the supernatants were filtered at 0.45 µm using Sartorius cellulose acetate filters to separate the solid (>0.45 µm) and the dissolved fraction (<0.45 µm). Finally, dissolved organic carbon (dissolved OC), major (Ca, Si, S, Fe, Al, P) and trace (Cr, Cu, Zn, Pb) elements were measured. Major and trace elements concentration in each filtrate were determined using ICP-AES analyzer. Dissolved OC was measured using a Shimadzu TOC-5050A.

2.3. Model description

Mineral phases. The solubility of major elements (Ca, Fe, Al, P, Si, S) is controlled by mineral phases described in Table 2. These phases were found to be the major mineral phases present in the tested SD samples (Drapeau et al., 2017). Among these phases only, amorphous $Fe(OH)_3$ and $Al(OH)_3$, further called HFO and HAO respectively, were allowed to precipitate. Similar to Dijkstra et al. (2009) HFO and HAO sorption capacity was modelled using the Generalized Two Layer Model (GTLM) of Dzombak and Morel (Dzombak and Morel, 1990). The oxides surface is composed by strong and weak monodentate amphoteric hydroxyl groups able to bind cations. Electrostatic fields around the charged oxides affects the intrinsic ionic sorption properties and also through non-specific interaction inside a diffuse (Gouy-Chapman) layer. Total amount of HFO and HAO reactive sites was automatically adjusted to the amount of precipitated HFO and HAO assuming specific surface area of 600 $m^2.g^{-1}$ of precipitated amorphous oxides. The amount of chemically reactive surface is set as define by Dzombak and Morel (1990): 0.2 mol of weak and 0.005 mol of strong binding sites per mol of precipitated HFO/HAO.

Table 2. Description of the mineral phases found in the SD according to results obtained by Drapeau et al. (2017) and used to model major elements solubility.

Mineral phase	Formula	Solubility constant
Albite	$NaAlSi_3O_8$	2.7
Calcite	$CaCO_3$	1.8
Chamosite	$Fe_2Al_2SiO_5(OH)_4$	32.8
HAO	$Al(OH)_3$	0.2
HFO	$Fe(OH)_3$	2.0
Illite	$K_{0.6}Mg_{0.25}Al_{1.8}Al_{0.5}Si_{3.5}O_{10}(OH)_2$	9.0
Pyrite	FeS_2	-24.6
Quartz	SiO_2	-3.9

Organic matter binding capacity. The sorption capacity of Dissolved and Solid Organic Matter (DOM and SOM, respectively) was modeled using Humic Ion-Binding Model VII described by Tipping et al, 2011. Model VII considers two types of cation binding to humic acids (HA) and fulvic acids (FA): (i) a specific binding involving a discrete binding sites distribution and (ii) a non-specific binding considered to occur through electrostatic accumulation of counter-ion in a Donnan volume surrounding the molecular surface and inversely proportional to the ionic strength of the solution. A total of 50 binding sites are described in Model VII, allowing to consider the heterogeneity of humic substances binding

capacity. These sites were described as composed of 4 carboxylic (type A sites) and 4 phenolic (type B sites) sites allowing them to form bidentate and tridentate recombination. Only the aqueous cations and their first hydrolysis product are likely to bind to HA and FA. The intrinsic equilibrium constants for cations binding to monodentate type A or B sites are described by two parameters log K_{MA} and log K_{MB}, respectively. These parameters are calculated as follow:

$$\log K_{MB} = \log K_{MA} \times \frac{pK_B}{pK_A}$$

In the previous equation pK_A and pK_B describe the intrinsic protonation constants for type A and type B sites, respectively.

Equilibrium constants for cations binding to bidentate or tridentate sites are defined as the sum of the log K of the monodentate sites constituting the multidentate site considered. The range of the metal binding strengths is also modulated by an empirical parameter called ΔLK_2 generating moderate and strong binding sites and by an electrostatic correction of charge development resulting from ion binding and release (Almas et al., 2007; Tipping et al., 2011). Non-specific ions accumulation in the Donnan volume surrounding humic molecules was neglected here, considering the high OM content and high concentration in background electrolyte (Bonten et al., 2008). The default binding constants from (Tipping et al, 2011) were not adjusted.

Model inputs. All the aqueous geochemical calculations were performed with PHREEQC-V3 software. The thermodynamic data which was used for the simulations comes from Lawrence Livermore National Laboratory (LLNL database). The input of the model consisted in several parameters concerning the SD physico-chemical characterization and the chemistry of the liquid, as follows:

1. pH and pE fixed according to values measured in the various solutions;
2. total content of the SD, in Zn, Cu, Cr, P, Pb determined by alkaline fusion (see § 2.1);
3. mineral phases controlling the solubility of major elements Fe, Al, Ca, Si and S further described in Table 2. These phases were already observed in IB sediments (Drapeau et al., 2017);
4. precipitate HFO and HAO for their sorption capacity
5. the cations binding capacity of the organic matter described following the two methodologies already presented. The cations binding capacity of the organic matter described in Model VII was implemented in PHREEQC using a Constant Capacitance Model following the methodology developed in Marsac et al. (2017).

Differences between the 3-model setup tested in this study are summarized in Table 3 and further described below:

Model setup I: The first multisurface model incorporates sorption to solid organic matter (SOM). Ion-binding to dissolved organic matter (DOM) is not considered in this first model setup. The quantity of strong and weak binding site used to model ion-binding to SOM remain constant over the tested pH range and is define previously in Drapeau (2018) as 0.06 and 0.08 mol for strong and weak binding site, respectively. Major and trace elements sorption to solid HFO and HAO is modeled using the GTLM (Dzombak and Morel, 1990).

Model setup II: This multisurface model incorporate sorption to solid HFO and HAO, SOM and DOM. Solid and dissolved OM sorption capacity is modeled using Model VII with reactive fraction used by Banc et *al.,* 2021 to model ion-binding to OM from constructed wetlands' sludge deposit. The SOM concentration have been calculated by subtracting to the total amount of OM introduced to the amount of DOM at each pH values.

Model setup III: Surfaces implemented in Model setup II are used and in addition in this model major and trace elements are able to be sorbed by released HFO. The same generic parameters for both released and solid HFO was used. The amount of HFO in the leached fraction have been calculated as the differences between the calculated concentration of Fe and the measured Fe concentration. When this amount is positive (Fe calculated < Fe measured) the corresponding amount of mol of HFO is considered as released.

Table 3. Description of the reactive surface and submodel used to model their reactivity in the three-model setups tested.

	Inputs	Mineral surface	Organic surface	Submodel
Model setup I	pH, pE, total content of major and trace elements	Solid HFO and HAO	SOM 0.06 mol of strong site 0.08 mol of weak site	SOM and DOM: from Drapeau, 2018 HFO/HAO: GTLM (Dzombak and Morel, 1990)
Model setup II	pH, pE, total content of major and trace elements	Solid HFO and HAO	SOM: 100% of measured content: 50-50 HA/FA DOM adapted from Banc et al., 2021	OM: MODELVII (Tipping et al., 2011) HFO/HAO: GTLM (Dzombak and Morel, 1990)
Model setup III	pH, pE, total content of major and trace elements	Solid HFO and HAO Colloidal HFO	SOM: 100% of measured content: 50-50 HA/FA DOM adapted from Banc et al., 2021	OM: MODELVII (Tipping et al., 2011) HFO/HAO: GTLM (Dzombak and Morel, 1990)

3. Results and discussion

3.1 pH-dependent leaching of major elements and trace metals

The measured concentration of DOC, major elements (Al, Ca, Fe, Mg, P, S, Si) and trace metals (Cu, Cr, Pb, Zn) are presented in Fig. 1. The minimum DOC concentration is measured for pH~7 representing the solution extracted with deionized water. DOC concentration increased considerably with progressive alkalization of the solutions until 30% of the total content in OC is released at pH 12. This phenomenon has been previously considered to be the result of the desorption of organic matter from solid organo-mineral association (Grybos et al., 2009a) leading to the release of high molecular weight organic molecules with increasing aromaticity (Banc et al., 2021; Wang et al., 2019). In a lesser extent, with acidification of the solution important increases in DOC concentrations were also measured in the SD solutions. In solid deposit from constructed wetlands, the molecules released under acidic conditions were mostly low molecular weight organics (Banc et al., 2021; Pédrot et al., 2009b). Major elements and trace metals solubility also strongly varied within the pH range. Dissolved Al and Fe varied up to 4 orders of magnitude, P and Ca within 3 orders of magnitude, Si and S by up to 2 orders of magnitude, trace metals by up to 3 orders of magnitude. Maximum leaching concentrations for Al, Ca, Fe and P is measured for acidic conditions with approximately 10, 75, 16 and 29% of the total content, respectively. Si and S are more sensible to alkaline conditions as maximum concentration is measured for pH 12 representing 0.7 and 42% of the total content. As observed in extract from soil solutions (Dijkstra et al., 2004) or sludge deposit from constructed wetlands (Kania et al., 2019), trace metals are more largely solubilized under acidic conditions. Zn and Cu being almost totally released in solution with 99 and 90% of the total content while Cr and Pb solubilization reach 17 and 78% of the total content.

These trends could be used as indicator of the preferential mechanism involved in the retention or the released of the considered trace metals. The large amount of Zn, Cu and Pb released under acidic conditions could suggest that these elements are in competition with proton for organic or mineral specific binding sites (Almas et al., 2007). The increase of solubility observed under alkaline conditions for these metals and more specifically for Cu may be attributed to the solubilization of organic matter and associated elements. Other the entire pH range, correlation coefficient between trace metals concentrations and DOC are relatively low suggesting low impact of DOC complexation - correlation coefficient for Cu, Zn Pb and Cr were 0.48, -0.03, -0.08, 0.07, respectively. However, for pH>7, these correlation coefficient increase highlighting the relative importance of DOC complexation in the released of trace metals - correlation coefficient for Cu, Zn, Pb, and Cr were 0.91, 0.81, 0.78, 0.90, respectively.

3.1. Response of the tested model setup vs experimental data

Figure 1 presents the measured concentrations obtained during the leaching tests and the simulated concentrations obtained with the three model setups (as described in section 2.3) as a function of pH, for major elements (Al, Ca, Fe, P, S, Si) and trace metals (Cr, Cu, Pb, Zn). The results obtained from the three approaches are discussed below.

3.2.1 Model setup I: simple implementation of the ion-binding to OM

Model setup I consider, besides the chemical mechanisms governed by the mineral assemblage (*i.e.* precipitation/dissolution and ion binding to Al/Fe oxides), ion binding to SOM contained in the SD. As shown in Fig. 1, model setup I globally fails to provide satisfactory results, despite several optimization steps concerning the parameters describing the sorption of metals onto OM (complexation constants, OM site density…). The best predictions obtained with this model are for Al, Ca, Si, S, as the leaching behavior of these elements is mainly controlled by the dissolution and precipitation of mineral phases. P solubilization is not controlled by mineral phases but by adsorption/desorption on HFO and HAO. Its solubilization increase gradually from acidic to alkaline conditions. The important quantity of precipitated HFO and their positive surface charge under acidic conditions induce strong complexation rates of P and thus, reduce the calculated concentration of P. On the other hand, increasing pH conditions induce an increase of the electronegativity of the HFO surface (Schwertmann and Taylor, 1989) reducing their affinity for P, increasing the release of P. Compared to major elements, trace metals solubilization is only controlled by complexation on OM and metal oxides as the formation of trace metals precipitates was not included in this first model setup. As shown in Fig. 1, the calculated concentrations of trace metals are globally overestimated for pH<8 and underestimated for pH>8. As observed with the correlation coefficient between DOC and trace metals, as well as in modeling studies of porous media (Almas et al., 2007; Dijkstra et al., 2004; Fang et al., 2016b) the solubilization of OM under alkaline conditions and the associated trace metals is greatly responsible for the solubilization of trace metals. However, in this first model setup, complexation of trace metals to DOM is not considered. Likewise, complexation of trace metals to SOM is not sufficient to reduce their solubilization under more acidic conditions. Thus, complexation constants between OM and cations used in this model setup fail to model ion binding to OM. Previous study using these thermodynamic constants for ion-binding to OM (Drapeau, 2018) had obtained good results (Thermodynamic constants available in supplementary materials). In the latter study, calculated complexation rate of trace metals to OM is low, trace metals solubilization is mainly controlled by precipitation and dissolution of mineral phases containing these elements. Including the formation of trace metals precipitates in the model setup I is possible. But this requires knowledge of the mineral phases present

in the sample and adequate thermodynamic constants not always disponible (Bonten et al., 2008). Thus, in this first model setup, the decision was made not to add precipitates as XRD results do not evidenced their presence (Drapeau et al., 2017). These results motivate the use of generic Model VII to model ion binding to OM.

3.2.2 Model setup II: ion binding to OM with Model VII

Previous modelling studies using Model VII as ion-binding model evidenced the need to modulate the quantity of reactive solid and dissolved OM (Amery et al., 2008; Golui et al., 2020b; Watmough and Orlovskaya, 2015). This modulation is an essential pre-requisite to adapt the reactivity of HA and FA described in Model VII to HA and FA from the modelled sample. Depending on the studies, the reactive fraction could be modulated either according to the measured physico-chemical characteristic of the OM contained in the samples (Fang et al., 2016b; Van Eynde et al., 2020) or according to information from the literature (Shi et al., 2020; Zhang et al., 2014). In this study information on the physico-chemical characteristics of the OM is not available. Banc et al. (2021), using similar modeling strategy on sludge desposit originating from constructed wetlands, evidenced the need to consider 100% of the measured solid OM as reactive and to adjust the reactive dissolved OM as function of pH conditions. The same modulation of the solid and dissolved OM used in Banc et al. (2021) was applied in this study and as shown in Fig. 1, significantly reduce the discrepancy between measured and calculated concentration of major elements and trace metals.

Ion-binding to SOM improved modeling calculation for acidic and near neutral conditions by reducing the leached content in most major elements and trace metals. Globally, under alkaline conditions, ion-binding to DOM increase the leaching content of cationic elements reducing discrepancy between measured and calculated concentrations. In this multisurface model, Si and S leaching content is independent of the OM binding capacity. The solubility of these two elements is mainly controlled by the dissolution of the mineral phases described in Table 2. Despite P complexation to OM was not included in this study, model setup II improves the calculation of P solubilization under acidic conditions. Indeed, OM by complexing Fe and Al ions reduce the amount of precipitated HFO/HAO which as consequence increase the solubilization of P. Over the entire pH range, but more importantly for alkaline conditions, despite possible complexation to DOM, Fe concentration remain largely underestimated by modeling calculations. This result could be attributed to the release of colloidal Fe-oxides from the infiltration basins SD. Integration of this phenomenon to the multisurface model will be tested in model setup III, described in the following paragraph. As observed in Fig.1, in model setup II, Pb and P concentration remain underestimated for near neutral to more alkaline conditions. Interestingly, these two elements are known for their important affinity for oxide binding sites (Baken

et al., 2016; Gu et al., 2020; Shi et al., 2013b). By integrating the remobilization of colloidal Fe-oxides, the amount of released P and Pb should increase and reduce discrepancy between measured and calculated concentrations.

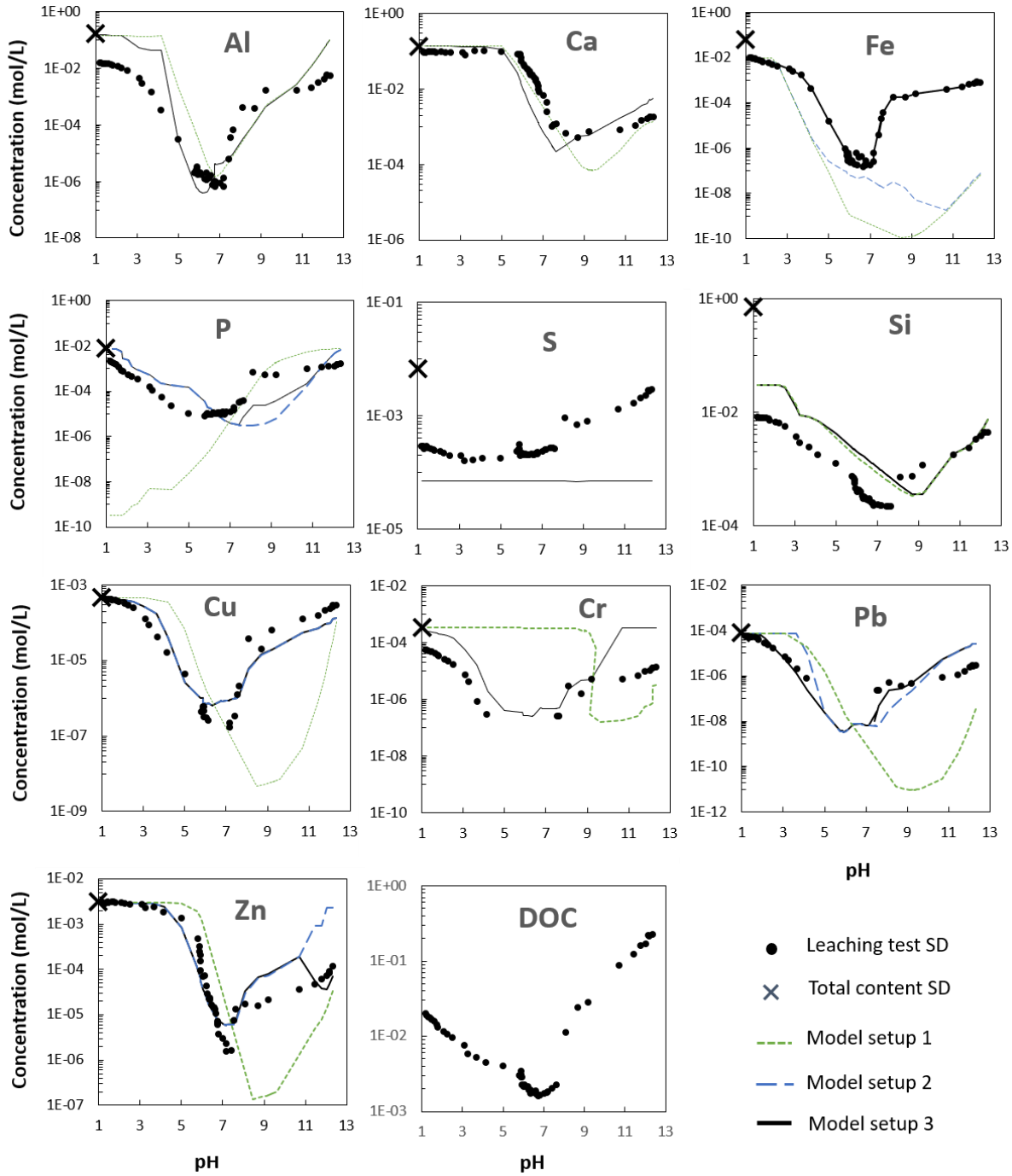

Fig.1: Element concentration (Al, Ca, Fe, P, S, Si, Cu, Cr, Pb, Zn and DOC) measured (points) during the leaching test and the element calculated concentration (line and dotted lines) as a function of pH.

3.3 Model setup III: evidence of the release of colloidal HFO

The construction of model setup III assumes that colloidal HFO are released from IB sediment in solution. The remobilization of colloidal metal oxides from soil has been evidenced in numerous studies (Pédrot et al., 2009b; Pokrovsky et al., 2005; Pokrovsky and Schott, 2002a). Such remobilization, associated or not with the release of OM, impact the mobility of many elements in soil waters. Previous modelling study (Almas et al., 2007; Tipping et al., 2003) allowed Al and Fe oxides to precipitate in various soil extract. To verify this assumption, saturations indices were calculated for $Fe(OH)_3$ based on the Fe concentration measured in the solution. With low solubility product of 2.5, used for aged $Fe(OH)_3$ in Tipping et al. (2003), almost all the solutions were oversaturated with respect to $Fe(OH)_3$ suggesting that part of the released Fe is under colloidal $Fe(OH)_3$ form. As shown in Fig. 1, the calculated concentration of P and Pb have been improved by considering the release of colloidal HFO. Other trace metals calculated concentrations are less impacted by model setup III, these elements being more largely complexed by OM.

As observed in model setup II, Pb concentrations were overestimated in the acidic pH range. By allowing $PbHPO_4$ to precipitates modeling concentration were improved. In soil samples, Pb phosphate phases are known to control Pb leaching in acidic conditions (Santillan-Medrano and Jurinak, 1975). Similarly, precipitation of $Zn(OH)_2$ under very alkaline conditions improved modeling calculation.

3.4 Performances of model setup III in calculating solid-solution distribution of trace metals

The logarithmic root mean squared errors ($RMSE_{log}$) and the mean-error (ME) have been calculated for the 4 trace metals (see table 4). The $RMSE_{log}$ is used as an indicator of the modeling performances and the ME is used as an indicator of the overestimation (ME>0) or underestimation (ME<0) of the predicted concentration. $RMSE_{log}$ and ME have been calculated for pH above and below pH 7.5 corresponding to pH of the solution extracted with deionized waters.

Table 4: Logarithmic root mean squared errors (RMSEs) and mean error (ME) between measured and calculated concentrations performed with model setup III above and below pH 7.5 for the Cr, Cu, Pb and Zn.

		Cr	Cu	Pb	Zn
$RMSE_{log}$	pH<7.5	0.86	0.39	0.35	0.43
	pH>7.5	1.19	0.40	0.79	0.40
ME	pH<7.5	0.71	0.17	-0.04	-0.12
	pH>7.5	0.97	-0.29	0.39	0.09

Table 4 confirms that model setup III is able to reproduce the concentration of 4 most concentrated trace metals of IB sediment (Badin, 2009; Clozel et al., 2006b; Drapeau et al., 2017) as calculated concentrations deviate for less than 1 order of magnitude compare to measured concentrations. The best calculated concentrations are obtained for Cu, Zn and Pb. According to Table 1, the quality of the model predictions is not influenced by pH conditions despite the large pH range and the consequent large variation of released concentrations already discuss. This multisurface model could thus be used to calculate the remobilization of trace metals from infiltration basin's SD submitted to natural and extreme pH conditions. Despite the improvement of the Cr concentration prediction with model setup II and III compared to model setup I, Cr calculated concentration remain overestimated, especially for alkaline pH. It is possible that a fraction of the Cr is normally precipitated in the recalcitrant fraction but tested precipitates do not give satisfactory results. Cr(III) is the only oxidation states that can be complexed by OM using Model VII (Tipping et al., 2011). However, under our pH-pE conditions, the Cr(V) and Cr(VI) forms are mainly released for pH>8. Two mechanisms of sorption of anionic Cr forms to OM, not integrated in ModelVII can be considered: (i) indirect sorption through cationic or metal oxide bridging (Gorny et al., 2016; Redman et al., 2002); and (ii) direct sorption of anionic Cr species on positively charged amino groups composing OM under acidic conditions (Park et al., 2008).

3.5 Influence of pH on the chemical speciation

According to modeling calculation obtained with model setup III, major elements and trace metals speciation in the solid and soluble phases are printed in Fig. 2. The percentage of each phase is printed as function of pH conditions. To clearly identified the speciation of these elements in the soluble phases, the distribution of major elements and trace metals between DOM, small inorganic species (*i.e.* comprising free ionic forms plus inorganic complex) and released Fe-oxides are displayed on Fig. 3.

3.5.1 Role of SOM, oxides and precipitates in the retention of major elements and trace metals

Major elements and trace metals speciation in the solid fraction largely depend on the considered elements and on the pH-conditions. Mineral phases precipitation largely controls the solubilization of Al, Ca and Fe. Calculation also evidenced the fundamental role of oxides in the retention of P in the solid fraction. The complexation to organic matter also contributes to the retention of these elements and particularly for Ca of which 20% is complexed to SOM at pH 8.

Trace metals are largely retained in the organic part of the solid fraction for most of the pH range. As also evidenced by Dijkstra et al. (2009) in various soil samples, precipitates also contribute to limit the

solubilization of elements, in this study Pb and Zn. Non-negligible proportion of trace metals are complexed to oxides for near neutral to more alkaline conditions. Approximately 20% of Cu and Zn are complexed to oxides for pH 8 while 90% of Pb is complexed to these surfaces. The preferential sorption of Pb to oxides surface compare to other trace metals have been also evidenced in soil and compost (Dijkstra et al., 2009; Fang et al., 2016b).

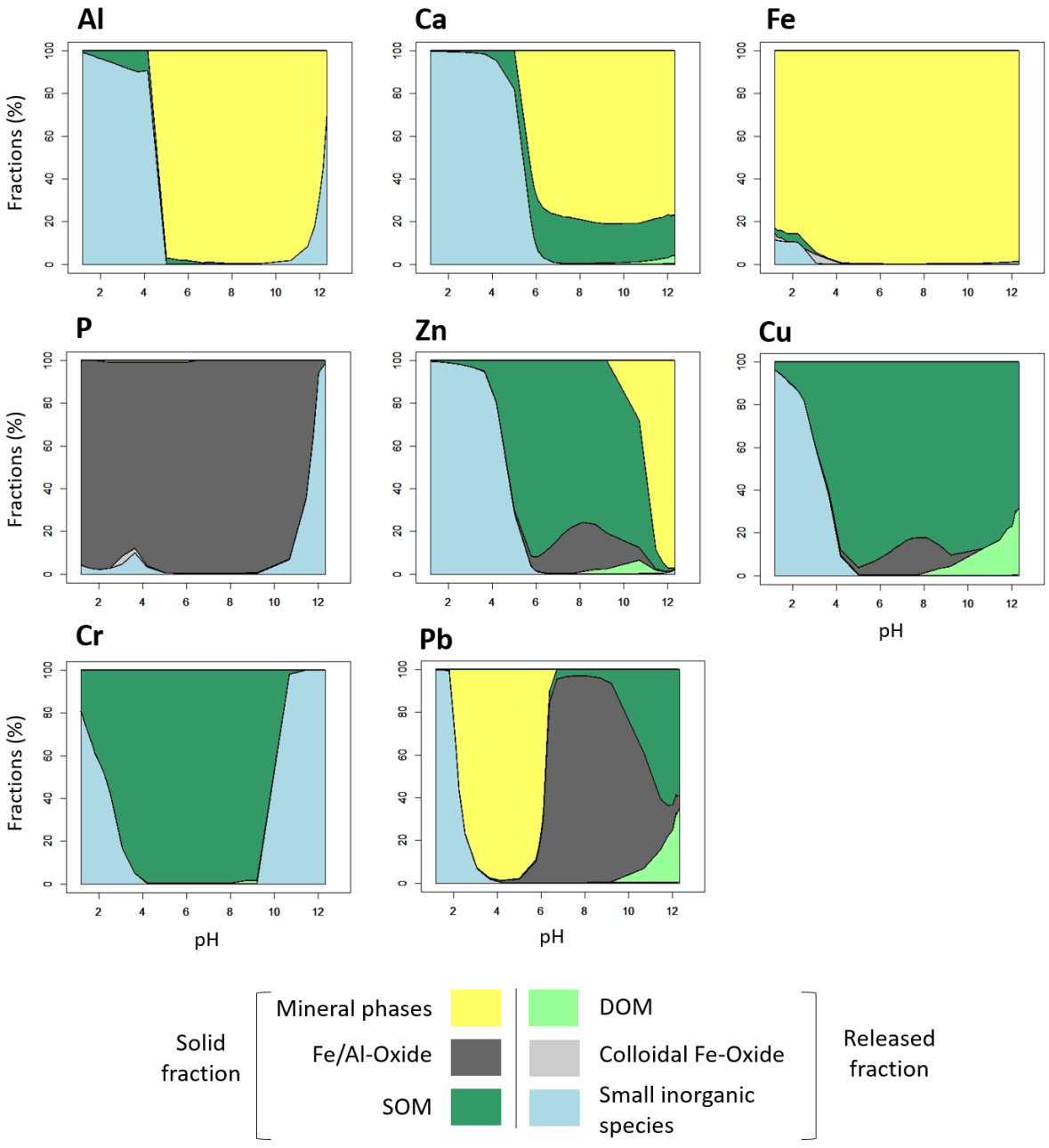

Fig.2: Distribution of major and trace elements in the particulate and released fractions. In the solid fraction elements could be precipitated (mineral phases such as $CaCO_3(s)$) or complexed to oxides (Fe/Al-oxides) and organic matter (SOM). In the released fraction, elements could be complexed to released organics (DOM) and colloidal oxides (Fe-oxides) or present as inorganic complex such as OH species and free ions such as Cu^{2+}, Pb^{2+} (Small inorganic species).

3.5.2 Role of DOM and oxides on the release of major elements and trace metals

Fig. 3 provides a detailed view of the speciation of the species in the released fraction only. The remobilization of Fe-oxides is largely controlling the releasing of Fe from SD of infiltration basin according to Fig. 3 and in accordance with previous modeling studies on soil solutions (Almas et al., 2007; Tipping et al., 2011). This phenomenon impacts the speciation of P in the soluble fraction. Indeed, from pH 7 to pH 10, P is mainly associated to Fe-oxides in solution. The role of Fe-oxides in the remobilization of P from soil samples have been also evidenced in natural soil samples (Baken et al., 2016; Gu et al., 2020). Similarly, remobilization of colloidal Fe-oxides favors the releasing of Pb. Once again, the process controlling the transfer of Pb are similar to those observed in soil solution (Pédrot et al., 2009b; Pokrovsky and Schott, 2002a). As shown in Fig. 3, other trace metals are largely complexed to DOM for pH>6. Among trace metals, Cu and Cr are more largely released associated with DOM as observed in several modeling studies (Dijkstra et al., 2004; Fang et al., 2016b). Indeed, for pH>5 the DOM-bound forms of Cu and Cr are preponderant while for other trace metals DOM complexation is predominant for pH>6. For high alkaline conditions, Cr(VI) is calculated as the main Cr species with no possible complexation to DOM explaining the large release of Cr as small inorganic species. For more acidic conditions, due to strong protonic competition for specific organic binding sites, trace metals are released as small inorganic species known to be more bioavailable compare to DOM-bound form for example (Aiken et al., 2011).

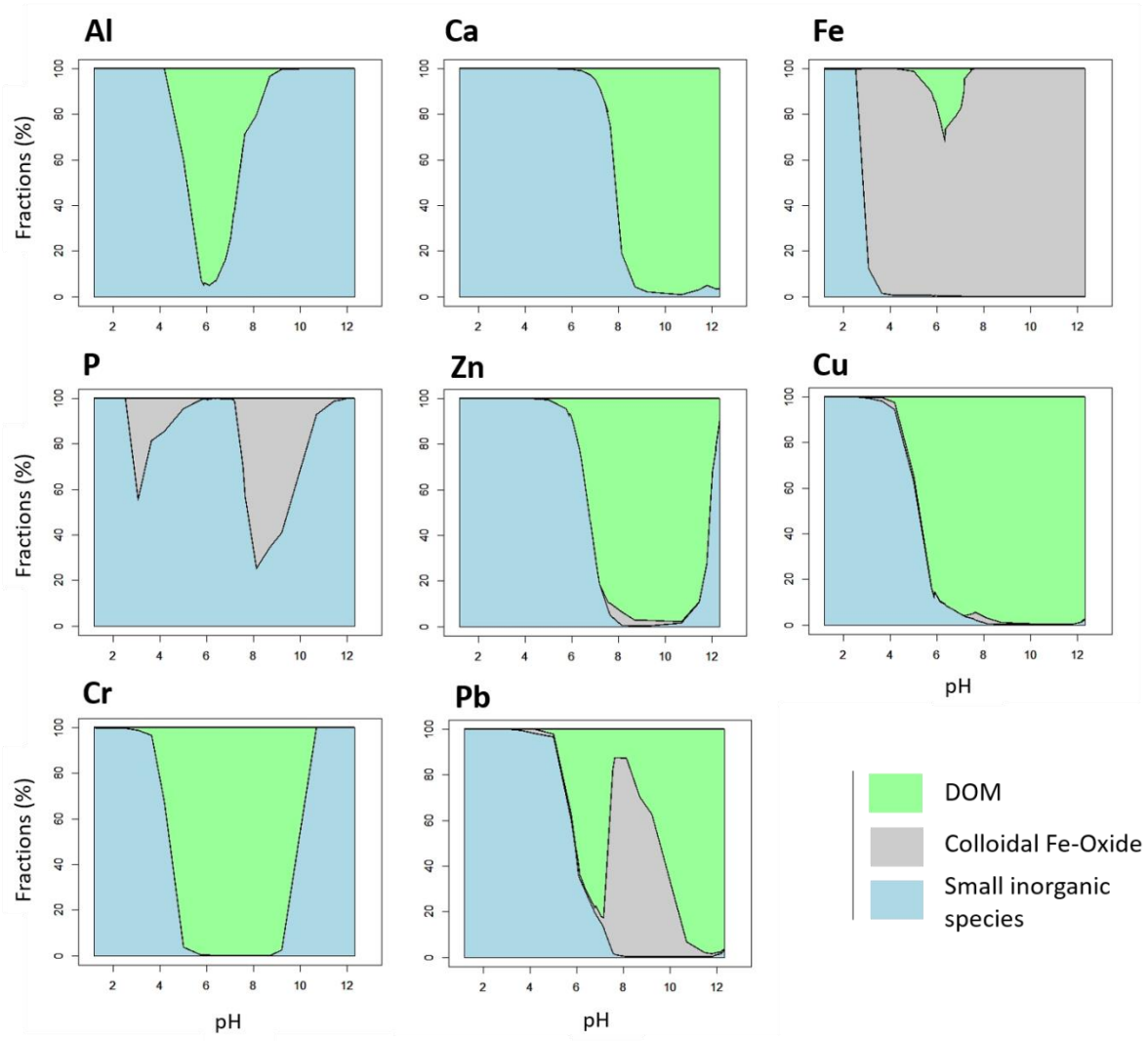

Fig.3: Focus on the major and trace elements speciation in the released fractions. In the released fraction, elements could be complexed to released organics (DOM) and colloidal oxides (Fe-oxides) or present as inorganic complex such as OH species and free ions such as Cu^{2+}, Pb^{2+} (Small inorganic species).

4. Conclusion

The aim of this study was to calibrate a multisurface model in order to produce a tool able to calculate trace metals release and speciation that can be used in the management of environmental risks associated to IB sediments. Two different way to model ion-binding to OM have been tested in multisurface modeling of pH-dependent solubilization of major elements and trace metals. In model setup I, ion-binding to OM have been modelled according to the strategy already used by Drapeau (2018) in multisurface modelling of SD originating from the same infiltration basins. Due to low complexation rates of trace metals to OM, model fail to calculate solubilization of these elements. These results led the authors of the present study to test the use of ModelVII to model ion binding to

OM. The discrepancy between calculated and measured concentration drastically reduce. Integration of the possible release of colloidal Fe-oxides, and the formation of Zn and Pb precipitates also improve model calculation.

OM and Fe/Al-oxides largely contribute to the retention of trace metals in the solid fraction of the sediment. However, attention should be paid to their remobilization from the solid fraction. Indeed, the remobilization of OM and Fe-oxide contribute to the release of associated elements. In this study, the remobilization of OM and Fe-oxides were induced by pH variations but change in the IB's hydrological regime due to varying storm event could also promote the remobilization of such carrier phases (C. Wang et al., 2020). Trace metals speciation affecting their transfer and mobility from the IB sediment to related aquifer (Tedoldi et al., 2016b; Zhu et al., 2020) the multisurface model developed in this study could be reused in reactive transport modeling.

Overall, this study showed that without any optimization of the chemical equilibrium parameters described in the models used in the multisurface model, the solubilization of major element and trace metals was adequately predicted. The quantity of reactive Fe/Al-oxides surface, usually based on various extraction procedure (Di Bonito et al., 2018), were based on Fe and Al total content in this study. Similarly, implementation of reactive fraction of solid and dissolved organic surface were based on measured content and reactive ratio from Banc et al. (2021). This implies, that this multisurface model could be reused for other SD originating from infiltration basins by adjusting total content in major elements and trace metals to the considered sample. The principal constraint of this model is the need to adequately implement the DOM concentration within pH variations. Further studies could be performed to correlate the DOM content to physico-chemical characteristics of the solid samples such as total content in OM in order to deduce DOM content thanks to total OM content.

Literature cited

Aiken, G.R., Hsu-Kim, H., Ryan, J.N., 2011. Influence of Dissolved Organic Matter on the Environmental Fate of Metals, Nanoparticles, and Colloids. Environ. Sci. Technol. 45, 3196–3201. https://doi.org/10.1021/es103992s

Allen, H.E., McGrath, S.P., McLaughlin, M.J., Peijnenburg, W.J.G.M., Sauvé, S., Lee, C., 2001. Bioavailability of metals in terrestrial ecosystems: importance of partitioning for bioavailability to invertebrates, microbes, and plants. Bioavailability of metals in terrestrial ecosystems: importance of partitioning for bioavailability to invertebrates, microbes, and plants.

Almås, Å.R., Lofts, S., Mulder, J., Tipping, E., 2007. Solubility of major cations and Cu, Zn and Cd in soil extracts of some contaminated agricultural soils near a zinc smelter in Norway: modelling with a multisurface extension of WHAM. European Journal of Soil Science 58, 1074–1086. https://doi.org/10.1111/j.1365-2389.2007.00894.x

Almas, Å.R., Lofts, S., Mulder, J., Tipping, E., 2007. 2 Solubility of major cations and trace metals (Cu, Zn and Cd) in soil 3 extracts of some contaminated agricultural soils near a zinc smelter in 4 Norway: modelling with a multisurface extension of WHAM 41.

Amery, F., Degryse, F., Cheyns, K., Troyer, I.D., Mertens, J., Merckx, R., Smolders, E., 2008. The UV-absorbance of dissolved organic matter predicts the fivefold variation in its affinity for mobilizing Cu in an agricultural soil horizon. European Journal of Soil Science 59, 1087–1095. https://doi.org/10.1111/j.1365-2389.2008.01078.x

Aryal, R., Vigneswaran, S., Kandasamy, J., Naidu, R., 2010. Urban stormwater quality and treatment. Korean J. Chem. Eng. 27, 1343–1359. https://doi.org/10.1007/s11814-010-0387-0

Badin, A.-L., 2009. Répartition et influence de la matière organique et des microorganismes sur l'agrégation et le relargage de polluants dans des sédiments issus de l'infiltration d'eaux pluviales urbaines (These de doctorat). Lyon, INSA.

Baken, S., Regelink, I.C., Comans, R.N.J., Smolders, E., Koopmans, G.F., 2016. Iron-rich colloids as carriers of phosphorus in streams: A field-flow fractionation study. Water Research 99, 83–90. https://doi.org/10.1016/j.watres.2016.04.060

Banc, C., Gautier, M., Blanc, D., Lupsea-Toader, M., Marsac, R., Gourdon, R., 2021. Influence of pH on the release of colloidal and dissolved organic matter from vertical flow constructed wetland surface sludge deposits. Chemical Engineering Journal 418, 129353. https://doi.org/10.1016/j.cej.2021.129353

Bonneau, J., Fletcher, T.D., Costelloe, J.F., Burns, M.J., 2017. Stormwater infiltration and the 'urban karst' – A review. Journal of Hydrology 552, 141–150. https://doi.org/10.1016/j.jhydrol.2017.06.043

Bonten, L.T.C., Groenenberg, J.E., Weng, L., van Riemsdijk, W.H., 2008. Use of speciation and complexation models to estimate heavy metal sorption in soils. Geoderma 146, 303–310. https://doi.org/10.1016/j.geoderma.2008.06.005

Chatain, V., Blanc, D., Borschneck, D., Delolme, C., 2013. Determining the experimental leachability of copper, lead, and zinc in a harbor sediment and modeling. Environ Sci Pollut Res 20, 66–74. https://doi.org/10.1007/s11356-012-1233-1

Chen, C., Guo, W., Ngo, H.H., 2019. Pesticides in stormwater runoff—A mini review. Front. Environ. Sci. Eng. 13, 72. https://doi.org/10.1007/s11783-019-1150-3

Clozel, B., Ruban, V., Durand, C., Conil, P., 2006. Origin and mobility of heavy metals in contaminated sediments from retention and infiltration ponds. Applied Geochemistry 21, 1781–1798. https://doi.org/10.1016/j.apgeochem.2006.06.017

Di Bonito, M., Lofts, S., Groenenberg, J.E., 2018. Chapter 11 - Models of Geochemical Speciation: Structure and Applications, in: De Vivo, B., Belkin, H.E., Lima, A. (Eds.), Environmental Geochemistry (Second Edition). Elsevier, pp. 237–305. https://doi.org/10.1016/B978-0-444-63763-5.00012-4

Dijkstra, J.J., Meeussen, J.C.L., Comans, R.N.J., 2009. Evaluation of a Generic Multisurface Sorption Model for Inorganic Soil Contaminants. Environ. Sci. Technol. 43, 6196–6201. https://doi.org/10.1021/es900555g

Dijkstra, J.J., Meeussen, J.C.L., Comans, R.N.J., 2004. Leaching of Heavy Metals from Contaminated Soils: An Experimental and Modeling Study. Environ. Sci. Technol. 38, 4390–4395. https://doi.org/10.1021/es049885v

Drapeau, C., 2018. Mesure et modélisation de la mobilité et de la spéciation des éléments majeurs et traces métalliques au sein de matrices complexes polluées en fonction du pH : application aux sédiments urbains et déchets miniers (These de doctorat). Lyon.

Drapeau, C., Delolme, C., Chatain, V., Gautier, M., Blanc, D., Benzaazoua, M., Lassabatère, L., 2017. Spatial and Temporal Stability of Major and Trace Element Leaching in Urban Stormwater Sediments. Open Journal of Soil Science 07, 347. https://doi.org/10.4236/ojss.2017.711025

Dzombak, D.A., Morel, F.M.M., 1990. Surface Complexation Modeling: Hydrous Ferric Oxide. John Wiley & Sons.

Faivre, N., Fritz, M., Freitas, T., de Boissezon, B., Vandewoestijne, S., 2017. Nature-Based Solutions in the EU: Innovating with nature to address social, economic and environmental challenges. Environmental Research 159, 509–518. https://doi.org/10.1016/j.envres.2017.08.032

Fang, W., Wei, Y., Liu, J., 2016. Comparative characterization of sewage sludge compost and soil: Heavy metal leaching characteristics. Journal of Hazardous Materials 310, 1–10. https://doi.org/10.1016/j.jhazmat.2016.02.025

Gangloff, S., Stille, P., Schmitt, A.-D., Chabaux, F., 2016. Factors controlling the chemical composition of colloidal and dissolved fractions in soil solutions and the mobility of trace elements in soils. Geochimica et Cosmochimica Acta 189, 37–57. https://doi.org/10.1016/j.gca.2016.06.009

Golui, D., Datta, S.P., Dwivedi, B.S., Meena, M.C., Trivedi, V.K., 2020. Prediction of free metal ion activity in contaminated soils using WHAM VII, baker soil test and solubility model. Chemosphere 243, 125408. https://doi.org/10.1016/j.chemosphere.2019.125408

Gong, P., Li, X., Zhang, W., 2019. 40-Year (1978–2017) human settlement changes in China reflected by impervious surfaces from satellite remote sensing. Science Bulletin 64, 756–763. https://doi.org/10.1016/j.scib.2019.04.024

Gorny, J., Billon, G., Noiriel, C., Dumoulin, D., Lesven, L., Madé, B., 2016. Chromium behavior in aquatic environments: a review. Environ. Rev. 24, 503–516. https://doi.org/10.1139/er-2016-0012

Grybos, M., Davranche, M., Gruau, G., Petitjean, P., Pédrot, M., 2009. Increasing pH drives organic matter solubilization from wetland soils under reducing conditions. Geoderma 154, 13–19. https://doi.org/10.1016/j.geoderma.2009.09.001

Gu, S., Gruau, G., Dupas, R., Jeanneau, L., 2020. Evidence of colloids as important phosphorus carriers in natural soil and stream waters in an agricultural catchment. Journal of Environmental Quality 49, 921–932. https://doi.org/10.1002/jeq2.20090

Hallberg, M., Renman, G., Lundbom, T., 2007. Seasonal Variations of Ten Metals in Highway Runoff and their Partition between Dissolved and Particulate Matter. https://doi.org/10.1007/S11270-006-9289-5

Kania, M., Gautier, M., Blanc, D., Lupsea-Toader, M., Merlot, L., Quaresima, M.-C., Gourdon, R., 2019. Leaching behavior of major and trace elements from sludge deposits of a French vertical flow constructed wetland. Science of The Total Environment 649, 544–553. https://doi.org/10.1016/j.scitotenv.2018.08.364

Klinkert, S., Comans, R.N.J., 2020. Geochemical Multisurface Modeling of Reactive Zinc Speciation in Compost as Influenced by Extraction Conditions. Environ. Sci. Technol. 54, 2467–2475. https://doi.org/10.1021/acs.est.9b04104

Maes, J., Jacobs, S., 2017. Nature-Based Solutions for Europe's Sustainable Development: Europe's sustainable development. CONSERVATION LETTERS 10, 121–124. https://doi.org/10.1111/conl.12216

Marsac, R., Banik, N.L., Lützenkirchen, J., Catrouillet, C., Marquardt, C.M., Johannesson, K.H., 2017. Modeling metal ion-humic substances complexation in highly saline conditions. Applied Geochemistry 79, 52–64. https://doi.org/10.1016/j.apgeochem.2017.02.004

Mermillod-Blondin, F., Simon, L., Maazouzi, C., Foulquier, A., Delolme, C., Marmonier, P., 2015. Dynamics of dissolved organic carbon (DOC) through stormwater basins designed for groundwater recharge in urban area: Assessment of retention efficiency. Water Research 81, 27–37. https://doi.org/10.1016/j.watres.2015.05.031

Natarajan, P., Davis, A.P., 2015. Hydrologic Performance of a Transitioned Infiltration Basin Managing Highway Runoff. Journal of Sustainable Water in the Built Environment 1, 04015002. https://doi.org/10.1061/JSWBAY.0000797

Park, D., Yun, Y.-S., Park, J.M., 2008. XAS and XPS studies on chromium-binding groups of biomaterial during Cr(VI) biosorption. Journal of Colloid and Interface Science 317, 54–61. https://doi.org/10.1016/j.jcis.2007.09.049

Pédrot, M., Dia, A., Davranche, M., 2009. Double pH control on humic substance-borne trace elements distribution in soil waters as inferred from ultrafiltration. Journal of Colloid and Interface Science 339, 390–403. https://doi.org/10.1016/j.jcis.2009.07.046

Pokrovsky, O.S., Dupré, B., Schott, J., 2005. Fe–Al–organic Colloids Control of Trace Elements in Peat Soil Solutions: Results of Ultrafiltration and Dialysis. Aquat Geochem 11, 241–278. https://doi.org/10.1007/s10498-004-4765-2

Pokrovsky, O.S., Schott, J., 2002. Iron colloids/organic matter associated transport of major and trace elements in small boreal rivers and their estuaries (NW Russia). Chemical Geology 190, 141–179. https://doi.org/10.1016/S0009-2541(02)00115-8

Pourret, O., Dia, A., Davranche, M., Gruau, G., Hénin, O., Angée, M., 2007. Organo-colloidal control on major- and trace-element partitioning in shallow groundwaters: Confronting ultrafiltration

and modelling. Applied Geochemistry, Metal interactions with natural organic matter and Watershed-scale geochemistry 22, 1568–1582. https://doi.org/10.1016/j.apgeochem.2007.03.022

Redman, A.D., Macalady, D.L., Ahmann, D., 2002. Natural Organic Matter Affects Arsenic Speciation and Sorption onto Hematite. Environ. Sci. Technol. 36, 2889–2896. https://doi.org/10.1021/es0112801

Santillan-Medrano, J., Jurinak, J.J., 1975. The Chemistry of Lead and Cadmium in Soil: Solid Phase Formation. Soil Science Society of America Journal 39, 851–856. https://doi.org/10.2136/sssaj1975.03615995003900050020x

Sauvé, S., Manna, S., Turmel, M.-C., Roy, A.G., Courchesne, F., 2003. Solid−Solution Partitioning of Cd, Cu, Ni, Pb, and Zn in the Organic Horizons of a Forest Soil. Environ. Sci. Technol. 37, 5191–5196. https://doi.org/10.1021/es030059g

Schwertmann, U., Taylor, R.M., 1989. Iron Oxides, in: Minerals in Soil Environments. John Wiley & Sons, Ltd, pp. 379–438. https://doi.org/10.2136/sssabookser1.2ed.c8

Shi, Z., Allen, H.E., Di Toro, D.M., Lee, S.-Z., Harsh, J.B., 2013. Predicting PbII adsorption on soils: the roles of soil organic matter, cation competition and iron (hydr)oxides. Environ. Chem. 10, 465. https://doi.org/10.1071/EN13153

Shi, Z., Yang, Y., Liu, F., Lu, Y., Ye, Q., Lin, X., Feng, C., Liang, Y., Dang, Z., 2020. Effect of soil particle size on the kinetics of Cu release from field-contaminated soils: Experiments and a quantitative model. Chemical Geology 552, 119780. https://doi.org/10.1016/j.chemgeo.2020.119780

Sigg, L., 2014. 4.15 - Metals as Water Quality Parameters – Role of Speciation and Bioavailability, in: Ahuja, S. (Ed.), Comprehensive Water Quality and Purification. Elsevier, Waltham, pp. 315–328. https://doi.org/10.1016/B978-0-12-382182-9.00090-6

Tedoldi, D., Chebbo, G., Pierlot, D., Kovacs, Y., Gromaire, M.-C., 2016. Impact of runoff infiltration on contaminant accumulation and transport in the soil/filter media of Sustainable Urban Drainage Systems: A literature review. Science of The Total Environment 569–570, 904–926. https://doi.org/10.1016/j.scitotenv.2016.04.215

Tipping, E., Lofts, S., Sonke, J.E., 2011. Humic Ion-Binding Model VII: a revised parameterisation of cation-binding by humic substances. Environ. Chem. 8, 225. https://doi.org/10.1071/EN11016

Tipping, E., Rieuwerts, J., Pan, G., Ashmore, M.R., Lofts, S., Hill, M.T.R., Farago, M.E., Thornton, I., 2003. The solid–solution partitioning of heavy metals (Cu, Zn, Cd, Pb) in upland soils of England and Wales. Environmental Pollution 125, 213–225. https://doi.org/10.1016/S0269-7491(03)00058-7

Treilles, R., Gasperi, J., Gallard, A., Saad, M., Dris, R., Partibane, C., Breton, J., Tassin, B., 2021. Microplastics and microfibers in urban runoff from a suburban catchment of Greater Paris. Environmental Pollution 287, 117352. https://doi.org/10.1016/j.envpol.2021.117352

Trusilova, K., Jung, M., Churkina, G., 2009. On Climate Impacts of a Potential Expansion of Urban Land in Europe. Journal of Applied Meteorology and Climatology 48, 1971–1980. https://doi.org/10.1175/2009JAMC2108.1

Van Eynde, E., Weng, L., Comans, R.N.J., 2020. Boron speciation and extractability in temperate and tropical soils: A multi-surface modeling approach. Applied Geochemistry 123, 104797. https://doi.org/10.1016/j.apgeochem.2020.104797

Wang, C., Wang, R., Huo, Z., Xie, E., Dahlke, H.E., 2020. Colloid transport through soil and other porous media under transient flow conditions—A review. WIREs Water 7, e1439. https://doi.org/10.1002/wat2.1439

Wang, Y., Zhang, Z., Han, L., Sun, K., Jin, J., Yang, Yu, Yang, Yan, Hao, Z., Liu, J., Xing, B., 2019. Preferential molecular fractionation of dissolved organic matter by iron minerals with different oxidation states. Chemical Geology 520, 69–76. https://doi.org/10.1016/j.chemgeo.2019.05.003

Watmough, S.A., Orlovskaya, L., 2015. Predicting Metal Release from Peatlands in Sudbury, Ontario, in Response to Drought. Water Air Soil Pollut 226, 103. https://doi.org/10.1007/s11270-015-2372-z

Zhang, C., Yu, Z., Zeng, G., Jiang, M., Yang, Z., Cui, F., Zhu, M., Shen, L., Hu, L., 2014. Effects of sediment geochemical properties on heavy metal bioavailability. Environment International 73, 270–281. https://doi.org/10.1016/j.envint.2014.08.010

Zhang, W., Ye, Y., Tong, Y., Ou, L., Hu, D., Wang, X., 2011. Contribution and loading estimation of organochlorine pesticides from rain and canopy throughfall to runoff in an urban environment. Journal of Hazardous Materials 185, 801–806. https://doi.org/10.1016/j.jhazmat.2010.09.091

Zhu, X., Chatain, V., Gautier, M., Blanc-Biscarat, D., Delolme, C., Dumont, N., Aubin, J.-B., Lipeme Kouyi, G., 2020. Combination of Lagrangian Discrete Phase Model and sediment physico-chemical characteristics for the prediction of the distribution of trace metal contamination in a stormwater detention basin. Science of The Total Environment 698, 134263. https://doi.org/10.1016/j.scitotenv.2019.134263

ARTICLE 5

Evaluation of multisurface modeling strategy to predict major and trace elements concentration released from solid deposits originating from nature-based solution facilities.

Banc, C. [*], Gautier, M. [*], Blanc, D. [*], Lupsea-Toader, Zhan, Q. [*], Chatain, V. [*], Marsac, R[**]. Gourdon, R. *

* Univ Lyon, INSA Lyon, DEEP, EA7429, 69621 Villeurbanne, France.

** Univ Rennes, CNRS, Géosciences Rennes, UMR **6118**, 35000 Rennes, France.

Keywords

Modeling, trace metals, speciation, sediment, pollutant

Abbreviations

DOC: Dissolved Organic Carbon

SD: Sludge Deposit

TOC: Total Organic Carbon

VFCW: Vertical Flow Constructed Wetlands

1. Introduction

Contaminants and nutrients immobilized and accumulated in porous media could be a major risk for surface and ground water ecosystems. The mobility of these elements is influenced by a multitude of geochemical factors complexifying the comprehension of the underlying mechanisms of their mobility and speciation. Among them, the colloidal fraction, remobilized from solid fraction strongly influence the solubilization of major and trace elements (Baken et al., 2016; Bauer and Blodau, 2009; Raudina et al., 2021b; Schijf and Zoll, 2011). The nature of this colloidal fraction is known to be determinant to understand the process regulating elements mobility. Indeed, numerous studies evidenced the co-transport of trace metals with colloidal organic matter (Raudina et al., 2021b; Regelink et al., 2011a). The colloidal fraction is not limited to the organic molecules. The remobilization of oxides in the colloidal fraction also promote the solubilization of poorly soluble elements such as Pb, P or As (Pokrovsky et al., 2005; Pourret et al., 2007b; Regelink et al., 2011b). The influence of the various chemical parameters of the solution largely complexify the comprehension of the remobilization process. Among the main chemical parameters of the solutions, pH is a key factor controlling either the quantity, the nature of the colloidal phases but also the complexation capacity of these colloids.

Infiltration basins (IB) and constructed wetlands (CW) are nature-based solution (NBS) designed to treat stormwaters and wastewaters, respectively. The filtration process inevitably leads to the formation of a deposit at the surface of these infrastructures (Drapeau et al., 2017; Kania et al., 2019). These deposits are the remaining residues of the retention of suspended solids contained in the waters. Numerous studies evidenced the complexity of these deposits composed by important amount of OM, similar to those observed for natural wetland soils (Drapeau et al., 2017; Kania et al., 2018; Kania et al., 2019; Kim et al., 2013). In the rest of the document, deposit originating from IB and CW shall be referred to as infiltration basin sediment (IBS) and sludge deposit (SD). By contrast to natural systems IBS and SD, accumulate important content of major cations such as Al and Fe, but also important amount of pollutants such as trace metals and nutrients (Clozel et al., 2006; Drapeau et al., 2017; Kania

et al., 2019). Remobilization of these contaminants is a major threat for the environment. Indeed, these NBS are the last buffer area between anthropic and natural environment. A tool able to predict the leaching content and the speciation of the contaminants in the solid and released fraction of SD from NBS could be used to reduce the environmental risk associated to SD management. In natural environment, such as soils or sediments, multisurface modeling has been successfully used in risk assessment.

Integration of several mechanistic sub-models into the so-called “multisurface” model allow to describe, understand and predict the speciation and remobilization mechanisms of various species. Integration of generics sub-model allow to predict the ion-binding to all the reactive surfaces of soil and solution compartment. The generic character of these model derived from a large variety of samples allow their utilization over a large range of chemical conditions (Bonten et al., 2008). This characteristic are highly important to widespread the use of these model. However, to obtain adequate results, studies pass through an important phase of chemical characterization of the reactive surface composing the samples. For instance, considering their impact on the predictions, the amount of chemically reactive Fe-Al-oxides are dosed through various extraction procedure (Di Bonito et al., 2018; Dijkstra et al., 2004; Fisher-Power et al., 2019). Unfortunately, under operational conditions, IBS and SD characterization methods used in routine are as simple as possible and mainly consist in an elemental analysis with the measure of major and trace elements total content as well as total organic carbon content. In order to be used for deposits environmental management, multisurface model need to be efficient with very limited amount of information and other wide environmental conditions (*i.e* various pH conditions, various content in reactive surfaces and large spectrum of majors and trace metals concentrations).

The objective of this paper is to test the reliability of a multisurface modeling strategy to predict the solubility of major and trace elements contained in complex deposit originating from NBS. To do so, we evaluated the use of multisurface model to predict solid-solution partitioning of a large number of elements in deposits with various soil properties and a wide range of elements total content. Modeling prediction obtained for IBS (Banc et al., 2021) and SD (Banc et al., 2021) using the same modeling strategy will be compared to one new SD and on IBS. The 4 deposits compared here encompass the large spectrum of total content usually measured in CW and IB sediments (Clozel et al., 2006b; Drapeau et al., 2017; M. Kania et al., 2019; Boram Kim et al., 2015). These works are even more challenging due to the limited amount of information available on the SD. Indeed, only the total content in solid and dissolved OM, and element total content available. The overview of the efficacity of the modeling

methodology showed in this study will be used to propose improvements of the modeling strategy dedicated to highly anthropic sediments.

2. Materials and methods

2.1 Chemical characterization of sediment samples and pH leaching experiments

Modeled samples are composed by two sludge deposit originating from the same CW (further called CW-SD 1 and 2) and by two sediment originating from the same IB (further caller IBS 1 and 2). CW-SD 1 and 2 are the results of respectively 7 years and 14 years of accumulation of suspended solids. Similarly, IBS-1 and 2 were sampled after 8 years and 13 years of operation. Ageing of the deposits causes changes in the physico-chemical characteristics measured which are notably highlighted by the elemental analysis. The methodology used to perform the elemental analysis of these 4 deposits are described in the studies were the data come from. These studies are listed in Table 1 describing the main results obtained from the elemental analysis. Results of the pH-leaching experiments used in this present article were also obtained by studies described in Table 1.

Table 1: Description of the SD elemental analysis.

		CW-SD-1 (Kania et al., 2019)	CW-SD-2 (Banc et al., 2021)	IBS-1 (Drapeau et al., 2017)	IBS-2 (Qiufang et al., 2021)
pH		6.42	6.55	7.52	7.23
LOI[1]	%	66.5	55.2	22.2	30
OC[2]	%	22.9	16.6	8.6	11.6
Fe	%	3.52	3.43	3.29	3.87
Al	%	2.09	2.13	4.23	4.97
Ca	%	3.84	6.29	5.43	3.36
P	%	2.04	2.11	0.23	0.21
Cu	mg/kg	623	584	286	319
Zn	mg/kg	1219	1019	1975	2816
Cr	mg/kg	57	55	178	198
Pb	mg/kg	64	68	162	268
As	mg/kg	7	6.6	nm	15.3
Co	mg/kg		6.4	nm	58
Cd	mg/kg	1.5	1.1	nm	3.4

[1] Loss On Ignition (LOI, %) measured as the weight loss after 24 hours at 550°C

[2] OC: organic carbon

2.2 Multisurface model description

The two modeling prediction reused in this study obtained for CW-SD-2 (From "Multi-surface sorption modelling of major and trace elements leaching from vertical flow constructed wetlands surface sludge deposits") and IBS-1 (From "Coupled organic-mineral geochemical modelling of the leaching behaviour of major and trace metals from stormwater infiltration basin sediments") followed the same modeling strategy further described below and applied on CW-SD-1 and IBS-2. All calculations were done using PHREEQC interface coupled with thermodynamic constant from Llnl database. Sub-models were integrated to model the organic matter and Al/Fe-oxides sorption capacity (sub-models described below).

Sorption to solid and dissolved oxides. In this study, sorption of ions was considered to occur only on amorphous iron and aluminum oxides. Indeed, in natural conditions the presence of high content in organic matter limits oxides crystallization but promotes the formation of amorphous forms (Guénet et al., 2017; Pédrot et al., 2011). Clay was not considered in order to simplify the approach. Cation binding to amorphous hydrous ferric oxides (HFO) and hydrous aluminum oxides (HAO) was modeled using the generalized two-layer model (GTLM) with generic parameters described by Dzombak and Morel, 1990. In this model, oxides binding capacity is also described by specific and non-specific binding. The default value of 600 $m^2.g^{-1}$ was used for the specific surface area of HFO/HAO. The oxides surface is composed of strong and weak monodentate amphoteric hydroxyl groups able to bind cations and anions. Relationship between precipitate amorphous Al and Fe-oxides and, the amount of chemically reactive surface is set as define by Dzombak and Morel (1990): 0.2 mol of weak and 0.005 mol of strong binding sites per mol of precipitated HFO/HAO. The electrostatic fields around the charged oxides affect the intrinsic ionic sorption capacity and also the non-specific interaction within a diffuse Gouy-Chapman layer.

Sorption to solid and dissolved organic matter. The sorption capacity of Dissolved and Solid Organic Matter (DOM and SOM, respectively) was modeled using Humic Ion-Binding Model VII described by Tipping et al, 2011. Model VII considers two types of cation binding to humic acids (HA) and fulvic acids (FA): (i) a specific binding involving a discrete binding sites distribution and (ii) a non-specific binding considered to occur through electrostatic accumulation of counter-ion in a Donnan volume surrounding the molecular surface and inversely proportional to the ionic strength of the solution. A total of 50 binding sites are described in Model VII, allowing to consider the heterogeneity of humic substances binding capacity. These sites were described as composed of 4 carboxylic (type A sites) and 4 phenolic (type B sites) sites allowing them to form bidentate and tridentate recombination. Only the

aqueous cations and their first hydrolysis product are likely to bind to HA and FA. The intrinsic equilibrium constants for cations binding to monodentate type A or B sites are described by two parameters log K_{MA} and log K_{MB}, respectively. These parameters are calculated as follow:

$$\log K_{MB} = \log K_{MA} \times \frac{pK_B}{pK_A}$$

In the previous equation pK_A and pK_B describe the intrinsic protonation constants for type A and type B sites, respectively.

Equilibrium constants for cations binding to bidentate or tridentate sites are defined as the sum of the log K of the monodentate sites constituting the multidentate site considered. The range of the metal binding strengths is also modulated by an empirical parameter called ΔLK_2 generating moderate and strong binding sites and by an electrostatic correction of charge development resulting from ion binding and release (Almas et al., 2007; Tipping et al., 2011). Non-specific ions accumulation in the Donnan volume surrounding humic molecules was neglected here, considering the high OM content and high concentration in background electrolyte (Bonten et al., 2008). The default binding constants from (Tipping et al, 2011) were not adjusted.

Model input files. In this study, the pH-dependent solid-solution partitioning of Al, Ca, Fe, P, Cu, Cd, Cr, Ni, Pb and Zn was composed by (i) fixed values of pH and pE measured in each solution, (ii) total concentrations of the various elements, (iii) total dissolved concentration of S and Si measured in each sample to account for competitive inorganic complexation, (iv) adapted concentrations of solid and dissolved concentration in OM (see Fig.1). The mineral phases allowed to precipitate are: calcite, HFO, HAO, strengite, hydroxylapatite and gibbsite.

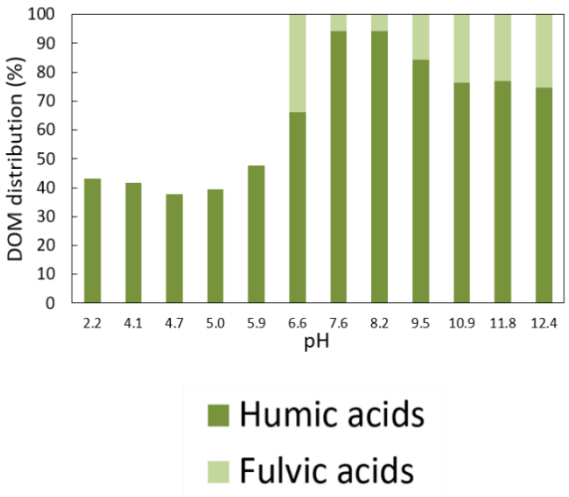

Fig.1: Modulation of the reactive fraction of measured DOM and the repartition between humic and fulvic acids used to model ion-binding to DOM (Banc et *al.,* 2021).

3. Results and discussion

3.1 pH dependence of the modelling results

To evaluate the influence of pH conditions on modeling performance, evolution of the of calculated on measured concentration ratio have been printed as function of pH conditions (Fig. 2). The continuous line represents 1:1 ratio while the upper and lower dotted line represent respectively 1:10 and 1:0.1 ratio.

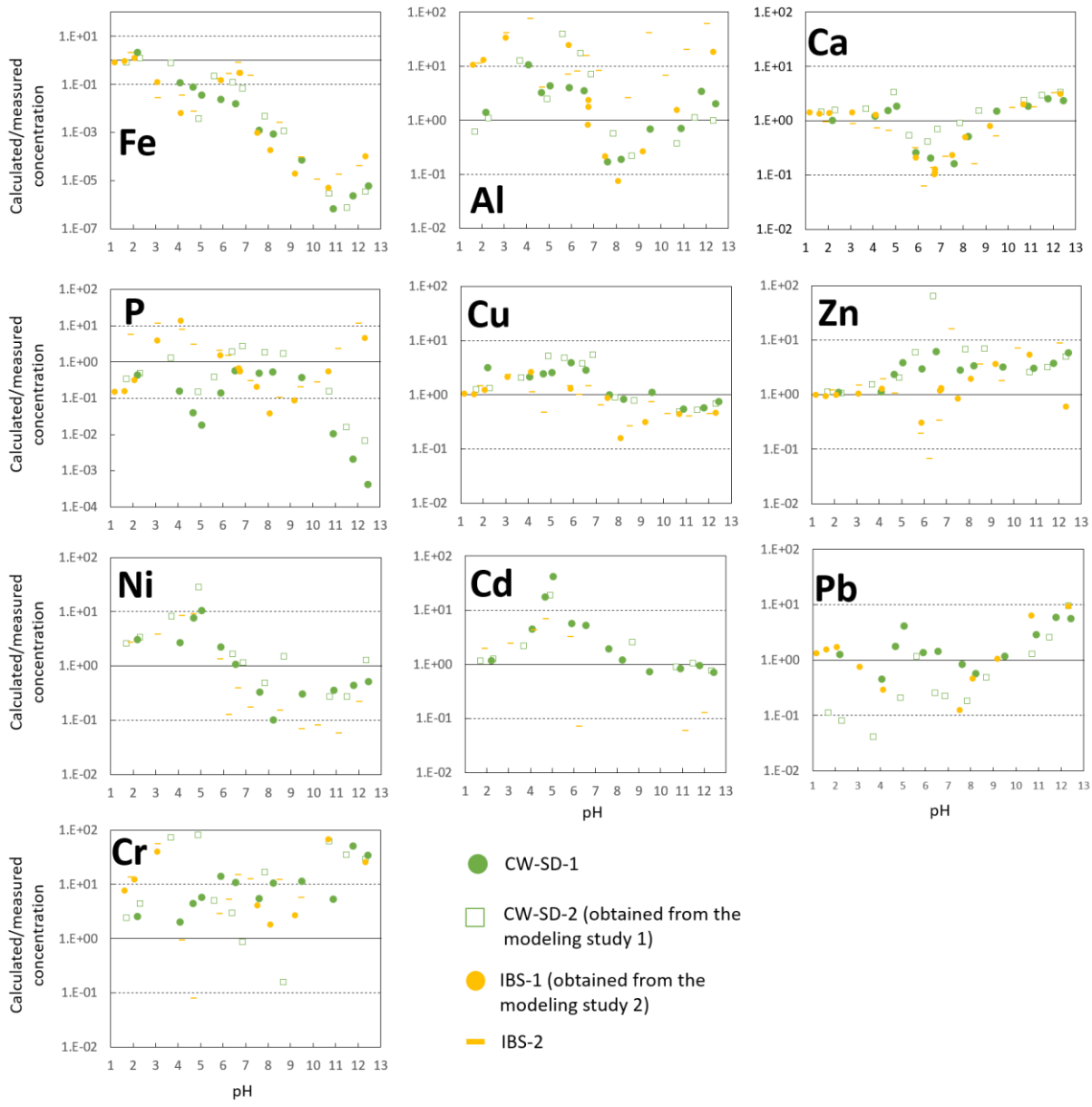

Fig.2: Evolution of the calculated over measured concentrations ratio as function of pH conditions. When the discrepancy between calculated and measured concentration reduce, the ratio tends to 1 (continuous line). The two dashed lines represent the limit whereby the deviation between the model calculations and the measurements does not exceed 10.

Modeling prediction for most Ca and Al concentrations are reasonably good over the entire pH range as most of the calculated:measured ratio are comprised between the two dotted lines. Thus, the discrepancy between measured and calculated concentration remain between one order of magnitude. In the multisurface model, the solubility of these elements is largely controlled by common mineral phases as described in section 2.2. This result emphasis that these mineral phases and the solubility constant used are sufficient to predict Ca and Al solubility. The calculated concentration of Fe is largely impacted by pH conditions. For Fe, the modeling discrepancy between measured and calculated concentration continuously increase from acidic to alkaline conditions. Models largely underestimate the Fe concentrations. Interestingly, Fe-oxides are calculated to be largely oversaturated in most of the pH range. As demonstrated in previous studies, the release of colloidal Fe-oxides from porous media is a well-known phenomenon (Pédrot et al., 2008; Pokrovsky et al., 2005; Pourret et al., 2007b). Using ultrafiltration experiments, lixiviation of Fe-organic matter particles has been evidenced in the constructed wetland SD (Banc et *al.,* 2021). According to these results, the release of colloidal Fe-oxides was included in the modeling calculation for each of the 4 deposits samples. The results presented for the other elements are considering this phenomenon. There is no clear evidence of strong influence of pH conditions on the quality of the modeling prediction for P as evidenced for Fe. However, it should be noted that under alkaline conditions, deviation between calculated and measured phosphorus concentrations increase. Especially for constructed wetlands SDs, models tend to underestimate the released P concentrations. Thus, these modeling results evidenced that sorption to colloidal and solid Fe-oxides is not sufficient to adequately predict P concentrations in alkaline conditions. Further chemical mechanisms need to be considered. Numerous studies evidenced that phosphorous and other anionic elements could be associated to organic matter through cationic bridging or through tertiary complex between oxides and organic matter (Al-Sid-Cheikh et al., 2015; Audette et al., 2020; Boram Kim et al., 2015). In our conditions of high loading in OM and divalent metals, this phenomenon could strongly impact the solubility of P but unfortunately, such mechanism is not considered in this study. Interestingly the largest deviation is observed for CW-SD that concentrates more important content in OM reinforcing the latter hypothesis suggesting that the remobilization of colloidal OM increase the solubilization of P through indirect complexation. Moreover, in conditions of high content of OM as it is the case of the CW-SD, adsorption of OM on the oxide surfaces causes the modification of the electrostatic properties of the organo-mineral particle and thus of the complexation capacity of the oxides (Arco-Lázaro et al., 2016; Lyvén et al., 2003; Saito et al., 2005). Thus, this results also question the ability of additive model to adequately predict the solubility of P in our conditions of high content in OM, both in the solid and released fraction. Indeed, previous studies evidenced that sorption of metal(loides) at oxides-organic matter interface is more

complex than a simple linear sorption additivity between OM and oxides (Christl, 2012; Moon and Peacock, 2013).

For trace elements presented in this study (Cu, Cd, Cr, Ni, Pb, Zn) varying pH conditions do not impact the modeling performances. This result is very encouraging since these metals are part of the monitored elements whose ecological impact of a remobilization might be important for environmental preservation and human health. According to these results, multisurface model used in this study could be used to model the leached concentrations under large variety of pH scenarios. For instance, the impact of acidification of wastewaters on the release and speciation of trace metals contained in the deposits could be tested with these models.

3.2 Influence of element concentration on model performance

Fig. 3 present the calculated concentrations of major and trace elements as function of the measured concentrations. The aim of these graphs is to highlighted a possible influence of the different species concentrations on the quality of the model prediction.

As demonstrated by these graphs, the release of major elements from the deposits has the particularity to be spread over a wide range of concentrations. For example, the maximum calcium concentration is 1000 folds higher than the minimum measured concentrations. For trace elements, the difference is also very important since, at least, 3 orders of magnitude separate the maximum and minimum measured concentrations. The modeling strategy is thus submitted to a wide range of major and trace concentrations. These variations could strongly influence the ionic strength of the solutions. In turn, ionic strength largely impacts the electrostatic parts of the models, notably by modifying the amount of elements complexed through nonspecific interactions (Tipping et al., 2011). As a reminder, in this study, the non-specific interaction between organic matter and various species have been neglected to simplify modelling calculations. As shown in Fig. 3, the deviation between measured and calculated concentrations is independent of the major and trace element concentrations. Even in low major and trace elements concentration, where increased deviation between measured and calculated concentration were expected due to perturbation of the electrostatic contribution of the sorption, the quality of the model prediction remains constant. This result is in agreement with Bonten et al. (2008) who evidenced low impact of the concentrations in major elements on the predicted concentrations of trace metals in natural soil samples. Thus, in conditions of high loading in reactive surfaces, as observed in our conditions, the specific interaction is sufficient to adequately describe pH-dependent solid-solution partitioning of most elements considered here. These results further expand the scope of potentially tested environmental scenarios. SD are largely reused as organic amendment in

agricultural soil. Calcic amendment could be also used in these soils to increase soil's pH. But what could be the consequences of such important increase of Ca concentration on trace metals remobilization from the SD? Results of this study confirm that multisurface modeling develop in this study could produce reliable predictions despite large variations of the content in major and trace elements.

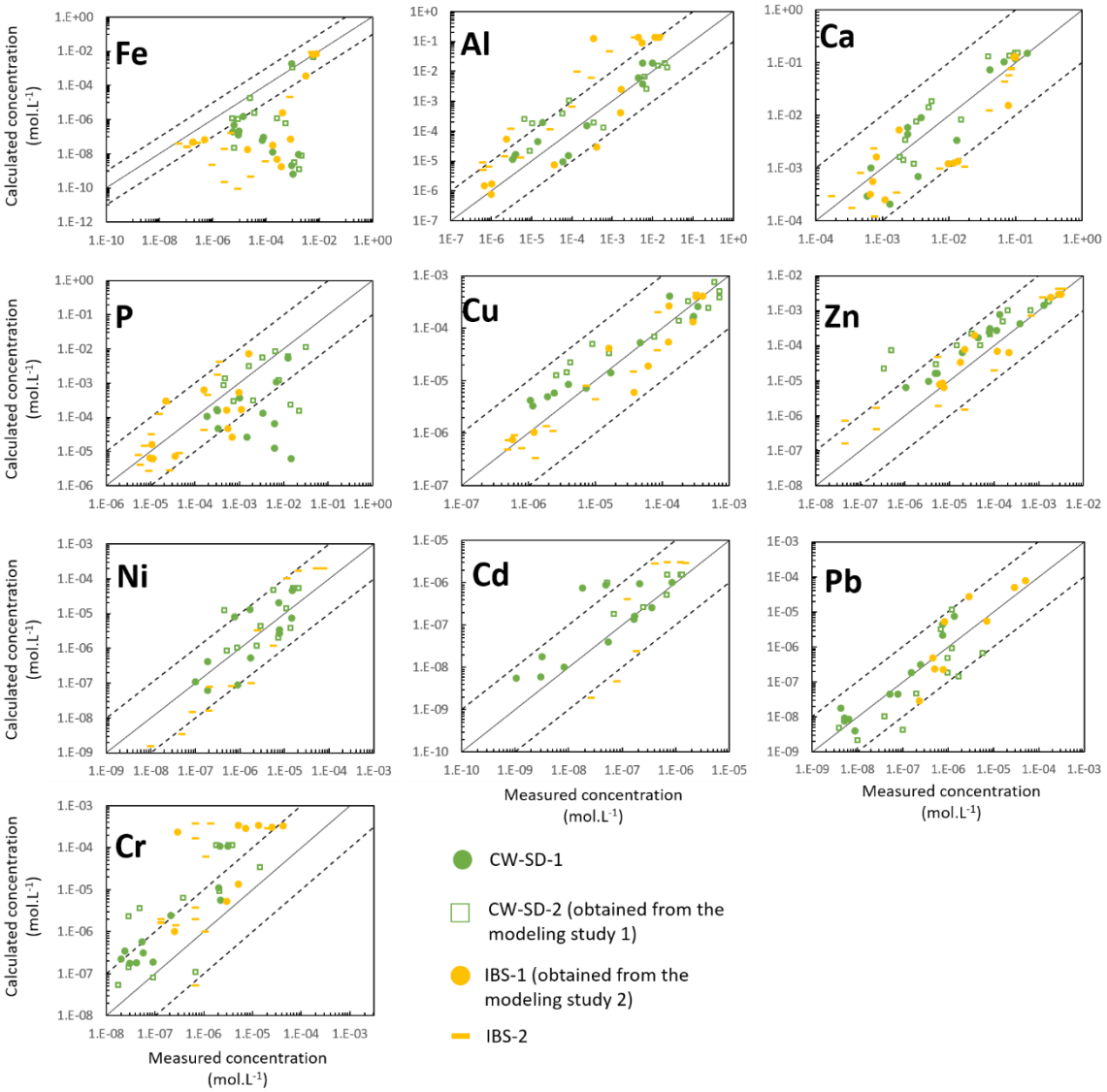

Fig.3: Calculated concentrations as function of the measured concentrations. When the discrepancy between calculated and measured concentration reduce, points tend to continuous line. The two dashed lines represent the limit whereby the deviation between the model calculations and the measurements does not exceed 10.

3.3 Quality of model predication as function of considered element

Fig. 4, represent the logarithmic Root Mean Square Error ($RMSE_{log}$) of the calculated element concentration for the entire pH range (pH~2 to pH~12). $RMSE_{log}$ will be used as an indicator of the modelling performances. In this modeling study, the solid-solution repartition of an important number of elements from different chemical class have been predicted simultaneously. Thus, this section aims

to provide an overview of the modeling performance depending on the chemical nature of the considered element.

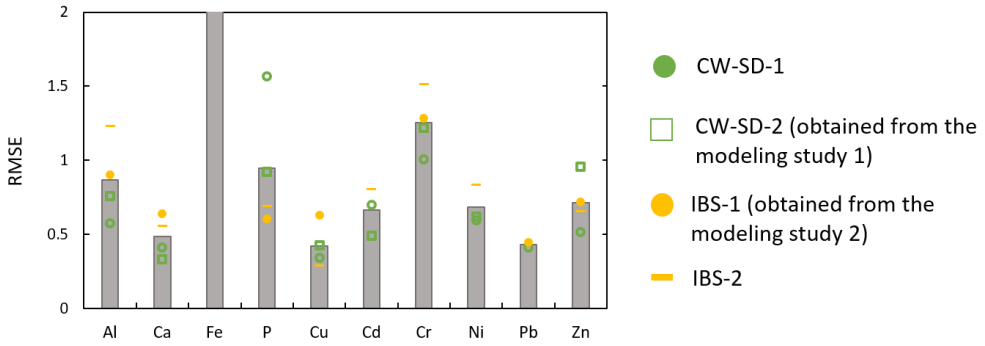

Fig.4: Calculated $RMSE_{log}$ as function of the considered elements. When $RMSE_{log}$ is below 1, deviation between measured and calculated concentrations are below 1 log unit.

The $RMSE_{log}$ values fluctuate from 0.4 for Cu to values ≥ 1 for P, As and Cr. Globally, the modeling results obtained with the multisurface model fluctuate with the considered element. The reason of the large discrepancy between calculated and measured concentration for Fe have been already discuss in the previous sections and will not be discuss again in the following paragraphs. The multisurface assemblage produce good modeling results for most major and trace metals (Ca, Al, Cu, Cd, Ni, Pb, Zn). More specifically, trace metals solubilization being largely controlled by OM in these model, low RMSE value observed for these elements suggest that OM have been adequately implemented. These results emphasis that for anionic elements (As, P), results are mitigated with $RMSE_{log}$ close to 1. As already discuss, by integrating anions complexation to OM, modeling calculation could be improved.

4. Conclusion

In this paper we evaluated the use of a multisurface modeling strategy dedicated to nature-based solutions deposits to predict the release of major and trace elements by applying the strategy for different deposits showing various reactive surface, major and trace metals contents. Indeed, to ensure that these models can be used by managers of these deposits in risk management, these models had to be simple, based on easily accessible data but especially perform on a large number of elements, under a wide variety of pH condition and a large spectrum of major and trace metals concentrations.

With the non-integration of nonspecific surface complexation to organic molecules defined in Model VII we hypothesis an increase of the deviation between measured and calculated concentration under low content in major and trace elements. The nonspecific interaction being important in low ionic strength conditions (Tipping et al., 2011). Multisurface model were tested over a wide range of major

and trace concentrations. The simplified Model VII model used in this study seem sufficient to adequately predict the release of most of the cationic metals released from deposits from high to low cations loading.

In multisurface modeling studies, the ratio of reactive solid or dissolved OM and their repartition in fulvic and humic acids is an important parameter (Fisher-Power et al., 2019; Klinkert and Comans, 2020). While some elements are more sensible to the quantity of reactive OM other are more sensible to the binding constants varying with humic and fulvic acids (Groenenberg, 2011). In this study, the ratio of reactive OM and repartition among humic and fulvic acids were reused from the chemical characterization performed on SD-CW2 (Banc et al., 2021). This result suggests that the reactivity of organic molecules remobilized from deposits under the influence of different pH conditions is relatively similar. In practice, the good modeling results obtained for trace metals suggests that further modeling studies on deposits originating from constructed wetlands or infiltration basins could use the same reactive OM parametrization used in this study.

The low influence of pH conditions on the quality of the modeling prediction is particularly important for constructed wetlands and infiltration basin sediments. As these deposits are subject to variable pH conditions (Huang et al., 2007; Kayhanian et al., 2007; Kim et al., 2014; Serrano et al., 2011), it was necessary for the model to be efficient over a wide range of pH conditions. Finally, according to the results of this study, the modeling strategy developed in this article could be reused for deposits with various physico-chemical characteristics, various ages, facing a wide range of pH conditions. The solid-solution partitioning and the speciation of the elements predicted by these models are precious information needed to evaluate the environmental risks associated to these deposits.

Literature cited

Aiken, G.R., Hsu-Kim, H., Ryan, J.N., 2011. Influence of Dissolved Organic Matter on the Environmental Fate of Metals, Nanoparticles, and Colloids. Environ. Sci. Technol. 45, 3196–3201. https://doi.org/10.1021/es103992s

Almas, Å.R., Lofts, S., Mulder, J., Tipping, E., 2007. 2 Solubility of major cations and trace metals (Cu, Zn and Cd) in soil 3 extracts of some contaminated agricultural soils near a zinc smelter in 4 Norway: modelling with a multisurface extension of WHAM 41.

Al-Sid-Cheikh, M., Pédrot, M., Dia, A., Guenet, H., Vantelon, D., Davranche, M., Gruau, G., Delhaye, T., 2015. Interactions between natural organic matter, sulfur, arsenic and iron oxides in re-oxidation compounds within riparian wetlands: NanoSIMS and X-ray adsorption spectroscopy evidences. Science of The Total Environment 515–516, 118–128. https://doi.org/10.1016/j.scitotenv.2015.02.047

Arco-Lázaro, E., Agudo, I., Clemente, R., Bernal, M.P., 2016. Arsenic(V) adsorption-desorption in agricultural and mine soils: Effects of organic matter addition and phosphate competition. Environmental Pollution 216, 71–79. https://doi.org/10.1016/j.envpol.2016.05.054

Audette, Y., Smith, D.S., Parsons, C.T., Chen, W., Rezanezhad, F., Van Cappellen, P., 2020. Phosphorus binding to soil organic matter via ternary complexes with calcium. Chemosphere 260, 127624. https://doi.org/10.1016/j.chemosphere.2020.127624

Baken, S., Regelink, I.C., Comans, R.N.J., Smolders, E., Koopmans, G.F., 2016. Iron-rich colloids as carriers of phosphorus in streams: A field-flow fractionation study. Water Research 99, 83–90. https://doi.org/10.1016/j.watres.2016.04.060

Banc, C., Gautier, M., Blanc, D., Lupsea-Toader, M., Marsac, R., Gourdon, R., 2021. Influence of pH on the release of colloidal and dissolved organic matter from vertical flow constructed wetland surface sludge deposits. Chemical Engineering Journal 418, 129353. https://doi.org/10.1016/j.cej.2021.129353

Bauer, M., Blodau, C., 2009. Arsenic distribution in the dissolved, colloidal and particulate size fraction of experimental solutions rich in dissolved organic matter and ferric iron. Geochimica et Cosmochimica Acta 73, 529–542. https://doi.org/10.1016/j.gca.2008.10.030

Bonten, L.T.C., Groenenberg, J.E., Weng, L., van Riemsdijk, W.H., 2008. Use of speciation and complexation models to estimate heavy metal sorption in soils. Geoderma 146, 303–310. https://doi.org/10.1016/j.geoderma.2008.06.005

Christl, I., 2012. Ionic strength-and pH-dependence of calcium binding by terrestrial humic acids. Environmental Chemistry 9, 89–96. https://doi.org/10.1071/EN11112

Clozel, B., Ruban, V., Durand, C., Conil, P., 2006. Origin and mobility of heavy metals in contaminated sediments from retention and infiltration ponds. Applied Geochemistry 21, 1781–1798. https://doi.org/10.1016/j.apgeochem.2006.06.017

Di Bonito, M., Lofts, S., Groenenberg, J.E., 2018. Chapter 11 - Models of Geochemical Speciation: Structure and Applications, in: De Vivo, B., Belkin, H.E., Lima, A. (Eds.), Environmental Geochemistry (Second Edition). Elsevier, pp. 237–305. https://doi.org/10.1016/B978-0-444-63763-5.00012-4

Dijkstra, J.J., Meeussen, J.C.L., Comans, R.N.J., 2004. Leaching of Heavy Metals from Contaminated Soils: An Experimental and Modeling Study. Environ. Sci. Technol. 38, 4390–4395. https://doi.org/10.1021/es049885v

Drapeau, C., Delolme, C., Chatain, V., Gautier, M., Blanc, D., Benzaazoua, M., Lassabatère, L., 2017. Spatial and Temporal Stability of Major and Trace Element Leaching in Urban Stormwater Sediments. Open Journal of Soil Science 07, 347. https://doi.org/10.4236/ojss.2017.711025

Fisher-Power, L.M., Shi, Z., Cheng, T., 2019. Testing the “component additivity” approach for modelling Cu and Zn adsorption to a natural sediment. Chemical Geology 512, 31–42. https://doi.org/10.1016/j.chemgeo.2019.02.038

Groenenberg, J.E., 2011. Evaluation of models for metal partitioning and speciation in soils and their use in risk assessment. [publisher not identified], Wageningen.

Huang, J., Du, P., Ao, C., Lei, M., Zhao, D., Ho, M., Wang, Z., 2007. Characterization of surface runoff from a subtropics urban catchment. Journal of Environmental Sciences 19, 148–152. https://doi.org/10.1016/S1001-0742(07)60024-2

Kania, Manon, Gautier, M., Blanc, D., Lupsea-Toader, M., Merlot, L., Quaresima, M.-C., Gourdon, R., 2019. Leaching behavior of major and trace elements from sludge deposits of a French vertical flow constructed wetland. Science of The Total Environment 649, 544–553. https://doi.org/10.1016/j.scitotenv.2018.08.364

Kania, M., Gautier, M., Imig, A., Michel, P., Gourdon, R., 2019. Comparative characterization of surface sludge deposits from fourteen French Vertical Flow Constructed Wetlands sewage treatment plants using biological, chemical and thermal indices. Science of The Total Environment 647, 464–473. https://doi.org/10.1016/j.scitotenv.2018.07.440

Kania, M., Gautier, M., Ni, Z., Bonjour, E., Guégan, R., Michel, P., Jame, P., Liu, J., Gourdon, R., 2018. Analytical indicators to characterize Particulate Organic Matter (POM) and its evolution in French Vertical Flow Constructed Wetlands (VFCWs). Science of The Total Environment 622–623, 801–813. https://doi.org/10.1016/j.scitotenv.2017.11.357

Kayhanian, M., Suverkropp, C., Ruby, A., Tsay, K., 2007. Characterization and prediction of highway runoff constituent event mean concentration. Journal of Environmental Management 85, 279–295. https://doi.org/10.1016/j.jenvman.2006.09.024

Kim, B., Gautier, M., Michel, P., Gourdon, R., 2013. Physical–chemical characterization of sludge and granular materials from a vertical flow constructed wetland for municipal wastewater treatment. Water Science and Technology 68, 2257–2263. https://doi.org/10.2166/wst.2013.485

Kim, B., Gautier, M., Prost-Boucle, S., Molle, P., Michel, P., Gourdon, R., 2014. Performance evaluation of partially saturated vertical-flow constructed wetland with trickling filter and chemical precipitation for domestic and winery wastewaters treatment. Ecological Engineering 71, 41–47. https://doi.org/10.1016/j.ecoleng.2014.07.045

Kim, B., Gautier, M., Rivard, C., Sanglar, C., Michel, P., Gourdon, R., 2015. Effect of Aging on Phosphorus Speciation in Surface Deposit of a Vertical Flow Constructed Wetland. Environ. Sci. Technol. 49, 4903–4910. https://doi.org/10.1021/es506164v

Klinkert, S., Comans, R.N.J., 2020. Geochemical Multisurface Modeling of Reactive Zinc Speciation in Compost as Influenced by Extraction Conditions. Environ. Sci. Technol. 54, 2467–2475. https://doi.org/10.1021/acs.est.9b04104

Lyvén, B., Hassellöv, M., Turner, D.R., Haraldsson, C., Andersson, K., 2003. Competition between iron- and carbon-based colloidal carriers for trace metals in a freshwater assessed using flow field-flow fractionation coupled to ICPMS. Geochimica et Cosmochimica Acta 67, 3791–3802. https://doi.org/10.1016/S0016-7037(03)00087-5

Moon, E.M., Peacock, C.L., 2013. Modelling Cu(II) adsorption to ferrihydrite and ferrihydrite–bacteria composites: Deviation from additive adsorption in the composite sorption system. Geochimica et Cosmochimica Acta 104, 148–164. https://doi.org/10.1016/j.gca.2012.11.030

Pédrot, M., Dia, A., Davranche, M., Bouhnik-Le Coz, M., Henin, O., Gruau, G., 2008. Insights into colloid-mediated trace element release at the soil/water interface. Journal of Colloid and Interface Science 325, 187–197. https://doi.org/10.1016/j.jcis.2008.05.019

Pokrovsky, O.S., Dupré, B., Schott, J., 2005. Fe–Al–organic Colloids Control of Trace Elements in Peat Soil Solutions: Results of Ultrafiltration and Dialysis. Aquat Geochem 11, 241–278. https://doi.org/10.1007/s10498-004-4765-2

Pourret, O., Dia, A., Davranche, M., Gruau, G., Hénin, O., Angée, M., 2007. Organo-colloidal control on major- and trace-element partitioning in shallow groundwaters: Confronting ultrafiltration and modelling. Applied Geochemistry 22, 1568–1582. https://doi.org/10.1016/j.apgeochem.2007.03.022

Raudina, T.V., Loiko, S.V., Kuzmina, D.M., Shirokova, L.S., Kulizhskiy, S.P., Golovatskaya, E.A., Pokrovsky, O.S., 2021. Colloidal organic carbon and trace elements in peat porewaters across a permafrost gradient in Western Siberia. Geoderma 390, 114971. https://doi.org/10.1016/j.geoderma.2021.114971

Regelink, I.C., Weng, L., van Riemsdijk, W.H., 2011a. The contribution of organic and mineral colloidal nanoparticles to element transport in a podzol soil. Applied Geochemistry, Ninth International Symposium on the Geochemistry of the Earth's Surface (GES-9) 26, S241–S244. https://doi.org/10.1016/j.apgeochem.2011.03.114

Regelink, I.C., Weng, L., van Riemsdijk, W.H., 2011b. The contribution of organic and mineral colloidal nanoparticles to element transport in a podzol soil. Applied Geochemistry, Ninth International Symposium on the Geochemistry of the Earth's Surface (GES-9) 26, S241–S244. https://doi.org/10.1016/j.apgeochem.2011.03.114

Saito, T., Koopal, L.K., Nagasaki, S., Tanaka, S., 2005. Analysis of Copper Binding in the Ternary System Cu2+/Humic Acid/Goethite at Neutral to Acidic pH. Environ. Sci. Technol. 39, 4886–4893. https://doi.org/10.1021/es0500308

Schijf, J., Zoll, A.M., 2011. When dissolved is not truly dissolved—The importance of colloids in studies of metal sorption on organic matter. Journal of Colloid and Interface Science 361, 137–147. https://doi.org/10.1016/j.jcis.2011.05.029

Serrano, L., de la Varga, D., Ruiz, I., Soto, M., 2011. Winery wastewater treatment in a hybrid constructed wetland. Ecological Engineering, Advances in pollutant removal processes and fate in natural and constructed wetlands 37, 744–753. https://doi.org/10.1016/j.ecoleng.2010.06.038

Tipping, E., Lofts, S., Sonke, J.E., 2011. Humic Ion-Binding Model VII: a revised parameterisation of cation-binding by humic substances. Environ. Chem. 8, 225. https://doi.org/10.1071/EN11016

A RETENIR

Les processus régissant la spéciation et le relargage des éléments au sein de milieux poreux sont particulièrement complexes. Comme mis en évidence avec les boues de filtres plantés de roseaux, la remobilisation des phases colloïdales joue un rôle prépondérant dans le relargage des métaux, métalloïdes et autres éléments d'intérêt comme le phosphore. La nature de ces phases colloïdales régit aussi leur réactivité vis-à-vis des éléments. Leur prise en compte au sein de modèle de prédiction est incontournable. Pour cela, leur intégration au sein de modèle multisurfacique en plus de l'intégration des processus de rétention des éléments en phase solide, est un challenge important.

Alors meme que le nombre de données d'entrée avait été volontairement limité (concentration totale en éléments majeurs et traces, la concentration en matière organique solide et dissoute), les travaux de modélisation présentés dans cette section permettent d'obtenir de bons résultats sur un large panel d'éléments. Une majeure partie du travail effectué lors de ces travaux de modélisation fut réalisé sur l'implémentation des surfaces réactives organique solides et relarguées avec ModelVII et des oxydes de fer et d'alumnium solides et relarguées avec le GTLM.

Comme démontré dans la synthèse bibliographique, la composition et la réactivité de la matière organique est largement dépendante de son origine. La prise en compte de cette hétérogénéité se concrétise souvent par l'application d'un ratio de matière organique active. Dans le cadre de la stratégie de modélisation utilisée ici et pour les dépôts, les meilleures prédictions sont obtenues considérant 100% de la matière organique solide comme active. La modulation du ratio de matière organique dissoute a aussi été nécessaire. Cette modulation est basée sur les résultats du fractionnement de la matière organique relarguée depuis une boue de filtre planté de roseaux (chapitre III). Ce ratio évolue en fonction du pH des solutions. Globalement, la capacité de sorption de la matière organique relarguée à pH acide était largement surestimée. La quantité de matière organique active à donc était largement réduite sur cette gamme de pH.

Dans cette étude, la quantité d'oxyde de fer et d'aluminium a été calculée à l'aide de la quantité totale en Fe et Al de l'échantillon considéré et des coefficients de solubilité de phases minérales utilisées. Pour chacun des quatre dépôts (2 boues de filtre planté et 2 sédiments de bassin d'infiltration), la considération du relargage d'oxyde de fer en solution a permis l'amélioration des prédictions. Ici, la quantité d'oxyde de fer sous forme colloïdale a été calculée comme la différence entre la concentration en Fe calculée (sous-estimée sur la quasi-totalité de la gamme de pH) et la concentration mesurée.

CHAPITRE V. CONCLUSION GENERALE ET PERSPECTIVES

1. Principales conclusions de l'étude

Sous l'impulsion de l'union européenne au travers du projet « Horizon 2020 », l'utilisation de solutions fondées sur la nature dans la gestion des eaux est promue et favorisée. Dans le cadre plus spécifique de la gestion des eaux usées en milieu rural (domestiques et industrielles) et des eaux de ruissellement en milieu urbain, deux types d'installation ont été largement développés : les filtres plantés de roseaux pour la gestion des eaux usées et les bassins de rétention et d'infiltration pour la gestion des eaux de ruissellement. Dans ces systèmes, la rétention des particules en suspension des eaux conduit à la formation de dépôts en surface des ouvrages. Ces dépôts montrent des teneurs importantes en matières organiques et en contaminants (*i.e.* métaux traces, métalloïdes et nutriments) dont les mécanismes de rétention et de remobilisation restent peu étudiés. Or, ces systèmes sont les dernières zones tampons séparant les systèmes fortement anthropisés produisant, par exemple, des eaux usées, des milieux naturels auxquels ils sont connectés. La remobilisation de contaminants stockés au sein de ces dépôts peut donc engendrer des pollutions diffuses ou accidentelles des zones de rejets naturels. Par ailleurs, ces dépôts sont amenés à être régulièrement évacués des installations pour éviter les problématiques de colmatage. Ils peuvent alors être valorisés comme une source d'amendement à moindre cout utilisée par les agriculteurs en raison des concentrations en matières organiques et nutriments. D'autres types de valorisation, notamment en lien avec le génie civil, sont actuellement à l'étude. Mais, à chaque fois, cela montre la nécessité de mieux comprendre les mécanismes de rétention et de remobilisation des contaminants de ces dépôts.

1.1. Nature et rôle des colloïdes remobilisés dans le relargage d'éléments majeurs et traces

Au sein des milieux poreux naturels comme des sols ou des sédiments, la remobilisation de phases colloïdales est à l'origine de la mobilité de polluants inorganiques et, plus particulièrement, des métaux traces. La nature de ces phases colloïdes, pouvant être organique et/ou minérale, est un facteur prépondérant dans cette mobilité. A l'instar des zones humides naturelles, les dépôts de boue générés au sein des filtres plantés de roseaux montrent une forte concentration en matière organique. L'utilisation de protocole de lixiviation (CENTS/TS 14429 European standard) couramment utilisé dans la caractérisation de déchets et de sols a permis de suivre l'impact des conditions de pH sur la remobilisation de colloïdes et des éléments majeurs et traces associés. Au regard de la problématique, une adaptation du protocole expérimental par l'ajout d'analyses des phases organiques a été nécessaire. Ainsi, les molécules organiques relarguées ont été fractionnées en fonction de leur poids moléculaire et leurs caractéristiques chimiques évaluées à l'aide de techniques d'UV-vis. Le compartiment colloïdal (> 3 kDa) contrôle largement le relargage de nombreux éléments (Fe, Al, Ca,

Mg, Li, Sr, Ba, Sr, Cr, Pb, Sc, Zn et Mn) quand d'autres sont plus faiblement associés à ces colloïdes (Cu, Ni, Co et Cd). Certains éléments (Na, Rb, P, As, Sb, S) sont en revanche peu associés aux phases colloïdales. Ces phases colloïdales sont largement constituées de matières organiques. Dans nos conditions, la forte quantité de matière organique relarguée semble promouvoir le relargage d'oxydes de fer et d'aluminium nanoparticulaire au sein de colloïdes organo-minéraux. Ainsi cette étude à pu mettre en évidence le rôle prépondérant de la remobilisation de ces colloïdes organo-minéraux dans le relargage du Pb, Sc, Y, Cr et d'éléments négativement chargés comme P et As. Le fort chargement en matière organique des solutions perturbe cependant la réactivité de ces complexes organo-minéraux comparativement aux études effectuées dans des milieux naturels. L'adsorption des molécules organiques à la surface des oxydes colloidaux réduit le nombre de sites disponibles et perturbe la charge de surface de ces oxydes diminuant ainsi la proportion d'éléments comme le phosphore ou l'arsenic complexés à ces oxydes. Le relargage de petites molécules organiques inférieures à 3 kDa assimilées à des acides fulviques joue aussi un rôle prépondérant en favorisant le relargage de métaux traces (Cu, Ni, Co et Cd).

En plus de contrôler la nature des phases colloïdales remobilisées, le pH impact aussi leur capacité de sorption. Avec l'acidification des solutions, la capacité de sorption des molécules organiques est largement réduite conduisant au relargage des ions sous la forme d'ions libres ou complexés à de petits ligands inorganiques. Finalement, la spéciation des éléments relargués depuis une boue de filtre planté est particulièrement complexe et la résultante de 3 principaux paramètres : les conditions de pH du milieu, la nature des phases colloïdales remobilisées et la nature de l'ion considéré ainsi que son état d'oxydation.

1.2. Modélisation multisurfacique avec prise en compte de la matière organique

Une même démarche de modélisation a été développée et appliquée sur 2 dépôts résidus du traitement des eaux par des solutions fondées sur la nature. Deux dépôts de boue issus de la filtration d'eaux usées principalement domestique après 7 et 14 ans de fonctionnement, et deux sédiments résidus d'infiltration d'eaux de ruissellement après 15 et 18 ans de fonctionnement ont été étudiés. Ces dépôts ont été choisis car ils représentent des dépôts dits matures mais les années séparant les dates d'échantillonnages permettent d'obtenir des disparités intéressantes afin de tester l'applicabilité des modèles à des matrices présentants des caractéristisques physico-chimiques différentes. Le défi de modélisation était important, notamment vis-à-vis de la nature de la matière organique et de la variabilité de ses proprietés de complexation. Par ailleurs, comme cela a été démontré dans le chapitre III, les processus géochimiques contrôlant la mobilité des éléments contenus dans ces dépôts sont particulièrement complexe, faisant notamment intervenir des colloïdes organo-minéraux. En outre, la quantité d'information à fournir a été volontairement réduite afin de

faciliter la réutilisation de ces modèles multisurfaciques dans des études de gestion du risque. Dans l'approche modélisatrice développée, la sorption des ions sur la matière organique a été calculée avec Model VII (Tipping et al., 2011). Afin de raccourcir les temps de calculs et de faciliter la réutilisation de la démarche de modélisation, la sorption non-spécifique des ions aux matières organiques n'a pas été intégrée aux calculs. La sorption sur les oxydes de fer et d'aluminium a été calculée avec le Generalized Two Layer Model de Dzombak and Morel (1990). Ces travaux de modélisation s'appuient sur 2 principales mesures : (i) la concentration totale en matière organique, en éléments majeurs et traces et (ii) la concentration de matière organique relarguée. Les résultats ont permis de montrer que l'utilisation de phases minérales simples permet de contrôler la solubilité des éléments majeurs comme le calcium, le magnésium, l'aluminium et le fer. Ces modèles sont particulièrement efficaces pour le calcul de la concentration en métaux traces divalents (Cu, Cd, Ni, Zn) relargués depuis les dépôts quelle que soit leur nature. Les écarts entre les concentrations mesurées et calculées, évalués à l'aide du « Root-mean-square error » sont globalement autour de 0,5 unité logarithmique. Ces travaux ont aussi permis de mettre en évidence le rôle prépondérant joué par la remobilisation des oxydes de fer mis en évidence plus tôt dans le chapitre dédié à l'ultrafiltration des solutions. La prise en compte du relargage d'oxyde de fer colloïdaux fut nécessaire pour améliorer les prédictions de la concentration relarguée du Pb ($RMSE_{log} < 0,5$) et d'élément chargé négativement, comme le phosphore et l'arsenic.

Pour les anions comme le phosphore et l'arsenic, des $RMSE_{log}$ compris entre 0,8 et 1,3 unité logarithmique, mettent en évidence des résultats de modélisation plus mitigés. Plusieurs phénomènes peuvent expliquer ces résultats. Il est possible que la forte concentration en matière organique exerce un contrôle important sur la solubilisation de ces éléments via une sorption directe sur les groupements fonctionnels (notamment les groupements thiols) ou bien une sorption indirecte via des ponts cationiques avec des cations ou des oxydes métalliques. La prise en compte de la compétition entre la matière organique et les anions pour les sites de sorptions des oxydes pourrait aussi améliorer les prédictions du modèle. En effet, le modèle additif utilisé dans cette thèse considérant la sorption d'un élément sur une particule organo-minérale comme étant la somme de sa complexation sur le minérale et sur la partie organique composant cette particule n'est pas démontré dans toute les études (Christl and Kretzschmar, 2001; Groenenberg and Lofts, 2014).

1.3. Utilisation des modèles multisurfaciques dans la gestion du risque associé aux dépôts de solutions fondées sur la nature

La perturbation des conditions chimiques rencontrées à l'intérieur des dépôts peut présenter des risques environnementaux majeurs en générant, par exemple, la dissolution des oxydes métalliques

et/ou la remobilisation de matières organiques et des contaminants associés. Les facteurs pouvant altérer ces conditions chimiques sont nombreux. Des changements de pH peuvent survenir au sein des solutions fondées sur la nature en réponse au déversement d'eaux plus acides ou plus alcalines, ou bien lors de l'intégration de ces dépôts dans des sols agricoles alcalins par exemple. L'hypersaturation hydrique des dépôts ou des sols amendés, l'altération de la circulation de l'air par le colmatage des dépôts ou la formation de semelle de labour et de croute de battance sur des sols agricoles peuvent conduire au développement de conditions anoxiques. Une multitude de phénomènes physico-chimiques peuvent donc entrainer des perturbations pouvant générer des pollutions. Pourtant les gestionnaires de ces infrastructures, responsables de l'efficacité des systèmes de traitement des eaux, mais aussi en charge de la gestion de ces dépôts jusqu'à leur réutilisation, ne disposent que de peu d'information sur les facteurs de risques liées à la remobilisation des polluants. Les outils de modélisation géochimique développés durant ces travaux pourraient trouver leur place au sein d'un panel d'outil d'aide à la décision dédié à la réduction des risques environnementaux. La capacité de ces modèles à prédire la concentration et la spéciation des polluants serait un atout majeur dans l'évaluation de la toxicité d'un relargage et donc la préservation de l'environnement.

Concrètement, la réutilisation des modèles multisurfaciques développés dans cette étude sur d'autres dépôts devra passer par deux principales étapes. Une première étape de mesure des contenus totaux sur l'échantillon à modéliser qui devra permettre l'ajustement de la concentration totale en matière organique, en éléments majeurs et traces du modèle. Ces mesures sont généralement effectuées en routine lors de la caractérisation des dépôts. Une seconde étape de mesure ou d'estimation de la concentration en matière organique relarguée en fonction du pH. Dans le chapitre IV, ces concentrations ont été obtenue lors des tests de lixiviations qui sont en revanche très peu pratiqués lors de la caractérisation de routine des dépôts. Or, les prédictions des modèles sont relativement sensibles à la quantité de matière organique relarguée. Il semble cependant possible d'estimer la concentration en matière organique relarguée en fonction de la concentration en matière organique totale de l'échantillon. En effet, en fonction de leur origine, les concentrations en matière organique relarguée depuis les dépôts montrent des signatures similaires.

2. Perspectives

Les travaux effectués dans cette thèse offrent des perspectives multiples dont certaines seront présentées ci-dessous. Deux principaux axes de recherche se détachent, (i) la poursuite des travaux de modélisation et (ii) le suivi de la transformation de la matière organique et des polluants associés le long du processus de filtration.

2.1. Application et amélioration des travaux de modélisation

Les travaux de modélisation effectués précédemment ont pu montrer quelques faiblesses pour reproduire l'influence du pH sur la concentration d'éléments chargés négativement comme l'As et le P. La fraction non négligeable de ces éléments relargués sous forme colloïdales pourrait être complexée à la matière organique via deux potentiels phénomènes : (i) des ponts cationiques (Audette et al., 2020) et/ou (ii) des complexes tertiaires matières organiques-oxides (Catrouillet et al., 2014). Cependant, les sous modèles utilisés dans cette étude et intégrés au sein des modèles « multi-surfaciques » ne permettent pas de prendre en compte ces associations. L'ajout de ce processus de complexation des éléments négativement chargé à la matière organique pourrait permettre de mieux représenter les processus à l'origine du transfert et de la biodisponibilité d'éléments cruciaux comme le phosphore que les boues de FPR accumulent années après années.

Les constantes de sorption thermodynamiques décrites dans ModelVII (Tipping et al., 2011) ont été obtenues en laboratoire sur des fractions d'acide humique et fulvique d'origine naturelle. Dans le cas de notre étude, l'introduction du ratio de matière organique solide et dissoute « réactive » a permis d'adapter la réactivité des substances humiques décrites dans ModelVII aux matières organiques anthropiques contenues dans nos échantillons. Bien que basées sur des expériences de caractérisation physico-chimique des fractions solides et dissoutes, des voies d'amélioration de cette démarche peuvent être explorées. L'approche proposée ici consisterait à adapter les constantes de sorption établies dans ModelVII. La finalité est encourageante : la création d'une base de données spécifiquement dédiée aux modélisateurs des matières organiques contenues dans des dépôts de solutions de traitement fondées sur la nature. Celle-ci pourrait, dans un premier temps, s'étendre sur les principaux éléments d'intérêt de ces matrices : As, P, N, Cu, Cr, Co, Ni, Pb, Zn. Succinctement, les humines, acides humiques et fulviques provenant de différents dépôts pourraient être isolés et purifiés en laboratoire. En utilisant un couplage PHREEQC-PHREEPLOT-ModelVII (Catrouillet et al., 2014), les pKa des sites carboxyliques et phénoliques mais aussi les LogK relatifs aux différents éléments étudiés pourraient être adaptés afin de modéliser le plus précisément possible les titrages potentiométriques et les isothermes d'adsorptions réalisés préalablement sur les fractions organiques isolées et purifiées.

Les modèles multisurfaciques développés durant cette thèse pourraient permettre de tester l'impact de différents scénarios de gestion très spécifique : Quel est l'impact d'une période d'inondation prolongée sur la remobilisation et la spéciation des polluants contenus dans ces dépôts ? L'ajout des dépôts à des sols agricoles dont les caractéristiques physico-chimiques sont connues engendre-t-il le relargage de polluants ? Les scénarios à tester sont nombreux, les prédictions du modèle pourraient être vérifiées en testant ces scénarios en laboratoire. L'intégration des modèles multisurfacique

développés ici à des modèles de transport pourraient permettre de tester l'impact de différents régimes hydrologiques (volume des bâchées etc.) sur la remobilisation et le transport de polluants au sein des matrices poreuses que sont les dépôts.

2.2. Dynamique des colloïdes le long du processus de traitement des eaux usées

L'application des techniques d'ultrafiltration le long du processus de traitement des filtres plantés de roseaux pourrait offrir une compréhension plus fondamentale des cycles biogéochimiques du carbone contenus dans ces ouvrages construits à l'instar de ce qui se fait à l'échelle du bassin versant (Pokrovsky et al., 2016; Pokrovsky and Schott, 2002b). L'application de techniques de séparation associée à des caractérisations physico-chimiques (UV, Fluo3D, Py-GC-MS, ICP-MS…) pourrait permettre de mieux comprendre l'impact des différentes étapes de filtrations (eaux brutes, lit bactérien éventuel, différents étages, etc.) sur la qualité, l'origine et la capacité des molécules organiques dissoutes à mobiliser des polluants. Le cycle du carbone ayant aussi un impact sur la capacité de nitrification et surtout de dénitrification de l'azote dans ce type d'ouvrage, il peut être cohérent d'envisager des analyses de biodisponibilité des molécules organiques en fonction de leur poids moléculaire. Au-delà même de l'amélioration de la compréhension du cycle du carbone et des nutriments dans les filtres, cette étude pourrait aussi permettre d'envisager des voies de valorisation des eaux traitées. En effet, l'emplacement rural des zones de FPR en fait un atout majeur pour permettre la réutilisation des eaux traitées en irrigation agricole. La concentration et la biodisponibilité des contaminants et nutriments contenus dans ces eaux est un frein à leur réutilisation. En réponse, l'apport d'information sur la spéciation et la biodisponibilité peut être un levier important pour améliorer et développer l'exploitation de ces eaux. Dans un contexte caractérisé par une insuffisance en eau entrainant des régulations de pompage et une raréfaction des nutriments (N/P), la réutilisation des eaux usées traitées peut être un enjeu agricole intéressant.

Références :

Audette, Y., Smith, D.S., Parsons, C.T., Chen, W., Rezanezhad, F., Van Cappellen, P., 2020. Phosphorus binding to soil organic matter via ternary complexes with calcium. Chemosphere 260, 127624. https://doi.org/10.1016/j.chemosphere.2020.127624

Catrouillet, C., Davranche, M., Dia, A., Bouhnik-Le Coz, M., Marsac, R., Pourret, O., Gruau, G., 2014. Geochemical modeling of Fe(II) binding to humic and fulvic acids. Chemical Geology 372, 109–118. https://doi.org/10.1016/j.chemgeo.2014.02.019

Christl, I., Kretzschmar, R., 2001. Interaction of copper and fulvic acid at the hematite-water interface. Geochimica et Cosmochimica Acta 65, 3435–3442. https://doi.org/10.1016/S0016-7037(01)00695-0

Dzombak, D.A., Morel, F.M.M., 1990. Surface Complexation Modeling: Hydrous Ferric Oxide. John Wiley & Sons.

Groenenberg, J.E., Lofts, S., 2014. The use of assemblage models to describe trace element partitioning, speciation, and fate: A review. Environmental Toxicology and Chemistry 33, 2181–2196. https://doi.org/10.1002/etc.2642

Pokrovsky, O.S., Manasypov, R.M., Loiko, S.V., Shirokova, L.S., 2016. Organic and organo-mineral colloids in discontinuous permafrost zone. Geochimica et Cosmochimica Acta 188, 1–20. https://doi.org/10.1016/j.gca.2016.05.035

Pokrovsky, O.S., Schott, J., 2002. Iron colloids/organic matter associated transport of major and trace elements in small boreal rivers and their estuaries (NW Russia). Chemical Geology 190, 141–179. https://doi.org/10.1016/S0009-2541(02)00115-8

Tipping, E., Lofts, S., Sonke, J.E., 2011. Humic Ion-Binding Model VII: a revised parameterisation of cation-binding by humic substances. Environ. Chem. 8, 225. https://doi.org/10.1071/EN11016

ANNEXES

ANNEXE A

Relative aux ultrafiltrations des solutions dépôt de boue.

Organic and organo-mineral colloids control of major and trace elements leached from treatment wetland sludge deposits. Influence of pH conditions.

Fig. S1: Diagramme pH-Eh des éléments rédox-sensible.

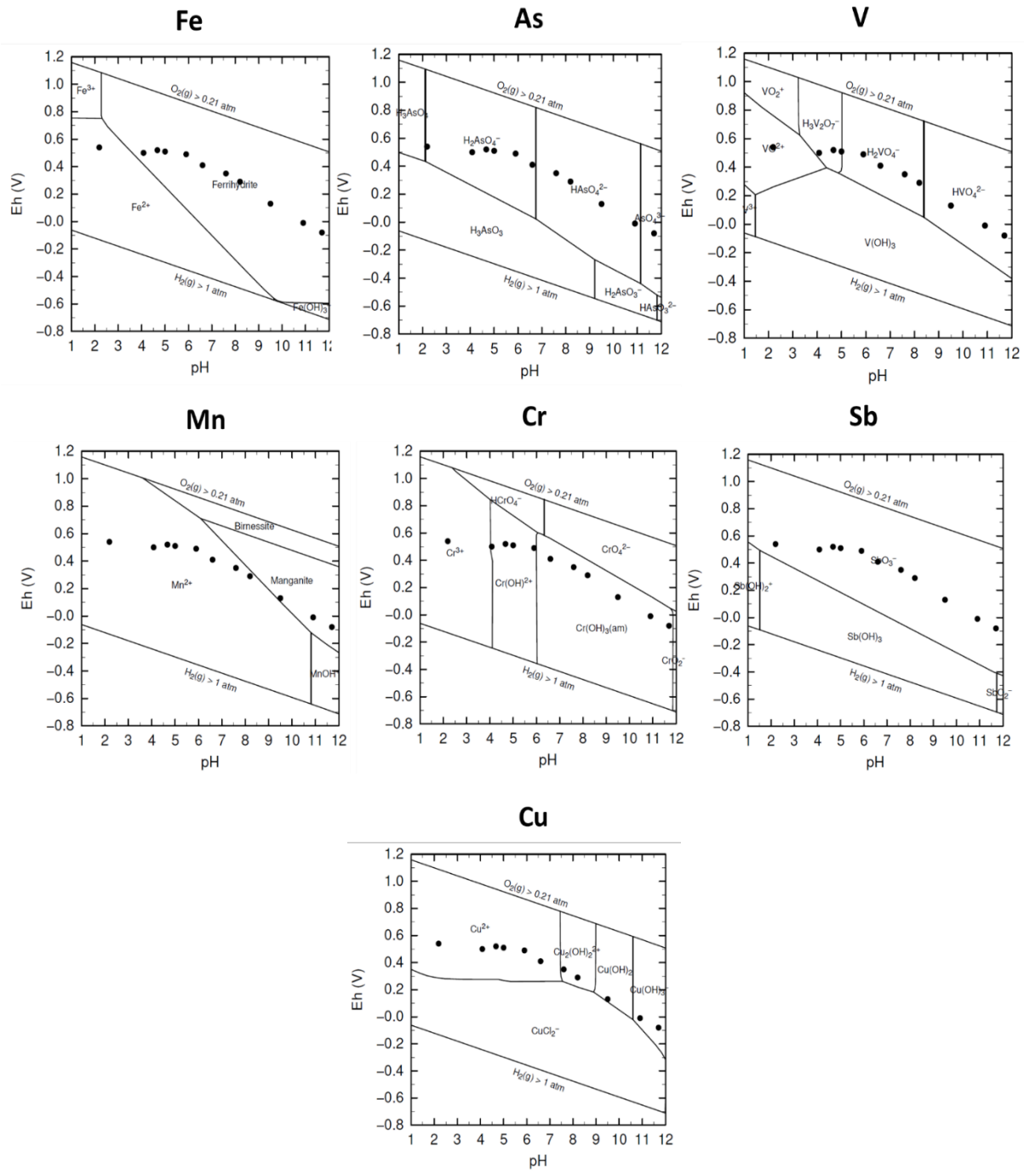

Tableau S1 : Concentrations ($mg.L^{-1}$) obtenues dans chacun des ultrafiltrats en fonction du pH des solutions de lixiviation utilisées sur le dépôt de boue de FPR.

	Fraction	DOC	Li	Na	Mg	Al	Ca	Sc
pH 12.4	<0.45 µm	5739.1	6.2	68051.4	6238.5	316667.6	179926.3	5.518
	<0.22 µm	5647.3	0.0	63131.3	5426.2	288106.8	161876.1	0.000
	<30kDa	2546.9	0.9	59131.7	611.3	302001.6	25020.0	0.858
	<10kDa	2267.4	0.2	50067.6	78.6	294777.1	5940.3	0.141
	<3kDa	1452.0	0.5	47779.7	162.7	294272.7	6509.2	0.254
pH 11.8	<0.45 µm	3892.2	6.9	51762.8	6594.4	195051.3	119125.1	3.792
	<0.22 µm	3730.7	4.1	49720.0	5818.1	189670.4	112680.6	3.394
	<30kDa	1224.1	0.5	41658.2	157.7	160482.5	4989.4	0.208
	<10kDa	1264.8	0.4	35420.3	118.7	155446.8	4242.1	0.181
	<3kDa	904.1	0.4	33772.2	42.4	158509.7	1341.9	0.025
pH 10.9	<0.45 µm	3389.3	6.7	50321.3	6369.9	193198.3	121194.6	3.055
	<0.22 µm	3397.7	3.8	42856.8	5098.5	175447.7	113859.2	4.435
	<30kDa	1312.6	0.6	40068.8	363.3	159917.9	10589.2	0.400
	<10kDa	1184.2	0.3	36205.7	114.0	160548.9	4245.9	0.122
	<3kDa	800.9	0.4	33547.8	53.5	157286.2	1594.0	0.030
pH 9.5	<0.45 µm	1083.6	5.6	41740.5	4276.9	10941.5	45754.8	0.942
	<0.22 µm	1063.9	4.5	35496.0	3644.3	9226.6	42940.6	1.285
	<30kDa	382.0	1.5	38945.0	910.7	2816.6	12247.9	0.090
	<10kDa	478.3	1.3	33240.5	1172.4	2640.3	15932.6	0.213
	<3kDa	168.9	1.0	32847.0	372.2	726.0	5161.2	0.010
pH 8.2	<0.45 µm	315.1	6.2	42806.2	2273.0	2132.1	39212.4	0.286
	<0.22 µm	320.8	2.4	28784.3	1609.3	2450.2	26244.8	n.d
	<30kDa	75.9	3.6	40476.7	1176.6	184.3	19236.1	0.012
	<10kDa	215.9	3.5	36241.8	1545.0	1094.3	27277.8	0.121
	<3kDa	18.0	3.3	37021.2	1094.4	108.8	18355.9	0.010
pH 7.6	<0.45 µm	163.4	5.8	44076.2	2996.2	1548.4	52553.1	n.d
	<0.22 µm	167.6	5.3	38155.8	2811.9	1342.5	49190.1	n.d
	<30kDa	43.9	5.6	42987.9	2558.8	155.9	41644.1	0.010
	<10kDa	52.3	4.9	39281.8	2449.5	51.8	41279.0	n.d
	<3kDa	9.5	5.0	39095.8	2494.5	154.2	41119.7	n.d
pH 6.5	<0.45 µm	65.3	7.4	43299.5	7893.9	88.3	138695.7	0.027
	<0.22 µm	63.7	7.4	43614.4	7765.0	85.6	137755.7	0.016
	<30kDa	34.1	7.8	44409.4	7910.1	36.0	138506.1	0.034
	<10kDa	25.2	7.0	39427.0	7439.1	32.6	138506.1	n.d
	<3kDa	22.1	7.0	38902.2	7511.5	24.9	137548.2	0.010
pH 5.9	<0.45 µm	79.4	10.6	52124.6	21023.0	100.6	522693.6	0.118
	<0.22 µm	77.1	10.2	50742.3	20940.0	69.5	513470.2	0.023
	<30kDa	42.3	10.7	51387.2	20863.3	39.5	500675.9	0.063
	<10kDa	40.5	9.3	46073.3	20293.2	19.4	525866.8	0.024
	<3kDa	41.6	9.5	46125.7	20225.5	16.4	504073.9	0.030
pH 5	<0.45 µm	178.7	13.9	55549.4	41409.2	105.2	1642558.2	0.156
	<0.22 µm	169.6	13.7	54903.2	40632.2	86.9	1649055.6	0.081

	<30kDa	132.6	14.8	56295.4	41310.6	29.2	1614240.6	0.178
	<10kDa	112.7	14.4	53749.7	41353.7	20.1	1703209.6	0.090
	<3kDa	108.0	15.5	54419.6	41145.3	11.6	1714375.1	0.130
pH 4.7	<0.45 µm	191.5	17.0	59506.0	53547.7	376.9	2723353.1	0.325
	<0.22 µm	188.5	16.7	57970.6	53505.2	125.4	2731654.1	0.106
	<30kDa	156.7	17.6	58792.5	53035.5	98.3	2714381.9	0.283
	<10kDa	125.4	16.3	55558.2	52734.2	57.1	2760162.9	0.199
	<3kDa	119.2	16.8	56073.6	52738.1	45.2	2796441.2	0.205
pH 4	<0.45 µm	227.5	25.9	67867.0	82920.5	989.8	5331001.8	0.320
	<0.22 µm	223.4	22.4	63580.2	77593.2	729.0	5186375.5	0.303
	<30kDa	154.6	26.1	63799.6	74024.8	520.9	5029332.7	0.393
	<10kDa	139.0	21.2	59452.8	73789.9	482.3	5225953.2	0.375
	<3kDa	132.8	21.4	59950.4	75206.6	446.9	5280995.4	0.364
pH 2.2	<0.45 µm	324.0	36.2	70923.7	102008.6	129783.3	6723848.8	0.542
	<0.22 µm	323.5	33.7	70675.1	100786.1	130419.2	6793262.7	0.542
	<30kDa	216.8	33.7	68248.2	98174.6	121842.4	6717693.9	0.850
	<10kDa	193.5	30.5	65750.8	94874.7	121165.0	6792039.3	0.828
	<3kDa	184.3	28.7	62884.6	92096.6	114381.6	6713142.5	0.857

Suite

	Fraction	V	Cr	Mn	Fe	Co	Ni	Cu
pH 12.4	<0.45 µm	641.0	208.0	263.3	114671.1	39.4	843.5	24651.6
	<0.22 µm	633.5	211.5	243.7	115432.7	37.1	707.8	23836.3
	<30kDa	663.1	42.3	54.5	17419.0	22.4	526.0	16134.9
	<10kDa	677.0	21.8	31.5	5283.3	19.1	494.4	14790.5
	<3kDa	668.2	15.6	14.0	4093.2	6.8	264.7	7189.7
pH 11.8	<0.45 µm	482.9	139.9	162.0	71204.5	23.4	452.7	22586.5
	<0.22 µm	470.9	131.5	156.5	70552.9	21.8	427.1	20980.9
	<30kDa	477.5	18.8	6.4	2379.6	9.6	231.1	11124.2
	<10kDa	505.2	18.3	6.4	2311.9	9.5	222.4	11048.2
	<3kDa	467.2	13.0	1.2	307.6	3.3	98.9	5289.5
pH 10.9	<0.45 µm	479.8	136.2	160.9	70934.2	23.3	441.8	22057.6
	<0.22 µm	495.8	129.5	147.6	66170.3	23.0	425.6	21362.4
	<30kDa	465.6	26.4	13.8	5731.3	9.9	239.1	11582.3
	<10kDa	508.2	19.6	6.2	2156.8	9.4	219.0	11292.4
	<3kDa	463.3	14.3	1.7	441.5	3.4	104.9	5587.5
pH 9.5	<0.45 µm	114.6	25.5	75.8	19913.0	9.1	102.4	5127.6
	<0.22 µm	116.5	23.2	59.2	17738.0	9.0	95.5	4945.2
	<30kDa	93.4	5.4	8.9	3342.0	5.1	52.5	2752.5
	<10kDa	102.2	7.6	14.4	5330.9	5.8	60.2	2935.9
	<3kDa	88.2	0.8	0.9	271.8	2.2	20.7	1400.0
pH 8.2	<0.45 µm	30.1	10.7	43.4	9577.6	3.9	52.7	1740.3
	<0.22 µm	25.2	7.7	26.4	6675.5	2.9	20.2	1337.2
	<30kDa	21.8	1.6	0.7	183.6	2.2	13.5	781.8
	<10kDa	26.8	4.0	11.2	3354.0	3.2	23.7	1336.6
	<3kDa	22.6	0.3	0.3	52.7	1.3	7.9	340.3

pH 7.6	<0.45 µm	14.9	3.0	0.0	4394.1	2.3	13.0	458.9
	<0.22 µm	16.4	4.8	21.5	4653.8	2.3	103.2	426.3
	<30kDa	13.5	1.3	0.7	101.0	1.8	11.5	264.3
	<10kDa	13.9	0.4	0.5	67.9	1.8	9.4	209.3
	<3kDa	14.0	0.2	0.4	33.5	1.3	6.9	142.7
pH 6.5	<0.45 µm	5.4	1.1	65.2	502.2	1.8	7.0	73.5
	<0.22 µm	5.4	1.0	60.9	307.5	1.6	7.0	67.8
	<30kDa	5.4	1.3	50.1	81.6	1.9	6.9	61.9
	<10kDa	5.6	0.2	16.5	24.5	1.6	9.7	53.9
	<3kDa	5.3	0.4	16.5	35.0	1.2	6.6	41.7
pH 5.9	<0.45 µm	3.5	1.3	359.0	544.9	4.2	11.2	67.3
	<0.22 µm	3.2	0.7	355.6	248.7	3.8	10.4	71.1
	<30kDa	3.0	1.0	340.6	40.7	4.0	13.2	62.3
	<10kDa	3.4	0.4	357.8	22.2	4.0	13.2	55.4
	<3kDa	3.2	0.3	311.6	14.4	3.4	11.3	48.2
pH 5	<0.45 µm	2.2	1.6	1899.4	325.5	15.3	44.3	123.4
	<0.22 µm	2.0	1.2	1942.5	220.8	14.6	46.1	126.4
	<30kDa	2.0	1.3	1922.5	57.9	15.7	50.9	118.5
	<10kDa	2.0	0.7	2077.8	36.0	15.7	48.1	117.2
	<3kDa	1.9	0.6	2093.8	19.8	15.1	46.3	104.4
pH 4.7	<0.45 µm	1.9	2.1	3873.3	356.0	33.9	99.0	153.9
	<0.22 µm	1.8	1.8	3749.2	212.5	30.0	97.5	161.9
	<30kDa	1.8	2.5	4009.3	314.2	33.0	102.6	144.8
	<10kDa	1.8	1.2	4013.3	62.6	33.0	102.2	143.9
	<3kDa	1.7	1.4	4208.0	52.7	32.3	96.3	127.7
pH 4	<0.45 µm	2.8	4.3	10102.6	892.2	92.0	437.1	333.1
	<0.22 µm	2.8	4.5	10102.6	639.8	89.2	312.1	318.9
	<30kDa	2.4	4.3	9765.8	353.7	91.8	333.7	291.3
	<10kDa	2.6	4.2	10099.6	281.1	95.2	326.8	283.2
	<3kDa	2.3	3.5	9716.9	178.2	90.8	292.1	264.6
pH 2.2	<0.45 µm	236.0	124.8	19949.4	56046.2	210.0	947.8	8848.7
	<0.22 µm	226.9	116.6	17119.5	56889.0	184.9	855.3	8376.0
	<30kDa	245.0	124.8	17654.6	58090.8	206.4	909.1	8522.9
	<10kDa	249.1	117.4	17934.3	56633.1	198.0	854.9	8202.2
	<3kDa	245.0	110.0	17959.0	54974.2	198.0	837.9	8147.8

Suite 2

	Fraction	Zn	As	Rb	Sr	Y	Cd	Pb	P	S
pH 12.4	<0.45 µm	9555.2	120.7	471.3	664.2	44.8	40.6	281.1	452.0	181.8
	<0.22 µm	8888.7	122.2	454.7	628.3	40.5	40.7	283.1	551.4	210.7
	<30kDa	3910.8	112.2	389.6	76.6	5.2	33.2	32.1	429.9	103.1
	<10kDa	3034.7	96.3	384.6	9.5	0.7	31.1	2.7	411.4	104.3
	<3kDa	1539.0	97.0	341.2	20.8	1.3	15.0	8.4	351.1	71.4
pH 11.8	<0.45 µm	6245.8	57.3	250.3	369.7	25.3	19.4	158.1	189.3	135.9
	<0.22 µm	5711.6	57.2	250.7	358.1	24.1	18.5	139.1	223.2	145.7
	<30kDa	1198.9	44.4	186.6	7.0	0.2	12.2	2.7	123.5	57.1
	<10kDa	1174.2	50.2	188.7	6.3	0.2	12.4	1.0	138.2	59.9
	<3kDa	376.0	40.6	175.7	2.0	0.0	5.2	0.2	110.3	46.1
pH 10.9	<0.45 µm	5955.4	57.8	245.0	370.3	24.7	18.8	154.7	192.3	113.7
	<0.22 µm	5769.9	61.5	251.8	364.0	24.6	19.7	146.7	157.4	100.4
	<30kDa	1438.9	43.6	182.3	25.7	1.5	12.0	9.5	123.5	59.4
	<10kDa	1211.9	48.7	195.5	5.9	0.2	12.3	0.9	135.9	58.2
	<3kDa	437.4	39.7	171.9	2.7	0.1	5.6	0.6	109.8	46.5
pH 9.5	<0.45 µm	2077.0	14.4	108.7	105.6	5.3	6.1	32.1	31.0	40.6
	<0.22 µm	1807.7	15.8	111.5	99.5	4.8	6.6	28.9	29.4	36.8
	<30kDa	417.2	10.3	91.3	23.5	0.7	3.9	4.8	28.3	38.0
	<10kDa	576.3	12.1	95.0	32.9	1.2	4.0	7.0	28.9	44.7
	<3kDa	76.2	9.6	89.4	8.5	0.0	1.8	0.2	20.7	30.6
pH 8.2	<0.45 µm	501.3	6.1	70.4	84.0	2.6	0.9	16.3	9.8	25.5
	<0.22 µm	318.4	6.6	55.0	56.7	1.7	0.7	11.2	5.1	11.9
	<30kDa	28.2	4.4	63.2	31.2	0.0	0.3	0.3	8.3	26.1
	<10kDa	196.2	4.6	65.2	52.1	0.9	0.6	5.3	11.8	37.6
	<3kDa	14.3	4.7	64.6	31.2	0.0	0.2	0.1	7.7	25.3
pH 7.6	<0.45 µm	222.9	n.d	58.4	101.3	1.4	0.3	10.9	10.0	32.2
	<0.22 µm	176.1	4.2	56.2	91.9	1.1	0.3	8.2	7.8	31.8
	<30kDa	24.7	2.7	54.4	69.6	0.0	0.1	0.3	5.2	25.5
	<10kDa	11.2	3.3	54.8	69.4	0.0	0.1	0.1	4.6	26.0
	<3kDa	12.2	3.3	55.9	69.7	0.0	0.3	0.3	4.6	26.3
pH 6.5	<0.45 µm	69.1	2.0	21.5	209.2	0.1	0.1	1.1	5.8	24.8
	<0.22 µm	58.1	1.7	21.9	212.0	0.1	0.1	0.8	5.7	24.5
	<30kDa	40.4	1.9	21.1	202.6	0.0	0.1	0.4	5.2	22.7
	<10kDa	33.0	2.3	21.1	206.6	0.0	0.1	0.1	4.3	23.0
	<3kDa	27.7	2.1	21.7	206.7	0.0	0.1	0.1	3.9	22.9
pH 5.9	<0.45 µm	348.0	2.9	27.6	759.0	0.1	0.4	1.3	10.4	27.5
	<0.22 µm	315.2	3.0	28.1	767.4	0.1	0.4	0.7	9.5	27.2
	<30kDa	209.6	2.8	26.9	734.0	0.0	0.3	0.3	8.7	24.7
	<10kDa	150.8	3.6	27.8	769.7	0.0	0.2	0.1	7.6	25.7
	<3kDa	29.4	3.3	27.7	747.4	0.0	0.1	0.1	6.6	25.1
pH 5	<0.45 µm	2886.7	7.5	27.6	2527.3	0.1	2.0	0.9	46.0	26.6
	<0.22 µm	2784.2	7.6	28.6	2607.1	0.1	2.1	0.6	44.1	26.4
	<30kDa	2635.3	7.6	27.2	2519.5	0.0	2.1	0.3	42.5	25.5

	<10kDa	2467.3	8.7	28.3	2620.6	0.0	2.1	0.1	42.7	26.0
	<3kDa	1252.7	8.6	28.6	2643.0	0.0	1.9	0.1	40.1	25.9
pH 4.7	<0.45 µm	7514.1	12.3	27.8	4353.1	0.3	5.6	1.1	103.4	29.0
	<0.22 µm	7081.4	12.3	28.5	4353.1	0.2	5.1	0.7	98.0	28.5
	<30kDa	7190.6	13.3	28.1	4332.6	0.2	5.2	0.5	92.2	27.5
	<10kDa	7289.2	13.4	27.9	4339.5	0.1	5.2	0.2	93.3	28.5
	<3kDa	7033.4	13.7	29.1	4423.8	0.0	5.2	0.1	98.7	27.5
pH 4	<0.45 µm	31984.7	22.6	30.2	8947.4	1.8	23.8	1.8	210.0	29.1
	<0.22 µm	29158.4	21.8	30.1	8704.1	1.5	22.3	1.1	250.1	31.3
	<30kDa	30253.5	21.9	29.7	8457.6	1.3	23.6	1.5	223.0	30.2
	<10kDa	29618.7	26.4	29.6	8711.7	1.2	22.7	0.4	235.1	30.2
	<3kDa	30151.4	24.9	30.5	9030.9	1.1	23.2	0.2	240.4	30.0
pH 2.2	<0.45 µm	86439.1	37.6	48.3	14067.6	192.6	101.9	51.0	381.0	33.6
	<0.22 µm	83556.4	28.1	48.0	13623.4	176.1	95.6	48.0	438.2	35.4
	<30kDa	89016.9	32.0	48.8	13977.5	188.5	100.9	50.1	425.5	32.0
	<10kDa	83621.9	35.7	48.5	13989.8	188.8	96.8	48.4	425.2	31.4
	<3kDa	82793.5	34.7	49.1	14180.8	188.8	95.9	47.2	429.7	30.5

ANNEXE B

Relative aux travaux de modélisations.

Coupled organic-mineral geochemical modelling of the leaching behaviour of major and trace metals from stormwater infiltration basin sediments

Tableau S2 : Constantes de complexation des ions à la matière organique utilisées dans Drapeau (2018)

Surface	Associated reaction	Log_K
≡Morg_s (strong organic matter)		
	≡Morg_sOH + Al3+ = ≡Morg_wOAl2+ + H+	2.58
	≡Morg_sOH + Ca2+ = ≡Morg_sOCa+ + H+	-1.75
	≡Morg_sOH + Fe2+ = ≡Morg_sOFe+ + H+	-0.46
	≡Morg_sOH + Fe3+ = ≡Morg_sOFe2+ + H+	4.75
	≡Morg_sOH + PO4-3 = ≡Morg_sOPO3-2 + H2O	6.6
	≡Morg_sOH + Cr3+ = ≡Morg_sOCr2+ + H+	3.6
	≡Morg_sOH + Cu2+ = ≡Morg_sOCu+ + H+	1.3
	≡Morg_sOH + Pb2+ = ≡Morg_sOPb+ + H+	0.1
	≡Morg_sOH + Zn2+ = ≡Morg_sOZn+ + H+	-3.7
≡Morg_w (weak organic matter)		
	≡Morg_wOH + Al3+ = ≡Morg_wOAl2+ + H+	10.5
	≡Morg_wOH + Ca2+ = ≡Morg_wOCa+ + H+	-1.7
	≡Morg_wOH + Fe2+ = ≡Morg_wOFe+ + H+	0.55
	≡Morg_wOH + Fe3+ = ≡Morg_wOFe2+ + H+	26.75
	≡Morg_wOH + PO4-3 = ≡Morg_wOPO3-2 + H2O	6.6
	≡Morg_wOH + Cr3+ = ≡Morg_wOCr2+ + H+	16
	≡Morg_wOH + Cu2+ = ≡Morg_wOCu+ + H+	7.6
	≡Morg_wOH + Pb2+ = ≡Morg_wOPb+ + H+	5.9
	≡Morg_wOH + Zn2+ = ≡Morg_wOZn+ + H+	0.8

FOLIO ADMINISTRATIF
THESE DE L'UNIVERSITE DE LYON OPEREE AU SEIN DE L'INSA LYON

NOM : BANC DATE de SOUTENANCE : 15/10/21
Prénoms : Camille

TITRE : Interactions matière organique-contaminants inorganiques dans des dépôts de solutions de traitement des eaux fondées sur la nature. Approche combinée ultrafiltration-modélisation

NATURE : Doctorat Numéro d'ordre : 2021LYSEI066

Ecole doctorale : Chimie Lyon

Spécialité : Environnement

RESUME :
Dans les systèmes de traitement des eaux qualifiés de « solutions fondées sur la nature » (i.e. filtres plantés de roseaux et bassin d'infiltration), la rétention des particules en suspensions peut conduire à la formation d'une couche de dépôts de surface. Tant du point de vue de sa capacité à interagir avec les polluants lors de sa présence sur l'unité de traitement, que lors de sa réutilisation notamment en épandage après curage, la spéciation des éléments au sein de ces dépôts et les mécanismes de remobilisation des polluants interrogent. Après évacuation, ces dépôts peuvent constituer une ressource intéressante notamment en agriculture en raison de la quantité de nutriments et de matière organique qu'ils contiennent. Ce travail avait pour objectifs de mieux décrire l'assemblage organo-minéral de ces matrices et de fournir une meilleure compréhension de l'influence des phases colloïdales sur la remobilisation d'éléments majeurs et traces afin de pouvoir fournir des modèles de prédictions, à la fois quantitatif et qualitatif, sur la remobilisation de polluants des dépôts soumis à des variations de pH.
Un dépôt de surface de filtre planté de roseaux à écoulement vertical a été soumis à différentes conditions de pH et les phases colloïdales ont été étudiées. La remobilisation de phases colloïdales organiques s'est montrée particulièrement sensible aux variations de pH. Dans la gamme de pH acide, de petites molécules organiques (< 3 kDa) sont majoritairement remobilisées des dépôts. Pour des pH proches de la neutralité et alcalins, les gros colloïdes organiques (> 30 kDa) prévalent en solutions. Ce relargage de matière organique semble favoriser la remobilisation d'oxydes de fer et d'aluminium au sein de colloïdes organo-minéraux. La nature et la quantité des phases colloïdales remobilisées exercent une large influence sur le relargage d'éléments majeurs et traces depuis les dépôts de filtre planté de roseaux. Cependant, l'affinité des éléments pour ces phases colloïdales est aussi contrôlée par la classe chimique de l'élément considéré, son état d'oxydation ainsi que le pH de la solution.
L'utilisation de ces données expérimentales a permis le développement et la calibration d'un modèle géochimique multi-surfacique capable de reproduire la spéciation d'une large gamme d'éléments (Fe, Al, P, Ca, Mg, Cu, Cd, Cr, Zn, Pb, As) contenue au sein d'une boue de filtre planté de roseaux et ainsi de reproduire le relargage de ces éléments. De par la concentration importante en matière organique mesurée dans la boue et leur importance dans le relargage et la spéciation des éléments, la modélisation de la complexation des métaux sur la matière organique par WHAM-ModelVII a fait l'objet d'un développement particulier. Les essais de modélisation combinés aux résultats d'ultrafiltrations ont permis l'obtention d'un ratio de matière organique active permettant d'améliorer la prédiction des concentrations en éléments. Afin d'évaluer la robustesse de la méthodologie employée sur cette première boue, la stratégie de modélisation a été appliquée à d'autres échantillons (i.e une deuxième boue de filtre planté de roseaux et deux sédiments de bassin d'infiltration). Les modèles multisurfaciques développés dans cette thèse ont tous montré leur efficacité à calculer le relargage de nombreux éléments quel que soit les conditions de pH et malgré des concentrations initiales en élément majeurs et traces très variables. Les informations fournies par ces travaux se sont avérées fondamentales dans la compréhension des risques associés notamment au relargage d'éléments traces métalliques. A terme ces modèles pourraient donc faire partie du panel d'outil d'aide à la décision à disposition des gestionnaires de ces dépôts.

MOTS-CLÉS : Solution fondée sur la nature, métaux traces, nutriments, spéciation, distribution phase solide et liquide, évaluation du risque

Laboratoire (s) de recherche : DEEP (Déchets Eaux Environnement Pollutions)

Directeur de thèse : GOURDON Rémy

Président de jury :

Composition du jury :
Béatrice BECHET, Directrice de Recherche Université Gustave Eiffel, Rapporteur
Oleg POKROSKY, Directeur de Recherche CNRS Géoscience Environnement Toulouse, Rapporteur
Philippe BATAILLARD, Chercheur BRGM, Examinateur
Rémi MARSAC, Chargé de Recherche CNRS Géoscience Rennes, Examinateur
Pascal MOLLE, Directeur de Recherche INRAE, Examinateur
Rémy GOURDON, Professeur des Universités INSA LYON, Directeur de thèse
Mathieu GAUTIER, Maître de Conférences INSA LYON, Co-directeur de thèse
Denise BLANC, Maître de Conférences INSA LYON, Examinateur